



Contracts for field projects
and supporting research on . . .

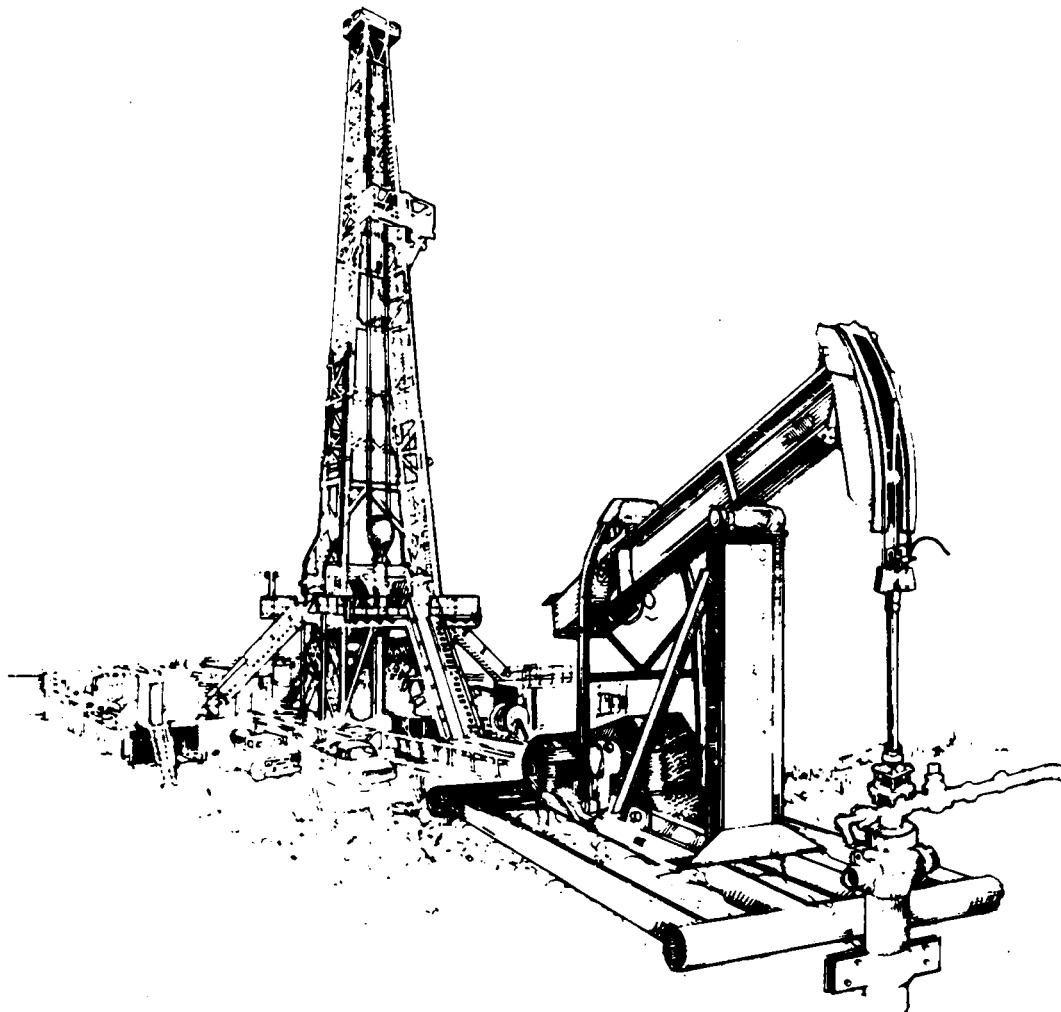
76

Enhanced Oil Recovery

Reporting Period July–September 1993

DOE/BC--93/4
(DE94000127)

PROGRESS REVIEW
Quarter Ending September 30, 1993



United States Department of Energy

Office of Gas and Petroleum Technology
and Bartlesville Project Office

DISCLAIMER

This report was prepared as an account of work sponsored by an agency of the United States Government. Neither the United States Government nor any agency thereof, nor any of their employees, makes any warranty, express or implied, or assumes any legal liability or responsibility for the accuracy, completeness, or usefulness of any information, apparatus, product, or process disclosed, or represents that its use would not infringe privately owned rights. Reference herein to any specific commercial product, process, or service by trade name, trademark, manufacturer, or otherwise does not necessarily constitute or imply its endorsement, recommendation, or favoring by the United States Government or any agency thereof. The views and opinions of authors expressed herein do not necessarily state or reflect those of the United States Government or any agency thereof.

Available to DOE and DOE contractors from the Office of Scientific and Technical Information, P.O. Box 62, Oak Ridge, Tennessee 37831; prices available from (615) 576-8401.

Available to the public from the U.S. Department of Commerce, Technology Administration, National Technical Information Service, Springfield, Virginia 22161; prices available from (703) 487-4650.

U.S. Department of Energy
Washington, D.C. 20545

JACK SIEGEL
*Acting Assistant Secretary
for Fossil Energy*
Room 4G-084 Forrestal Building
Telephone Number 202-586-4695

REGINAL SPILLER
*Deputy Assistant Secretary for Gas
and Petroleum Technologies*

SANDRA WAISLEY
*Director for Oil and Gas Exploration
and Production*

Bartlesville Project Office
P.O. Box 1398
Bartlesville, Oklahoma 74005
Telephone No. 918-337-4401

THOMAS C. WESSON
Director

R. M. RAY
Deputy Director

BETTY J. FELBER
*Program Coordinator,
Enhanced Oil Recovery*

HERBERT A. TIEDEMANN
*Project Manager for
Technology Transfer*

DOE/BC--93/4
(DE94000127)
Distribution Category UC-122

PROGRESS REVIEW NO. 76

CONTRACTS FOR FIELD PROJECTS AND SUPPORTING RESEARCH ON ENHANCED OIL RECOVERY

Date Published - August 1994

UNITED STATES DEPARTMENT OF ENERGY



PUBLICATIONS LIST

Bartlesville Project Office

Thomas C. Wesson, Director

AVAILABILITY OF PUBLICATIONS

The Department of Energy makes the results of all DOE-funded research and development efforts available to DOE and DOE contractors from the Office of Scientific and Technical Information, P.O. Box 62, Oak Ridge, TN 37831; prices available from (615) 576-8401, FTS 626-8401.

Available to the public from the National Technical Information Service, U.S. Department of Commerce, 5285 Port Royal Road, Springfield, VA 22161; prices available from (703) 487-4650.

Give the full title of the report and the report number.

Sometimes there are slight delays between the time reports are shipped to NTIS and the time it takes for NTIS to process the reports and make them available. Accordingly, we will provide one copy of any individual report as long as our limited supply lasts. Please help us in our effort to eliminate wasteful spending on government publications by requesting only those publications needed. Order by the report number listed at the beginning of each citation and enclose a self-addressed mailing label. Available from DOE Bartlesville Project Office, ATTN: Herbert A. Tiedemann, P.O. Box 1398, Bartlesville, OK 74005; (918) 337-4293.

Quarterly Reports

DOE/BC-93/1 **Contracts for Field Projects and Supporting Research on Enhanced Oil Recovery. Progress Review No. 73. Quarter ending December 1992. December 1993. 144 pp. Order No. DE93000136.** Status reports are given for various enhanced oil recovery and gas recovery projects sponsored by the Department of Energy. The field tests and supporting research on enhanced oil recovery include chemical flooding, gas displacement, thermal/heavy oil, resource assessment, geoscience technology, microbial technology, field demonstrations in high-priority reservoir classes, novel technology, and environmental technology.

General Research

NIPER-691 **1992 Annual Report. October 1, 1991-September 30, 1992. National Institute for Petroleum and Energy Research. October 1993. 104 pp. Order No. DE94000103.** This report covers the second full year of research by the National Institute for Petroleum and Energy Research (NIPER) under the DOE's National Energy Strategy-Advanced Oil Recovery Program Implementation Plan. The Plan outlines an integrated, highly targeted research, development, and demonstration program focusing on near-, mid-, and long-term objectives to maximize the economic producibility of the domestic oil and gas resource and to assure that new and advanced recovery technologies are implemented in the field within the earliest possible time frame. NIPER also performs research for the DOE Advanced Extraction and Processing Technology (AEPT) Program to develop crosscutting tools, techniques, and scientific/technical understanding in both extraction and conversion/upgrading technologies which can be applied to a broad range of petroleum resources. NIPER performs exploratory research to identify and test novel concepts, and fundamental applied research to develop and apply improved technical and scientific understanding to the solution of generic problems. The report covers research accomplishments, publications, and presentations resulting from the FY92 research conducted under 14 Base Program projects, 11 of which were funded under DOE's Light Oil and Heavy Oil Programs, and three funded under the AEPT Program.

Chemical Flooding

NIPER-698

NIPER/DOE Chemical EOR Workshop. Final Report. National Institute for Petroleum and Energy Research. October 1993. 96 pp. Order No. DE93000173. The subject of this report is the Chemical EOR Workshop held on June 23-24, 1993, in Houston, Texas. The objectives of this workshop were to evaluate the potential for chemical enhanced oil recovery (EOR) to recover significant quantities of remaining domestic oil, to assess the role of the DOE and petroleum industry to achieve this potential, and to assess the research needs in chemical EOR. Fifty-six research engineers and scientists from major oil companies, independent oil companies, academic institutes, research institutes, and DOE attended this workshop. Ten papers on the state-of-the-art in chemical EOR technologies and recent field test experience were presented on the first day. Two workshops, one on surfactant/alkali flooding and the other on profile modification/polymer flooding, were held on the second day. It was concluded that chemical EOR has the potential of recovering significant quantities of remaining oil, and it is the only method that has the potential of economically recovering residual oil from reservoirs of shallow and medium depth.

NIPER-705

User's Guide and Documentation Manual for "PC-Gel" Simulator. Topical Report. National Institute for Petroleum and Energy Research. October 1993. 196 pp. Order No. DE94000104. PC-Gel is a three-dimensional, three-phase (oil, water, and gas) permeability modification simulator developed by incorporating an in situ gelation model into a black oil simulator (BOAST) for personal computer application. The features included in the simulator are transport of each chemical species of the polymer/crosslinker system in porous media, gelation reaction kinetics of the polymer with crosslinking agents, rheology of the polymer and gel, inaccessible pore volume to macromolecules, adsorption of chemical species on rock surfaces, retention of gel on the rock matrix, and permeability reduction caused by the adsorption of polymer and gel. The in situ gelation model and simulator were validated against data reported in the literature. The simulator PC-GEL is useful for simulating and optimizing any combination of primary production, waterflooding, polymer flooding, and permeability modification treatment.

NIPER-710

Screening of Mixed Surfactant Systems: Phase Behavior Studies and CT Imaging of Surfactant-Enhanced Oil Recovery Experiments. Topical Report. National Institute for Petroleum and Energy Research. November 1993. 128 pp. Order No. DE94000105. A systematic chemical screening study was conducted on selected anionic-nonionic and nonionic-nonionic systems. The objective of this study was to evaluate and determine combinations of these surfactants that would exhibit favorable phase behavior and solubilization capacity. The effects of different parameters, including (a) salinity, (b) temperature, (c) alkane carbon number, (d) HLB of nonionic component, and (e) type of surfactant, on the behavior of the overall chemical system were evaluated. The current work was conducted using a series of ethoxylated nonionic surfactants in combinations of several anionic systems with various hydrocarbons. Efforts to correlate the behavior of these mixed systems led to the development of several models for the chemical systems tested. The models were used to compare the different systems and provided some guidelines for formulating them to account for variations in salinity, oil hydrocarbon number, and temperature. The models were also evaluated to determine conformance with the results from experimental measurements. The models provided good agreement with experimental results.

DOE/BC/14880-5 Improved Techniques for Fluid Diversion in Oil Recovery. First Annual Report. New Mexico Institute of Mining and Technology. December 1993. 284 pp. Order No. DE94000113. This report describes work performed during the first year of the project, "Improved Techniques for Fluid Diversion in Oil Recovery." This three-year project has two objectives: (1) to compare the effectiveness of gels in fluid diversion with those of other types of processes, and (2) to identify the mechanisms by which materials (particularly gels) selectively reduce permeability to water more than to oil. To establish a baseline for the applicability of gel treatments, previously published field results were examined to determine if they reveal usable guidelines for the selection of candidates for gel treatments. Views of seven gel vendors and experts from eight major oil companies were also surveyed concerning the selection and implementation of gel treatments. After analyzing the literature and the survey responses, criteria were proposed for candidate selection, both for injection wells and production wells.

NIPER-714 Surfactant-Enhanced Alkaline Flooding Field Project. Annual Report. National Institute for Petroleum and Energy Research. December 1993. 36 pp. Order No. DE94000111. The Tucker sand from Hepler field, Crawford County, Kansas, was characterized using routine and advanced analytical methods. The characterization is part of a chemical flooding pilot test to be conducted in the field, which is classified as a DOE Class I (fluvial-dominated deltaic) reservoir. Routine and advanced methods of characterization were compared. Traditional wireline logs indicate that the reservoir is vertically compartmentalized on the foot scale. Routine core analysis, X-ray computed tomography (CT), minipermeameter measurement, and petrographic analysis indicate that compartmentalization and lamination extend to the microscale. An idealized model of how the reservoir is probably structured (complex layering with small compartments) is presented.

Thermal Recovery

DOE/BC/93000174 Fundamentals of Foam Transport in Porous Media. Topical Report. University of California, Berkeley. October 1993. 76 pp. Order No. DE93000174. Foam in porous media is a fascinating fluid both because of its unique microstructure and dramatic influence on the flow of gas and liquid. A wealth of information is now compiled in the literature describing foam generation, destruction, and transport mechanisms. Yet there are conflicting views of these mechanisms and on the macroscopic results they produce. By critically reviewing how surfactant formulation and porous media topology conspire to control foam texture and flow resistance, an attempt is made to unify the disparate viewpoints. Evolution of texture during foam displacement is quantified by a population balance on bubble concentration, which is designed specifically for convenient incorporation into a standard reservoir simulator. Theories for the dominant bubble generation and coalescence mechanisms provide physically based rate expressions for the proposed population balance. Stone-type relative permeability functions along with the texture-sensitive and shear-thinning nature of confined foam complete the model. Quite good agreement is found between theory and new experiments for transient foam displacement in linear cores.

DOE/BC/14899-8 Drawdown Behavior of Gravity Drainage Wells. SUPRI TR 97. Stanford University Petroleum Research Institute. October 1993. 84 pp. Order No. DE93000175. An analytical solution for drawdown in gravity drainage wells is developed. The free-surface flow is viewed as incompressible, and anisotropy effects are included. The well is a line source well, and the reservoir is infinitely large. The model is valid for small drawdowns. The uniform wellbore potential inner boundary condition is modelled using the proper Green's function. The discontinuity at the wellbore is solved by introducing a finite skin radius, and the formulation produces a seepage face. The calculated wellbore flux distribution and wellbore pressures are in fair agreement with results obtained using a numerical gravity drainage simulator. Three distinct flow periods are observed. The wellbore storage period is caused by the moving liquid level, and the duration is short. During the long intermediate flow period, the wellbore pressure is nearly constant. In this

period the free surface moves downwards, and the liquid is produced mainly by vertical drainage. At long times the semilog straight line appears. The confined liquid solutions by Theis (1935) and van Everdingen and Hurst (1949) may be used during the pseudoradial flow period if the flowrate is low. New type curves are presented that yield both vertical and horizontal permeabilities.

DOE/BC/94000102 A Growing-Drop Technique for Measuring Dynamic Interfacial Tension. Topical Report. University of California, Berkeley. October 1993. 52 pp. Order No. DE94000102. A novel, growing-drop technique is described for measuring dynamic interfacial tension as a result of sorption of surface-active solutes. The proposed method relates the instantaneous pressure and size of expanding liquid drops to interfacial tension and is useful for measuring both liquid/gas and liquid/liquid tensions over a wide range of time scales, currently from 10 ms to several hours. Growing-drop measurements on surfactant-free water/air and water/octanol interfaces yield constant tensions equal to their known literature values. For surfactant-laden, liquid drops, the growing-drop technique captures the actual transient tension evolution of a single interface, rather than interval times as with the classic maximum-drop-pressure and drop-volume tension measurements. Dynamic tensions measured for 0.25 mM aqueous 1-decanol solution/air and 0.02 kg/m³ aqueous Triton X-100 solution/dodecane interfaces show nonmonotonic behavior, indicating slow surfactant transport relative to the imposed rates of interfacial dilation. The dynamic tension of a purified and fresh 6 mM aqueous sodium dodecyl sulfate (SDS) solution/air interface shows only a monotonic decrease, indicating rapid surfactant transport relative to the imposed rates of dilatation. Conversely, an aged SDS solution, naturally containing trace dodecanol impurities, exhibits dynamic tensions which reflect a superposition of the rapidly equilibrating SDS and the slowly adsorbing dodecanol.

NIPER-722 Thermal Process for Heavy Oil Recovery. Topical Report. National Institute for Petroleum and Energy Research. November 1993. 76 pp. Order No. DE94000109. This report summarizes research activities conducted in FY93. A major portion of project research during the year was concentrated on modeling and reservoir studies to determine the applicability of steam injection oil recovery techniques in Texas Gulf Coast heavy oil reservoirs. In addition, an in-depth evaluation of a steamflood predictive model developed by Mobil Exploration and Production Company (Mobil E&P) was performed. Details of these two studies are presented. A topical report (NIPER-675) assessing the NIPER Thermal EOR Research Program the past 10 years was written during the fiscal year and delivered to DOE. Results of the Gulf Coast heavy oil reservoir simulation studies indicated that though these reservoirs can be successfully steamflooded and could recover more than 50% of oil-in-place, steamflooding may not be economical at current heavy oil prices. Assessment of Mobil E&P's steamflood predictive model capabilities indicate that the model in its present form gives reasonably good predictions of California steam projects, but fails to predict adequately the performance of non-California steam projects.

NIPER-661 Feasibility of Steam Injection Process in a Thin, Low-Permeability Heavy Oil Reservoir of Arkansas — A Numerical Simulation Study. Topical Report. National Institute for Petroleum and Energy Research. December 1993. 112 pp. Order No. DE94000112. This report details the findings of an in-depth study undertaken to assess the viability of the steam injection process in the heavy oil bearing Nacatoch sands of Arkansas. Published screening criteria and DOE's steamflood predictive models were utilized to screen and select reservoirs for further scrutiny. Although, several prospects satisfied the steam injection screening criteria, only a single candidate was selected for detailed simulation studies. The selection was based on the availability of needed data for simulation and the uniqueness of the reservoir. The reservoir investigated is a shallow, thin, low-permeability reservoir with low initial oil saturation and an underlying water sand. The study showed that the reservoir will respond favorably to steamdrive, but not to cyclic steaming. Steam stimulation, however, is necessary to improve steam injectivity during subsequent steamdrive. Further, in such marginal heavy oil reservoirs (i.e., reservoir characterized by thin pay zone and low initial oil

saturation) conventional steamdrive (i.e., steam injection using vertical wells) is unlikely to be economical, and nonconventional methods must be utilized. It was found that the use of horizontal injectors and horizontal producers significantly improved the recovery and oil-steam ratio and improved the economics. It is recommended that the applicability of horizontal steam injection technology in this reservoir be further investigated.

Geoscience

NIPER-713

Field Guide to Muddy Formation Outcrops, Crook County, Wyoming. Topical Report. National Institute for Petroleum and Energy Research. November 1993. 116 pp. Order No. DE94000106. The purpose of this report and a similar report containing Almond Formation outcrop data is to provide the data and analyses generated from this research project so that other workers may use and build upon it. The objectives of this research program are to (1) determine the reservoir characteristics and production problems of shoreline barrier reservoirs; and (2) develop methods and methodologies to effectively characterize shoreline barrier reservoirs to predict flow patterns of injected and produced fluids. Two reservoirs were selected for detailed reservoir characterization studies — Bell Creek field, Carter County, Montana that produced from the Lower Cretaceous (Albian-Cenomanian) Muddy Formation, and Patrick Formation of the Mesaverde Group. An important component of the research project was to use information from outcrop exposures of the producing formations to study the spatial variations of reservoir properties and the degree to which outcrop information can be used in the construction of reservoir models. This report contains the data and analyses collected from outcrop exposures of the Muddy Formation, located in Crook County, Wyoming 40 miles south of Bell Creek oil field. The outcrop data set contains, permeability, porosity, petrographic, grain size and geologic data from 1-inch-diameter core plugs drilled from the outcrop face, as well as geological descriptions and sedimentological interpretations of the outcrop exposures. The outcrop data set provides information about facies characteristics and geometries and the spatial distribution of permeability and porosity on interwell scales. Appendices within this report include a micropaleontological analyses of selected outcrop samples, an annotated bibliography of papers on the Muddy Formation in the Powder River Basin, and over 950 permeability and porosity values measured from 1-inch-diameter core plugs drilled from the outcrop. All data contained in this report are available in electronic format upon request. The core plugs drilled from the outcrop are available for measurement.

NIPER-712

Reservoir Condition Special Core Analyses and Relative Permeability Measurements on Almond Formation and Fontainebleu Sandstone Rocks. Topical Report. National Institute for Petroleum and Energy Research. November 1993. 32 pp. Order No. DE94000107. This report describes the results from special core analyses and relative permeability measurements conducted on Almond formation and Fontainebleu sandstone plugs. Almond formation plug tests were performed to evaluate multiphase, steady-state, reservoir-condition relative permeability measurement techniques and to examine the effect of temperature on relative permeability characteristics. The Fontainebleu sandstone was selected for tests because of its uniformity and 100-mD permeability range. In addition to rock tests, a fluid system consisting of propane and 1-bromopropane was designed and evaluated for tests simulating condensate deposition. In condensate systems, liquid and gas phase volumes within the rock are pressure and temperature sensitive. Insufficient time was available to use the fluid in flow tests. Progress was made toward using the PC version of the BOAST simulator, DOE's black oil reservoir simulator, for coreflood history matching. The simulator may be very useful in determining rock relative permeability functions from reservoir-rate displacement tests while accounting for capillary effects.

NIPER-720

Investigation of Wettability by NMR Microscopy and Spin-Lattice Relaxation. Topical Report. National Institute for Petroleum and Energy Research. November 1993. 16 pp. Order No. DE94000108. The wettability of reservoir rock has an important impact on the efficiency of oil

recovery processes and the distribution of oil and water within the reservoir. One of the potentially useful tools for wettability measurements is nuclear magnetic resonance (NMR) and spin-lattice relaxation. More recently, using NMR microscopy, NIPER has developed the capability of imaging one- and two-phase fluid systems in reservoir rock at resolutions to 25 microns. Effects seen in the images of fluids within the pore space of rocks near the rock grain surfaces hinted at the possibility of using NMR microscopy to map the wettability variations at grain sites within the pore space. Investigations were begun using NMR microscopy and spin-lattice relaxation time measurements on rock/fluid systems and on well-defined fractional wet model systems to study these effects. Relaxation data has been modelled using the stretched exponential relationship recently introduced. Comparisons of the NMR microscopy results of the model system with the rock results indicate that the observed effects probably do not reflect actual wettability variations within the pore space. The results of the relaxation time measurements reveal that even in the simple model studies, the behavior of two phases is somewhat ambiguous and much more complex and requires more study.

NIPER-724

Data from Selected Almond Formation Outcrops — Sweetwater County, Wyoming. Topical Report. National Institute for Petroleum and Energy Research. December 1993. 76 pp. Order No. DE94000110. The objectives of this research program are to: (1) determine the reservoir characteristics and production problems of shoreline barrier reservoirs; and (2) develop methods and methodologies to effectively characterize shoreline barrier reservoirs to predict flow patterns of injected and produced fluids. Two reservoirs were selected for detailed reservoir characterization studies — Bell Creek field, Carter County, Montana, that produces from the Lower Cretaceous (Albian-Cenomanian) Muddy Formation, and Patrick Draw field, Sweetwater County, Wyoming, that produces from the Upper Cretaceous (Campanian) Almond Formation of the Mesaverde Group. An important component of the research project was to use information from outcrop exposures of the producing formations to study the spatial variations of reservoir properties and the degree to which outcrop information can be used in the construction of reservoir models. A report similar to this one presents the Muddy Formation outcrop data and analyses performed in the course of the study. Two outcrop localities, RG and RH, previously described by Roehler (1988) provided good exposures of the Upper Almond shoreline barrier facies and were studied during 1990-1991. Core from core well No. 2 drilled approximately 0.3 miles downdip of outcrop RG was obtained for study. The results of the core study will be reported in a separate volume. Outcrops RH and RG, located about 2 miles apart were selected for detailed description and drilling of core plugs. One 257-ft thick section was measured at outcrop RG, and three sections 145 ft thick located 490 and 655 ft apart were measured at the outcrop RH. Cross-sections of these profiles were constructed to determine lateral facies continuity and changes. This report contains the data and analyses from the outcrops. The outcrop data set includes 4 measured sections and descriptions of outcrop exposures; grain-size distribution data from image analysis of 30 thin section; permeability and porosity measurements from 25 1-inch diameter coreplugs drilled from the face of the outcrops; and 923 fracture azimuths measured from the outcrop face. This data is available in electronic format from the Department of Energy, Bartlesville Project Office.

BNL 47046

Effects of Selected Thermophilic Microorganisms on Crude Oils at Elevated Temperatures and Pressures. 1991 Annual Report. Brookhaven National Laboratory. October 1993. 32 pp. Order No. DE93000172. During the past several years, a considerable amount of work has been carried out showing that microbial enhanced oil recovery (MEOR) is promising and the resulting biotechnology may be deliverable. In this laboratory systematic studies are being conducted which deal with the effects of thermophilic and thermoadapted bacteria on the chemical and physical properties of selected types of crude oils at elevated temperatures and pressures. Particular attention is being paid to heavy crude oils such as Boscan and Cerro Negro (Venezuela), Monterey (California) and those from Alabama and Arkansas. Current studies indicate that during the biotreatment several properties of crude oils are affected. The oils are (1) emulsified; (2) acidified; (3) there is a qualitative and quantitative change in light and heavy fractions of the crudes; (4) there are chemical changes in fractions containing sulfur compounds; (5)

ere is an apparent solubilization of trace metals; and (6) the qualitative and quantitative chemical and physical changes appear to be microbial species dependent. Effects on heavy crude oils are also compared to those on lighter oils such as oils from the Wyoming petroleum reserve. Microbial oil interactions are monitored routinely by a consortium of analytical techniques which are continuously upgraded and are capable of multiparameter analysis. The results generated in fiscal year 1991, describing (1) through (6), are presented and discussed in this report.

PER-703 **User's Guide and Documentation Manual for Microbial Transport Simulator. Topical Report. National Institute for Petroleum and Energy Research. October 1993. 76 pp. Order No. DE94000101.** The microbial transport simulator (MTS) is a three-dimensional, three-phase, multiple-component numerical model that permits the study of the transport of microorganisms and nutrients in porous media. Microbial parameters incorporated into MTS include: microbial growth and decay, microbial deposition, chemotaxis, diffusion, convective dispersion, tumbling, and nutrient consumption. Governing equations for microbial and nutrient transport are coupled with continuity and flow equations under conditions appropriate for black oil reservoir. The model's mathematical formulations and preparation procedures of data files for conducting simulations using MTS are described.

DE/BC/14663-11 **New Microorganisms and Processes for MEOR. Final Report. INJECTECH, Inc. December 1993. 48 pp. Order No. DE94000114.** Oil reservoirs naturally contain inorganic and organic materials which may be exploited through simple mineral supplementation to support the growth of denitrifying microorganisms. The growth and metabolic products from the presence of these microorganisms will aid in the release of oil from the rock matrix and improve crude oil quality and oil field operations. These studies have been successful in defining new microorganisms and processes for MEOR. Materials which may serve as nutritional sources for microorganisms are present in the connate or flood waters or may be added to reservoirs during drilling and production operations of oil fields. These materials include sulfate, carbonate, volatile fatty acids, nitrogen-containing corrosion inhibitors, phosphorous-containing scale inhibitors and trace elements. The experiments show that, with simple minimal mineral supplementation to the

flood waters, the increased growth of naturally-occurring microorganisms can contribute to the enhancement of oil recovery and are important aspects of many EOR technologies. Sulfate reducing bacteria (SRB), heterotrophic denitrifying bacteria, and denitrifying *Thiobacillus* species were successfully isolated from oil field waters. The SRB and *Thiobacillus* cultures, as a consortium, can utilize the volatile fatty acids and dissolved carbonates found in these waters and formations. These cultures were shown to feed each other sequentially and survive in mixed cultures. In a reservoir environment, these types of organisms are limited because of the development of an additional microflora containing heterotrophic denitrifying bacteria.

Fundamental Petroleum Chemistry

NIPER-531 **Microcarbon Residue Yield and Heteroatom Partitioning Between Volatiles and Solids for Whole Vacuum Resids and Their Liquid Chromatographic Fractions. Topical Report. National Institute for Petroleum and Energy Research. October 1993. 40 pp. Order No. DE93000171.** Five petroleum resids >1000° F were separated into compound type fractions using liquid chromatography. The coking tendency of each compound type was assessed using the micro-carbon residue (MCR) test (ASTM D 4530). Heteroatom (N, S, Ni, V) partitioning between MCR solids versus volatiles was determined through analysis of the starting fractions and the corresponding MCR solids. The weighted sum of MCR solid yields over all compound types in a given resid was typically in good agreement with the MCR yield of the whole resid. This finding agrees with prior studies indicating coke yield to be an additive property. Sulfur partitioning was also an additive property, was predictable from MCR yield, and was nearly independent of the initial form (sulfide, thiophenic, sulfoxide) present. Nitrogen and nickel partitioning were nonadditive and therefore composition dependent. Partitioning of vanadium into solids was essentially quantitative for all resids and their fractions. MCR solid yield was generally dependent only on H/C ratio. However, there is some evidence indicating secondary dependence on hydrocarbon structure; i.e., that naphthenic rings reduce MCR in proportion to H/C by virtue of their effective hydrogen transfer properties. Deposition of N and Ni into MCR solids over the fractions was often appreciably less than that of the whole resids, thereby indicating that interaction among various compound types was required for maximum incorporation of those elements into coke.

INDEX

COMPANIES AND INSTITUTIONS

	Page		Page
American Oil Recovery, Inc.		Reservoir Engineering Research Institute	
Applications of Advanced Petroleum Production Technology and Water-Alternating-Gas Injection for Enhanced Oil Recovery—Mattoon Oil Field, Illinois	86	Research Consortium on Fractured Petroleum Reservoirs	65
Anderman/Smith Operating Company		Sandia National Laboratories	
Secondary Oil Recovery from Selected Carter Sandstone Oil Fields—Black Warrior Basin, Alabama	92	Geodiagnostics for Fossil Energy Recovery	61
Columbia University		Sierra Energy Company	
Dynamic Enhanced Recovery Technologies	75	Enhanced Oil Recovery Utilizing High-Angle Wells in the Frontier Formation, Badger Basin Field, Park County, Wyoming	80
Surfactant Loss Control in Chemical Flooding: Spectroscopic and Calorimetric Study of Adsorption and Precipitation on Reservoir Minerals	19	Stanford University	
Illinois Institute of Technology		Productivity and Injectivity of Horizontal Wells	29
Surfactant-Enhanced Alkaline Flooding for Light Oil Recovery	12	Stanford University Petroleum Research Institute	
Lawrence Berkeley Laboratory		Research on Oil Recovery Mechanisms in Heavy Oil Reservoirs	41
Electrical and Electromagnetic Methods for Reservoir Description and Process Monitoring	53	Surtek, Inc.	
Lawrence Berkeley Laboratory/Industry Heterogeneous Reservoir Performance Definition Project	54	Detailed Evaluation of the West Kiehl Alkaline-Surfactant-Polymer Field Project and Its Application to Mature Minnelusa Waterfloods	42
Lawrence Livermore National Laboratory		Investigation of Oil Recovery Improvement by Coupling an Interfacial Tension Agent and a Mobility Control Agent in Light Oil Reservoirs	1
Oil Field Characterization and Process Monitoring Using Electromagnetic Methods	39	University of Alaska	
Lomax Exploration Company		Study of Hydrocarbon Miscible Solvent Slug Injection Process for Improved Recovery of Heavy Oil from Schrader Bluff Pool, Milne Point Unit, Alaska	25
Green River Formation Waterflood Demonstration Project, Uinta Basin, Utah	71	University of Kansas	
Maurer Engineering		Improved Oil Recovery in Fluvial Dominated Deltaic Reservoirs of Kansas—Near-Term	84
Horizontal Oil Well Applications and Oil Recovery Assessment	37	Improving Reservoir Conformance Using Gelled Polymer Systems	17
New Mexico Institute of Mining and Technology		University of Michigan	
Field Verification of CO ₂ -Foam	23	Characterization and Modification of Fluid Conductivity in Heterogeneous Reservoirs To Improve Sweep Efficiency	51
Improved Techniques for Fluid Diversion in Oil Recovery	9	University of Southern California	
Oklahoma Geological Survey		Modification of Reservoir Chemical and Physical Factors in Steamfloods To Increase Heavy Oil Recovery	49
Continued Support of the Natural Resources Information System for the State of Oklahoma	67	University of Southern Mississippi	
ParaMagnetic Logging, Inc.		Responsive Copolymers for Enhanced Petroleum Recovery	5
Fabrication and Downhole Testing of Moving Through Casing Resistivity Apparatus	64		

University of Texas

Development of Cost-Effective Surfactant
Flooding Technology 14

University of Tulsa

Integrated Approach Toward the Application
of Horizontal Wells To Improve
Waterflooding Performance 93

CONTENTS BY EOR PROCESS

Chemical Flooding—Supporting Research 1
Gas Displacement—Supporting Research 23
Thermal Recovery—Supporting Research 25
Geoscience Technology 51
Resource Assessment Technology 67
Field Demonstrations in High-Priority
Reservoir Classes 71

**DOE Technical Project Officers for
Enhanced Oil Recovery**

DIRECTORY

Name	Phone number	Name of contractor
U. S. Department of Energy Gas and Petroleum Technology Oil and Gas Exploration and Production 3E-028/FORS Washington, D.C. 20585		
Bartlesville Project Office P. O. Box 1398 Bartlesville, Oklahoma 74005		
Edith Allison	918-337-4390	Columbia University Lomax Exploration Company Sierra Energy Company
Jerry Casteel	918-337-4412	Columbia University Illinois Institute of Technology New Mexico Institute of Mining and Technology Surtek, Inc. University of Kansas University of Southern Mississippi University of Texas
Robert Lemmon	918-337-4405	Lawrence Berkeley Laboratory ParaMagnetic Logging, Inc. Sandia National Laboratories University of Michigan
Rhonda Lindsey	918-337-4455	Reservoir Engineering Research Institute University of Kansas University of Tulsa
R. Michael Ray	918-337-4403	Oklahoma Geological Survey
Thomas Reid	918-337-4233	Lawrence Livermore National Laboratory Maurer Engineering Stanford University Stanford University Petroleum Research Institute Surtek, Inc. University of Alaska University of Southern California
Metairie Site Office 900 Commerce Road, East New Orleans, Louisiana 70123		
Gene Pauling	504-734-4131	American Oil Recovery, Inc. Anderman/Smith Operating Company
Morgantown Energy Technology Center P. O. Box 880 Morgantown, West Virginia 26505		
Royal Watts	304-291-4218	New Mexico Institute of Mining and Technology

CHEMICAL FLOODING— SUPPORTING RESEARCH

**INVESTIGATION OF OIL RECOVERY
IMPROVEMENT BY COUPLING AN
INTERFACIAL TENSION AGENT AND
A MOBILITY CONTROL AGENT
IN LIGHT OIL RESERVOIRS**

Contract No. DE-AC22-92BC14886

**Surtek, Inc.
Golden, Colo.**

**Contract Date: Sept. 28, 1992
Anticipated Completion: Sept. 30, 1995
Government Award: \$219,925
(Current year)**

**Principal Investigator:
Malcolm J. Pitts**

**Project Manager:
Jerry Casteel
Bartlesville Project Office**

Reporting Period: July 1–Sept. 30, 1993

Objectives

The study will investigate two major areas concerning coinjecting an interfacial tension (IFT) reduction agent(s) and

a mobility control agent into petroleum reservoirs. The first will consist of defining the mechanisms of interaction of an alkaline agent, a surfactant, and a polymer on a fluid–fluid and a fluid–rock basis. The second is the improvement of the economics of the combined technology.

This report examines the effect of the addition of polymer to different combinations of alkaline agents and surfactants. Xanthan gum and polyacrylamide polymers were evaluated. In addition, the effect of alkali and polymer on the critical micelle concentration (CMC) of different surfactant types was investigated.

Summary of Technical Progress

A 42 °API gravity crude oil from the Adena Field¹ was selected for the study. Solutions were dissolved in 1000 mg/L NaCl except where designated.

Interfacial Tension with Alkali and Surfactant

A series of IFT measurements at 72 °F were made with 0.1 and 0.2 wt % surfactant in the presence of alkali from 0 to 2 wt %. Surfactant structures and molecular weights were varied. The five alkaline agents tested were Na₂CO₃, NaHCO₃, Na₃PO₄, Na₂HPO₄, and NaOH. The addition of alkali alone did not reduce the IFT. Na₃PO₄ is the exception and did achieve IFT reductions of up to 400-fold. The IFT reduction with surfactant in the absence of alkali ranged from less than

2-fold to in excess of 3200-fold. The addition of alkali to the surfactant solutions lowered the IFT values for all surfactants tested. Ultralow IFT values of 0.001 dyne/cm or less were measured for a number of the surfactants. Surfactant structure and alkali type resulted in different IFT reduction characteristics. Differences were also observed with alkali concentration for each surfactant and alkali type.

Effect of Temperature on Interfacial Tension

The IFT of selected alkaline-surfactant solutions was determined at 125 and 180 °F, and the data were compared with the 72 °F data. Changes in IFT were observed with the various alkaline-surfactant solutions. How the IFT changed with temperature was generally consistent for the different alkaline agents for a single surfactant. No consistent trend was observed for the different surfactants.

Effect of Polymer on Interfacial Tension of Alkaline-Surfactant Solutions

A xanthan gum and a polyacrylamide polymer were added to selected solutions of alkali and surfactant at 400, 800, and 1200 mg/L. Each of the five alkaline types was tested with a linear alkyl aryl sulfonate, a branched alkyl aryl sulfonate, and an alpha olefin sulfonate. Each of the alkali concentrations tested showed an increase in IFT values with the addition of polymer. Increasing the polymer concentration above 400 mg/L resulted in only minimal changes of IFT values. Polymer type and alkali type did not affect the alteration of IFT values.

Effect of Alkali and Surfactant on the Viscosity of Polymer Solutions

The effect of blending alkali, surfactant, and alkali plus surfactant on polyacrylamide, xanthan gum, and hydroxyethyl cellulose was monitored. As expected, when only alkali was added, the polymer solution viscosities for each of the three polymers decreased at 72 °F. At 180 °F, polyacrylamide and hydroxyethyl cellulose solution viscosities decreased as well, but the xanthan gum solution viscosities increased. The addition of surfactant to the alkaline-polymer or polymer solutions resulted in increases and decreases of viscosity which were dependent on surfactant type for polyacrylamide and hydroxyethyl cellulose. The alkyl aryl sulfonate and alpha olefin sulfonate significantly reduced the viscosity of the polyacrylamide and hydroxyethyl cellulose at 180 °F with a slight reduction of solution viscosity at 72 °F. The addition of the linear alkyl aryl sulfonate to the polyacrylamide solution increased the solution viscosity significantly at 180 °F and to a lesser extent at 72 °F. Xanthan gum solution viscosities increased with the addition of branched alkyl aryl sulfonate and linear alkyl aryl sulfonate but not with alpha olefin sulfonate. With the addition of alkali to the polymer solution,

the addition of the linear alkyl aryl sulfonate and alpha olefin sulfonate increased xanthan gum solution viscosity whereas the addition of branched alkyl aryl sulfonate did not. In both the polymer and alkaline-polymer solutions, surfactant addition effects were more pronounced at 72 °F than at 180 °F.

The intrinsic viscosity and hydrodynamic radius were calculated from the apparent viscosity data.² The data for sodium carbonate are listed in Table 1.

Critical Micelle Concentration

Critical micelle concentrations of 0.02 to 0.06 wt % active were measured for alpha olefin, linear alkyl aryl, branch alkyl aryl, and internal olefin sulfonates. The addition of Na₂CO₃, NaOH, NaHCO₃, Na₃PO₄, and Na₂HPO₄ to the surfactant solution decreased the CMC to 0.005 to 0.02 wt %. The addition of polyacrylamide and xanthan gum polymers to the surfactant solutions appeared to decrease the CMC like the addition of alkali but did not alter the CMC of the alkaline plus surfactant solution.

Effect of the Addition of Sodium Chloride on Interfacial Tension, Critical Micelle Concentration, and Polymer Solution Viscosity

The addition of sodium chloride to the surfactant plus alkali solutions resulted in a decrease in CMC until the surfactant precipitated from solution. The addition of sodium chloride and alkali affected the CMC in a similar manner.

The addition of sodium chloride to the alkaline plus surfactant solutions generally showed an increase of the IFT. As the sodium chloride concentration increased, the alkyl aryl sulfonate surfactants precipitated from solution. Increasing the temperature resulted in solution stability at higher sodium chloride concentrations. The data for the addition of 0.5 to 2.0 wt % NaOH plus surfactant are listed in Table 2.

The addition of sodium chloride to either a polyacrylamide or surfactant plus polyacrylamide solution resulted in a decrease in polymer solution viscosity. When alkali was dissolved in the polymer or surfactant plus polymer solution, the solution viscosity did not change significantly until the sodium chloride concentration approached 30,000 mg/L. Then the apparent viscosity decreased. The difference between the alkaline plus surfactant plus polymer solutions is that, with alkali added to the solution, it becomes stable at a lower salinity. The data for polyacrylamide with Na₂CO₃ and a linear alkyl aryl sulfonate are listed in Table 3.

Xanthan gum solutions demonstrated a different trend. As the salinity was increased, the addition of sodium chloride increased the xanthan gum solution viscosity with salinity at 180 °F, but it had little effect on the solution viscosity at 72 °F. Xanthan gum plus surfactant showed similar characteristics. The addition of alkali to the xanthan gum or surfactant plus xanthan gum solutions did not alter the effect of sodium chloride. Like polyacrylamide solutions, the solutions were unstable at lower sodium chloride concentrations when xanthan

TABLE 1

Effect of Alkali and Surfactant on the Viscosity of Polymer Solutions

Polymer type	Alkaline agent	Surfactant type	[η], mL/g	Hydrodynamic
				radius, μm
Xanthan gum	None	None	6,370	0.256
	None	0.1 wt % LXS 420	7,969	0.276
	None	0.2 wt % LXS 420	10,801	0.305
	None	0.5 wt % LXS 420	10,134	0.299
	2 wt % Na ₂ CO ₃	None	8,535	0.282
	2 wt % Na ₂ CO ₃	0.1 wt % LXS 420	3,117	0.202
	2 wt % Na ₂ CO ₃	0.2 wt % LXS 420	2,287	0.182
	2 wt % Na ₂ CO ₃	0.5 wt % LXS 420	3,547	0.211
	Polyacrylamide	None	None	21,710
None		0.1 wt % LXS 420	15,621	0.498
None		0.2 wt % LXS 420	12,290	0.460
None		0.5 wt % LXS 420	12,208	0.459
2 wt % Na ₂ CO ₃		None	4,685	0.333
2 wt % Na ₂ CO ₃		0.1 wt % LXS 420	3,137	0.292
2 wt % Na ₂ CO ₃		0.2 wt % LXS 420	3,118	0.291
2 wt % Na ₂ CO ₃		0.5 wt % LXS 420	3,726	0.309
Hydroxyethyl cellulose		None	None	2,293
	None	0.1 wt % LXS 420	2,025	0.114
	None	0.2 wt % LXS 420	2,144	0.116
	None	0.5 wt % LXS 420	2,269	0.118
	2 wt % Na ₂ CO ₃	None	1,376	0.100
	2 wt % Na ₂ CO ₃	0.1 wt % LXS 420	1,067	0.092
	2 wt % Na ₂ CO ₃	0.2 wt % LXS 420	1,162	0.095
	2 wt % Na ₂ CO ₃	0.5 wt % LXS 420	1,259	0.097

TABLE 2

Effect of the Addition of Sodium Chloride Plus Surfactant Solutions on Interfacial Tension (dyne/cm)

Surfactant	Temp., °F	Sodium chloride concentration, mg/L					
		1,000	5,000	10,000	15,000	20,000	30,000
Alpha olefin sulfonate	72	0.167	0.159	0.161	0.143	0.108	0.112
	125	0.095	0.218	0.160	0.152	0.154	0.158
	170	0.103	0.190	0.326	0.166	0.192	0.179
Internal olefin sulfonate	72	0.148	0.116	0.105	0.081	0.079	0.067
	125	0.072	0.128	0.161	0.175	0.166	0.100
	170	0.060	0.197	0.148	0.135	0.142	0.149
Branched alkyl toluene sulfonate	72	0.008	0.075	0.154	ppt*	ppt	ppt
	125	0.001	0.014	0.054	0.054	0.080	ppt
	170	0.001	0.009	0.009	0.022	0.036	0.103
Linear alkyl toluene sulfonate	72	0.105	0.281	0.256	ppt	ppt	ppt
	125	0.019	0.284	0.243	0.169	ppt	ppt
	170	0.014	0.184	0.153	0.126	0.045	ppt
Linear alkyl aryl sulfonate	72	0.008	0.040	0.104	0.008	0.002	ppt
	125	0.105	0.006	0.054	0.036	0.024	0.004
	170	0.046	0.003	0.002	0.048	0.025	0.005
Linear alkyl aryl sulfonate	72	0.002	0.303	0.416	0.464	ppt	ppt
	125	0.014	0.188	0.350	0.409	0.376	0.576
	170	0.046	0.003	0.002	0.048	0.025	0.005
Branched alkyl aryl sulfonate	72	0.007	0.003	0.001	ppt	ppt	ppt
	125	0.001	0.012	0.009	ppt	ppt	ppt
	170	0.001	0.033	0.018	ppt	ppt	ppt

*ppt, precipitated.

gum was added to the solution. The effect of the addition of sodium chloride to the hydroxyethyl cellulose solutions was similar to that of the xanthan gum solutions.

Solution Long-Term Stability

NaOH, Na₂CO₃, and Na₃PO₄ were mixed with a linear alkyl aryl sulfonate, a branched alkyl aryl sulfonate, and an alpha olefin sulfonate in 500, 1,000, and 1,500 mg/L polyacrylamide solutions. The solutions were aged at 72, 92, 132, and 180 °F for 50 d. The alkaline solutions and the alkaline

plus surfactant solutions were stable. The addition of polyacrylamide polymer to the linear and branched alkyl aryl sulfonates plus alkali solutions resulted in solution instability at the higher polymer concentrations and at higher surfactant concentrations. Table 4 shows the data for Na₂CO₃ plus a branched alkyl aryl sulfonate solution.

A linear alkyl aryl sulfonate demonstrated the same relationship between surfactant and polyacrylamide for solutions stability. An alpha olefin sulfonate demonstrated no solution instability at any polymer or surfactant concentration.

TABLE 3
Apparent Viscosity (cP) of 800 mg/L of Polyacrylamide Solution with Na₂CO₃ and a Linear Alkyl Aryl Sulfonate Added at 72 °F

Alkali	Surfactant	Sodium chloride concentration, mg/L					
		1,000	5,000	10,000	15,000	20,000	30,000
None	None	26.2	11.4	8.2	6.9	6.4	5.6
2% Na ₂ CO ₃	None	5.4	6.1	6.0	5.6	5.5	5.4
2% Na ₂ CO ₃	0.1% LXS 420	6.1	6.1	6.1	5.9	5.6	ppt
2% Na ₂ CO ₃	0.2% LXS 420	6.1	6.1	6.1	6.1	ppt*	ppt
2% Na ₂ CO ₃	0.5% LXS 420	6.6	6.4	6.4	6.8	ppt	ppt
None	0.1% LXS 420	26.6	11.6	8.4	7.0	6.5	6.0
None	0.2% LXS 420	27.1	12.3	8.7	7.2	6.8	6.6
None	0.5% LXS 420	28.4	13.9	9.4	7.8	7.9	8.0

*ppt, material precipitated from solution.

TABLE 4
Polyacrylamide Solution Stability* Data for Na₂CO₃ Plus a Branched Alkyl Aryl Sulfonate Solution

Alkali	Surfactant	Polyacrylamide	Temperature, °F			
			72	92	132	180
1% Na ₂ CO ₃	None	None	S	S	S	S
1% Na ₂ CO ₃	0.1% Petro B-100	None	S	S	S	S
1% Na ₂ CO ₃	0.2% Petro B-100	None	S	S	S	S
1% Na ₂ CO ₃	0.5% Petro B-100	None	S	S	S	S
1% Na ₂ CO ₃	None	500	S	S	S	S
1% Na ₂ CO ₃	0.1% Petro B-100	500	S	S	S	S
1% Na ₂ CO ₃	0.2% Petro B-100	500	S	S	S	I
1% Na ₂ CO ₃	0.5% Petro B-100	500	SI	SI	S	I
1% Na ₂ CO ₃	None	1000	S	S	S	S
1% Na ₂ CO ₃	0.1% Petro B-100	1000	S	S	S	S
1% Na ₂ CO ₃	0.2% Petro B-100	1000	S	S	S	I
1% Na ₂ CO ₃	0.5% Petro B-100	1000	S	S	S	I
1% Na ₂ CO ₃	None	1500	S	S	S	S
1% Na ₂ CO ₃	0.1% Petro B-100	1500	S	S	S	S
1% Na ₂ CO ₃	0.2% Petro B-100	1500	SI	I	I	I
1% Na ₂ CO ₃	0.5% Petro B-100	1500	I	I	I	I

*S, stable solution; SI, slightly instable solution; and I, instable solution.

Future Work

Future studies will investigate the effect of increasing cation as well as salinity with cation on the IFT, apparent viscosity, and CMC. Rock-fluid interactions and the effect of chemical composition and rock type will be investigated.

References

1. L. W. Holm, Propane-Gas-Water Miscible Floods in Watered-Out Areas of the Adena Field, Colorado, *J. Pet. Technol.*, 1264-1270 (October 1972).
2. K. S. Sorbie, *Polymer-Improved Oil Recovery*, pp. 45-48, Blackie, Glasgow and London, CRC Press Inc., Boca Raton, Florida, 1991.

RESPONSIVE COPOLYMERS FOR ENHANCED PETROLEUM RECOVERY

Contract No. DE-AC22-92BC14882

University of Southern Mississippi
Hattiesburg, Miss.

Contract Date: Sept. 22, 1992
Anticipated Completion: Sept. 21, 1995
Government Award: \$273,400
(Current year)

Principal Investigators:
Charles McCormick
Roger Hester

Project Manager:
Jerry Casteel
Bartlesville Project Office

Reporting Period: July 1-Sept. 30, 1993

Objective

The overall objective of this research is the development of advanced water-soluble copolymers that rely on reversible microheterogeneous associations for mobility control and reservoir conformance for use in enhanced oil recovery.

Summary of Technical Progress

Advanced Copolymer Synthesis

AM/AMBA/BPAM Terpolymers

Synthetic efforts have included synthesis of hydrophobically modified terpolymers based on acrylamide (AM) and one of three anionic monomers: acrylic acid (AA), 2-acrylamido-2-methyl-propanesulfonic acid (AMPS), or 3-acrylamido-3-methylbutanoic acid (AMBA). The hydrophobic monomer used was *n*-(4-butyl)phenylacrylamide (BPAM); it possesses both the hydrophobic character desired and a chromophore which allows the use of ultraviolet (UV) spectroscopy for accurate determination of hydrophobic monomer content in the terpolymers.

Polymer synthesis. Monomers used in polymer synthesis are depicted in Fig. 1. The micellar polymerization of Turner et al.¹ was used for all polymerizations. This aqueous polymerization method uses a surfactant, sodium dodecyl sulfate (SDS), to solubilize the hydrophobic BPAM monomer. A total monomer concentration of 0.44M was used with monomer feeds of 0.5 mol % BPAM and 5 or 25 mol % AA, AMBA, or AMPS; the remaining balance of the feed was acrylamide. The acidic monomers were neutralized just before polymerization. Potassium persulfate, $K_2S_2O_8$, was used as a free radical initiator [(monomer)/($K_2S_2O_8$) = 3000]. Polymerizations were conducted at 50 °C for 4 to 6 h, followed by precipitation into acetone. The terpolymers were dried under

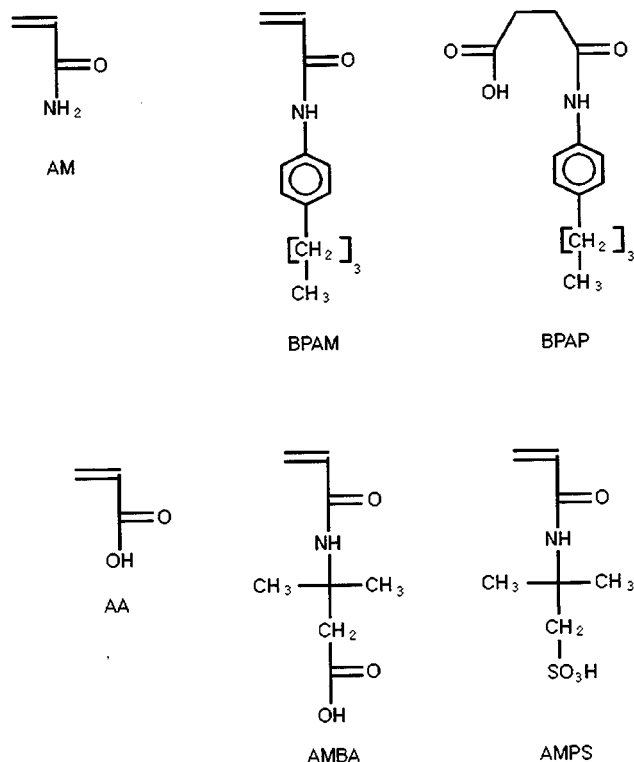


Fig. 1 Monomers used in polymer synthesis and the BPAM model compound.

vacuum, crushed, and redissolved in water, followed by dialysis against deionized water to remove residual surfactant and monomers. The terpolymers were then lyophilized to a constant weight.

NaAMPS/AMPTAC Copolymers and AM/NaAMPS/AMPTAC Terpolymers

Efforts have centered on the synthesis of ionically modified polymers that possess both anionic and cationic functionalities pendant from the polymer backbone. Prior research in the laboratories has demonstrated that solution behavior of polymers containing both anionic and cationic functionalities is strongly dependent on the ratio of the anionic to cationic charged groups.²⁻⁴ This behavior allows selective synthesis of polymers operative over a wide range of conditions. This section describes the synthesis and solution behavior of copolymers of sodium 2-(acrylamido)-2-methyl-propanesulfonic acid (NaAMPS) and [2-(acrylamido)-2-methylpropyl]trimethylammonium chloride (AMPTAC), the ATAS series, as well as terpolymers of acrylamide (AM), NaAMPS, and AMPTAC, the ATASAM series. Monomers used in the ATAS and ATASAM polymer series are shown in Fig. 2.

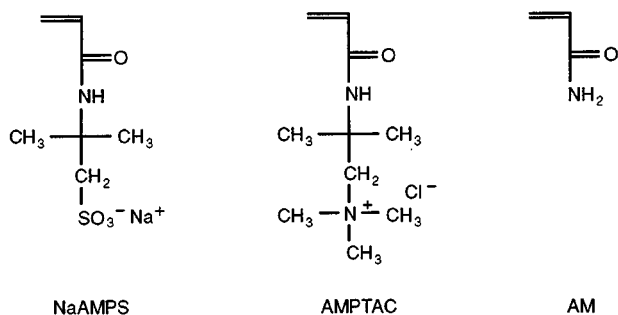


Fig. 2 Monomers used in ATAS and ATASAM polymer series.

Monomer and polymer synthesis. The AMPTAC monomer was prepared by reacting 2-acrylamido-2-methylpropanedimethylamine⁵ with methyl iodide to afford [2-(acrylamido)-2-methylpropyl]trimethylammonium iodide (AMPTAI). Dowex Cl⁻ resin was used to ion-exchange the iodide ion to obtain the desired AMPTAC. Acrylamide and AMPS, which was neutralized to NaAMPS before polymerization, were obtained from Aldrich. The copolymers and terpolymers were prepared by free radical polymerization in a 0.5M NaCl aqueous solution under nitrogen at 30 °C using 0.1 mol % potassium persulfate as the initiator. The feed ratio of NaAMPS/AMPTAC copolymers was varied from 90:10 to 30:70 mol %, whereas the feed ratio of AM/NaAMPS/AMPTAC terpolymers was varied from 99:0.5:0.5 to 70:15:15 mol %. Total monomer concentration was held constant at 0.45M for all polymerizations. All polymers were dialyzed against deionized water to remove residual monomers and salts and isolated by lyophilization.

AM/APS Copolymers

Photophysical studies were conducted on copolymers of acrylamide containing less than 0.5 mol % 2-(1-pyrenylsulfonamido) ethyl acrylamide to relate the aqueous solution behavior to the molecular structure. The copolymer prepared by a surfactant technique was shown to possess some inherent blockiness or short runs of the pyrenesulfonamide label in dilute solution. Intermolecular associations were observed above a critical concentration of polymer. Excimer emission intensity (I_E/I_M) values paralleled the rheological response as a function of concentration. The copolymer prepared by solution polymerization showed random incorporation of the pyrenesulfonamide comonomer and no intermolecular association tendency over the concentration range studied. Associative thickening behavior observed in the surfactant-polymerized copolymer is consistent with microphase organization of hydrophobic pyrenesulfonamide aggregates above a critical concentration.

Monomer and polymer synthesis. The synthesis of pyrenesulfonamide labeled copolymers **1** and **2** (Fig. 3) was described previously.⁶ Labeled copolymer **1** was prepared via a surfactant copolymerization technique and contains 0.25 mol % pyrenesulfonamide label. Copolymer **2** was synthesized via a solution copolymerization technique and contains 0.35 mol % pyrenesulfonamide label. Copolymer compositions were determined by UV spectroscopic analysis in water of the pyrenesulfonamide chromophore at 351 nm ($\epsilon = 24,120 \text{ m}^{-1}\text{cm}^{-1}$).

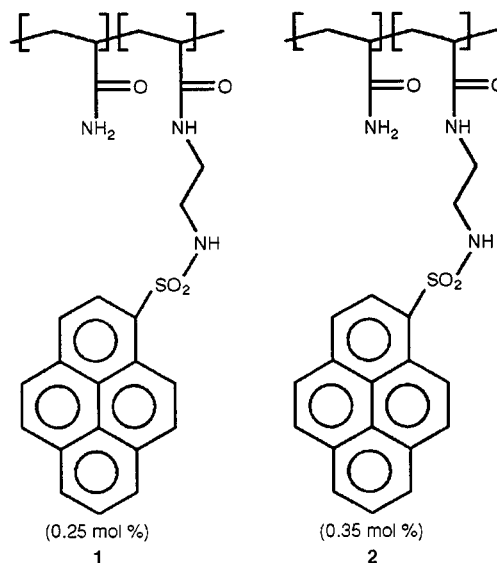


Fig. 3 Surfactant-polymerized (1) and solution-polymerized (2) AM/APS.

Characterization of Molecular Structure

AM/AMBA/BPAM Terpolymers

Polymerization conversions were estimated gravimetrically. Polymer compositions were determined by a

combination of UV spectroscopy and elemental analysis. The method of Valint et al.⁷ was used to determine the percentage of BPAM incorporation into the terpolymers. The BPAM model compound, BPAP (Fig. 1), was used to establish a calibration curve in water, which was used in subsequent determinations of BPAM incorporation. Incorporation of BPAM was consistent with the feed level for polymerizations using 5 mol % of the anionic monomers. However, incorporation of BPAM was retarded in the polymerizations in which greater amounts of the anionic monomers were used because of ionic interferences between the anionic SDS micelles and the growing macro-radicals. Elemental analysis was used to determine the content of the anionic monomers in the terpolymers as reported previously.⁸ Incorporation of the anionic monomers was slightly higher than the feed ratios in all cases.

Characterization of polymer associative behavior. Associative behavior of these terpolymers was determined by low shear viscometry in salt solutions. These studies were performed as a function of terpolymer concentration as well as of salt concentration. Three-dimensional plots best demonstrate the viscometric behavior of these systems. An example is shown in Fig. 4 for BPAM/NaAMB-5 containing approximately 0.5 mol % BPAM and 6 mol % NaAMB (the neutralized form of AMBA). As demonstrated by Fig. 4, the BPAM/NaAMB-5 polymer exhibits a rapid increase in viscosity as a function of terpolymer concentration as a result of interpolymer hydrophobic associations through the BPAM moieties. The onset of these associations occurs at very dilute concentration (below 0.1 g/dL), well below the critical overlap concentration of polyacrylamide. Also, these associations persist at NaCl concentrations approaching 0.5M, which indicates that

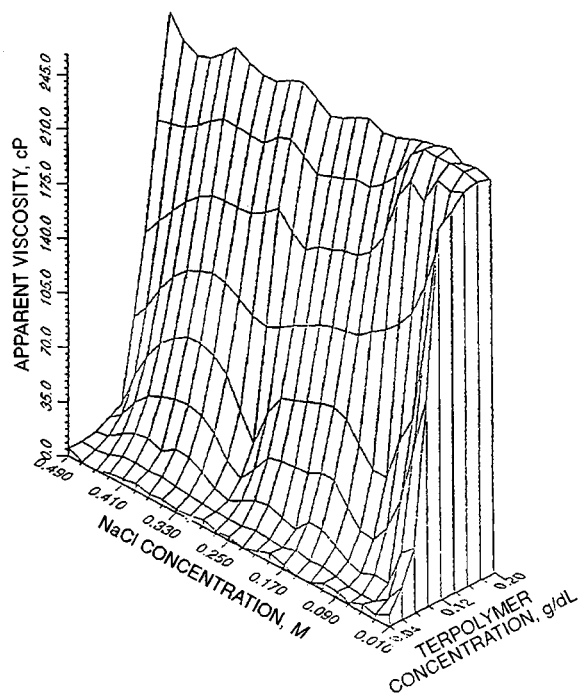


Fig. 4 Apparent viscosity as a function of polymer and NaCl concentration for the BPAM/NaAMB-5 terpolymers.

these hydrophobically modified polyelectrolytes show promise as salt-resistant thickening agents. More detailed studies of the viscometric properties of these terpolymer systems will be discussed in a forthcoming report.

NaAMPS/AMPTAC Copolymers and AM/NaAMPS/AMPTAC Terpolymers

Elemental analyses for carbon, hydrogen, nitrogen, and sulfur were conducted by M-H-W Laboratories of Phoenix, Ariz., on the low-conversion copolymer samples. Copolymer compositions were confirmed with the use of ¹³C NMR by integration of the amide carbonyl peaks. Molecular weight studies were performed on a Chromatix KMX-6 Low Angle Laser Light Scattering instrument. Refractive index increments were obtained with a Chromatix KMX-16 Laser Differential Refractometer. For quasielastic light scattering, a Langley-Ford Model LF1-64 channel digital correlator was used in conjunction with the KMX-6. All measurements were conducted at 25 °C in 1M NaCl. Polymer stock solutions were made by dissolving a specified amount of polymer in solvent and allowing it to age for 2 to 3 weeks before analyzing it with a Contraves LS-30 rheometer.

Polymer solution behavior. The effects of sodium chloride on the intrinsic viscosities of the ATAS copolymers and ATAS-0 and ATAS-100 were determined at a shear rate of 5.96 s⁻¹ at 25 °C (Fig. 5). ATAS-0, the anionic homopolymer of NaAMPS, shows the greatest decrease in viscosity as the NaCl concentration increases. As more AMPTAC is incorporated into the copolymer this effect becomes less pronounced with the transition from polyelectrolyte to polyampholyte character. ATAS-40 lies near the polyampholyte composition

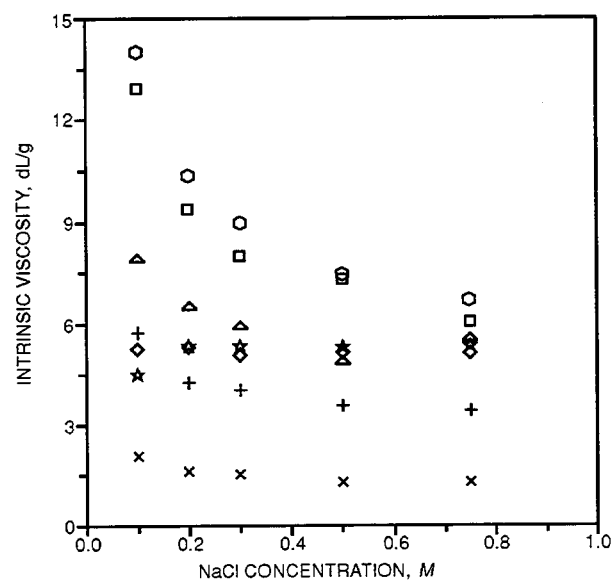


Fig. 5 Intrinsic viscosities for the ATAS copolymers as a function of NaCl concentration determined at a shear rate of 5.96 s⁻¹. ○, ATAS-0. □, ATAS-10. △, ATAS-25. ◇, ATAS-40. ☆, ATAS-50. +, ATAS-70. ×, ATAS-100.

region but still possesses a net charge. This leads to a small change in viscosity for ATAS-40 with increasing ionic strength. At equal molar concentrations of each monomer (ATAS-50), there is an increase in the viscosity. The copolymer ATAS-70 lies on the edge of the polyelectrolyte/polyampholyte transition and thus shows a small decrease in intrinsic viscosity. The effects of sodium chloride on the intrinsic viscosities of the ATASAM terpolymers are shown in Fig. 6. ATASAM 5-5 displays a dramatic increase in viscosity with the addition of a small amount of sodium chloride. This is indicative of the elimination of intramolecular interactions and the resulting coil expansion. ATASAM 10-10 and ATASAM 15-15 display complex behavior with increasing salt concentration. A small amount of electrolyte is required to solubilize both terpolymers. A slight increase in the ionic strength initially produces a decrease in intrinsic viscosity as a result of the elimination of intermolecular and molecular interactions with increasing ionic strength. As the ionic strength increases further, the intrinsic viscosities increase as intramolecular interactions are reduced and chain solvation is enhanced.

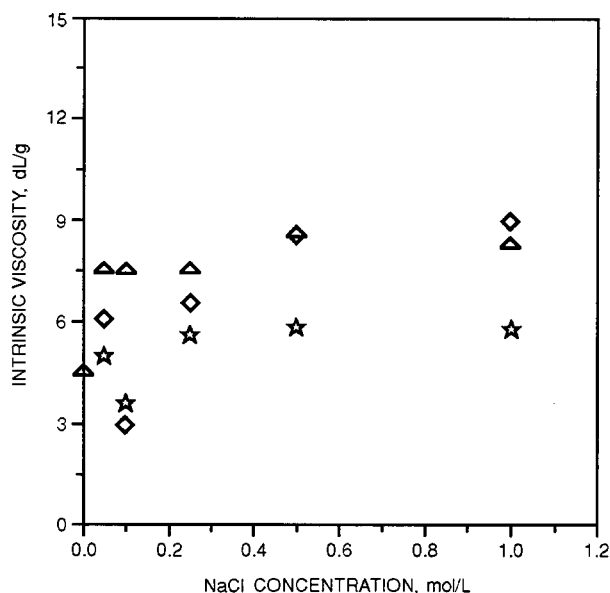


Fig. 6 Effects of sodium chloride on the intrinsic viscosities of ATASAM terpolymers determined at 25 °C at a shear rate of 5.96 s⁻¹. Δ , ATASAM 5-5. \diamond , ATASAM 10-10. \star , ATASAM 15-15.

AM/APS Copolymers

Viscosity measurements were performed on solutions ranging from 20 to 200 mg/dL in concentration. Measurements were recorded with a Contraves LS-30 rheometer at 25 °C and a shear rate of 6.0 s⁻¹.

Steady-state fluorescence emission studies were performed on a Spex Fluorolog-2 fluorescence spectrophotometer equipped with a DM3000F data system. All samples were run in the front-face mode to avoid inner filter effects. Slit widths

were varied from 0.5 to 2.5 nm, depending on sample concentration. Samples were deaerated by bubbling with nitrogen for 25 to 30 min. Particularly "foamy" samples were sparged by first bubbling with helium and then with argon.

Results and Discussion

In Fig. 7, I_E/I_M and the reduced viscosity of copolymer 1 are plotted as a function of concentration. Viscosity and I_E/I_M both increase dramatically above an initial concentration, C^* (ca. 0.1 g/dL), which provides strong evidence that intermolecular hydrophobic association of the labels is facilitated. It has been proposed that hydrophobic molecules can locate each other at distances greater than 100 Å as a result of the strong influence of water structuring.⁹ This is reflected on a molecular level by enhancement of I_E/I_M values. On a macroscopic scale, hydrophobic associations are indicated by a sharp increase in the viscosity profile at C^* .

Copolymerization dependencies of reduced viscosity and I_E/I_M are shown in Fig. 8 for copolymer 2 prepared in DMF/H₂O. The zero Huggins constant of the reduced viscosity vs. concentration curve suggests a compact polymer conformation that is independent of polymer concentration. The I_E/I_M values confirm this premise. The microstructure of this polymer—random label distribution—no doubt strongly influences the polymer conformation. In water, the hydrophobic labels are compelled to aggregate by the hydrophobic effect. The homogeneous polymerization medium results in a random microstructure. The random interspacing of the hydrophobe along the polymer backbone leads to compaction of the polymer coil as a result of intramolecular associations. Such a compact structure is reflected in the viscosity profile of 2.

Although 1 contains less pyrenesulfonamide label than 2, the I_E of 1 is enhanced relative to 2. A greater local concentration therefore exists for 1, which suggests that microstructural

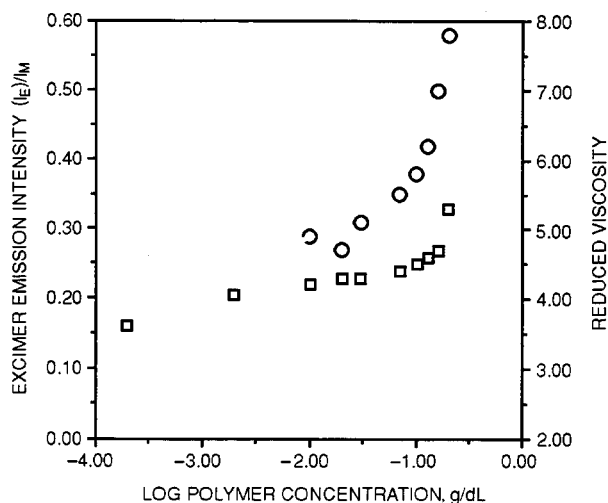


Fig. 7 Reduced viscosity and excimer emission intensity (I_E/I_M) as a function of the concentration for copolymer 1 prepared in deionized water. \circ , Reduced viscosity. \square , I_E/I_M .

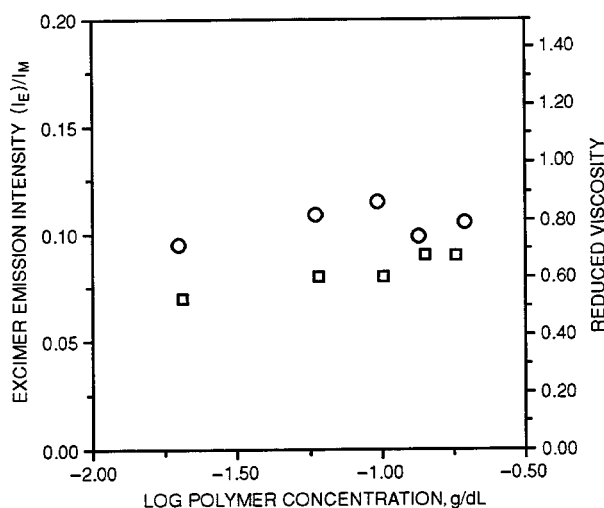


Fig. 8 Reduced viscosity and excimer emission intensity (I_E/I_M) as a function of the concentration for copolymer 2 prepared in deionized water. ○, Reduced viscosity. □, I_E/I_M .

differences exist between these polymers. It is probable that 1 has a more blocky microstructure because of partitioning of the pyrenesulfonamido monomer within the micelle during copolymerization, which allows some degree of blockiness even at low feed composition.

References

1. S. R. Turner, D. B. Siano, and J. Bock, U.S. Patent 4 426 485, 1984.
2. C. L. McCormick and C. B. Johnson, *Macromolecules*, 21: 686 (1988).
3. C. L. McCormick and C. B. Johnson, *Macromolecules*, 21: 694 (1988).
4. C. L. McCormick and C. B. Johnson, *Polym.*, 31: 1000 (1990).
5. C. L. McCormick and K. P. Blackmon, *Polym.*, 27: 1971 (1986).
6. S. A. Ezzell and C. L. McCormick, *Macromolecules*, 25: 1881 (1992).
7. P. L. Valint, Jr., J. Bock, and D. Schultz, *Polym. Mater. Sci. Eng. Prepr.*, 57: 482 (1987).
8. C. L. McCormick, J. C. Middleton, and D. F. Cummins, *Macromolecules*, 25: 1201 (1992).
9. J. Israelachvili and R. Pashley, *Nature*, 300: 341 (1982).

IMPROVED TECHNIQUES FOR FLUID DIVERSION IN OIL RECOVERY

Contract No. DE-AC22-92BC14880

New Mexico Institute of Mining and Technology
Petroleum Recovery Research Center
Socorro, N. Mex.

Contract Date: Sept. 17, 1992

Anticipated Completion: Sept. 30, 1995

Government Award: \$192,590

Principal Investigators:

Randall S. Seright

F. David Martin

Project Manager:

Jerry Casteel

Bartlesville Project Office

Reporting Period: July 1–Sept. 30, 1993

Objectives

This three-year project has two general objectives. The first objective is to compare the effectiveness of gels in fluid diversion with those of other types of processes. Several different types of fluid-diversion processes will be compared, including those using gels, foams, emulsions, and particulates. The ultimate goals of these comparisons are to (1) establish which of these processes are most effective in a given application and (2) determine whether aspects of one process can be combined with those of other processes to improve performance. Analyses will be performed to assess where the various diverting agents will be most effective (e.g., in fractured vs. unfractured wells, in deep vs. near-wellbore applications, in reservoirs with vs. without crossflow, or in injection wells vs. production wells). Experiments will be performed to verify which materials are the most effective in entering and blocking high-permeability zones. Another objective of the project is to identify the mechanisms by which materials (particularly gels) selectively reduce permeability to water more than to oil. In addition to establishing why this occurs, this research will attempt to identify materials and conditions that maximize this phenomenon.

Summary of Technical Progress

For the investigation of the performance of gels and gelants in fractured systems, several experiments were conducted with fractured Berea sandstone cores. The nominal permeability of the rock matrix (k_m) for most of these cores was 650 mD (see the second column of Table 1). However, one core (Core 6) had a brine permeability of 66 mD. All these

TABLE 1

Core and Fracture Permeabilities*

Core	Normal k_m , darcys	k_{av} , darcys	$k_f w_f$, darcy-cm	Relative flow capacity, $k_f w_f h_f / A k_m$	Fracture outlet sealed?
3	0.65	31	84	46.5	No
4	0.65	7.4	18.8	10.4	Yes
5	0.65	18.4	49.7	27.3	No
6	0.066	17.0	47.2	256	No

* k_m , rock matrix; k_{av} , average brine permeabilities; $k_f w_f$, calculated fracture conductivities; and $k_f w_f h_f / A k_m$, ratio of flow capacity of fracture to that of the rock matrix.

experiments were performed at 41 °C. The cylindrical cores were 14 cm long with a cross-sectional area of 10 cm². These cores were fractured lengthwise with a core splitter. The two halves of the core were repositioned as shown in Fig 1 and cast in epoxy. Two internal pressure taps were drilled 2 cm from the inlet sand face. One tap was located 90° from the fracture in order to measure pressure in the rock matrix, whereas the other tap was drilled to measure pressure in the fracture. During corefloods the fracture was always oriented vertically.

After the core was cast in epoxy and saturated with brine, the permeability to brine was determined. The third column in Table 1 lists average brine permeabilities (k_{av}) for several fractured cores. These permeabilities average the effects of flow through the fracture and the rock matrix. When brine is the only mobile fluid, the conductivity of the fracture can be estimated by using the Darcy equation for flow in parallel. In particular, the total flow rate is the sum of the flow rate through the rock matrix and the flow rate through the fracture. The fourth column in Table 1 lists calculated fracture conductivities ($k_f w_f$). If the fracture width is about 0.01 cm, then the permeabilities for these fractures range from 1880 to 8400 D. The flow capacity of the fracture relative to that of the rock matrix is given by the ratio $k_f w_f h_f / A k_m$. This ratio is listed in the fifth column of Table 1. The flow capacity of the fracture ranged from 10 to 256 times as great as the flow capacity of the rock matrix. For one core listed in Table 1 (Core 4), the outlet end of the fracture was blocked with epoxy. This block was placed to prevent gel from washing out of the fracture.

During the experiments, water-tracer studies were routinely performed before and after gel placement. These tracer

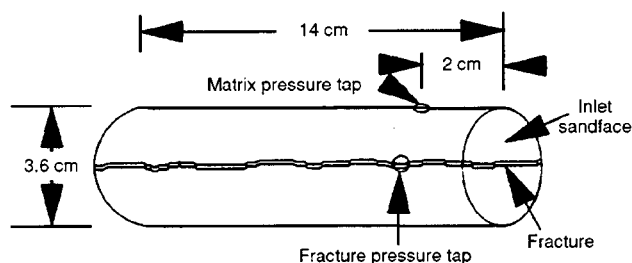


Fig. 1 Schematic of a fractured core.

studies were used to characterize pore volumes and dispersivities of the cores. These studies involved the injection of a brine bank that contained potassium iodide as a tracer. The tracer concentration in the effluent was monitored spectrophotometrically at a wavelength of 230 nm. In Fig. 2 the solid curve illustrates the results from a tracer study for an unfractured Berea core that was saturated with brine. Tracer curves for unfractured cores could be described very well with the error-function solution. Dispersivities of unfractured Berea sandstone cores were typically 0.1 cm, and the effluent tracer concentration reached 50% of the injected concentration after the injection of 1 pore volume (PV) of tracer solution. The dashed curve in Fig. 2 shows the tracer results from a fractured Berea core. For this fractured core, the first tracer was detected in the effluent after the injection of 0.04 PV of tracer solution. In contrast, for the unfractured core, the first tracer was detected after the injection of 0.8 PV of tracer solution.

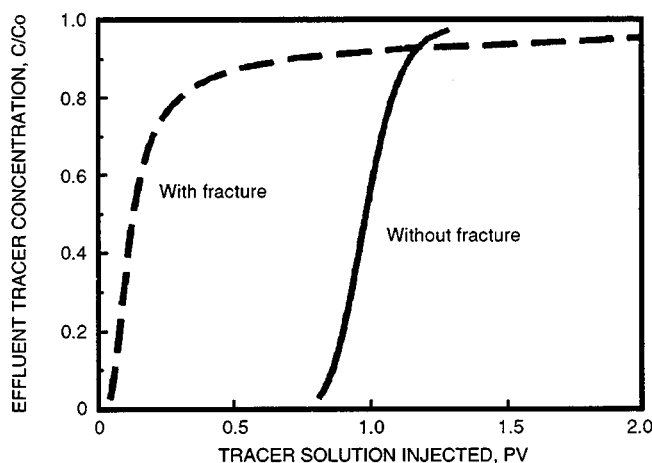


Fig. 2 Tracer results in fractured vs. unfractured Berea sandstone cores. Cores are saturated with water only.

Injection of Cr³⁺ (Acetate)-HPAM Gelants

A Cr³⁺ (acetate)-HPAM gel was used to conduct a set of experiments in fractured cores. This gelant contained 5000-ppm HPAM (Allied Colloids Alcoflood 935®), 417-ppm chromium triacetate, and 1% NaCl at pH 6. The gelation time for this gelant was about 5 h. One experiment was performed in a fractured core with an epoxy block at the outlet end of the fracture (Core 4 in Table 1), whereas another experiment used a fractured core with no epoxy block (Core 3 in Table 1). In both experiments, 0.3 PV of gelant was injected at an injection rate of 200 mL/h. After the gelant was injected, the cores were shut in for 6 d.

For Core 3 (with the open fracture), tracer studies (Fig. 3) indicated that the gel treatment did not improve sweep efficiency. In contrast, for Core 4 (with the fracture outlet sealed), tracer studies (Fig. 4) revealed that the gel significantly delayed tracer breakthrough in the core, which indicated that the gel treatment significantly increased sweep efficiency.

Apparently, less gel washed out from the core with the sealed fracture. However, the sweep efficiency was still much less than that expected for an unfractured core (Fig 2).

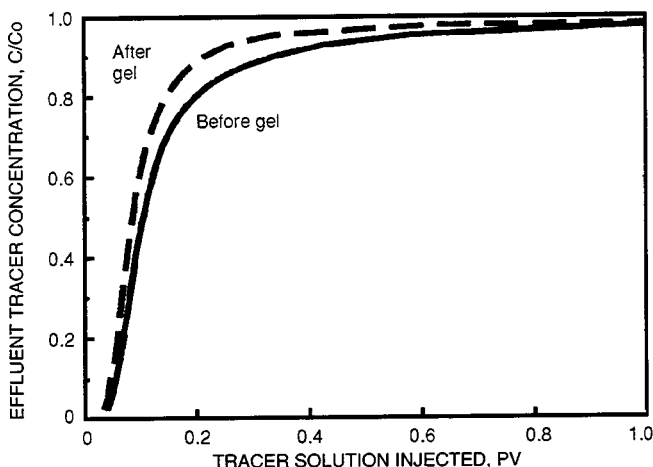


Fig. 3 Tracer results before and after placement of gelant in fractured Core 3 with fracture outlet open.

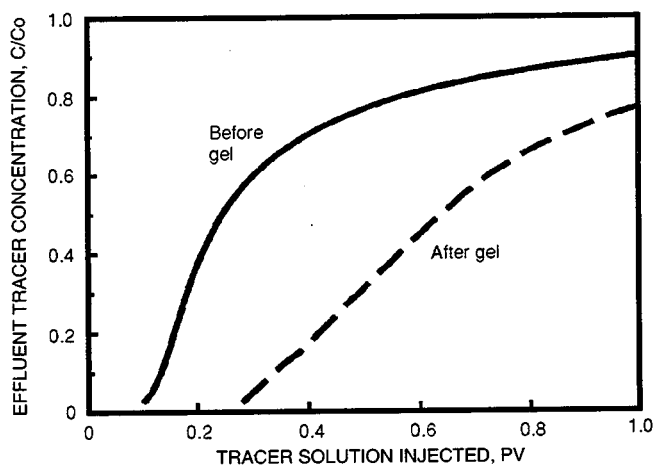


Fig. 4 Tracer results before and after placement of gelant in fractured Core 4 with fracture outlet sealed.

Injection of Cr^{3+} (Acetate)-HPAM Gels

Two experiments were performed in which gels (rather than gelants) were injected into fractured cores. Properties of these cores are given in Table 1. The fracture outlets for these cores were not sealed.

Again, the gel contained 5000-ppm HPAM (Allied Colloids Alcoflood 935), 417-ppm chromium triacetate, and 1% NaCl at pH 6. For gelation to occur, a 24-h delay occurred between gelant preparation and gel injection into the fractured cores. For Cores 5 and 6, between 0.4 and 0.6 PV of gel (12 to 16 mL) was injected. Of course, this volume was more than enough to fill the fractures. After the gel was injected, the cores were shut in for 4 d. The inlet and outlet end caps were then removed from the core holder, and gel was scraped from

flow lines and the inlet and outlet rock faces. The end caps were then repositioned, and brine injection commenced.

Figures 5 and 6 show tracer results before and after gel placement for Cores 5 and 6, respectively. Both figures indicate that the gel has substantially improved sweep efficiency. Particularly in Fig. 6, the post-gel tracer curve suggests that the fracture is almost completely healed. For this curve, the first tracer was detected in the effluent at 0.73 PV, the 50% concentration level was reached at 0.96 PV, and the dispersivity associated with the tracer curve was 0.2 cm. For comparison, in an unfractured core with no gel, the first tracer was detected in the effluent at 0.80 PV, the 50% concentration level was reached at 1.0 PV, and the dispersivity associated with the tracer curve was 0.1 cm.

For both Cores 5 and 6, the permeability reduction values were fairly constant during the injection of 35 PV of brine. Thus the gel did not appear to wash out easily. The gels provided permeability reduction values that averaged 30 and

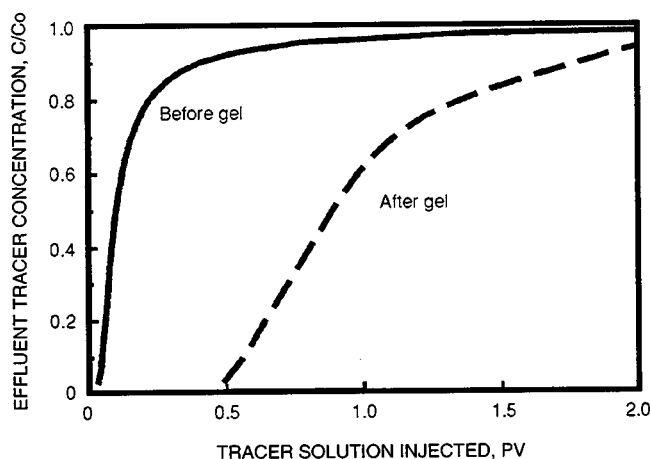


Fig. 5 Tracer results before and after placement of a gel in fractured Core 5 (650-mD rock matrix).

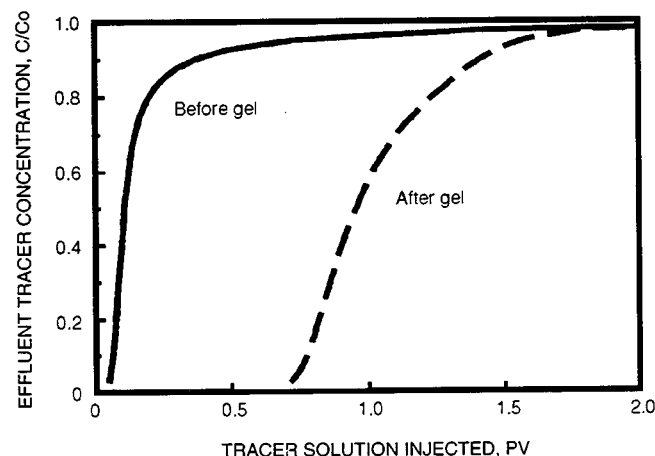


Fig. 6 Tracer results before and after placement of gel in fractured Core 6 (66-mD rock matrix).

180, respectively. Before the gels were injected, the flow capacities of the fracture relative to those of the rock matrix were 27.3 and 256 for Cores 5 and 6, respectively (Table 1). The similarity of these values to the corresponding permeability reduction values is consistent with the idea that the gels, in effect, healed the fractures.

The preceding results suggest that, in fractured systems, superior diversion may be obtained by injecting gels rather than gelants. Before this suggestion can be accepted, however, it must be determined whether gels can be injected into fractures without "screening out" or developing excessive pressure gradients. These tests will be described in a future report.

(2) a high-acid number (Long Beach). The Adena crude oil has transient interfacial tensions on the order of 0.1 mN/m, and the minimum in interfacial tension occurs at a short time of 100 s. The low-acid number of Adena oil does not prevent sufficient interfacial activity. Sufficient interfacial activity occurs at a high pH of 13. A second minimum was found to occur at higher times. This second minimum results from the formation of the middle phase.

Materials and Experiments

In this study, two crude oils containing natural organic acids were contacted with an alkaline pH aqueous solution. One crude oil used in this investigation is a Long Beach crude oil, obtained from THUMS Long Beach Company, with an acid number of 1.0 determined from ASTM procedure D-664 and an API gravity of 24.9. It was centrifuged at 40,000 G's for 30 min to remove water and clays. The viscosity of the crude oil after centrifuging was 52 cP at 25 °C and the interfacial tension (IFT) against deionized water was 24.5 mN/m. The other crude oil (Adena) used was obtained from SURTEK from the Adena field located in Morgan County, Colo. The oil is a light oil with an API gravity of 41.95, a viscosity of 3.75 cP at 25 °C, and an acid number less than 0.002. The IFT against deionized water is 39 mN/m.

The alkaline solutions are a mixture of sodium hydroxide, sodium bicarbonate, and sodium chloride. All alkalis were obtained from Fisher Scientific Company.

A preformed surfactant Petrostep B-105 (55% active) was added to the alkaline solution. The surfactant was obtained from Stepan Chemical Company, and the surfactant solutions were made on a 100% basis.

The spinning-drop technique was employed to measure transient (non-equilibrated) IFT. The volumetric ratio of water to oil in the spinning-drop tensiometer is about 140. The pH was measured with an Orion microprocessor analyzer/901 with a Ross combination electrode designed for low sodium error. All experiments were performed at 25 °C.

Throughout this study, the solutions were made by diluting an equimolar ratio of sodium bicarbonate/NaOH (referred to as 20/20) with either the same molarity of sodium bicarbonate plus NaCl to keep the total sodium constant or the same molarity of NaOH plus enough NaCl to keep the total sodium constant. By changing the ratio of sodium bicarbonate/NaOH, the pH is changed. Lower pH is obtained by adding the sodium bicarbonate plus NaCl solution to the 20/20 mixture, or a higher pH is obtained by adding the NaOH plus NaCl solution to the 20/20 mixture. It should be noted that 343 mol/m³ total sodium is about 2.0 wt % sodium bicarbonate/NaOH mixture.

Effect of Different Oils

Shown in Fig. 1 is the minimum in transient IFT as a function of pH for both the Adena and Long Beach crude oils. The Long Beach crude oil has a minimum at a typical pH of 10.7, which is about the same as most acidic crude oils.

SURFACTANT-ENHANCED ALKALINE FLOODING FOR LIGHT OIL RECOVERY

Contract No. DE-AC22-92BC14883

**Illinois Institute of Technology
Chicago, Ill.**

**Contract Date: Sept. 21, 1992
Anticipated Completion: Sept. 20, 1995
Government Award: \$150,000
(Current year)**

**Principal Investigator:
Darsh T. Wasan**

**Project Manager:
Jerry Casteel
Bartlesville Project Office**

Reporting Period: July 1–Sept. 30, 1993

Objective

The overall objective of this project is to develop a very cost-effective method for formulating a successful surfactant-enhanced alkaline flood by appropriately choosing mixed alkalis that form inexpensive buffers to obtain the desired pH (between 8.5 and 12.0) for ultimate spontaneous emulsification and ultralow tension. In addition, the novel concept of pH gradient design to optimize floodwater conditions will be tested.

Summary of Technical Progress

The interfacial behavior of two different crude oils was compared this quarter: (1) a low-acid number (Adena) and

However, the Adena oil has a minimum at a pH of 13, which is considerably higher. This unusual behavior with the Adena oil likely results from saponification of esters, because the Adena oil does not have much organic acid. Future experiments are planned to determine the constituents responsible for producing this minimum in IFT.

Figure 2 shows the transient IFT as a function of time for both the Long Beach crude oil and the Adena crude oil. This figure shows that there is sufficient interfacial activity result-

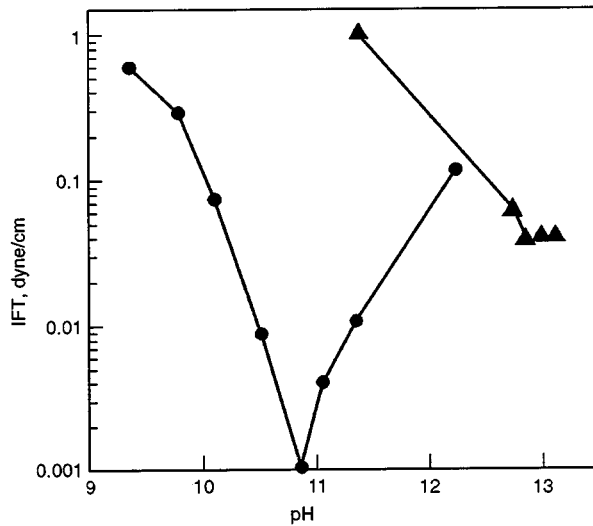


Fig. 1 Effect of pH on the transient interfacial tension minimum. $\text{NaHCO}_3/\text{NaOH}$, 0.343 M [Na], 0.1% PB105. ●, Long Beach crude oil. ▲, Adena crude oil.

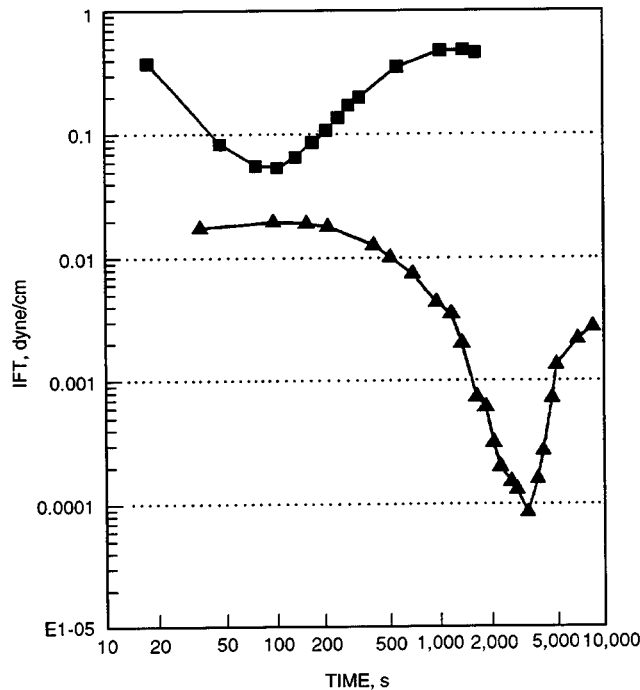


Fig. 2 Transient interfacial tension for Adena and Long Beach oil. 0.343 M Na + 0.1% Petrostep. ■, Adena oil. ▲, Long Beach oil.

ing from the interaction of the alkaline solution with the Adena oil to lower IFT. The minimum with the Adena oil occurs at a much shorter time than the Long Beach crude oil, and the IFT is almost three orders higher. Both the shorter time for minimum and the depth of the minimum for the Adena oil likely result from a low concentration of surface active material. Interfacial turbulence was not observed with the Adena oil, however it was observed with the Long Beach oil.

Effect of Sodium and Surfactant Concentration on Middle Phase Formation

Figure 3 shows the transient interfacial tension as a function of sodium concentration. This figure clearly shows that the 0.684 M sodium has two minimums. The first minimum results from monolayer behavior of the surfactants at the interface. The second minimum results from middle phase formation. The spontaneous formation of the middle phase was observed under the microscope. The formation of the middle phase is advantageous in the recovery process. Also, Fig. 3 shows that the extent of the middle phase is increased by an increase in sodium concentration.

Figure 4 shows that an increase in surfactant concentration causes more middle phase to form, which is similar to that for the effect of sodium concentration. The middle phase settles

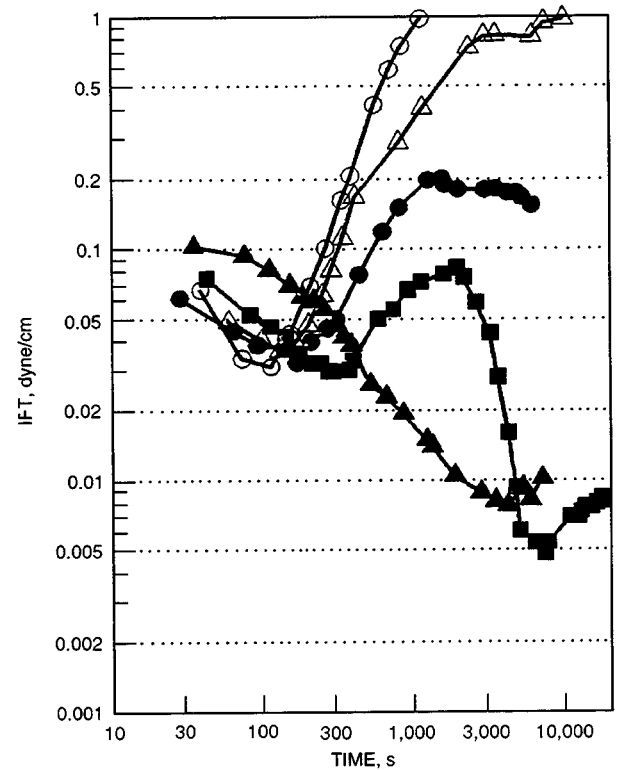


Fig. 3 Effect of sodium concentration on transient interfacial tension for Adena oil. pH, 12.9; constant rpm; T, 29 °C. ○, 0.171 M [Na] total. △, 0.343 M [Na] total. ●, 0.513 M [Na] total. ■, 0.684 M [Na] total. ▲, 1.0 M [Na] total.

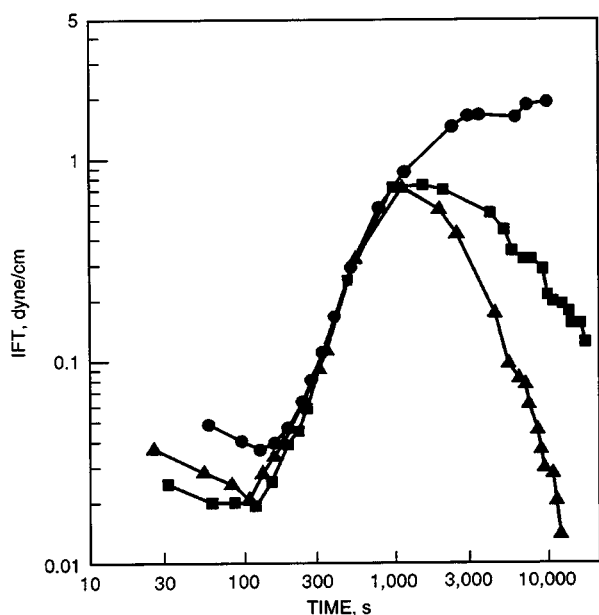


Fig. 4 Effect of added surfactant on transient interfacial tension for Adena oil. 0.343 M [Na]; Na HCO₃/NaOH; pH, 12.9. ●, 0.1% PB105. ■, 0.2% PB105. ▲, 0.5% PB105.

o the interfacial region, and the tension between the oil/middle phase and the alkali/middle phase is lower than that between the alkali/oil. As a result, the IFT goes lower as more middle phase accumulates.

Conclusions

Although the acid concentration of the Adena oil is very low, the oil exhibits sufficient interfacial activity when contacted both with and without added surfactant in the alkaline solution. The minimum in IFT of the Adena oil occurs at very short times, indicating that the interfacial reaction is completed quickly. The formation of the middle phase occurs with the Adena oil, resulting in a second minimum in transient IFT. With an increase in either sodium or surfactant concentration, the extent of middle phase formation increases.

DEVELOPMENT OF COST-EFFECTIVE SURFACTANT FLOODING TECHNOLOGY

Contract No. DE-AC22-92BC14885

University of Texas
Austin, Tex.

Contract Date: Sept. 30, 1992
Anticipated Completion: Sept. 29, 1995
Government Award: \$765,557

Principal Investigators:

Gary A. Pope
Kamy Sepehrnoori

Project Manager:

Jerry Casteel
Bartlesville Project Office

Reporting Period: July 1–Sept. 30, 1993

Objective

The objective of this research is to develop cost-effective surfactant flooding technology by using surfactant simulation studies to evaluate and optimize alternative design strategies and taking into account reservoir characteristics, process chemistry, and process design options such as horizontal wells. Task 1 is the development of an improved numerical method for the simulator so that a wider class of these difficult simulation problems can be solved accurately and affordably. Task 2 is the application of this simulator to the optimization of surfactant flooding to reduce its risk and cost.

Summary of Technical Progress

The tasks of reducing the cost and risk of surfactant flooding are closely related since any reduction in risk will directly improve the economics of a commercial field application. The importance of good reservoir characterization and the large impact of reservoir characteristics on surfactant flooding as well as on other tertiary oil recovery processes has been well established during the past twenty years. Improved means of assessing the risk and performance of surfactant flooding that take into account realistic reservoir characteristics are clearly needed. The most important of these reservoir characteristics is heterogeneity.

In the past, the traditional layered reservoir description has been used in simulations of surfactant flooding. Although the theoretical basis for using more flexible and realistic reservoir descriptions based upon geostatistical methods has been available now for several years, these methods have been applied to the simulation of other processes such as waterflooding.

Their application to surfactant flooding has not been attempted to date. This is unfortunate because surfactant flooding is generally more sensitive to reservoir characteristics than simpler processes, hence the need for cost and risk reduction is much greater. Clearly, the use of stochastic simulations lends itself to the quantitative assessment of uncertainty because multiple realizations of the same statistical description can be made and some idea of the probability distribution of outcomes computed. In addition, the stochastic approach can be used to explore the impact of reservoir characteristics better and then to improve the design of the surfactant flood so that it will be more robust and efficient so that predictions are more accurate. A few simulation results are illustrated in this report.

A comparison is made between a surfactant flood in a reservoir described with uniform permeability layers and one described stochastically with the same average permeability and standard deviation of permeability (or Dykstra–Parsons coefficient, V_{DP}). In both cases, a quarter five-spot well pattern is simulated using the chemical flooding simulator, UTCHEM. The well spacing is 20 acres and the thickness of the reservoir is 140 ft. The grid is $11 \times 11 \times 5$, so the gridblocks are 60 ft in the x and y directions and 28 ft in the z direction. The five vertical gridblocks for the layered description had permeabilities from top to bottom of 275 mD, 4.5 mD, 197 mD,

12.8 mD, and 104 mD and a uniform porosity of 0.136. The Dykstra–Parsons coefficient is 0.8 and the geometric mean permeability is 50 mD. This description is an idealization of an actual mid-Continent U.S. sandstone oil reservoir that is a potential candidate for surfactant flooding because it has already been waterflooded to nearly its economic limit and is otherwise subject to abandonment. The stochastic reservoir description was generated with a University of Texas program based upon the matrix decomposition method. A spherical variogram and a log normal permeability distribution with the same average and standard deviation as above and several different correlation lengths were used. The permeability distribution with correlation lengths (λ_x and λ_y) of 660 ft in the x and y directions and 28 ft in the z direction is shown in Fig. 1.

First a waterflood was simulated until 98% watercut was reached, then 2.5 vol % surfactant injected for 0.25 pore volumes (PV). The surfactant slug contained 1000 ppm polymer and was followed by another 0.5 PV of polymer slug at the same concentration and finally by water for another 3.25 PV. Although the surfactant and polymer properties are extremely important and have been carefully selected as favorable but still realistically based upon the best of recent surfactant research, the research focus is on the stochastic simulation aspect instead of the process simulation aspect.

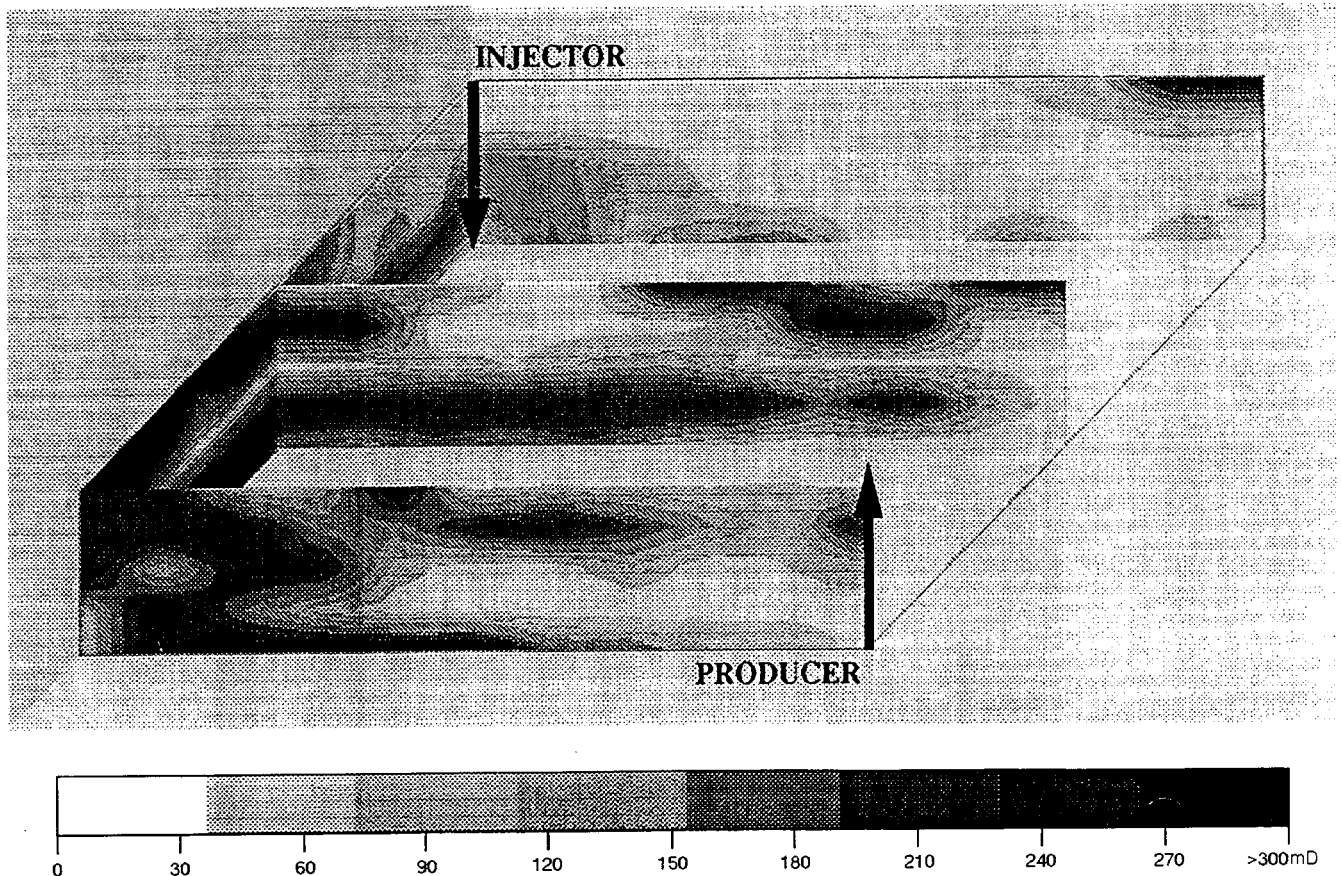


Fig. 1 Permeability distribution for reservoir with correlation lengths of 660 ft in horizontal plane.

The simulated chemical properties will be reported and discussed as well as varied in future reports.

Figure 2 shows the cumulative oil recovery as a fraction of the oil in place after the waterflood for the layered description and for four stochastic cases with correlation lengths ranging from 330 to 2640 ft in the x and y directions (the value in the vertical direction is kept fixed at 28 ft here). These results are represented as a function of time rather than PV to emphasize the impact of injectivity on this important geostatistical parameter. Both the injector and producer are pressure-constrained wells in this case, so the injection rate varies with time as a sensitive function of the reservoir description. This has a major impact on the project life and thus on the economics of the project. As the ratio of the correlation length in the x and y directions to the length in the z direction increases, the reservoir looks more and more like a layered reservoir, and this is clearly reflected in the oil recovery curves of Fig. 2. In this case, the results of the layered reservoir are more optimistic than those of the stochastic reservoirs, which are more like actual reservoirs. This shows that there is indeed an incentive to consider reservoir descriptions other than the layered description traditionally used to simulate surfactant flooding.

Figure 3 shows multiple realizations of the results for the stochastic description with correlation lengths of 660 ft in both the x and y directions. These unconditioned simulations show the very large variation in oil recovery and timing that can result merely by the use of different random assignments of permeability to the reservoir gridblocks from a permeability distribution with the same statistical parameters. Conditioning these reservoir distributions with reservoir data, such as core data, well logs, or tracers, can reduce this variation to an acceptable level. Comparisons with conditioned simulations will be shown in future reports.

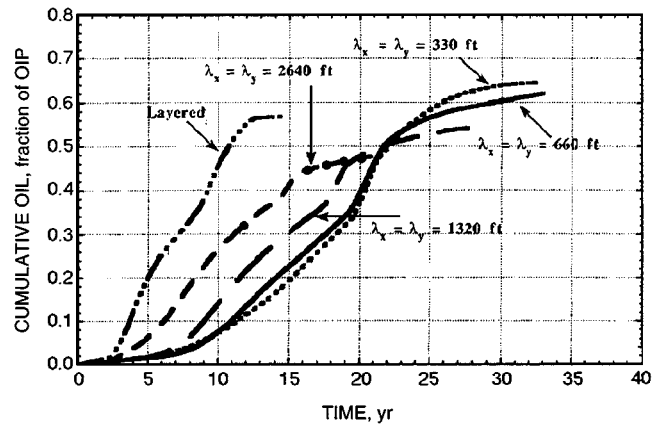


Fig. 2 Comparison of oil recovery for layered and stochastic reservoir descriptions. Realization #1. V_{DP} , 0.8.

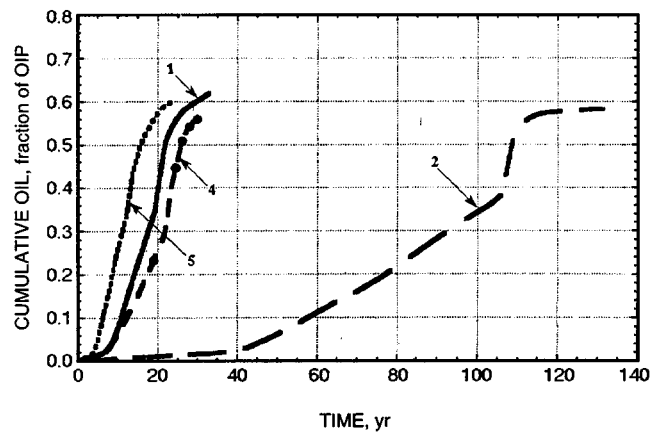


Fig. 3 Oil recovery for multiple realizations 1, 2, 4, and 5 of the same permeability field. V_{DP} , 0.8. λ_x , 660 ft. λ_y , 660 ft. λ_z , 28 ft.

IMPROVING RESERVOIR CONFORMANCE USING GELLED POLYMER SYSTEMS

Contract No. DE-AC22-92BC14881

University of Kansas
Center for Research
Lawrence, Kans.

Contract Date: Sept. 25, 1992
Anticipated Completion: Sept. 24, 1995
Government Award: \$707,123

Principal Investigators:
Don. W. Green
G. Paul Willhite

Project Manager:
Jerry Casteel
Bartlesville Project Office

Reporting Period: July 1–Sept. 30, 1993

Objectives

The general objectives of this project are to (1) identify and develop gelled polymer systems that have potential to improve reservoir conformance of fluid displacement processes, (2) determine the performance of these systems in bulk and in porous media, and (3) develop methods to predict the capability of these systems to recover oil from petroleum reservoirs.

This work focuses on three types of gel systems—an aqueous polysaccharide (KUSP1) system that gels as a function of pH, the chromium (III)–polyacrylamide system, and the aluminum citrate–polyacrylamide system. Laboratory research is directed at the fundamental understanding of the physics and chemistry of the gelation process in bulk form and in porous media. This knowledge will be used to develop conceptual and mathematical models of the gelation process. Mathematical models will then be extended to predict the performance of gelled polymer treatments in oil reservoirs.

Summary of Technical Progress

Development and Selection of Gelled Polymer Systems

Selection of Organic Crosslinking System To be Investigated

A database of gelled polymer systems was constructed and three systems were identified as candidates to be studied in detail. Screening experiments indicated problems with the piperazine di-HCl–polyacrylamide system and the sodium aluminate–polyacrylamide system. Gelation was not observed in samples prepared at selected pH values and concentrations

of piperazine di-HCl and polyacrylamide. It is suspected that the piperazine di-HCl does not crosslink polyacrylamides as claimed in patent literature. Piperazine di-HCl was the only organic crosslinker that was identified as less hazardous than chromium. The sodium aluminate–polyacrylamide system is prepared at pH values of approximately 12 and gels upon reduction of pH below a value of 10. Screening experiments took the form of identifying and testing chemical agents (e.g., esters) that can reduce the pH of solutions from 12 to 10 over a period of several days. Mono-ethyl phthalate met this requirement but produced precipitates when added to the sodium aluminate–polyacrylamide system.

The third candidate, the aluminum citrate–polyacrylamide system, was selected to be investigated in detail. Aluminum citrate and polyacrylamide were rated less toxic than at least one of the components in all of the organic crosslinked systems. Another factor that influenced the selection of the aluminum citrate–polyacrylamide system was the renewed interest of the oil industry, which was due in part to the system's reputation as a low-toxicity system.

Physical and Chemical Characterization of Gel Systems

Chemical Reaction Kinetics

A study was conducted to determine chemical kinetics of the Cr(III)–polyacrylamide system. Rate data were obtained on the uptake reactions of Cr(III) monomers, dimers, and trimers with polyacrylamide. Oligomer uptake was determined by separating the unreacted Cr(III) by equilibrium dialysis, oxidizing the Cr(III) to Cr(VI), and measuring the Cr(VI) concentration by ultraviolet (UV) spectroscopy. Slopes of storage modulus–time data obtained from dynamic rheological measurements were used as a measure of the gelation rate.

Uptake rate and gelation rate increased with oligomer size, oligomer concentration, polymer concentration, and pH. The gelation reaction, as indicated by the value of storage modulus, generally tracked the Cr(III)-uptake data for the monomer and trimer species as shown in Figs. 1 and 2. This tracking

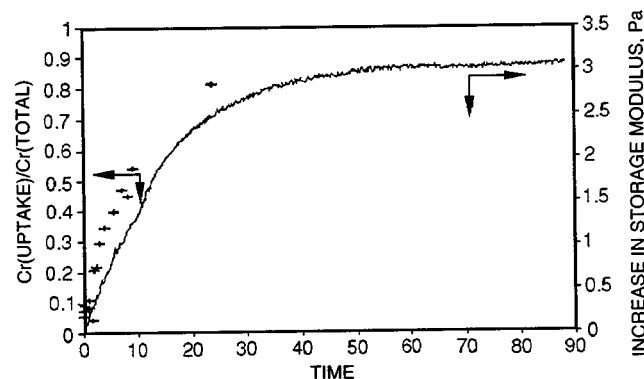


Fig. 1 Comparison of Cr(III)-uptake data and gelation data for the chromium monomer species. 11 ppm chromium; 15,000 ppm polyacrylamide; pH = 5.0.

suggests that the gelation or crosslinking reaction occurred a short but finite time after the chromium first reacted with the polymer (the uptake reaction). A kinetic model was developed that described very well the uptake data for the monomer but fit the dimer data less well and the trimer data poorly.

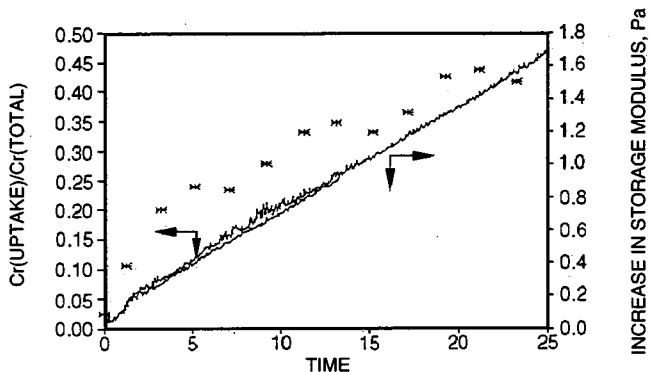


Fig. 2 Comparison of Cr(III)-uptake data and gelation data for the chromium dimer species. 23 ppm chromium; 14,500 ppm polyacrylamide; pH = 4.0.

Mathematical Modeling of Gel Systems

Development of Mathematical Model(s) of Laboratory In Situ Gelation

The kinetics of gelation of polymers is usually related to the pH of the polymer solution. The pH of polymer solutions, in turn, is affected by chemical interactions with the reservoir rock. The effects of sodium-hydrogen ion exchange in simple coreflood experiments with high-pH NaCl brine solutions were modeled. A mechanism proposed by Bunge and Radke¹ was used to describe the ion-exchange reaction on the surface of the rock. This mechanism was incorporated into a flow model by assuming local equilibrium between the fluid-phase concentrations and the adsorbed-phase concentrations.

Figures 3 and 4 show the simulated concentration profiles of the Na⁺ species and the pH as the injected solution advances along the length of the core. The trends shown by the results may be rationalized on the basis of the study of cation-exchange reactions.^{2,3}

Each profile shows the formation of two distinct fronts:

1. The first front travels at the interstitial velocity with no retardation. This front simply entails the displacement of the initial solution and is termed the salinity wave.
2. The second front moves at a velocity less than the interstitial velocity and involves a change in both the solid-phase composition and the fluid-phase concentrations. This front is termed the ion-exchange wave. The region before the ion-exchange wave corresponds to the injected fluid-phase composition and solid-phase concentrations in equilibrium with the injected concentrations.

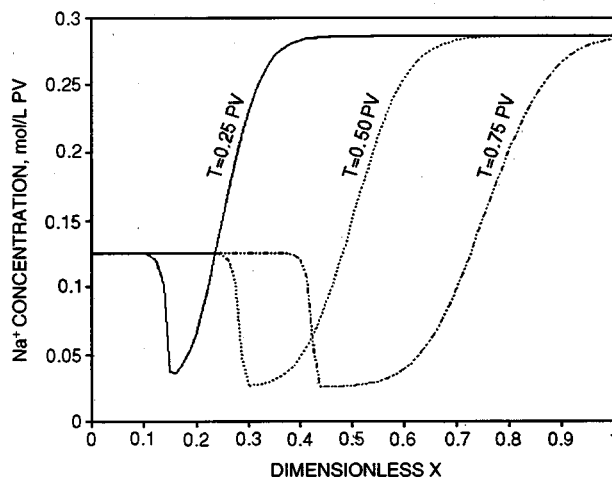


Fig. 3 Na⁺ concentration profiles along the length of the core as a function of pore volumes of injection. T, dimensionless time.

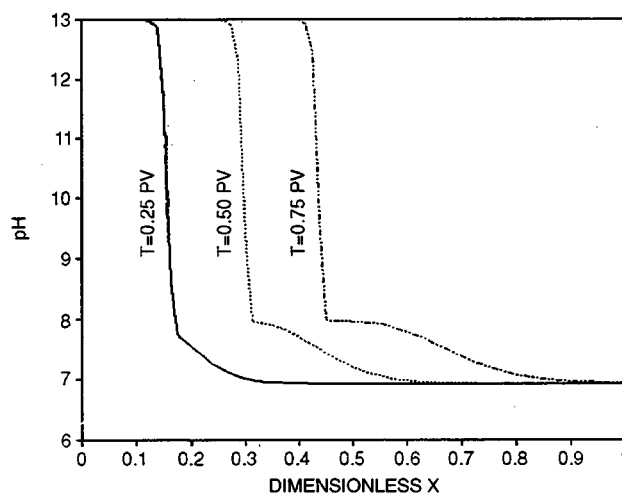


Fig. 4 pH profiles along the length of the core as a function of pore volumes of injection. T, dimensionless time.

The velocity and shape of the ion-exchange wave is a function of the sodium-hydrogen ion-exchange equilibrium and the dispersion in the core. The Langmuir-like nature of the ion-exchange equilibria produces fronts that continuously sharpen as they propagate through the core. Dispersion, however, tends to smother the sharp concentration gradients and opposes the sharpening character of the wave fronts. These competing phenomena balance each other and the resultant ion-exchange waves are indifferent with respect to sharpening behavior as they progress through the core.

Because the velocities of the salinity wave and the ion-exchange wave are different, an intermediate plateau in the concentration profiles is formed. This plateau consists of a modified fluid-phase composition in equilibrium with the initial solid-phase composition. Because the sodium-ion concentration in the intermediate region is less than its injected value, the model predicts an overall uptake of sodium ions from the injected solution.

References

1. A. L. Bunge and C. J. Radke, The Origin of Reversible Hydroxide Uptake on Reservoir Rock, *SPEJ, Soc. Pet. Eng. J.*, 25: 711-718 (October 1985).
2. G. A. Pope, L. W. Lake, and F. Helfferich, Cation Exchange in Chemical Flooding: Part 1—Basic Theory Without Dispersion, *SPEJ, Soc. Pet. Eng. J.*, 18: 418-434 (December 1978).
3. L. W. Lake and F. Helfferich, Cation Exchange in Chemical Flooding: Part 2—The Effect of Dispersion, Cation Exchange, Polymer/Surfactant Adsorption in Chemical Flood Environment, *SPEJ, Soc. Pet. Eng. J.*, 18: 435-444 (December 1978).

**SURFACTANT LOSS CONTROL
IN CHEMICAL FLOODING:
SPECTROSCOPIC AND CALORIMETRIC
STUDY OF ADSORPTION AND
PRECIPITATION ON RESERVOIR
MINERALS**

Contract No. DE-AC22-92BC14884

**Columbia University
New York, N.Y.**

**Contract Date: Sept. 30, 1992
Anticipated Completion: Sept. 29, 1995
Government Award: \$602,232**

**Principal Investigator:
P. Somasundaran**

**Project Manager:
Jerry Casteel
Bartlesville Project Office**

Reporting Period: July 1–Sept. 30, 1993

Objective

The objective of this contract is to elucidate the mechanisms underlying adsorption and surface precipitation of flooding surfactants on reservoir minerals. The effect of surfactant structure, surfactant combinations, and other inorganic and polymeric species will also be determined. Solids of relevant mineralogy and a multipronged approach consisting of microspectroscopy and nanospectroscopy, microcalorimetry, electrokinetics, surface tension, and wettability will be used to achieve the goals. The results of this study should help in controlling surfactant loss in chemical flooding and also in developing optimum structures and conditions for efficient chemical flooding processes.

Summary of Technical Progress

Adsorption/desorption of single surfactant and surfactant mixtures at the kaolinite–water and alumina–water interfaces were studied during this quarter.

The adsorption of sodium dodecyl sulfate (SDS) and octaethylene glycol mono-*n*-decyl ether (C₁₂EO₈) on kaolinite was found to be higher from their mixtures than as single components. This enhanced adsorption was attributed to hydrophobic chain–chain interactions. The effect of pH on the adsorption of single and surfactant mixtures on kaolinite was also elucidated.

Desorption of cationic tetradecyl trimethyl ammonium chloride (TTAC) studied at the alumina–water interface indicated that adsorption was reversible. Electrokinetic measurements supported this observation.

Adsorption of Surfactant Mixtures at Solid–Liquid Interfaces

Adsorption of surfactant mixtures at solid–liquid interfaces is of practical importance for many industrial operations because commercially available surfactants are invariably mixtures of many compounds. However, study of surfactant mixture adsorption at solid–liquid interfaces is very limited. During this reporting period, the adsorption of ionic–nonionic surfactant mixtures at the kaolinite–water interface was systematically studied.

Isotherms obtained for the adsorption of anionic SDS on kaolinite are shown in Fig. 1. The adsorption of SDS decreases as the pH is increased from 5 to 10. Both positive and negative sites coexist on the kaolinite surface and the number of positive sites will decrease with increasing pH. As a result it can be stated that the adsorption mechanism prevalent here is purely electrostatic. At pH 5, the saturation adsorption is $\approx 1.6 \times 10^{-6}$ mol/m²; when a cross-sectional area of 53 Å² for an SDS molecule is used, this translates into a surface coverage of roughly 56%, which suggests that roughly half the surface is covered by positive sites.

As in the case for the adsorption of SDS, C₁₂EO₈ adsorption on kaolinite decreases with an increase in pH. A hydrogen bonding mechanism has been proposed for the adsorption of ethylene oxide (EO) groups on oxide surfaces, and it can be expected that a similar effect predominates here. Reduced adsorption at higher pH values can be attributed to the deprotonation of the surface hydroxyl groups, which will result in a decrease in the number of hydrogen bonding sites available for C₁₂EO₈ adsorption. When a molecular cross-sectional area of 65 Å² for C₁₂EO₈ in the adsorbed state is used, the surface coverage at saturation can be estimated to be 12%.

Unlike alumina (which does not adsorb ethoxylated alcohols) and silica (which adsorbs ethoxylated alcohols but not SDS), kaolinite adsorbs both SDS and C₁₂EO₈ to about the same order of magnitude, suggesting that the kaolinite surface exhibits the characteristics of both alumina and silica with respect to the adsorption of these two surfactants.

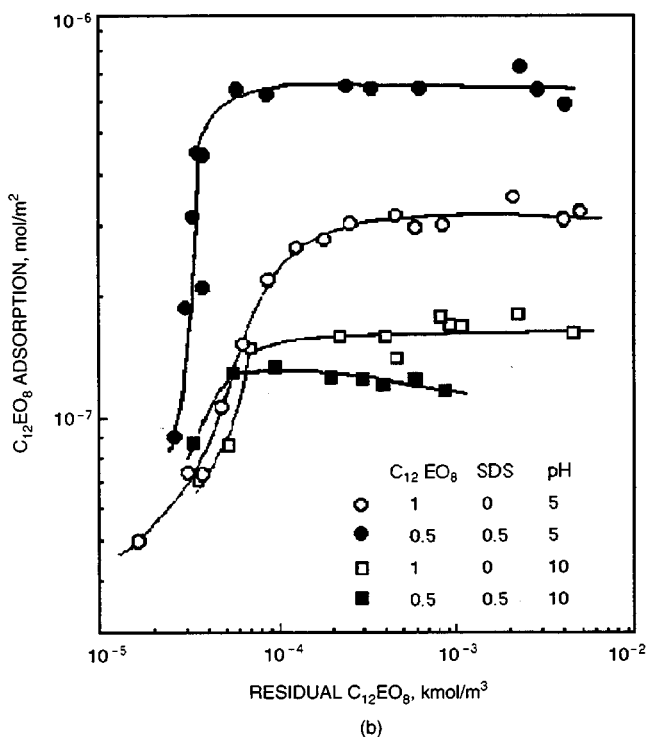
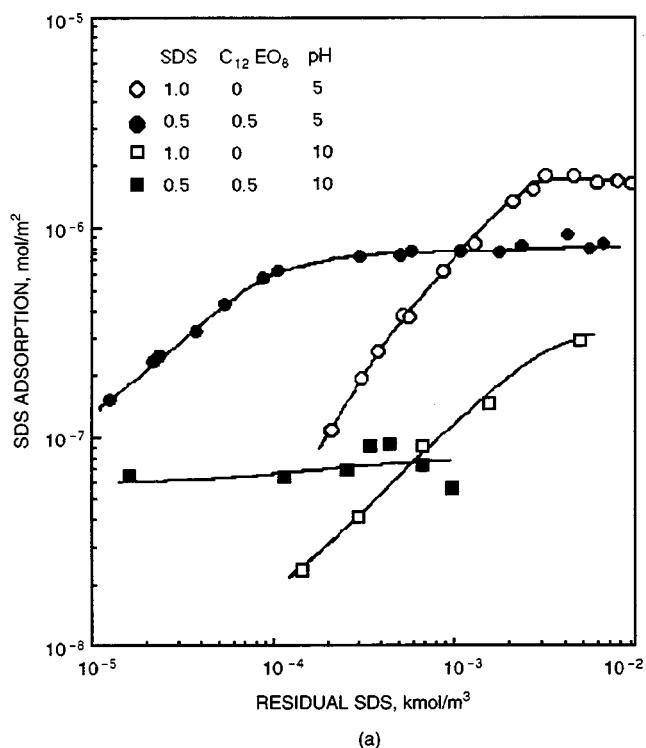


Fig. 1 Effect of pH on the adsorption of (a) sodium dodecyl sulfate (SDS) and (b) octaethylene glycol mono-*n*-decyl ether (C₁₂EO₈) from SDS-C₁₂EO₈ mixtures: 0.03 M NaCl, 25 °C.

Adsorption of SDS-C₁₂EO₈ mixtures on kaolinite was conducted at different pH values. The adsorption of SDS from the mixtures is shown in part a of Fig. 1, and that for C₁₂EO₈ is shown in part b of Fig. 1. At pH 5, the adsorption of the

nonionic C₁₂EO₈ is markedly enhanced by the presence of the anionic SDS, suggesting cooperative adsorption through hydrocarbon chain-chain interactions in the adsorbed layer. At pH 10, adsorption of the nonionic C₁₂EO₈ is suppressed by the presence of SDS, indicating competition between the anionic SDS and the nonionic C₁₂EO₈ for the limited number of common adsorption sites available.

The mechanisms of the effect of pH on surfactant mixture adsorption are schematically presented in Fig. 2. Although hydrocarbon chain-chain interaction between the adsorbed surfactant species is predominant at low pH, it is not likely to be as predominant at high pH because the adsorbed surfactant species cannot be close to each other as a result of the lack of adjacent adsorption sites for both surfactant species. Instead competition from the anionic SDS for limited common adsorption sites leads to suppression of C₁₂EO₈ adsorption.

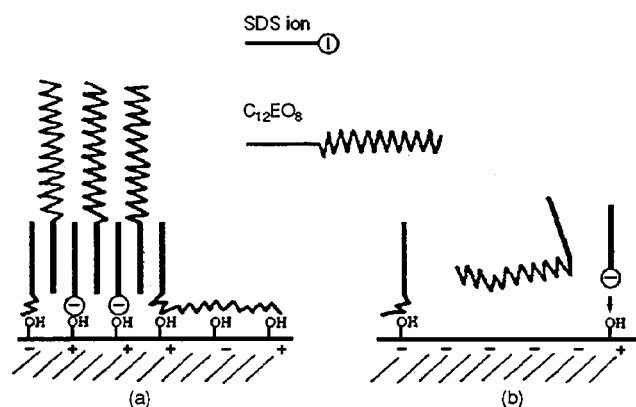


Fig. 2 Schematic presentation of pH effect on the adsorption of sodium dodecyl sulfate-octaethylene glycol mono-*n*-decyl ether (SDS-C₁₂EO₈) mixtures on kaolinite. (a) low pH, hydrocarbon chain-chain interaction results in cooperative adsorption; (b) high pH, competition for limited adsorption sites on kaolinite suppresses adsorption of C₁₂EO₈.

Fluorescence Probing of Mixed-Surfactant Adsorbed Layers

Fluorescence spectroscopy could not be conducted at the kaolinite-water interface because kaolinite quenched the fluorescence signal from pyrene. Therefore fluorescence probing of the adsorbed layer was performed for adsorption on alumina.

As mentioned in the previous quarterly reports, pyrene monomer fluorescence is sensitive to the medium in which pyrene resides. In hydrophobic environments, the ratio of the intensities of the third and first peaks (I_3/I_1) on a pyrene emission spectrum is higher than when pyrene is in a hydrophilic environment. The value for I_3/I_1 is 0.5–0.6 in water, 0.8–0.9 in surfactant micelles, and > 1 in nonpolar solvents. Since this ratio can be used to characterize the polarity of environments, it can be termed the polarity parameter.

The adsorption of mixtures of SDS and C₁₂EO₈ on alumina was studied. The I_3/I_1 values of pyrene obtained for the mixed

adsorbed layers are given in Fig. 3 along the isotherms. It is seen that the polarity parameter is nearly constant along each adsorption isotherm. This can be explained if the increased adsorption is realized by self-replication of the surfactant aggregates with the overall structure of the aggregate remaining unaltered. The I_3/I_1 values for surfactant micelles are given in Table 1. It is seen that the polarity parameter for SDS micelles is lower than that obtained for SDS aggregates at the alumina-water interface (Fig. 3). The aggregates at the solid-liquid interface are more compact than micelles so that water molecules are more effectively excluded from the hydrocarbon core.

The values obtained for the mixed micelle of SDS and $C_{12}EO_8$, however, are close to those obtained at the alumina-water interface, suggesting that the presence of the ethoxyl chains of the nonionic $C_{12}EO_8$ could be a key factor in determining the polarity in mixed surfactant aggregates.

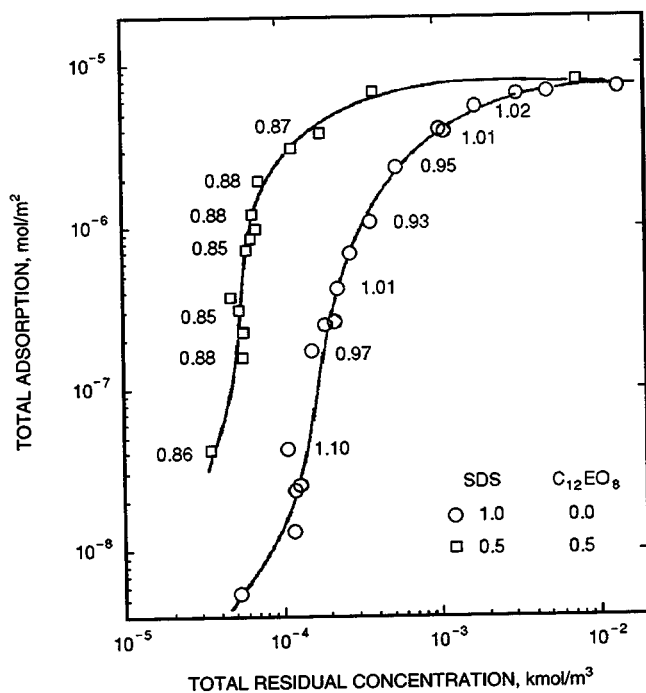


Fig. 3 Polarity parameter of pyrene (I_3/I_1) in the adsorbed layer of 1:1 SDS- $C_{12}EO_8$ mixtures on alumina.

TABLE 1

Polarity Parameter (I_3/I_1) Values for Surfactant Micelles in Aqueous Solution

Surfactant	Concentration studied, kmol/m ³	Critical micelle concentration, kmol/m ³	I_3/I_1
SDS	3×10^{-2}	1.5×10^{-3}	0.88
$C_{12}EO_8$	1.0×10^{-3}	1.0×10^{-4}	0.80
1:1 SDS- $C_{12}EO_8$	2.6×10^{-3}	1.1×10^{-4}	0.85

Subsequent studies will be directed toward discerning the evolution of the adsorbed layer in greater detail.

Effect of Hydrocarbon Chain Length of Nonionic Surfactant on Its Adsorption

Figure 4 shows the isotherms for the adsorption of the nonionic surfactants C_nEO_8 with different hydrocarbon chain length ($n=10, 12, 14, 16$) on kaolinite. The isotherms are consistently shifted to the lower concentration region as the hydrocarbon chain length is increased from C_{10} to C_{16} . It can be noticed that the plateau adsorption tends to increase slightly with increase in hydrocarbon chain length. When a parking area of 9.2 \AA^2 per $(-O-CH_2CH_2-)$ group is used on the basis of adsorption on silica, it can be found that the kaolinite surface is only partly covered by the nonionic surfactant (Table 2).

Subsequent studies will focus on the effect of nonionic surfactant's hydrocarbon chain length on adsorption on kaolinite from 1:1 SDS- C_nEO_8 mixtures.

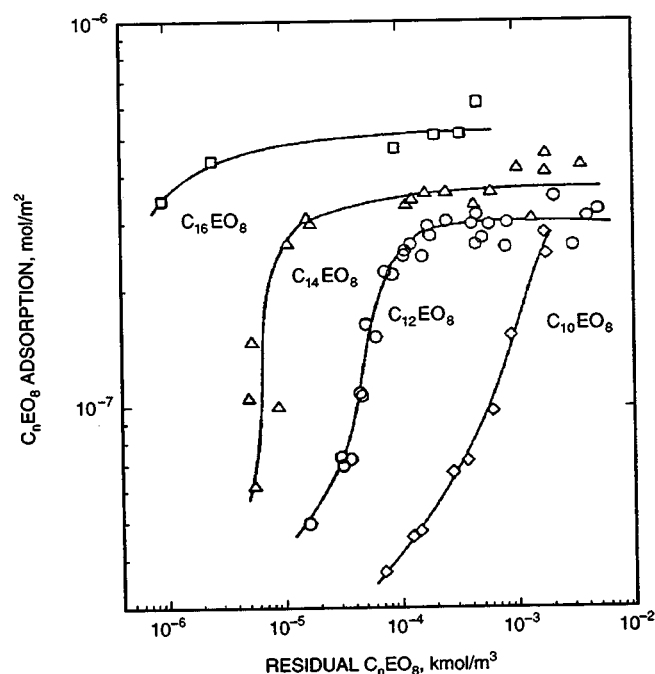


Fig. 4 Effect of hydrocarbon chain length (C_nEO_8) on the adsorption of nonionic surfactant on kaolinite. 0.03 M NaCl , 25°C , $\text{pH } 5$.

TABLE 2

Effect of Hydrocarbon Chain Length on Plateau Adsorption

Surfactant	Plateau adsorption, mol/m ²	Surface coverage, Θ
$C_{12}EO_8$	2.5×10^{-7}	0.11
$C_{14}EO_8$	3.1×10^{-7}	0.14
$C_{16}EO_8$	4.4×10^{-7}	0.19

Adsorption/Desorption of Cationic Surfactant at Alumina–Water Interface

Results reported during the third quarter indicated that electrostatic forces were predominant during the adsorption of cationic TTAC on alumina. Desorption of TTAC from the alumina surface was studied during this reporting period. The adsorption isotherm of TTAC on alumina was first determined. Supernatant solutions of varying residual concentrations along the isotherm were diluted with water and the slurry conditioned for 15 h. This procedure was repeated several times depending upon the concentration. The results are shown in Fig. 5. The solid line represents the initial adsorption isotherm. It is observed that adsorption is reversible in most cases except at low concentrations. At low concentrations, it does appear that there is some hysteresis, but this could result

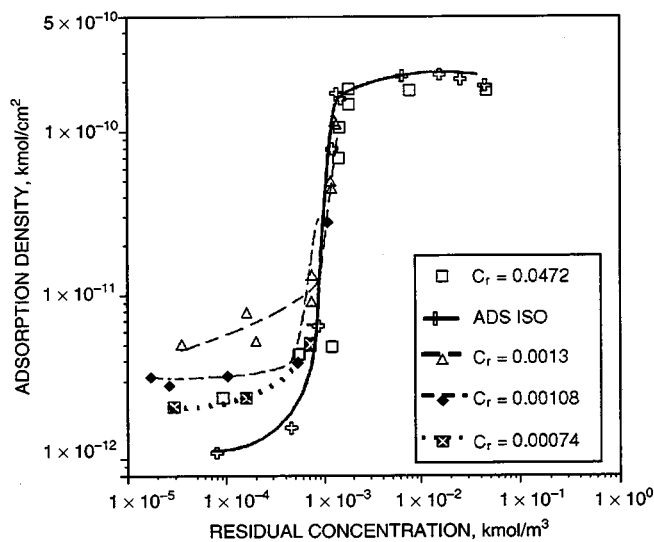


Fig. 5 Desorption of tetradecyl trimethyl ammonium chloride (TTAC) from alumina: dilutions from different residual concentrations. ADS ISO, adsorption isotherm. C_r , residual concentration.

from experimental error as a result of loss of material during dilution.

Electrokinetic measurements were also performed on the same samples and from the results seen in Fig. 6, it does appear that the adsorption of cationic TTAC on alumina is reversible. Further studies will concentrate on spectroscopic characterization of the adsorbed layer.

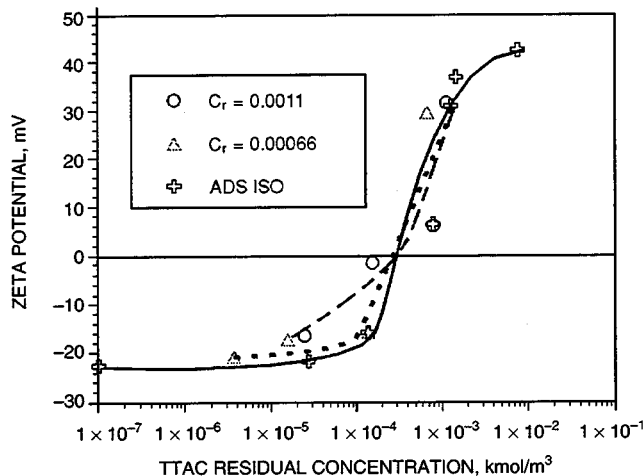


Fig. 6 Electrokinetic measurements of tetradecyl trimethyl ammonium chloride (TTAC)–alumina system after adsorption and upon dilution from different residual concentrations. ADS ISO, adsorption isotherm. C_r , residual concentration.

Future work

The following areas will be investigated as this project continues.

1. Fluorescence spectroscopy of TTAC adsorbed layer on alumina.
2. Microstructure of mixed SDS– $C_{12}EO_8$ adsorbed layer.
3. Calorimetry on adsorbed alkyl xylene sulfonate layers.

GAS DISPLACEMENT— SUPPORTING RESEARCH

FIELD VERIFICATION OF CO₂-FOAM

Contract No. DE-FG21-89MC26031

**New Mexico Institute of Mining and Technology
Petroleum Recovery Research Center
Socorro, N. Mex.**

Contract Date: Sept. 30, 1989

Anticipated Completion: Sept. 30, 1993

Principal Investigators:

**F. David Martin
John P. Heller
William W. Weiss**

Project Manager:

**Royal Watts
Morgantown Energy Technology Center**

Reporting Period: July 1–Sept. 30, 1993

Objective

This project is a cooperative effort of industry, university, and government to transfer laboratory research technology to a field demonstration test. The primary objective of the project

is to evaluate the use of foam for mobility control and fluid diversion in a field-scale CO₂ flood.

Summary of Technical Progress

The East Vacuum Grayburg/San Andres Unit (EVGSAU), operated by Phillips Petroleum Company, was the site selected for a comprehensive evaluation of the use of foam for improving the effectiveness of a CO₂ flood. The Petroleum Recovery Research Center (PRRC), a division of the New Mexico Institute of Mining and Technology (NMIMT), is providing laboratory and research support for the project. The project is jointly funded by the EVGSAU Working Interest Owners (WIO), the U.S. Department of Energy (DOE), and the State of New Mexico. A Joint Project Advisory Team (JPAT) composed of WIO technical representatives from several major oil companies provides input, review, and guidance for the project. The four-year project began in late 1989 and is now in the fourth and final year. During this quarter a no-cost extension was granted by DOE for 6 months.

The favorable production responses resulting from the first foam injection test are described in the previous progress reports. On the basis of that favorable response, a second foam test was initiated during the last quarter in the same injection well as that used for the first foam test. At some period after the initiation of the second foam test on May 21, 1993, however, a facilities problem was discovered at the field site.

Normal injection operations involved the blending of about one-third produced gas (containing 70 to 75% CO₂) with about two-thirds purchased CO₂. Because of the high temperatures observed in June and July and the corresponding higher injection pressures, a greater than normal volume of produced gas was being injected. This condition resulted in a lower hydrostatic gradient and a somewhat higher surface injection pressure. Since it would be difficult to distinguish the pressure response caused by the foam injection from the pressure increases caused by the change in injected gas composition, the decision was reached to abort the second foam test until a stabilized baseline could be reestablished.

Following the JPAT meeting on June 30 and July 1, 1993, in Socorro, a smaller working group of the JPAT met in Odessa on July 26 and 27 to evaluate results of the foam test. The nature of the facilities problem was unknown and not discussed at the JPAT meeting, but it was discussed at the subgroup meeting in late July. The recommendation of the subgroup was to establish a minibaseline by injecting CO₂ until a baseline injectivity is reached followed by about 6 to 8 weeks of water and 6 to 8 weeks of CO₂ before reinitiating the second foam test. The baseline injectivity with CO₂

stabilized in mid-September, and water injection began on Oct. 1, 1993.

The subgroup has proposed an alternative foam generation scheme to the JPAT. After an analysis of the injection well profile results, the subgroup is proposing that near-wellbore diversion might be more effective if a large surfactant slug were injected into the higher permeability zones and then followed by continuous CO₂ injection rather than using a rapid surfactant-alternating-gas (SAG) process. Details of the second foam test will be decided by the JPAT during the next quarter.

During this quarter the application of the simulated annealing method for inverse reservoir modeling at the EVGSAU pilot was presented¹ at the Annual Society of Petroleum Engineers Meeting. Results of all the reservoir simulation runs will be compiled during the next quarter in preparation for completion of the final report.

Reference

1. A. J. Sultan, A. Ouenes, and W. W. Weiss, Reservoir Description by Inverse Modeling: Application to EVGSAU Field, in *Proceedings of the Annual Technical Conference and Exhibition of the Society of Petroleum Engineers*, Houston, Tex., Oct. 3-6, 1993, pp. 637-652.

THERMAL RECOVERY— SUPPORTING RESEARCH

**STUDY OF HYDROCARBON MISCIBLE
SOLVENT SLUG INJECTION PROCESS
FOR IMPROVED RECOVERY OF HEAVY
OIL FROM SCHRADER BLUFF POOL,
MILNE POINT UNIT, ALASKA**

Contract No. DE-FG22-93BC14864

**University of Alaska
Fairbanks, Alaska**

Contract Date: Dec. 1, 1992

Anticipated Completion: June 30, 1996

Total Project Cost:

DOE Funding for FY93	\$200,000
Contractor	129,726
Total	\$329,726

**Principal Investigator:
G. D. Sharma**

**Project Manager:
Thomas Reid
Bartlesville Project Office**

Reporting Period: July 1–Sept. 30, 1993

Objectives

The ultimate objective of this 3-yr research project is to evaluate the performance of the hydrocarbon miscible solvent slug process and to assess the feasibility of this process for improving recovery of heavy oil from Schrader Bluff reservoir. This will be accomplished through measurement of pore-volume-temperature (PVT) and fluid properties of Schrader Bluff oil, determination of phase behavior of Schrader Bluff oil solvent mixtures, asphaltene precipitation tests, slim-tube displacement tests, coreflood experiments, and reservoir simulation studies. The expected results from this project include determination of optimum hydrocarbon solvent composition suitable for hydrocarbon miscible solvent slug displacement process, optimum slug sizes of solvent needed, solvent recovery factor, solvent requirements, extent and timing of solvent recycle, displacement and sweep efficiency to be achieved, and oil recovery.

Summary of Technical Progress

During this quarter reservoir oil and gas samples were acquired. The General Equation-of-State Model (GEM) simulator, developed by the Computer Modeling Group, was used to simulate the slim-tube displacement runs for various

solvents. Displacement experiments in the slim tube are to be conducted to verify the slim-tube simulation results.

Slim-Tube Simulation

The equation-of-state (EOS) parameters obtained from the PVT simulator are used to simulate slim-tube displacement runs on the GEM simulator. The EOS parameters are included in Table 1. The GEM is a multidimensional EOS compositional simulator that can simulate all the important mechanisms of a miscible gas injection process (i.e., vaporization and swelling of oil, condensation of gas, viscosity and interfacial tension reduction, and the formation of a miscible solvent bank through multiple contacting). The GEM can be run in explicit, fully implicit, and adaptive implicit modes. It uses a dual-porosity and dual-permeability model and can perform flash calculation (the quasi-Newton successive substitution method is used to solve the nonlinear equations associated with flash calculation). The GEM uses either the Peng–Robinson or the Soave–Redlich–Kwong EOS (the Peng–Robinson EOS is used in the simulation of slim-tube experiments).

The GEM simulator has two models, a large-memory model and a small-memory model. The small-memory model handles more components than the large-memory model. The small-memory model uses up to ten components. All the EOS parameters for the regular components are stored in the simulator. For user-defined components, all the EOS parameters must be input into the simulator. The EOS parameters listed in Table 1 for pseudocomponents and plus fraction are input into GEM simulator.

In the experimental setup the slim tube is 40 ft long and is coiled in 1-ft diameter. The slim tube has an outer diameter of 0.236 in., and it is filled with Ottawa sand of 5 D permeability and 0.352 porosity. For the purpose of simulation, the slim tube is represented by a one-dimensional model of $40 \times 1 \times 1$ grid blocks. Each grid block is 1 ft long, and in *j* and *k* directions the lengths are adjusted to represent exact slim-tube volume. One injector and one producer are included in this model at the first and last block, respectively. The grid diagram is shown in Fig. 1. The slim-tube porosity and permeability values are input into the simulator. The solvent injection rate was maintained at 3 cm³/h, and a total

TABLE 1
EOS Parameters for GEM Simulator*

Component	Zi	MW	PC, psia	TC, R	OMEGA	OMEGB	PCHOR	AC	REFD
N2	0.0024	28.02	493	227.6	0.457236	0.0778	41	0.04	0.804
C1	0.263	16.04	673.1	344.2	0.452477	0.08793	77	0.008	0.3
CO ₂	0.0022	44.01	1070	547.8	0.457236	0.0778	79.7	0.225	0.777
C2	0.0035	30.07	709.8	550.3	0.457236	0.0778	108	0.098	0.3771
C3	0.008	44.09	617.4	666.4	0.457236	0.0778	150.3	0.152	0.5077
C4	0.0159	58.12	550.7	765.6	0.457236	0.0778	189.9	0.193	0.5844
C5	0.0101	72.14	489.5	845.9	0.457236	0.0778	231.5	0.251	0.6109
C6–C8	0.0667	104.71	382.8	994	0.28	0.05945	325.059	0.3684	0.7444
C9–C10	0.102	128.8	318.4	1090.7	0.470967	0.04968	392.557	0.466	0.7764
C11+	0.5621	363	210.8	1605.7	0.303265	0.07023	1121	0.7303	0.9895

*Abbreviations used are: Zi, mole fraction; MW, molecular weight; PC, critical pressure of component, psia; TC, critical temperature of component, °R; OMEGA, equation-of-state constant; OMEGB, equation-of-state constant; PCHOR, parachor of component; AC, eccentric factor of component; REFD, reference saturated liquid density.

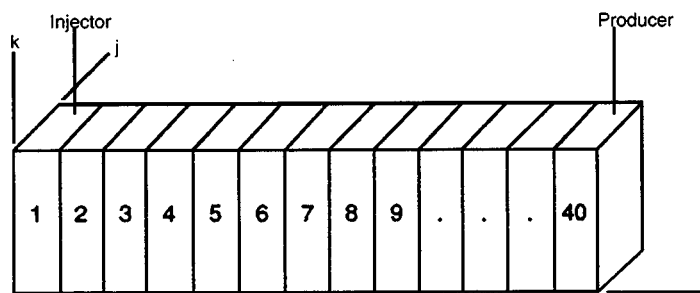


Fig. 1 Grid blocks for simulating slim-tube experiment.

of 1.2 pore volumes (PV) of solvent was injected in each simulation run.

Five slim-tube simulations were conducted with 0, 5, 15, 25, and 35% natural gas liquid (NGL) in the injected gas. Recoveries vs. pore volumes injected for the preceding five simulation runs are plotted in Figs. 2 to 6. Gas/oil ratio vs. pore volumes injected are plotted in Figs. 7 to 9. Figure 6 shows that the injected gas (65% KUPSCH gas and 35% NGL) is near miscible with the oil on the basis of recovery.

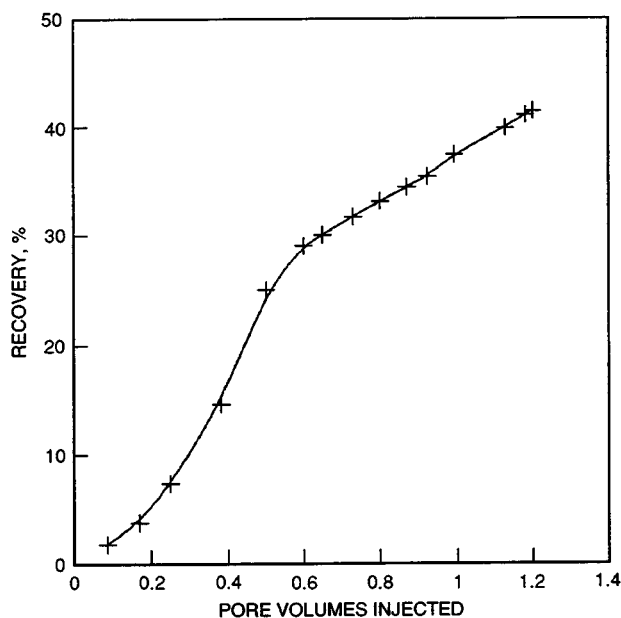


Fig. 2 Recovery vs. pore volumes injected (100% KUPSCH gas). +, slim-tube simulation.

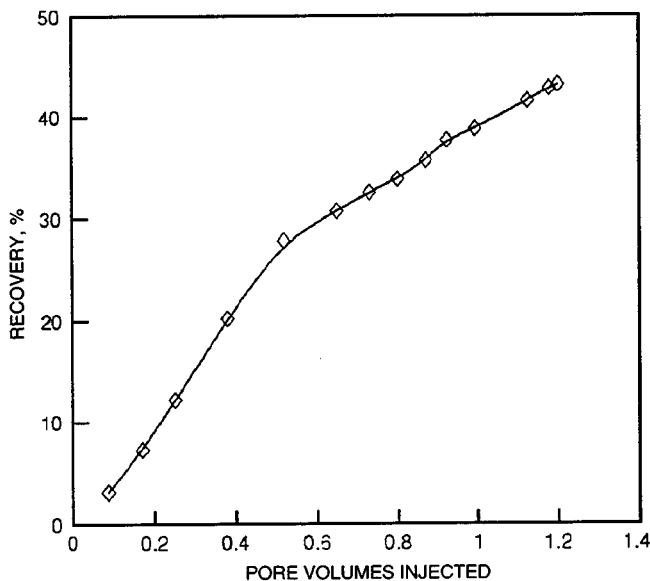


Fig. 3 Recovery vs. pore volumes injected (95% KUPSCH gas and 5% natural gas liquid injection). -◇-, slim-tube simulation.

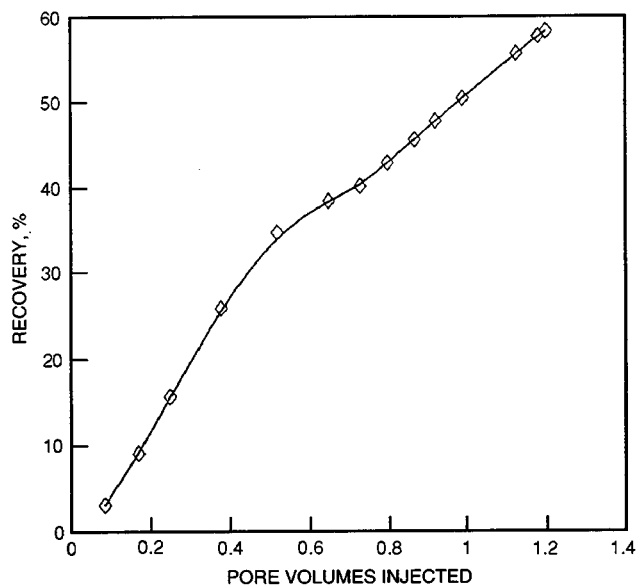


Fig. 4 Recovery vs. pore volumes injected (85% KUPSCH gas and 15% natural gas liquid injection). -◇-, slim-tube simulation.

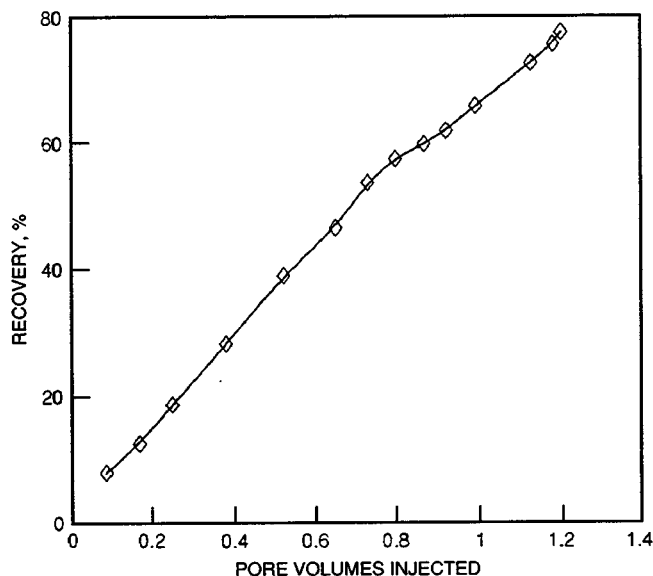


Fig. 5 Recovery vs. pore volumes injected (75% KUPSCH gas and 25% natural gas liquid injection). -◇-, slim-tube simulation.

The recoveries at 1.2 PV injection obtained from the simulation runs are listed in Table 2.

Future Work Plan

In the coreflood displacement experiments to be performed, water and gas will be used as displacing fluids. Displacement experiments will also be continued in a slim tube to study the miscibility of various solvents with Schrader Bluff crude.

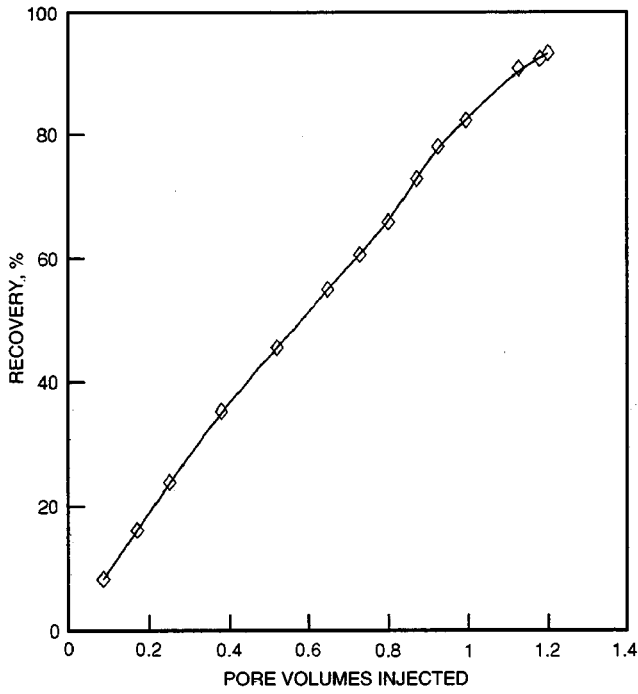


Fig. 6 Recovery vs. pore volumes injected (65% KUPSCH gas and 35% natural gas liquid injection). \diamond —, slim-tube simulation.

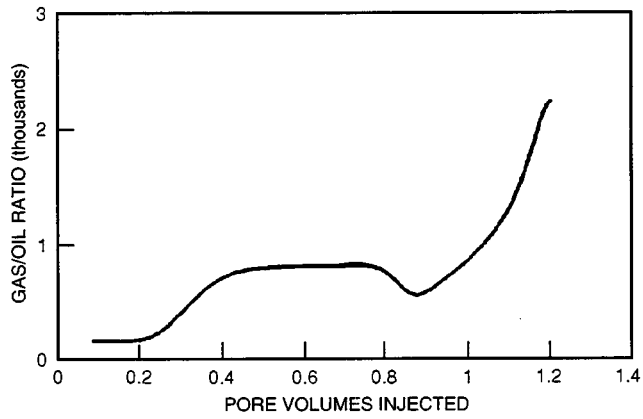
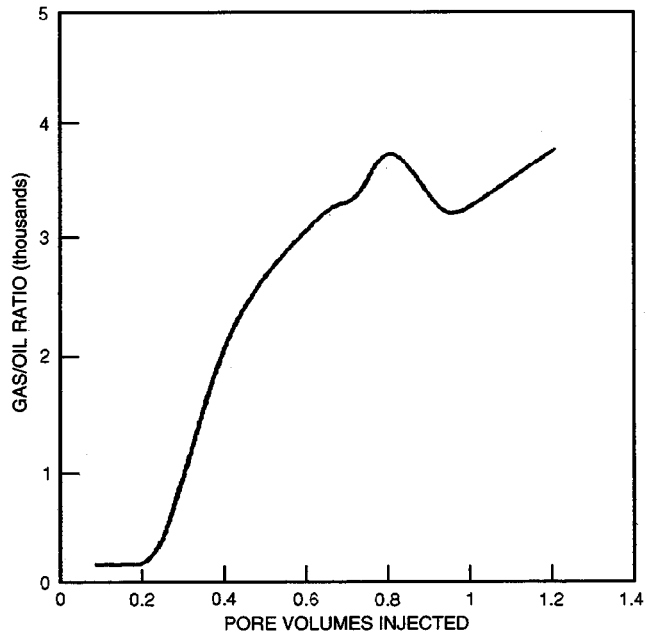
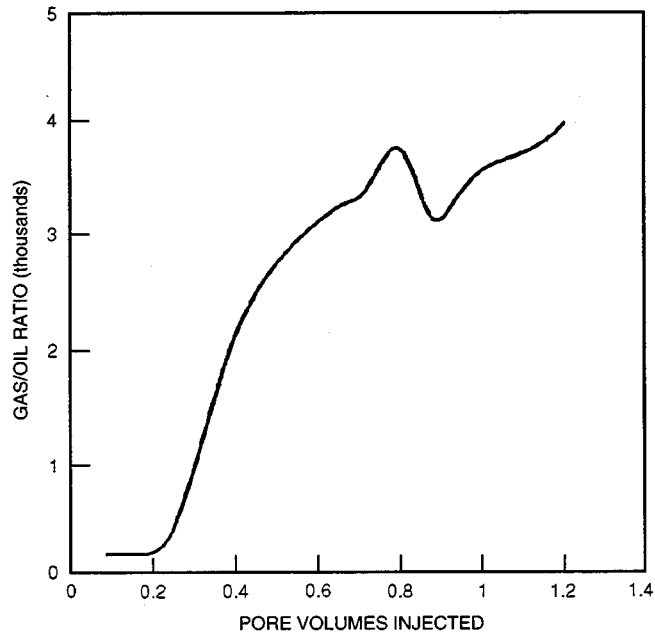


Fig. 7 Illustration showing gas/oil ratio vs. pore volumes injected (65% KUPSCH gas and 35% natural gas liquid injection). —, slim-tube simulation.

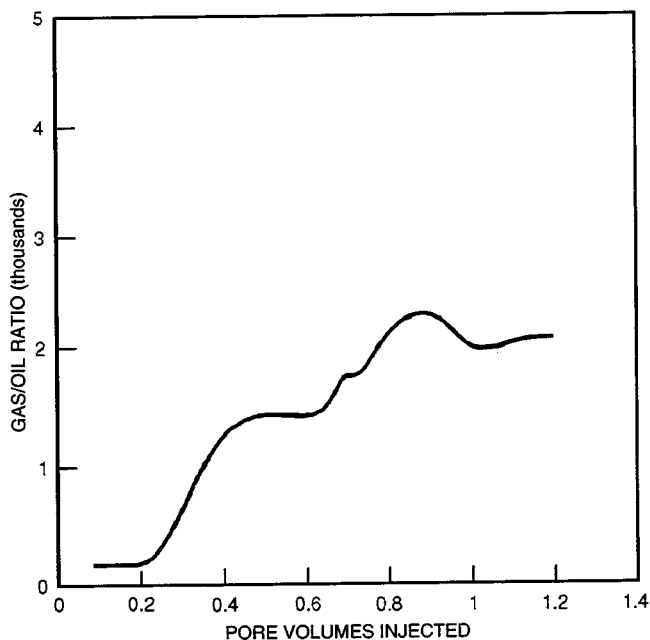


(a)

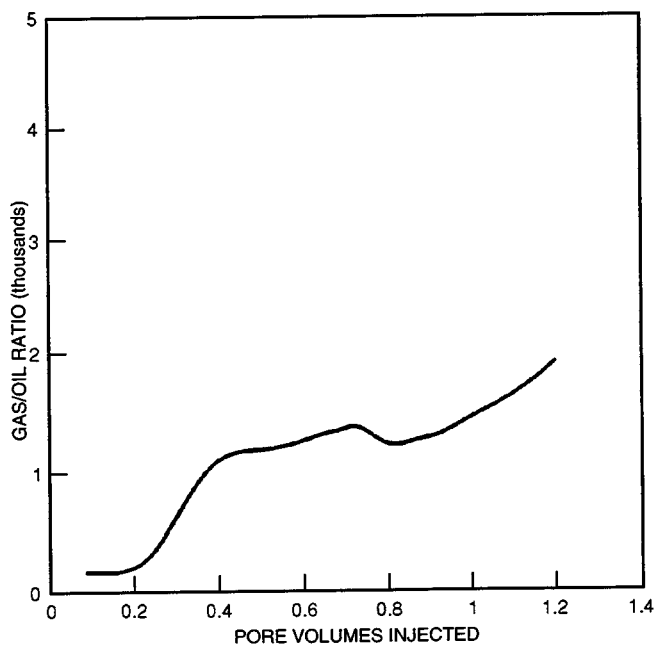


(b)

Fig. 8 Illustrations showing gas/oil ratio vs. pore volumes injected. —, slim-tube simulation. (a) KUPSCH gas injection. (b) 95% KUPSCH gas and 5% natural gas liquid injection.



(a)



(b)

Fig. 9 Illustrations showing gas/oil ratio vs. pore volumes injected. —, slim-tube simulation. (a) 85% KUPSCH gas and 15% natural gas liquid injection. (b) 75% KUPSCH gas and 25% natural gas liquid injection.

TABLE 2

Recoveries from Various Simulation Runs Injecting Various Solvents

Solvents injected	Recovery, %
100% KUPSCH gas*	41.471
95% KUPSCH gas and 5% natural gas liquid	43.103
85% KUPSCH gas and 15% natural gas liquid	58.213
75% KUPSCH gas and 25% natural gas liquid	77.39
65% KUPSCH gas and 35% natural gas liquid	93.27

*KUPSCH gas is a Kuparuk and Schrader Bluff gas mixture.

PRODUCTIVITY AND INJECTIVITY OF HORIZONTAL WELLS

Contract No. DE-FG22-93BC14862

Stanford University
Stanford, Calif.

Contract Date: Mar. 10, 1993
Anticipated Completion: Mar. 10, 1998
Government Award: \$359,000
(Current year)

Principal Investigators:
F. John Fayers
Khalid Aziz
Thomas A. Hewett

Project Manager:
Thomas Reid
Bartlesville Project Office

Reporting Period: July 1–Sept. 30, 1993

Objectives

The project objectives include the following:

- *Modeling horizontal wells*—Establish detailed three-dimensional (3-D) methods of calculation that will successfully predict horizontal well performance under a range of

reservoir and flow conditions, review both commercial simulators and simple inflow performance relationships used by the industry, investigate the sensitivity of various parameters on the performance of horizontal wells, and develop modeling techniques and computer codes based on generalized 3-D flexible gridding techniques that can be incorporated into reservoir simulators.

- *Reservoir characterization*—Investigate reservoir heterogeneity descriptions of interest to applications of horizontal wells, develop averaging techniques in three dimensions that will adequately compute the effective single-phase and two-phase directional permeabilities within the variable gridding characteristics of the model developed in task 1, and perform sensitivity studies of the averaging technique to uncertainties in the heterogeneity distribution.

- *Experimental planning and interpretation*—Critically review technical literature on two-phase flow in pipes and the correlation of these results in terms of their relevance to horizontal wells; perform sensitivity studies to choose parameter spaces of interest for some typical field conditions using the advice of oil companies; plan key experiments to investigate sensitivity to parameter variation, including inflow distribution, completion variations, void fractions, etc.; perform data analysis, including flow pattern distribution, scaling, dependence on perforation intervals, confidence levels, etc.; revise two-phase pressure drop in horizontal wells; and incorporate this capability in the analytic solutions for critical rates task.

Summary of Technical Progress

A number of research activities were carried out in the last three months. A list outlining these efforts followed by a brief description of each activity in the subsequent sections of this report follows.

- The available analytical solutions in the literature for steady-state critical rates of horizontal wells were examined. The application of these methods to a cresting example showed significant uncertainties in the prediction of critical rates.

- Sensitivity computations for evaluating the effects of shale distribution on the performance of horizontal wells in heterogeneous reservoirs were run.

- A number of single-phase (water and oil) and two-phase (water and air) experiments were completed in the Marathon Wellbore Model and the collected data are being analyzed.

- A presentation of the project was given at the International Technology Forum DEA-44/67 on Horizontal, Slimhole, and Coiled Tubing held by Maurer Engineering on September 29–October 1 in Houston.

- A draft review report entitled “Opportunities for Horizontal Wells and Problems in Predicting Their Performance”¹ is complete.

Analytic Solutions for Critical Rates

Reservoirs with bottom water and/or gas cap can exhibit coning and cresting behavior. For instance, oil production through a horizontal well underlain by a water zone causes the oil–water interface to deform into a crest shape. The height of the water crest increases as the production rate is increased. At a certain production rate, the water crest becomes unstable, and water is produced into the well. The maximum rate at which oil is produced without production of gas or water is defined as the critical rate.

At least four analytical methods exist for quantifying critical rates for horizontal wells. These methods, reviewed in Ref. 1, have been applied to a base example. The calculation example is given in this quarterly report, whereas the mathematical details are given in Ref. 1.

Calculation Example

A numerical example is devised to determine the range of critical rates ($Q_{o,c}$) predicted by the different methods. A reservoir with a gas cap is considered and the data given in Example 8-7 of Joshi’s book⁹ is used. In this example a horizontal well with length $L = 1640$ ft is drilled 72 ft below the gas–oil contact. The isotropic case is considered with $k_h = k_v = 70$ mD. For the anisotropic case, $k_v = 0.1 k_h$. Other parameters in the example are $y_e = 2640$ ft, $\mu_o = 0.42$ cP, $B_o = 1.1$ reservoir barrels/stock tank barrels (RB/STB) $\Delta p = 0.48$ g/cm², $r_w = 0.328$ ft, and $r_e = 1489$ ft. The predicted critical oil rate for each method is calculated using the corresponding equation in the form of field units (see Ref. 2). The results are summarized in Table 1.

Results in Table 1 show a vast discrepancy among the preceding methods for prediction of critical oil rates for a single horizontal well. They differ by as much as a factor of 22 in the isotropic case. To further test these methods, a simulation study of the steady-state cresting behavior for horizontal wells has been assigned to a new graduate student.

TABLE 1
Estimates of Critical Oil Rates for a Single Horizontal Well from Different Methods*

Method	Isotropic $Q_{o,c}$, STB/d	Anisotropic [(k_v/k_h) = 0.1] $Q_{o,c}$, STB/d
Efros ³ and Giger ⁴	114†	–
Giger ⁵ and Karcher et al. ⁶	457	–
Joshi ^{2,7}	492‡	–
Chaperon ⁸	1122	985
Guo and Lee ⁹	2576	810

*STB, stock tank barrels.

†This value is listed as 57 STB/d in Ref. 2.

‡This value is calculated to be 470 STB/d in the corrections to Ref. 2.

Reservoir Heterogeneity

A Master's Thesis¹⁰ on this aspect of the project is near completion. In this work stochastic and flow simulations are used to investigate the variability of production behavior for a horizontal well in a heterogeneous reservoir. For the construction of a probability distribution of oil recovery, a flow simulator must be run on as many stochastic realizations as possible just to compile the data. Such a process requires a great deal of time and effort. However, if the ranking of oil recovery can be realized by a single parameter, the distribution of oil recovery can be computed without performing massive flow calculations. In Ref. 10 such a parameter is introduced, and an application is demonstrated for a water-flooding problem with horizontal injectors and producers. Details of this work will be given in the first annual report. Only a sample example of the results is presented here. Figure 1 shows four cases in which 3-D impermeable shale distributions are generated by sequential indicator simulation. Short (250 ft) and long (1000 ft) horizontal ranges of correlations with five shale densities, ranging from 0.1 to 0.5 (shale/10 ft), are considered. The production performance of the distributions is illustrated in Figs. 2 to 4. Figure 2 is a plot of oil rate and water cut vs. time for two extreme cases, namely, density of 0.1 with correlation range

of 250 ft and density of 0.5 with correlation range of 1000 ft. The effects of shale density and correlation range on oil recovery are shown in Figs. 3 and 4, respectively. The preceding results indicate that the well productivity is significantly reduced as the shale density increases, especially for longer correlation ranges. Extensive work in this area is planned for the continuation of the project.

Experiments at Marathon Oil Company

During the last 3 months the first batch of experiments was completed. The experiments performed up to now include (1) single-phase water core flow with and without inflow, (2) single-phase oil core flow with no inflow, (3) two-phase water core flow with air inflow, and (4) two-phase water/air core flow. These experiments are run for a number of core and radial flow rates. A sketch of the Marathon Wellbore Model is shown in Fig. 5, in which Q refers to the core flow and q to the radial flow. The interpretation of the first batch of data is under way, and samples (for cases 2 and 3) of the results are shown here. Figure 6 shows the pressure-drop data (measured per 10-ft section along the wellbore) for two different oil core flow rates. The lines are based on analytical predictions for the single-phase smooth-pipe flows. Despite the observed scatter in the data, the calculated smooth-pipe pressure drops provide

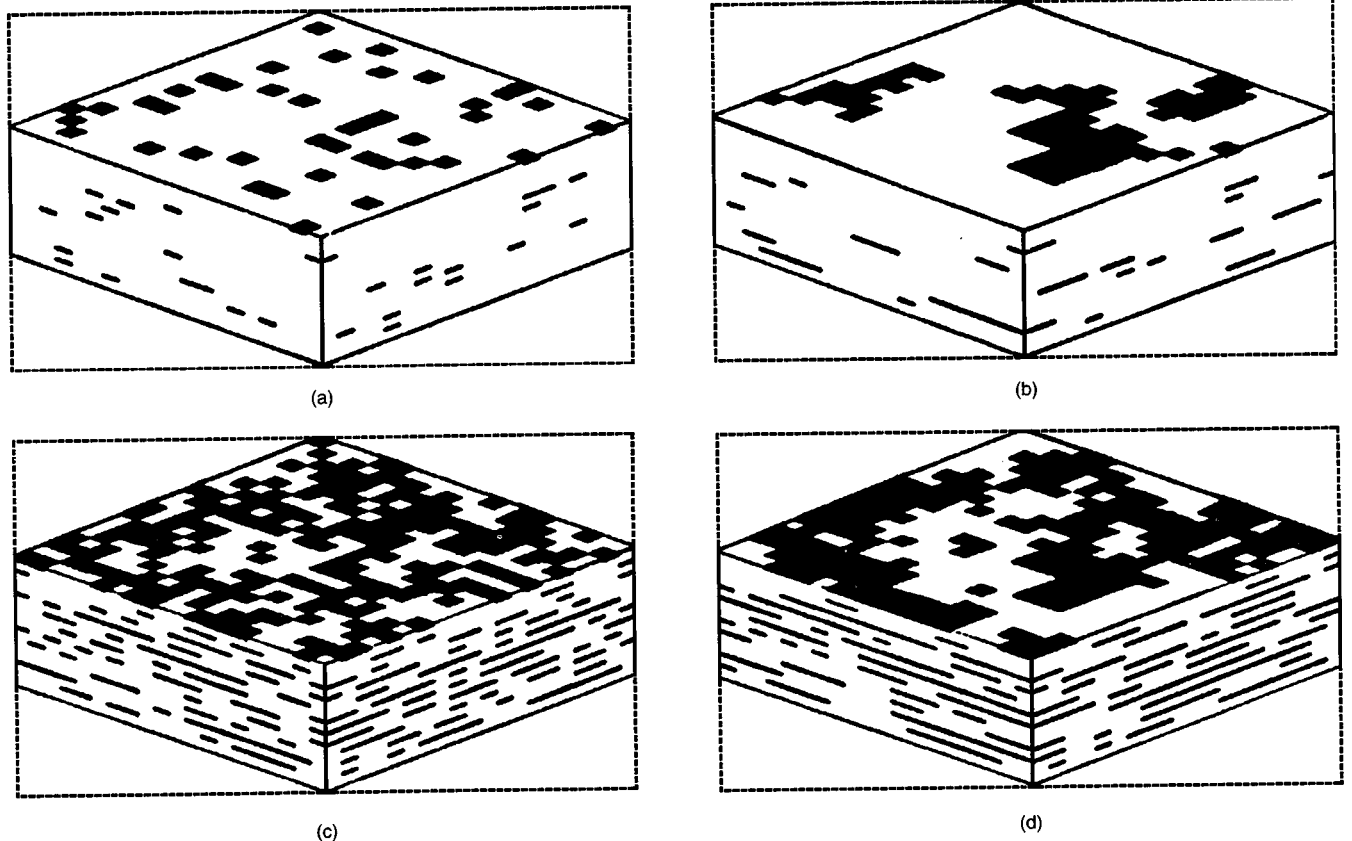


Fig. 1 Stochastic shale distributions. (a) 0.1 shale/10 ft; range, 250 ft. (b) 0.1 shale/10 ft; range, 1000 ft. (c) 0.5 shale/10 ft; range, 250 ft. (d) 0.5 shale/10 ft; range, 1000 ft.

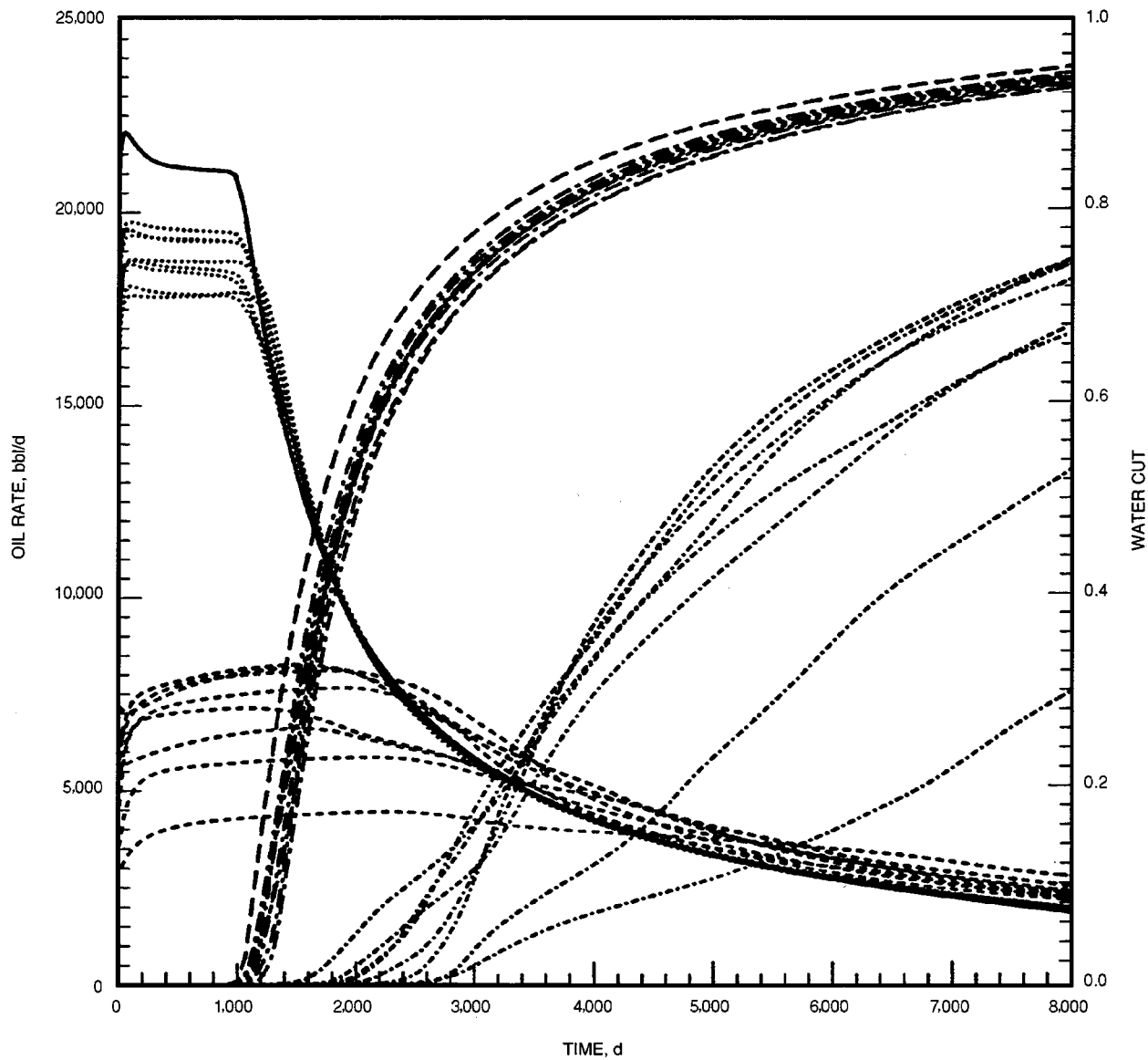


Fig. 2 Plot of oil rate and water cut vs. time., oil rate case a (density of 0.1 with correlation range of 250 ft). ----, oil rate case d (density of 0.5 with correlation range of 1000 ft). ———, oil rate homogeneous. ———, water cut case a (density of 0.1 with correlation range of 250 ft). - - - - -, water cut case d (density of 0.5 with correlation range of 1000 ft). ———, water cut homogeneous.

reasonable estimates of the data. Figure 7 is for the case in which water enters the wellbore from the right (at the 100-ft mark) and air is supplied in the radial direction starting from the 55-ft mark (see Fig. 5). The resulting two-phase flow causes a larger pressure drop, as the data indicate. The lines in Fig. 7 show predictions of two-phase pressure drops computed from the empirical correlations of Beggs and Brill¹¹

(with 0.001- and 0.002-ft roughness) and those of Dukler et al.¹² (with 0.001-ft roughness). All the computations are done with the Aziz, Spencer & Associates, Inc. (ASA) multiphase flow system program.¹³ The results in Fig. 7 indicate the need to use larger roughness (or friction factors) to predict the two-phase flow pressure drops. The complete analyses of the data will be given in the annual report.

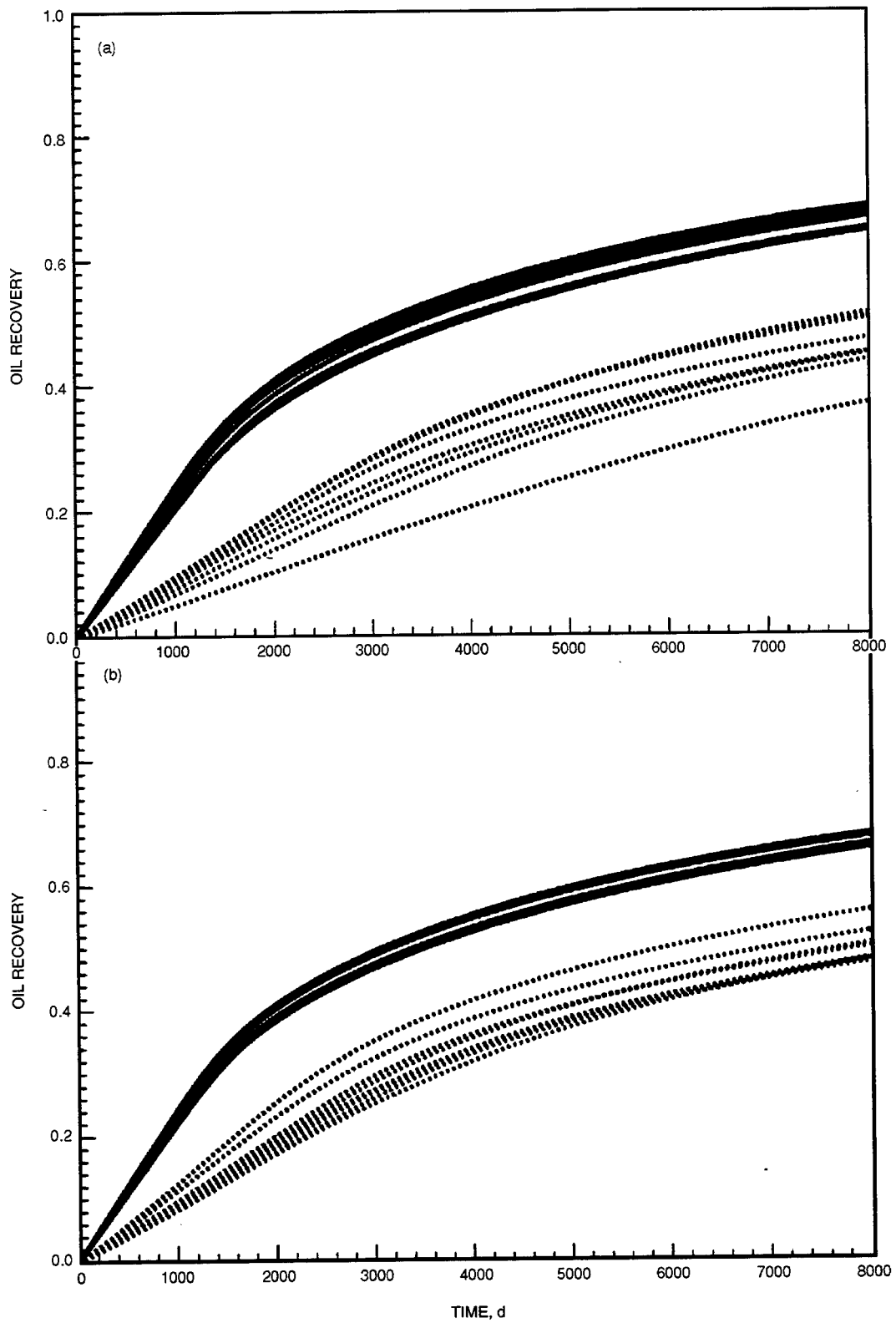


Fig. 3 Effect of shale density at ranges of 1000 ft (a) and 250 ft (b). —, 0.1 shale/10 ft. . . . , 0.5 shale/10 ft.

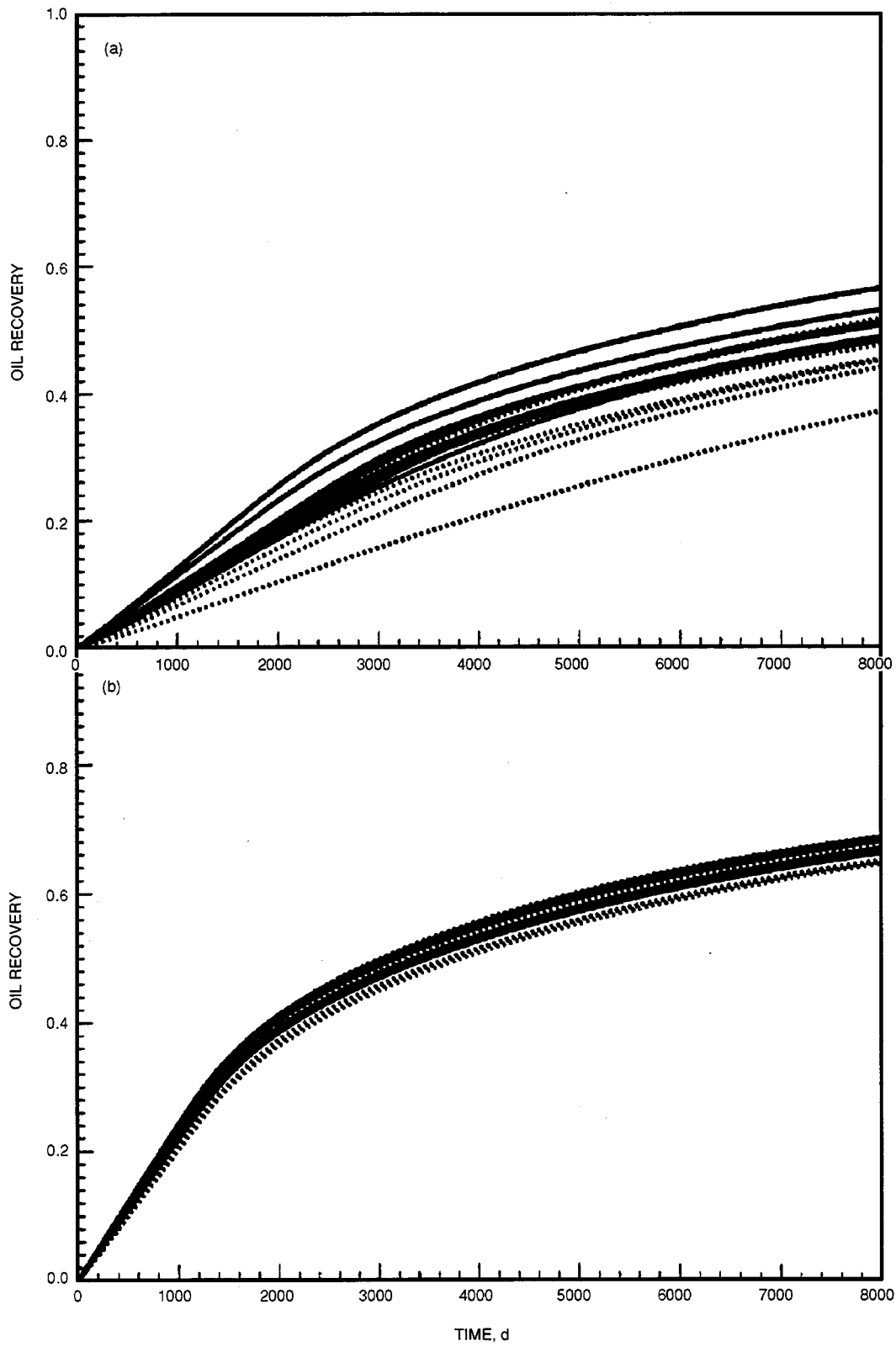


Fig. 4 Effect of correlation range. (a) 0.5 shale/10 ft. (b) 0.1 shale/10 ft. —, range, 250 ft. . . . , range, 1000 ft.

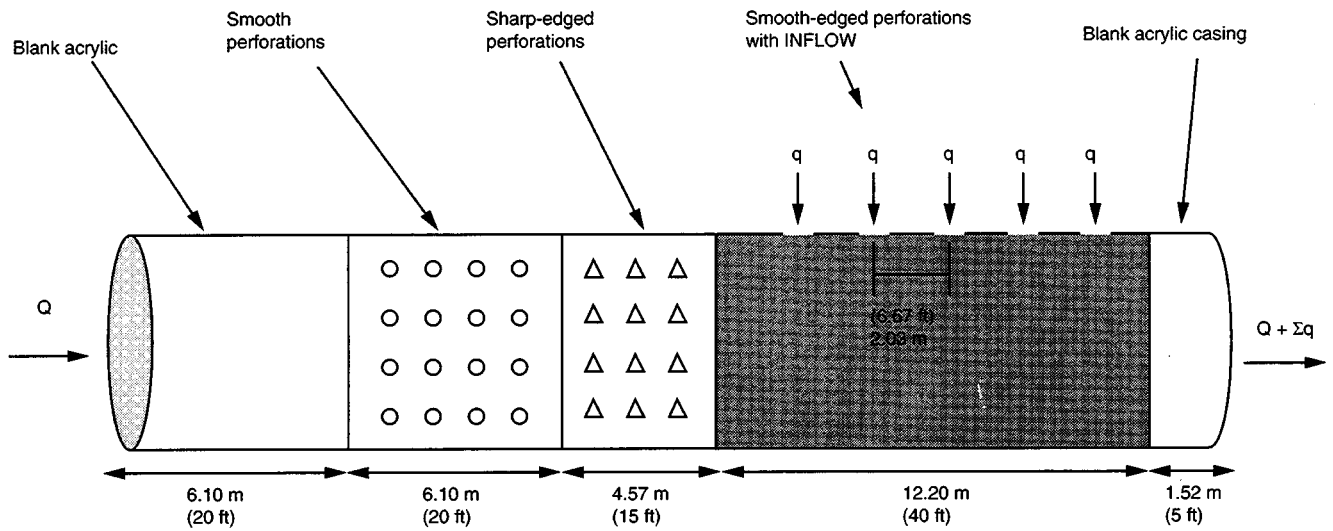


Fig. 5 Layout of the Marathon Wellbore Model.

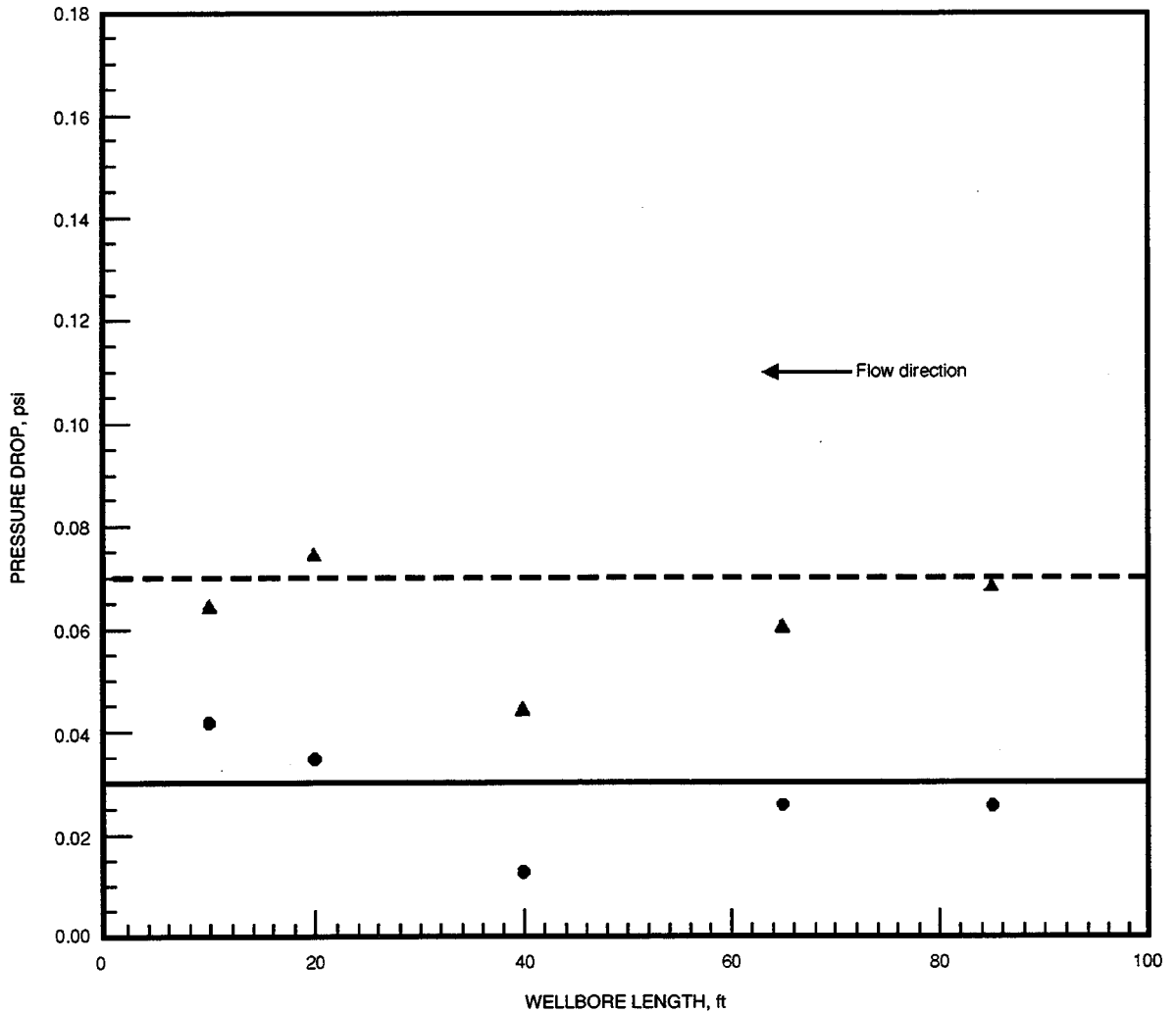


Fig. 6 Pressure drop along the wellbore for single-phase oil core flow. ●, data ($Q = 311$ gpm). ▲, data ($Q = 493$ gpm). —, $Q = 311$ gpm, calculated smooth pipe. - - -, $Q = 493$ gpm, calculated smooth pipe.

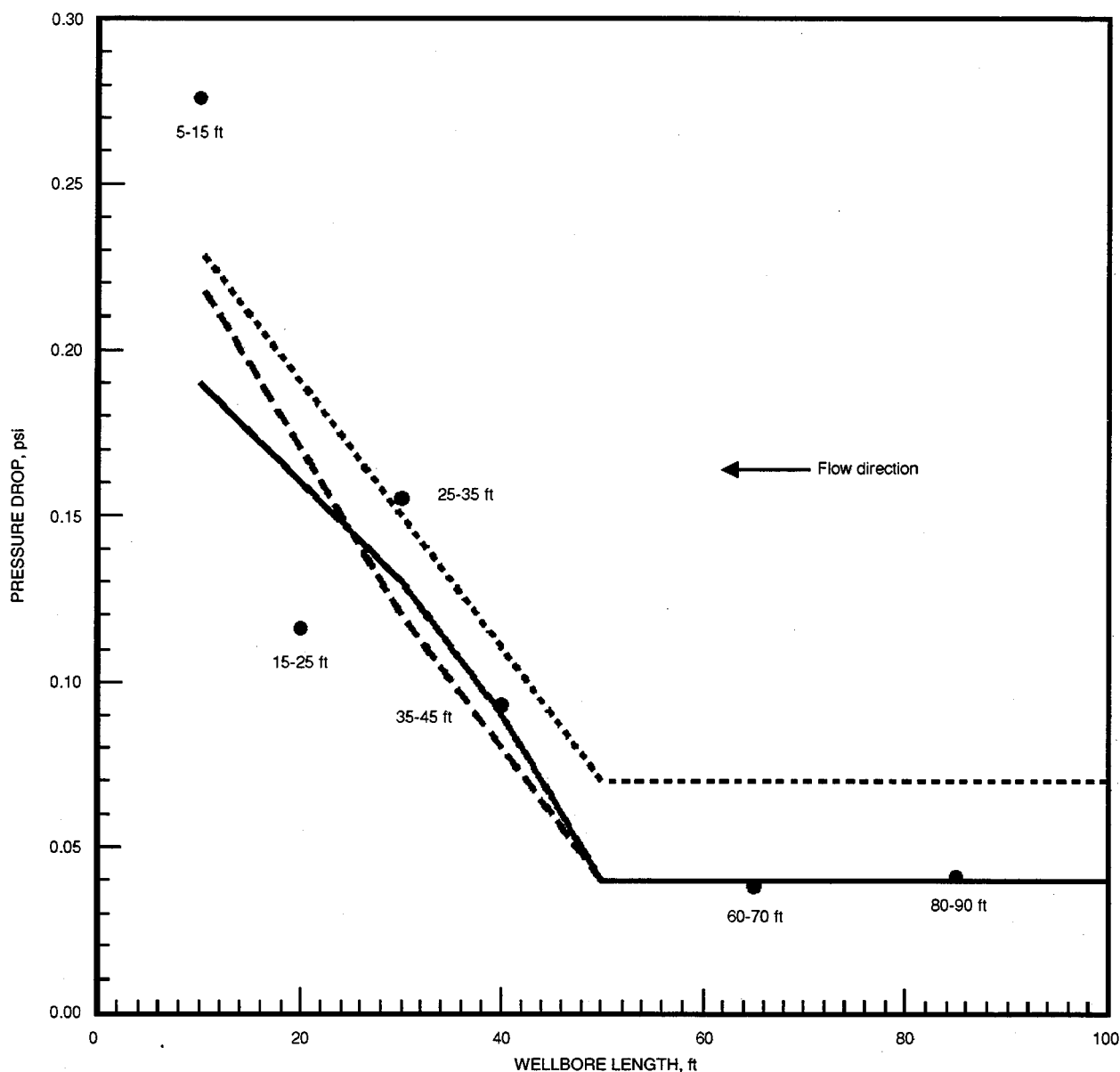


Fig. 7 Pressure drop along the wellbore for $Q = 400$ gpm (water, core flow), $q = 215$ scfm (air, inflow). ●, data (flow from 100 to 0 ft). ----, roughness, 0.001 ft (Ref. 12). —, roughness, 0.001 ft (Ref. 11). ·····, roughness, 0.002 ft (Ref. 11).

References

1. F. J. Fayers, S. Arbabi, and K. Aziz, *Opportunities for Horizontal Wells and Problems in Predicting Their Performance*, Project Report, Department of Energy, in preparation.
2. S. D. Joshi, *Horizontal Well Technology*, pp. 288-292, Pennwell Books, Oklahoma, 1991.
3. D. A. Efros, Study of Multiphase Flow in Porous Media, *Gastoptexizdat*, Leningrad, 1963 (in Russian).
4. F. M. Giger, Evaluation theorique de l'effet d'arete d'eau sur la production par horizontaux, *Rev. Inst. Fra. Pet.*, 38(3) (May-June 1983) (in French).
5. F. M. Giger, Analytic 2-D Models of Water Cresting Before Breakthrough for Horizontal Wells, *SPE Reserv. Eng.*, 409-416 (November 1989).
6. B. J. Karcher, F. M. Giger, and J. Combe, *Some Practical Formulas to Predict Horizontal Well Behavior*, paper SPE 15430 presented at the Society of Petroleum Engineers 61st Annual Technical Conference and Exhibition, New Orleans, La., Oct. 5-8, 1986.
7. S. D. Joshi, Augmentation of Well Productivity with Slant and Horizontal Wells, *J. Pet. Technol.*, 729-739 (June 1988).
8. I. Chaperon, *Theoretical Study of Coning Toward Horizontal and Vertical Wells in Anisotropic Formations: Subcritical and Critical Rates*, paper SPE 15377 presented at the Society of Petroleum Engineers 61st Annual Technical Conference and Exhibition, New Orleans, La., Oct. 5-8, 1986.
9. B. Guo and R. L. Lee, *An Exact Solution to Critical Oil Rate of Horizontal Wells with Water-Oil-Interface Cresting*, in Proceedings of the Lerkendal Petroleum Engineering Workshop, Trondheim, Feb. 5-6, 1992, pp. 55-66.
10. T. Yamada, *Production-Based Vertical Permeability for a Horizontal Well in the Presence of Stochastic Distribution of Shales*, M.S. Thesis, Stanford University, in preparation.
11. H. D. Beggs and J. P. Brill, A Study of Two Phase Flow in Inclined Pipes, *J. Pet. Technol.*, 25: 607-617 (May 1973).

12. A. E. Dukler, M. Wicks, and R. G. Cleveland, Frictional Pressure Drop in Two-Phase Flow: An Approach Through Similarity Analysis, *A.I.Ch.E.J.*, 10: 44-51 (January 1964).
13. *ASA Multiphase Flow Software Systems User Guide*, Aziz, Spencer & Associates Inc., 1993.

**HORIZONTAL OIL WELL APPLICATIONS
AND OIL RECOVERY ASSESSMENT**

Contract No. DE-AC22-93BC14861

**Maurer Engineering, Inc.
Houston, Tex.**

**Contract Date: June 3, 1993
Anticipated Completion: June 2, 1994
Government Award: \$124,119**

**Principal Investigator:
William J. McDonald**

**Project Manager:
Thomas Reid
Bartlesville Project Office**

Reporting Period: July 1–Sept. 30, 1993

Objectives

The primary objective of this project is to examine factors affecting technical and economic success of horizontal well applications. The goals of the project will be accomplished through five tasks designed to evaluate the technical and economic success of horizontal drilling, ascertain its limitations, and outline technical needs to overcome these limitations. Data describing the experiences of the operators throughout the domestic oil and gas industry will be gathered and organized. Maurer Engineering, Inc., databases containing detailed horizontal case histories will also be used. All these data will be categorized and analyzed to assess the status of horizontal well technology and determine the impact of horizontal wells on present and future domestic oil recovery and reserves.

Summary of Technical Progress

Information Base on Horizontal Wells

A spreadsheet data file was constructed from well data describing 3885 domestic horizontal wells, the total as of the summer of 1993. Most domestic effort in horizontal drilling has been focused on fractured carbonate formations. Three principal

formations are the focus of this activity: the Austin Chalk in Texas, the Bakken Shale in North Dakota, and the Niobrara in Colorado and Wyoming. Results from this formation type are well-known, and a large volume of published results is available. Given the scope of this study, the analyses will be limited to formations other than these three fractured carbonates. On the basis of domestic well data, 431 horizontal wells have been completed in other formations (Fig. 1). These wells were highlighted for detailed study.

About 180 operators drilled these other wells in a total of 112 formations. Contacts for 150 of these companies were located, telephoned about the project, and sent a questionnaire. A copy of the project questionnaire is shown as Fig. 2. No names or addresses could be tracked down for the remaining operators. As of the end of the reporting period, questionnaires covering almost half the wells have been returned.

An extensive review of the literature was conducted on the wells of interest. Over 70 technical articles were reviewed and analyzed for data pertinent to the study. Information from these articles is being compiled into a comprehensive discussion of horizontal applications to be included as a section of the final project report.

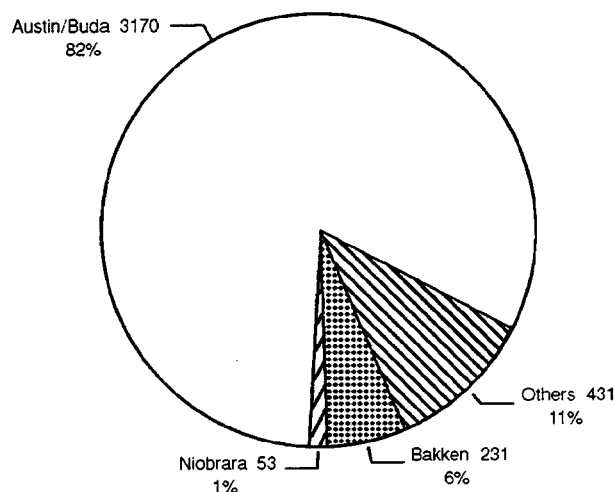


Fig. 1 U.S. horizontal well distribution through December 1992.

Specialized Database for Horizontal Well Forecasting

A database for the questionnaire formation data was constructed in dBASE IV. A computer data entry form with the same format as the questionnaire was developed to facilitate data entry. Questionnaires were received from several sources, including operators listed in the original well data file, participant companies in the DEA-44 Horizontal Well Technology joint-industry project, attendees of the Horizontal Technology Forum held in Calgary during July 1993, and attendees of the Horizontal Technology Forum held in Houston during September 1993.

HORIZONTAL WELL PRODUCTION QUESTIONNAIRE

PLEASE COMPLETE FOR EACH FIELD (MAKE COPIES IF NECESSARY).

NAME: _____ COMPANY: _____
 ADDRESS: _____ FAX NO.: _____
 FIELD: _____ FORMATION: _____
 LITHOLOGY: _____ STATE: _____ COUNTY: _____

- NUMBER OF HORIZONTAL WELLS DRILLED: 1-4 5-10 11-25 26-50 > 50
 APPROXIMATE NUMBER OF NEW WELLS _____; APPROXIMATE NUMBER OF RE-ENTRIES _____
- TYPE OF APPLICATION: (Check all applicable)

<input type="checkbox"/> INTERSECT FRACTURES	<input type="checkbox"/> IMPROVE WATER DRIVE/WATER INJECTION
<input type="checkbox"/> THIN BEDS (Increase production rate)	<input type="checkbox"/> LOW PERMEABILITY (Poor fracture candidate)
<input type="checkbox"/> LAYERED BEDS (Establish communication)	<input type="checkbox"/> IMPROVE GRAVITY DRAINAGE
<input type="checkbox"/> MINIMIZE CONING (Water, gas, etc.)	<input type="checkbox"/> ENHANCED OIL RECOVERY (Steam, polymer, etc.)
<input type="checkbox"/> SURFACE RESTRICTIONS (Lakes, bldgs., etc.)	<input type="checkbox"/> FAVORABLE ECONOMICS OVER VERTICAL
- PRIMARY OBJECTIVE: REDUCE COST (vs. vertical) INCREASE PRODUCTION RATE INCREASE RESERVES
- HORIZONTAL TO VERTICAL PRODUCTION RATIO: 1:1 1.5:1 2:1 3:1 4:1 5:1 OTHER _____
- HORIZONTAL TO VERTICAL COST RATIO: 1:1 1.25:1 1.5:1 1.75:1 2:1 2.5:1 3:1 OTHER _____
- WERE HORIZONTAL WELLS A TECHNICAL SUCCESS? YES NO COMMENTS: _____
- WERE HORIZONTAL WELLS AN ECONOMIC SUCCESS? YES NO COMMENTS: _____
- WERE ANY OF THESE HORIZONTAL WELLS STIMULATED? YES NO
 TYPE OF STIMULATION: FRACTURE MATRIX (Acid, washing, etc.)
- INCREASE IN RESERVES DUE TO HORIZONTAL: _____% 0% 1-5% 6-10% 11-15% 16-25%
- PLEASE DESCRIBE YOUR FUTURE HORIZONTAL ACTIVITY: NONE DECREASE SAME INCREASE
- WHAT DEVELOPMENT(S) WOULD INCREASE THE USE OF HORIZONTAL WELLS IN YOUR FIELDS? _____
- WHAT HORIZONTAL WELL PRODUCTION PROBLEMS HAVE YOU ENCOUNTERED?:

<input type="checkbox"/> ARTIFICIAL LIFT	<input type="checkbox"/> CEMENT PROBLEMS	<input type="checkbox"/> COMPARTMENTALIZATION
<input type="checkbox"/> FORMATION DAMAGE	<input type="checkbox"/> FORMATION HETEROGENEITY	<input type="checkbox"/> LOGGING (Prod., MWD, Other)
<input type="checkbox"/> RESERVOIR MODELING	<input type="checkbox"/> SAND CONTROL	<input type="checkbox"/> SCALE OR CORROSION
<input type="checkbox"/> STIMULATION	<input type="checkbox"/> WATER OR GAS CONING	<input type="checkbox"/> WORKOVER PROBLEMS
- WOULD YOU LIKE A SUMMARY OF THE SURVEY RESULTS? YES NO
 COMMENTS (include additional sheets if necessary) _____

PLEASE RETURN FORM BY FAX TO MAURER ENGINEERING INC. AT FAX: (713) 683-6418 PH.: (713) 683-8227

Fig. 2 Horizontal well production questionnaire.

Over 160 records (1 for each returned questionnaire) have been generated. A few questionnaires describing formations outside the scope of this study, including Austin Chalk wells and wells outside the United States, have been returned. These data may be evaluated and compared at a later date.

Economic and Technical Trend Analysis

Preliminary analyses were performed on the database. Two types of trends are being examined in the horizontal well data. Overview analyses will determine the types and frequencies of the various applications of horizontal technology (fractures, thin beds, low permeability, enhanced oil recovery, etc.). Preliminary results for 48 formations are shown in Fig. 3. Multiple responses were typical; therefore the results shown in the figure total more than 100%. The three most common applications include intersecting fractures (52%), delaying coning (35%), and economics (31%).

The average production and cost ratios for horizontal applications as compared to vertical applications will be computed. Trends will also be examined within various application subsets. For example, early results show that less than 40% of "Intersect Fracture" applications reported economic success.

Final analyses of technical and economic trends will proceed rapidly after all questionnaire data are received and entered.

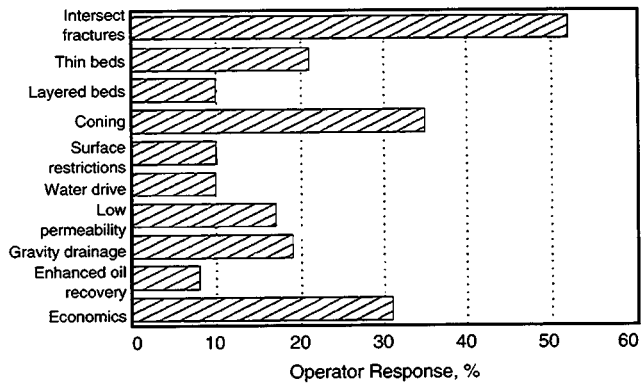


Fig. 3 Horizontal technology applications (48 formations).

Horizontal Well Application Forecast

Another key parameter in the questionnaire data is the estimated increase in reserves from horizontal technology. Preliminary results from 38 questionnaires (Fig. 4) show that half the operators expect no increase in reserves as a result of drilling horizontal wells in their particular field. However, the next most common response was an increase in the range of 16 to 25%. In a significant number of applications, horizontal wells are expected to increase recoverable reserves through, for example, delaying the onset of water coning or accessing oil not economically recoverable with vertical wells.

Final survey results are expected to yield interesting trends. The Department of Energy has been queried regarding the best numbers to use for oil-in-place estimates for forecasting the overall effect of horizontal wells on domestic reserves.

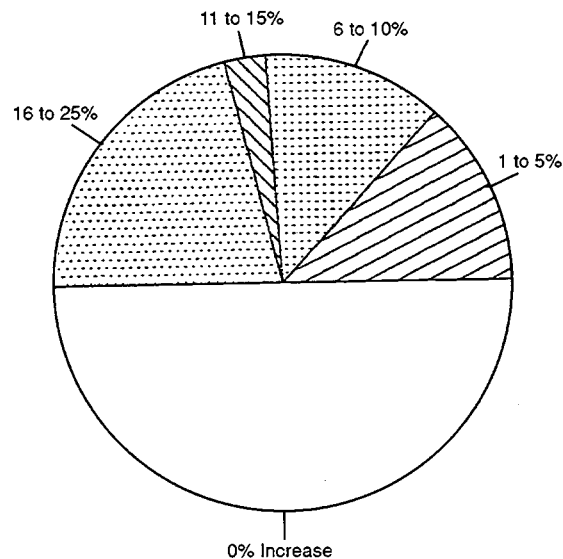


Fig. 4 Chart showing increase in reserves with horizontal wells (38 responses).

OIL FIELD CHARACTERIZATION AND PROCESS MONITORING USING ELECTROMAGNETIC METHODS

Lawrence Livermore National Laboratory
Livermore, Calif.

Contract Date: Oct. 1, 1984
Anticipated Completion: Oct. 1, 1993
Government Award: \$350,000

Principal Investigator:
Mike Wilt

Project Manager:
Thomas Reid
Bartlesville Project Office

Reporting Period: July 1–Sept. 30, 1993

Objectives

The objectives of this project are to apply surface and borehole electromagnetic (EM) methods for oil field characterization and to monitor in situ changes in the electrical conductivity during enhanced oil recovery (EOR) operations. The goal of this project is to develop practical tools for geophysical characterization of oil strata and monitoring of EOR processes in a developed field. Crosshole and surface-to-borehole EM are being applied to map oil field structure and to provide an image of electrical conductivity changes associated with EOR operations.

Summary of Technical Progress

During the third quarter the initial interpretation of data collected at the Lost Hills field site in May was concluded. This consisted of fitting the surface-to-borehole data to one-dimensional (1-D) models. The composite section, consisting of pieced-together 1-D models, will be used as a first guess for interpretation with two-dimensional (2-D) codes. In addition some modifications have been made to the tomographic imaging code developed by Alumbaugh.¹ These changes allow the use of the code in areas with high resistivity contrasts, such as oil fields.

After some initial failures field tests on the new borehole transmitter are complete. This report demonstrates that some drift and bias errors that were prevalent with the old transmitting tool have apparently been eliminated. This means that new data will probably be more repeatable than previous data sets.

Interpretation of Lost Hills No. 3 Field Data

Surface-to-borehole profiles collected at the Lost Hills site in May 1993 have been interpreted using 1-D models. Each profile

consists of a surface transmitter loop, broadcasting a monochromatic 1 kHz signal, and a series of induction coil receivers in borehole DRL35N spaced at 6 m intervals from the surface to a depth of 150 m. A separate profile was made for each of the eight surface transmitters extending westward from borehole DRL35N to DRL61, a distance of 125 m. The data set consists of 8 profiles, each including 22 measurements. Surface-to-borehole profiles were modeled separately with a 1-D (layered) modeling code developed by Schenkel.² The resulting 1-D models were then pieced together to form a pseudo-section.

A sample of an individual inversion with the accompanying layered section is given in Figs. 1 and 2. Figure 1 shows the fit of observed to calculated data for one of the measurement profiles. As shown, the fit is very close except for the

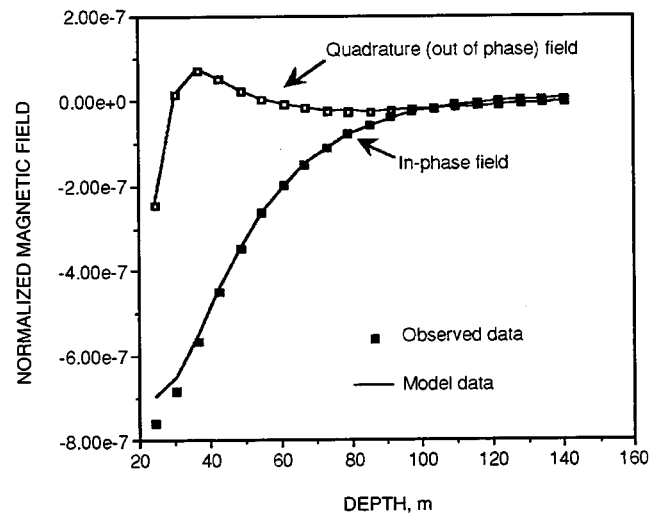


Fig. 1 Comparison of observed and calculated data for Lost Hills surface-to-borehole profile. Data for transmitter location 25 m from borehole DRL35N.

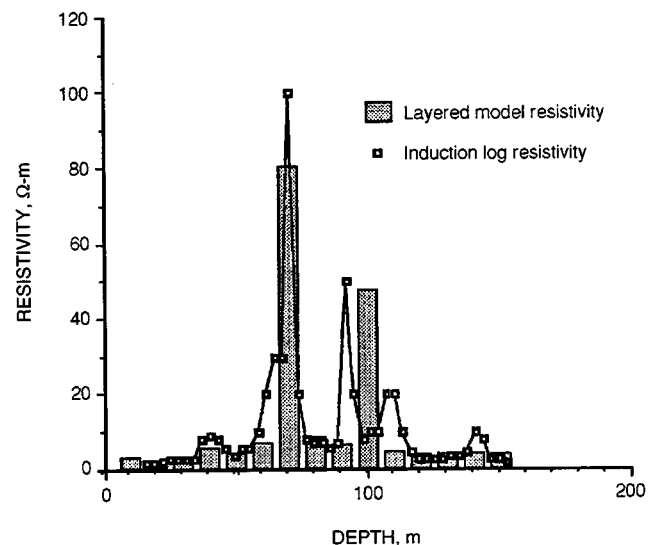


Fig. 2 Comparison of the layered model obtained from the above inversion and the borehole induction log from well DRL35N.

initial two measurements. This suggests that the data can be well described by a multilayered model, which is expected for the gently dipping structures at Lost Hills.

The 11-layer 1-D resistivity model was obtained by fixing the thickness of each layer at 10 m and assuming that each layer has a resistivity of 5 Ω -m. The computer then is free to change the resistivity of the layers until the model-generated results fit the observed data. For all of the profiles the inversions indicate the presence of two separate resistive layers at a depth below 50 m. These layers represent the oil sands that are the targets for upcoming EOR steamflood activities. In the coming months the field survey will be repeated to observe changes in these layers. Comparison of the results to the borehole induction log from well DRL35N shows an excellent agreement in the depth and resistivity of the target oil sands (Fig. 2).

A resistivity cross section can be formed by plotting the layered section derived from the 1-D inversions for each sounding beneath the position of the surface loop transmitters. The layered models are then pieced together along the profile to form a quasi-2-D model of the earth along the surface profile (Fig. 3). For a smoothly varying section, such as Lost Hills, this model is probably a good first guess for a 2-D structure. This assertion will be tested in the near future when the 2-D code is applied to the Lost Hills data set.

The pseudo-section shown in Fig. 3 accurately reflects the configuration of the upper two oil sands at Lost Hills as known from the borehole induction logs. It shows that the sands form two distinct gently dipping resistive units in a low resistivity background predominantly consisting of finer grained clays and silts.

Inversion Code

A tomographic inversion code developed by Alumbaugh¹ is being modified to make the code more robust and improve the performance. Alumbaugh's code employs cylindrical symmetry and makes use of the "Born" approximation to provide an image of crosshole EM data. Such simplifications allow for data interpretation using desktop computer workstations, but a price is paid in accuracy. The code has proven effective in cases where the geology is simple and the resistivity variation between formations is less than a factor of 10. For example, the code performed well on experimental data collected during saltwater injection experiments at the University of California, Richmond Field station. The code has not performed well, however, using EM data collected at the Lost Hills oil field, presumably because of the high resistivity contrast between clays and oil-bearing sands.

The new code, based on a formulation developed by Habashy et al.,³ provides much more accurate solutions in regions of high resistivity contrast. In addition, it runs between two and four times faster than the Alumbaugh code. The code is being tested

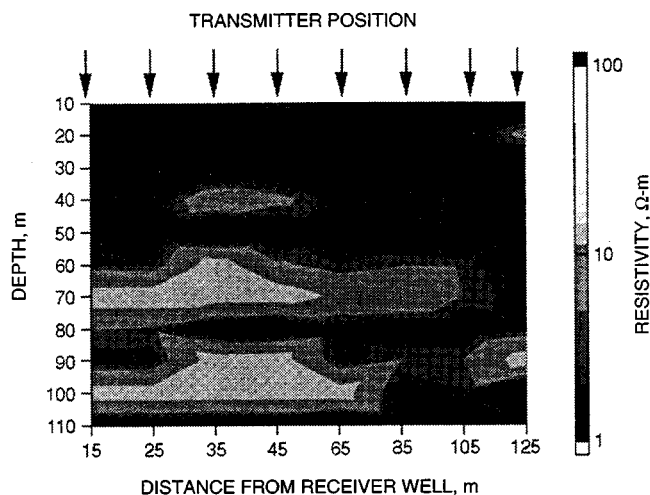


Fig. 3 Resistivity cross section formed by piecing together the one-dimensional inversions from the surface-to-borehole inversions.

on theoretical data and will be applied to field data after these tests are complete.

Field Test of New Borehole Transmitter

Results from a recent field test with a new borehole transmitter show that data collected with the new source repeat to better than 0.2 percent in amplitude and 0.1 degrees in phase over a two-day period. This is a significant improvement from the previous transmitter. The improvement is the result of the design, in which all of the signal-generating components are located within the tool and only dc power is supplied from the surface to operate it. This design eliminates many ground loop paths and thereby reduces noise and measurement drift.

In addition, the tool is considerably more powerful than the initial measurements indicated. At an operating current of 10 A the tool provides a peak moment of about 700 A-m², or about 30% higher than original estimates. The testing did reveal a shortcoming when operating in the presence of metal. Large metallic objects (such as steel well casing) serve to de-tune the oscillator and cause the transmitter not to function. This is unimportant in plastic- or fiberglass-lined wells, but in steel-cased wells the old transmitter tool must be used.

References

1. D. L. Alumbaugh, *Iterative Electromagnetic Born Inversion Applied to Earth Conductivity Imaging*, Ph.D. dissertation, University of California, Berkeley, 1993.
2. M. Wilt and C. Schenkel, Cross-Borehole Electromagnetic Induction at the Dynamic Stripping Clean Site, *Expanded Abstracts of the Society of Exploration Geophysicists Annual Meeting*, New Orleans, La., 1992.
3. T. M. Habashy, R. W. Groom, and B. R. Spies, Beyond the Born and Rytov Approximations: A Nonlinear Approach to Electromagnetic Scattering, *J. Geophys. Res.*, 98(B2): 1759-1775 (1993).

**RESEARCH ON OIL RECOVERY
MECHANISMS IN HEAVY OIL
RESERVOIRS**

Contract No. DE-FG22-93BC14899

**Stanford University
Petroleum Research Institute
Stanford, Calif.**

**Contract Date: Feb. 8, 1993
Anticipated Completion: Feb. 7, 1997
Government Award: \$800,000
(Current year)**

**Principal Investigators:
William E. Brigham
Henry J. Ramey, Jr.**

**Project Manager:
Thomas Reid
Bartlesville Project Office**

Reporting Period: July 1–Sept. 30, 1993

Objectives

The goal of the Stanford University Petroleum Research Institute (SUPRI) is to conduct research directed toward increasing the recovery of heavy oils. Presently SUPRI is working in five main directions:

1. Flow properties studies—to assess the influence of different reservoir conditions (temperature and pressure) on the absolute and relative permeability to oil and water and on capillary pressure.
2. In situ combustion—to evaluate the effects of different reservoir parameters on the in situ combustion process. This project includes the study of the kinetics of the reactions.
3. Steam with additives—to investigate the mechanisms of the process using commercially available surfactants for reduction of gravity override and channeling of steam.
4. Formation evaluation—to develop and improve techniques of formation evaluation, such as tracer tests and pressure transient tests.
5. Field support services—to provide technical support for design and monitoring of Department of Energy (DOE)-sponsored or industry-initiated field projects.

Summary of Technical Progress

Flow Properties Studies

The images from the computerized axial tomography (CAT) scanner can now be fully visualized by the addition of a zoom in and out function, a color map capability, a histogram

feature, and a threshold to the interpretation software. The software package provides for standard calculations. For other calculations, a C code generator has been developed to process computerized tomography (CT) pictures. That program follows a syntax that is a subset of the C language grammar and enables the user to consider images as basic data types. The result is a ready-to-use, user-friendly Motif application prompting the user for different parameters specified by the user. This allows any researcher to perform calculations on CT images without the need to know the internal format of the files or the Motif tool kit.

On the end effect project, more experiments were conducted using the same brine-oil (8% sodium bromide brine-cyclohexane) at 8.0, 4.0, and 1.0 cm³/min flow rates to check the repeatability of the saturation measurements. The analysis of results shows good agreement with the previous runs. The 1.0 cm³/min run indicated that the fluids at the early stage of the imbibition displacement are flowing through only part of the core face. Thus there is a strong possibility of counter current flow of oil at the inlet. Complete analysis of the experiments is being done. The development of software for calculating relative permeabilities by history-matching technique is in progress. Both one-dimensional and two-dimensional simulators will be included in the history-matching method. Different relative permeability models will be used to obtain the best match. The complete drainage capillary pressure curve for the Berea Sandstone core and cyclohexane-brine system has been measured. The measurement of the imbibition capillary pressure curve is in progress.

In Situ Combustion

Most of the quarter was spent moving the kinetics experiment and the tube run apparatus to a specially dedicated laboratory. Data acquisition computers have been connected in the control room and the equipment is now being recalibrated and tested. One of the projects assigned to the new student researchers will involve a repeat of the kinetic runs with metallic additives, with emphasis on understanding the cause of the changes in reactions previously observed. Postburn analysis of the samples should give insight on the transport properties of the metallic salts used to increase the oil reactivity.

SUPRI personnel will help the National Institute for Petroleum and Energy Research organize the symposium on In Situ Combustion Practices to be held in Tulsa, Okla., on April 21 and 22, 1994.

Steam with Additives

The building of the experimental model for steam injection in fractured media has continued. The steam injection system was calibrated. Pressure transducers and plates were cleaned and calibrated. It was necessary to rebuild the injection pumps because of excessive wear of the pistons. A new positioning system to secure the model on the scanning table was also built. Scans were made to determine the best locations for

scanning during the experiments. It is possible to scan between the thermocouple rows and hence avoid artifacts while measuring saturation at two different locations. Data acquisition software was developed for temperatures, heat fluxes, pressure, and production data. Analytical heat transfer calculations for the composite system in two dimensions are sought.

A paper summarizing our research results on steam foam has been written and will be presented at the International Energy Agency (IEA) meeting on October 18 and 19, 1993, in Austria.

Formation Evaluation

The following are the abstracts of the two reports sent to DOE on well testing in gravity drainage situations.

A Finite Difference Model for Free Surface Gravity Drainage¹

A finite-difference model has been developed to simulate the free surface gravity flow of an unconfined single phase, infinitely large reservoir into a well. The model was verified with experimental results in sandbox models in the literature and with classical methods applied to observation wells in the Groundwater literature. The simulator response was also compared with analytical approaches for wellbore pressure at late producing times.

The seepage face in the sandface and the delayed yield behavior were reproduced by the model considering a small liquid compressibility and incompressible porous medium.

The potential buildup (recovery) simulated by the model evidenced a different phenomenon from the drawdown, contrary to statements found in the Groundwater literature. Graphs of buildup potential vs. time, buildup seepage face length vs. time, and free surface head and sand bottom head radial profiles evidenced that the liquid refills the desaturating cone as a flat moving surface. The late time pseudo radial behavior was only approached after exaggerated long times.

Drawdown Behavior for Gravity Drainage Wells²

An analytical solution for drawdown in gravity drainage wells is developed. The free surface flow is viewed as incompressible, and anisotropy effects are included. The well is a line source well, and the reservoir is infinitely large. The model is valid for small drawdowns.

The uniform wellbore potential inner boundary condition is modeled using the proper Green's function. The discontinuity at the wellbore is solved by introducing a finite skin radius, and the formulation produces a seepage face.

The calculated wellbore flux distribution and wellbore pressures are in fair agreement with results obtained using a numerical gravity drainage simulator. Three distinct flow periods are observed. The wellbore storage period is caused by the moving liquid level, and the duration is short. During the long intermediate flow period, the wellbore pressure is nearly constant. In this period, the free surface moves downwards, and the liquid is produced mainly by vertical drainage. At long times, the semilog straight line appears. Confined liquid solutions may be used during the pseudoradial flow period if the flowrate is low. New types curves are presented that yield both vertical and horizontal permeabilities.

Field Support Services

A SUPRI researcher participated in a study of the Wilmington steamflood. Heat and mass balance calculations were used to develop a procedure to estimate heat losses from the surface lines and wells, heat loss to the produced fluids, and the overburden and heat retained in the reservoir. A predictive model for oil production was then derived and run using several scenarios of steam injection rates. If the company allows, this work will be published.

A new researcher has been assigned to the multiphase flow ultrasonic testing loop. The goal of this project is to find a reliable tool for multiphase flow measurements in wells. Preliminary results were presented in January 1993 (Ref. 3). Future work will extend the research to different flow regimes and oil/water systems.

References

1. F. R. Couri and H. J. Ramey, Jr., *A Finite Difference Model for Free Surface Gravity Drainage*, SUPRI Report TR-96, Stanford University Petroleum Research Institute, July 1993.
2. J. A. Aasen and H. J. Ramey, Jr., *Drawdown Behavior for Gravity Drainage Wells*, SUPRI Report TR-97, Stanford University Petroleum Research Institute, September 1993.
3. David A. Dannert and Roland Horne, SUPRI Report TR-89, Stanford University Petroleum Research Institute, January 1993.

DETAILED EVALUATION OF THE WEST KIEHL ALKALINE-SURFACTANT-POLYMER FIELD PROJECT AND ITS APPLICATION TO MATURE MINNELUSA WATERFLOODS

Contract No. DE-AC22-93BC14860

**Surtek, Inc.
Golden, Colo.**

**Contract Date: Jan. 7, 1993
Anticipated Completion: Sept. 30, 1994
Government Award for FY93: \$165,148**

**Principal Investigator:
Malcolm J. Pitts**

**Project Manager:
Thomas Reid
Bartlesville Project Office**

Reporting Period: July 1-Sept. 30, 1993

Objectives

The objectives of this project are to (1) quantify the incremental oil produced from the West Kiehl alkaline-surfactant-polymer (ASP) project by classical engineering and numerical simulation techniques, (2) quantify the effect of chemical slug volume injection on incremental oil in the two swept areas of the field, (3) determine the economic ramifications of the application of the ASP technology, (4) forecast the results of injecting an ASP solution to mature waterfloods and polymer floods, and (5) provide the basis for independent operators to book additional oil reserves by using the ASP technology.

This report documents the initial geological and reservoir engineering data gathering. In addition, some of the initial laboratory results will be discussed. Some evaluation of the West Kiehl has been published.^{1,2}

Summary of Technical Progress

Geological and Reservoir Engineering Evaluation

A geological study of 72 fields surrounding the West Kiehl is complete. Of the 72 fields, 35 were studied in detail. Table 1 lists the fields studied in more detail as well as some information about each field.

Current and estimated ultimate oil recovery data were developed for each of the 35 fields using decline curve analysis. The data are summarized in Table 1. From this list of 35 fields, two were selected for numerical simulation: Simpson Ranch (polymer flood) and South Prairie Creek (waterflood).

Initially Semlek North was selected as the comparative polymer flood. After a more extensive reservoir engineering study, however, Simpson Ranch was thought to be a better analog reservoir to the West Kiehl. A series of geologic maps and cross sections have been prepared for Prairie Creek South and Simpson Ranch. The Minnelusa producing zone was subdivided into separate horizons based on log characteristics and reservoir parameters in both of the analog fields and the West Kiehl. These maps provide the basis for determining pore volumes for each of these zones. Porosity and water saturations from the logs were used to calculate hydrocarbon pore volumes. Reservoir simulation models will be run on both of these fields.

The remaining 33 fields were also being subjected to reservoir analysis. Each of these fields has been mapped in a slightly less rigorous manner than West Kiehl and the two additional fields to be numerically simulated. Pore volumes and oil saturations were calculated. The production histories were subjected to decline analysis to determine ultimate oil recoveries, both primary and secondary. From the primary performance characteristics, reservoirs with a water drive, a partial water drive, and no water drive were defined. A table of information about each field; an isopachous map; and a

plot of the oil production, oil cut, and injection rate was developed for each of the 35 fields. For the Edsel, the information sheet is included as Table 2, the isopachous map as Fig. 1, and the production and injection information as Fig. 2.

Laboratory Study

Two linear corefloods and seven radial corefloods were completed. Relative permeability analysis indicated the Minnelusa Lower B sand is water-wet and the mobility ratio for water-displacing oil averages 2.2. Oil saturation shifts were from 0.836 PV to 0.358 PV, for a recovery of 47.8% of the initial oil saturation. Injection of polymer (Pusher 700) after the waterflood recovered no additional oil. Injection of 0.8 wt % Na_2CO_3 plus 0.1 wt % Petrostep B-100 plus Pusher 700 reduced the oil saturation to 0.224 PV for an additional recovery of 0.134 PV of incremental oil or 37.4% of the waterflood residual oil. Dynamic retention of chemical from the linear corefloods averaged 72,966 lb/acre-ft for Na_2CO_3 , 5,123 lb/acre-ft for Petrostep B-100, and 723 lb/acre-ft for Pusher 700 injected with Na_2CO_3 plus Petrostep B-100 and averaged 314 lb/acre-ft when injected dissolved in Fox Hills water prior to ASP solution. When Pusher 700 dissolved in injection water was injected after the ASP solution, an additional 49 lb/acre-ft was retained by the Minnelusa sand. On the basis of resistance factor and chemical retention data of these linear corefloods, the injection concentration of 1050 mg/L Pusher 700 is sufficient for mobility control if 1 PV of polymer were injected.

Chemical oil recoveries of the radial corefloods using 4-in. radial discs are summarized in Table 3. The chemical floods were performed with no waterflood prior to chemical injection with the exception of two corefloods.

The average polymer flood performed no better than the average waterflood, 45.1% initial oil saturation (S_{oi}) vs. 46.6% S_{oi} , respectively. However, injection of 0.8 wt % Na_2CO_3 plus 0.1 wt % Petrostep B-100 plus 1050 mg/L Pusher 700 recovered 15% S_{oi} . Additional oil was recovered when 30% PV or more of ASP slug was injected. Reducing the volume of ASP slug injected to 13% PV lowered the incremental oil production to 6.2% S_{oi} .

Numerical Simulation of the West Kiehl Field

The net sand isopachous maps have been input into the simulator and the grid system designed. A history match has not been achieved. A radial coreflood history match to calibrate the chemical option of the numerical simulator has been initiated, but a history match has not been achieved.

Simulation Analyses Application to Waterflooded Minnelusa Fields

This section has not been started.

TABLE 1

Listing of Select Minnelusa Reservoirs in Study Area*

FIELD	PROD ZONE	DRIVE MECHANISM PRIMARY SECONDARY	LOCATION TWP SEC	RGE	CUM PROD thru 1992		INJECTION thru 1992		DISC DATE	UNIT DATE	OIL GRAV	TOTAL PROD	WELLS INU	VOLUME acre ft	AREA acres	AVG NET PAY FEET	AVG POR	
					OIL Mbbbls	WTR Mbbbls	in 1992	thru 1992										Mbbbls
ALPHA	MNLS C	PART WTR DR	1,241 51N	68W	954,237	3,958.3	1,468,600	4,107.8	1986	1989	25.3	10	5	13,922.21	393.78	35.36	18.60%	
AMERICAN	MNLS UB	POL-WTRFLD	336 52N	68W	29,205	64.1	63,028	3,001.1	1986	1988	20.3	4	2	3,023.56	14.79	17.58%		
AMMO	MNLS UB	WATER FLOOD	16 17 52N	68W	13,207	171.0	18,160	650.3	1985	1988	19.9	2	1	9,680.00	78.00	13.00	20.10%	
ART CREEK	MNLS A:UB	SOL GAS	6 5 51N	67W	10,989	868.3	715.0	282,700	1,725.0	1981	23.3	3	1	3,949.70	145.33	27.19	19.34%	
ASH	MNLS UB	PART WTR DR	27 26 52N	68W	35,734	275.0	3.0	21,378	21.4	1975	20.0	3	2	2,085.70	95.54	21.60	18.78%	
BERGER HILL	MNLS UB	WATER DRIVE	6 5 51N	67W	35,407	1,019,955	921.3	10,609.4	10,609.4	1975	19.9	3	1	5,078.55	183.38	14.72	25.00%	
BRACKEN	MNLS UB	POL-WTRFLD	12 18 52N	68W	30,977	471.2	988.5	422,655	1,476.6	1983	21.4	3	2	3,019.31	109.92	15.47	17.32%	
BREKENS	MNLS UB	WATER DRIVE	28 52N	68W	329,751	37,216	1,774.5	1,604.0	1978	1980	21.0	3	2	5,056.73	205.82	30.34	22.98%	
CAMBRIDGE	MNLS UB	AUG WTR DR	28 53N	68W	38,185	1,174	0	0	1989	1993	20.2	6	4	5,066.23	218.06	23.33	20.22%	
CAMBRIDGE	MNLS UB	POL-WTRFLD	18 19 53N	67W	65,127	119,829	1,254.7	5,461.1	1973	1979	22.6	6	4	5,461.10	585.63	24.82	18.07%	
DEADMAN CREEK	MNLS UB	POL-WTRFLD	18 19 53N	67W	208,157	187,884	4,669.9	1,895,200	12,343.7	1981	1984	21.0	7	5	10,059.79	375.82	27.05	22.52%
EDSEL	MNLS A:UB	WATER FLOOD	25 26 53 54 N	67W	193,754	92,214	3,945.8	1,037,399	9,688.5	1983	1988	21.0	6	4	8,338.47	217.87	38.37	21.32%
GUTHRY	MNLS A:UB	WATER FLOOD	8 9 52N	68W	24,972	17,234	718.0	2,740.4	1980	1986	22.0	6	3	6,845.34	247.87	27.75	21.50%	
HEATH	MNLS C	WATER DRIVE	4 8 52N	68W	12,282	595.1	684.1	1,116.4	1987	1987	22.0	5	3	2,060.07	87.86	19.64	28.65%	
HEATH NORTH	MNLS UB	WATER FLOOD	24 52N	68W	305,759	353,160	2,537.7	43,590	220.0	1974	1986	19.0	2	2,078.19	123.89	13.59	16.73%	
HOOPER GULCH	MNLS UB	POL-WTRFLD	30 8 1 53N	68W	74,500	136,074	2,824.2	810,300	3,264.1	1973	1985	21.8	6	3	11,985.32	383.37	30.88	22.10%
NIHIL	MNLS UB	AST-WTRFLD	23 50 53N	68W	74,500	136,074	2,824.2	220,821	1,072.5	1985	1987	24.0	6	1	2,086.45	145.02	14.39	19.05%
NIHIL WEST	MNLS UB	WATER FLOOD	17 18 54 55 N	68W	18,534	328,535	2,464.3	1,890.0	4,674.2	1978	1982	21.3	6	3	6,912.08	323.08	27.58	21.20%
LAD	MNLS A:UB	WATER FLOOD	18 19 54 N	68W	18,534	328,535	2,464.3	853,503	3,364.2	1984	1987	21.7	5	3	5,077.03	213.30	23.80	21.30%
LITTLE MISSOURI	MNLS UB	POL-WTRFLD	5 1 52 54 55 N	68W	210,902	96,838	1,984.7	332,364	1,228.2	1986	1989	22.9	8	5	2,283.82	272.56	19.04	19.17%
LITTLE MITCHELL CRK	MNLS UB	WATER FLOOD	8 9 52N	67W	204,692	340,848	9,481.3	3,574.7	12,665.8	1986	1989	25.4	10	8	19,076.52	663.82	28.75	20.44%
LONGSTAR	MNLS UB	POL-WTRFLD	8 9 52 53 N	68W	390,692	89,831	2,005.6	1,250,481	5,001.1	1984	1987	25.0	10	5	7,218.94	261.00	27.66	20.70%
LONGSTAR	MNLS A:UB	WATER FLOOD	21 10 51 52 N	68W	139,015	1,457,911	6,195.0	1,990,428	27,000.9	1980	1985	20.7	12	4	14,171.89	518.21	27.35	22.65%
MELCOTT RANCH	MNLS UB	WATER FLOOD	22 6 53N	68W	72,532	165,319	1,477.9	1,477.9	1983	1983	22.4	4	2	3,471.31	249.68	13.93	22.91%	
OSHTO NORTH	MNLS LB	WATER DRIVE	24 53N	68W	83,481	123,288	1,037.1	792.3	1984	1984	22.4	2	2	2,754.58	107.20	25.70	22.00%	
PERDUE CREEK SO	MNLS UB	WATER FLOOD	16 52N	68W	50,772	115,159	652.5	135.4	1985	1985	21.2	3	1	1,851.12	94.08	17.55	20.94%	
REYNOLDS RANCH	MNLS UB	WATER DRIVE	6 1 52N	68W	24,617	972,181	1,968.8	10,927.7	1974	1981	24.0	2	2	1,839.91	87.78	20.86	26.60%	
RIELE	MNLS LB	PART WTR DR	15 52N	68W	68,668	320,062	0	205,805	279.8	1985	1991	25.0	1	1	2,577.00	86.50	29.79	17.10%
SEMLEK	MNLS LB	WATER DRIVE	27 52N	68W	44,841	118,910	3,223.7	5,009.8	1982	1982	22.6	4	2	6,437.54	253.48	25.40	21.20%	
SEMLEK NORTH	MNLS UB	WATER DRIVE	16 52 1 52N	68W	51,661	118,910	1,438.0	888.8	1975	1988	23.0	4	3	3,846.19	207.00	18.58	16.51%	
SEMLEK WEST	MNLS UB	WATER DRIVE	28 50 52N	68W	128,646	1,285,170	5,790.9	536,708	12,369.4	1982	23.6	14	5	15,284.43	574.49	28.81	18.73%	
SEMPSON RANCH	MNLS UB	AUG WTR DR	11 5 51N	68W	21,746	242,655	781.7	2,749.0	1977	1980	21.0	4	2	3,587.05	172.00	20.85	18.03%	
TERACE	MNLS LB	WATER DRIVE	11 3 51N	68W	419,311	585,989	3,631.1	2,847.0	1985	1985	21.0	6	2	8,885.54	268.05	33.15	23.52%	
WAGONSPOKE	MNLS LB	PART WTR DR	3 3 52 54 53 N	68W	38,635	119,234	2,915.6	7,468.8	1,102,741	13,639.8	1972	28.0	3	2	6,265.52	258.00	24.46	19.60%
WOLF DRAW	MNLS UB	POL-WTRFLD	18 24 52N	68 66 68 W	121,299	7,152	503.6	92.5	1986	1986	21.5	4	2	4,436.48	298.26	16.48	17.31%	
TOTALS					4,746,538	15,031,995	69,938.8	16,121,136	127,130.3			207	119	53	211,294.59	8,480.17		
AVERAGE					135,672	429,474	1,998.3	597,079	4,708.5	1979	1985	22.1	6	3	6,036.99	242.29	23.50	20.27%
MAXIMUM					894,237	1,871,993	9,481.3	1,990,428	27,000.9	1980	1985	28.0	14	6	19,076.52	663.82	38.37	26.65%
MINIMUM					12,734	0	0.0	0	0.0	1980	1985	19.0	2	1	968.00	76.00	13.00	16.60%

TABLE 1 (Continued)

FIELD	PROD ZONE	AVG SW %	FVF factor	FM TEMP	RW @ FM TEMP	PORE VOLUME Mbbbl	ORIGINAL O.I.P. Mbbbl	CURR OIL-CUT %	PROJ REM RES Mbbbl	TOT RES Mbbbl	EST RECOVERY %	ULTR % O.O.P.	DEPL FACTOR %	EST PRI TOT REC Mbbbl	EST PRI % O.O.P.	OOIP PV	UI TOIL REC PV	CUM OIL REC PV	CUM WTR REC PV	CUM INI BALANCE	ABD O.I.P. PV	
																						150
ALPHA	MNLS C	32.68%	1.050	150	0.65	17,920.4	11,449.2	2,340	61.32%	1,179.2	5,035.5	60	43.98%	76.59%	16.54%	1,893.6	0.281	0.215	0.076	0.229	-0.062	0.358
AMERICAN	MNLS UB	27.00%	1.050	133	0.39	4,124.1	2,887.2	78	54.13%	290.6	290.6	28	10.14%	84.00%	2.54%	0.695	0.639	0.070	0.020	0.062	0.003	0.625
AMMO	MNLS ABUB	31.20%	1.043	134	0.22	1,540.6	1,168.0	42	33.15%	31.1	294.1	40	17.47%	80.76%	3.26%	0.738	0.132	0.112	0.297	0.422	0.013	0.626
ART CREEK	MNLS UB	15.50%	1.025	104	0.20	5,931.8	3,952.7	110	33.11%	88.4	956.7	49	24.20%	90.76%	12.41%	0.666	0.666	0.161	0.121	0.291	0.024	0.505
ASH	MNLS UB	45.00%	1.044	138	0.49	2,715.1	2,263.7	35	91.59%	368.4	640.4	60	28.29%	42.47%	28.10%	0.834	0.236	0.100	0.001	0.008	-0.093	0.588
BERGER HILL	MNLS UB	25.00%	1.040	140	2.00	5,970.8	3,444.7	97	33.5%	47.8	989.1	20	28.15%	95.08%	28.13%	0.577	0.162	0.154	1.775	0.353	0.176	0.524
BRACKEN	MNLS UB	25.00%	1.050	132	0.13	4,181.0	2,966.4	222	60.85%	326.3	3,629.0	117	26.70%	49.91%	147.7	0.714	0.191	0.113	0.064	0.425	-0.179	0.356
BREAGNS	MNLS UB	25.00%	1.050	143	0.30	11,332.8	7,663.1	903	48.00%	1,854.1	3,629.0	176	44.90%	63.44%	316.2	0.680	0.298	0.027	0.004	0.000	-0.031	0.364
CAMBRIDGE	MNLS UB	32.00%	1.030	133	0.30	7,655.8	5,246.7	105	78.58%	2,138.6	2,356.0	63	7.04%	8.55%	271.4	0.620	0.258	0.164	0.108	0.713	0.442	0.472
DEADMAN CREEK	MNLS UB	32.00%	1.040	120	0.24	13,669.8	5,594.6	178	35.25%	723.2	1,977.9	248	35.35%	63.44%	271.4	0.680	0.288	0.242	0.425	0.697	0.029	0.374
EDSEL	MNLS ABUB	32.00%	1.030	147	0.25	17,575.5	11,603.2	325	10.98%	1,064.8	4,102.6	81	15.99%	87.05%	822.4	0.524	0.300	0.289	0.415	0.709	0.005	0.325
GUTHRY	MNLS UB	35.00%	1.040	130	0.30	13,669.8	8,543.5	360	20.60%	1,167.0	8,008.0	25	32.66%	85.43%	800.8	0.571	0.187	0.073	0.279	0.005	0.005	0.440
HEATH	MNLS C	45.00%	1.050	154	1.00	9,291.2	5,146.2	89	42.51%	304.8	654.8	173	33.54%	53.45%	128.1	0.724	0.243	0.130	0.157	0.082	-0.205	0.481
HEATH NORTH	MNLS UB	40.00%	1.050	150	1.02	2,697.3	1,952.1	824	37.61%	220.4	1,003.1	64	46.22%	78.03%	96.4	0.704	0.175	0.123	0.033	0.159	0.003	0.573
HOOPER GULCH	MNLS UB	24.00%	1.030	137	0.15	20,566.2	15,374.0	208	20.56%	183.7	2,848.0	42	33.45%	93.55%	385.0	0.631	0.325	0.254	0.079	0.348	0.015	0.379
MIEHL	MNLS UB	23.00%	1.030	134	0.28	13,501.3	8,520.2	498	21.06%	215.4	2,166.2	31	31.65%	90.06%	788.0	0.740	0.234	0.211	0.157	0.364	0.009	0.420
MIEHL WEST	MNLS ABUB	35.00%	1.030	140	0.13	9,240.2	6,841.3	578	66.54%	996.8	1,955.6	137	33.80%	49.80%	303.5	0.740	0.253	0.211	0.157	0.364	-0.004	0.506
LAV	MNLS UB	23.00%	1.030	120	0.14	7,858.1	5,874.5	561	37.53%	785.4	1,955.6	115	47.51%	92.35%	2,143.0	0.714	0.339	0.313	0.118	0.419	-0.013	0.375
LITTLE MISSOURI	MNLS UB	25.00%	1.050	136	0.07	30,250.3	21,607.4	1,070	32.04%	1,788.1	4,388.7	115	46.76%	59.26%	842.2	0.810	0.379	0.224	0.176	0.431	0.032	0.431
LITTLE MITCHELL CRK	MNLS ABUB	15.00%	1.050	136	0.27	21,173.8	15,135.0	381	8.71%	102.1	6,297.1	13	41.61%	98.38%	992.0	0.715	0.297	0.293	0.997	1.275	-0.014	0.417
LONE CEDAR	MNLS UB	24.00%	1.040	116	0.27	11,592.9	9,384.8	199	30.49%	438.2	1,611.1	162	42.83%	72.80%	1,611.1	0.635	0.272	0.198	0.249	0.082	-0.032	0.363
MELLOTT RANCH	MNLS ABUB	34.00%	1.040	120	0.45	5,927.4	3,761.6	229	40.37%	430.2	1,467.3	52	38.22%	85.15%	1,330.0	0.615	0.312	0.221	0.169	0.327	0.034	0.462
OSMOTO NORTH	MNLS UB	36.00%	1.030	120	0.45	4,701.4	2,893.2	139	30.60%	113.8	766.3	36	58.22%	85.15%	973.4	0.748	0.286	0.243	0.050	0.327	0.034	0.363
PRAIRIE CREEK SO	MNLS UB	23.00%	1.030	120	0.09	2,682.3	2,005.2	67	2.47%	(23.4)	973.4	0	44.01%	122.95%	973.4	0.583	0.256	0.315	2.878	0.082	-0.032	0.326
REYNOLDS RANCH	MNLS UB	40.00%	1.030	128	1.60	3,418.7	2,179.4	243	100.00%	262.9	651.6	70	29.90%	59.65%	425.2	0.638	0.191	0.114	0.000	0.473	0.380	0.380
RULE	MNLS UB	33.70%	1.040	110	0.15	10,587.8	7,431.8	123	12.29%	187.5	3,411.2	69	45.90%	94.50%	3,411.2	0.702	0.322	0.304	0.473	0.177	-0.208	0.350
SEMLEK	MNLS UB	27.00%	1.040	110	0.15	5,015.9	3,279.6	142	30.29%	187.8	1,525.8	60	46.52%	94.24%	1,051.1	0.654	0.304	0.281	0.098	0.557	-0.408	0.353
SEMLEK NORTH	MNLS UB	32.00%	1.040	120	0.15	22,209.4	13,890.9	352	9.10%	256.0	6,046.9	33	43.56%	95.77%	5,297.4	0.625	0.272	0.261	0.704	0.577	0.848	0.448
SEMLEK WEST	MNLS UB	35.00%	1.050	120	0.20	5,017.4	3,106.0	60	8.22%	78.8	870.5	78	28.02%	90.96%	1,302.0	0.619	0.173	0.158	0.377	0.548	0.013	0.448
SIMPSON RANCH	MNLS UB	35.00%	1.050	140	0.18	16,213.3	11,889.7	1,149	41.71%	2,160.8	5,791.9	147	48.71%	62.69%	5,791.9	0.733	0.357	0.224	0.176	0.425	0.340	0.429
TERRACE	MNLS UB	23.00%	1.050	128	0.05	9,572.8	6,928.9	100	2.98%	(90.8)	2,824.8	0	40.77%	103.21%	1,123.7	0.724	0.295	0.305	0.780	1.425	0.340	0.429
WAGONSPOKE	MNLS UB	24.00%	1.050	128	0.05	5,957.8	4,369.0	332	93.99%	746.9	1,250.5	114	28.62%	40.27%	480.5	0.733	0.210	0.085	0.016	0.087	-0.013	0.523
WOLF DRAW	MNLS UB	23.00%	1.050	130	0.65	329,754.3	225,179.5	13,010	19.0731	88,012.0	37,890.1											
TOTALS																						
AVERAGE		29.03%	1.040	130	0.39	9,421.6	6,433.7	372	24.01%	2,160.8	2,514.6	81	39.09%	79.47%	1,082.6	0.663	0.267	0.212	0.338	0.386	0.165	0.416
MAXIMUM		45.00%	1.050	154	2.00	30,250.3	21,607.4	2,340	100.00%	5,168.0	10,266.7	248	50.72%	122.95%	5,791.9	0.834	0.379	0.315	2.878	1.425	0.442	0.626
MINIMUM		15.00%	1.014	104	0.05	1,540.6	1,168.0	35	2.47%	(23.4)	204.1	0	10.14%	9.23%	39.2	0.524	0.070	0.027	0.000	0.000	-0.408	0.303

*Minnelusa Field Production, T. 51 N. to 55 N., R. 67 W. to 69 W. Prod-sel Oct. 2, 1993. Total Fields, 35. Waterfloods, 13; polymer waterfloods, 12; alkaline-surfactant-polymer waterfloods, 1. Water drives, 8; augmented water drives, 3.

TABLE 2

Edsel Field Information Summary

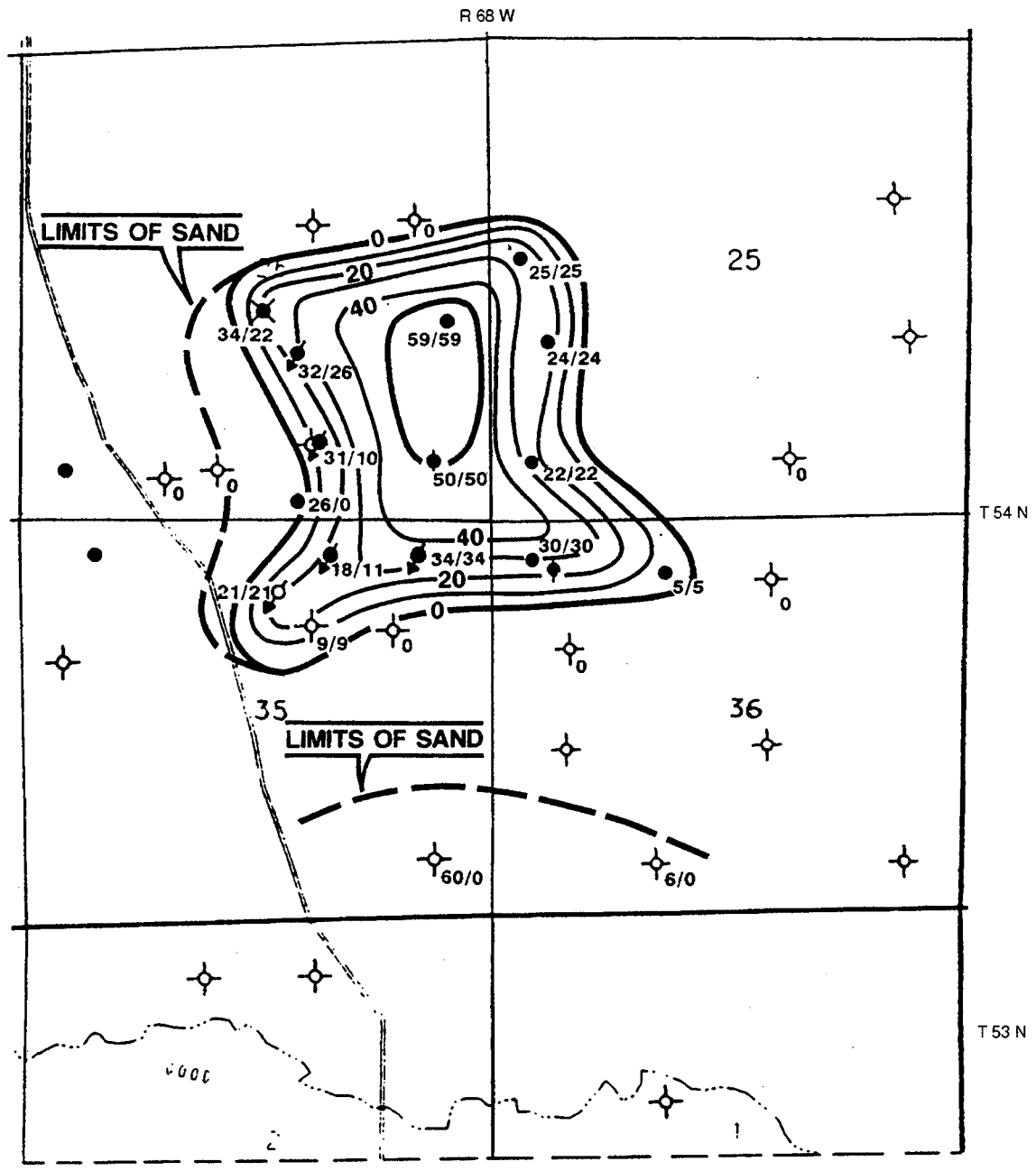
Field	Edsel	Discovery	1981
Producing Zone	Minnelusa Upper B	Unit	1984
Location	Crook County, Wyo.	Oil gravity	21.0
	Sec. 25, 26, 35, and 36,	Oil viscosity, cP	17.2
	and T. 54 N., R. 68 W.	Water viscosity, cP	0.46
Drive Mechanism	Waterflood	Depth, ft.	6,431
		Formation Temperature, °F	147
		R _w @ Formation temperature, Ω	0.25
Current Production		Reservoir Properties	
1/1 to 12/31/92			
Oil, bbl	208,157	Volume, acre-ft	10,059.79
Water, bbl	1,671,895	Area, acre	375.82
		Average net pay, ft	27.05
		Average porosity, %	22.52
		Average S _w , %	32.00
		Formation volume factor	1.030
Cumulative Production			
through 12/31/92			
Oil/mdbl	4,260.2	Pore volume, Mdbl	17,575.5
Water, Mdbl	7,468.9	Oil in place, Mdbl	11,603.2
Injection, Mdbl	12,243.7	Estimated ultimate recovery, % OOIP	43.34
		Current recovery % OOIP	36.72
		Current depletion, %	84.71
Current Rates		Primary Decline Analysis	
Oil, BOPD	570	Economic cutoff	
Oil cut, %	11.07	Oil, BOPD	90
		End of primary decline	03/1984
		Estimated decline, %	45.00
		Projected ultimate recovery, Mdbl	817.2
		Primary recovery, % OOIP	7.04
		Cumulative oil, PV	0.242
		Cumulative water, PV	0.425
		Cumulative injection, PV	0.697
		Balance	0.029
Waterflood Decline Analysis		Primary Decline Analysis	
Economic cutoff		Economic cutoff	
Oil, BOPD		Oil, BOPD	90
Oil cut, %	5.00	End of primary decline	03/1984
Estimated decline, %	15.00	Estimated decline, %	45.00
Projected ultimate recovery, Mdbl	5028.9	Projected ultimate recovery, Mdbl	817.2
Projected remaining reserves, Mdbl	768.8	Primary recovery, % OOIP	7.04
Estimated remaining life, yr (from 1/1/93)	5.25	Cumulative oil, PV	0.242
Original oil in place (OOIP), PV	0.660	Cumulative water, PV	0.425
Ultimate recovery, PV	0.286	Cumulative injection, PV	0.697
Remaining oil in place, PV	0.374	Balance	0.029

Production

Location	Name	Cumulative oil, bbl	Cumulative water, bbl	Status
SWSW 25-54-68	Brislawn #7	571,285	1,385,670	Pump-oil
NWSW 25-54-68	Brislawn #8	393,139	71,992	Pump-oil
SWNW 25-54-68	Unit #9	343,769	110,273	Pump-oil
NWSE 26-54-68	Brislawn #1	93,064	48,139	Inj
NESE 26-54-68	Brislawn #4	1,888,014	3,765,755	Pump-oil
SESE 26-54-68	Brislawn #5	432,390	339,238	Si-oil
NWSE 26-54-68	Brislawn #2	2,760	14,843	Swd
SWSE 26-54-68	Good Lad #1	20,518	17	Inj
NENE 35-54-68	Unit #7	22,152	29,344	Inj
NWNW 36-54-68	State #1	465,649	1,647,019	Pump-oil
NENW 36-54-68	State #2	54,587	31	Pump-oil
SWNW 36-54-68	State #3	265	5,280	Ta-oil

Injection

Location	Name	Current injection, bbl	Cumulative injection, bbl	Status
SWSE 26-54-68	Good Lad #1	412,991	3,572,024	Inj
NWSE 26-54-68	Brislawn #1	430,515	3,839,904	Inj
NENE 35-54-68	Unit #7	1,051,676	4,851,724	Inj



- Legend
- | | |
|----------------------|--------------------------------|
| ◆ Dry hole | ◊ Water injector |
| ● Producing oil well | ◻ Water disposal |
| ◆ Shut-in oil well | 70/65 Net porosity/net oil pay |
| ◆ Abandoned oil well | |

Fig. 1 Isopachous map of Edsel Field, Minnelusa Upper B. Isopach: net oil pay. Scale 1 in. = 2000 ft.

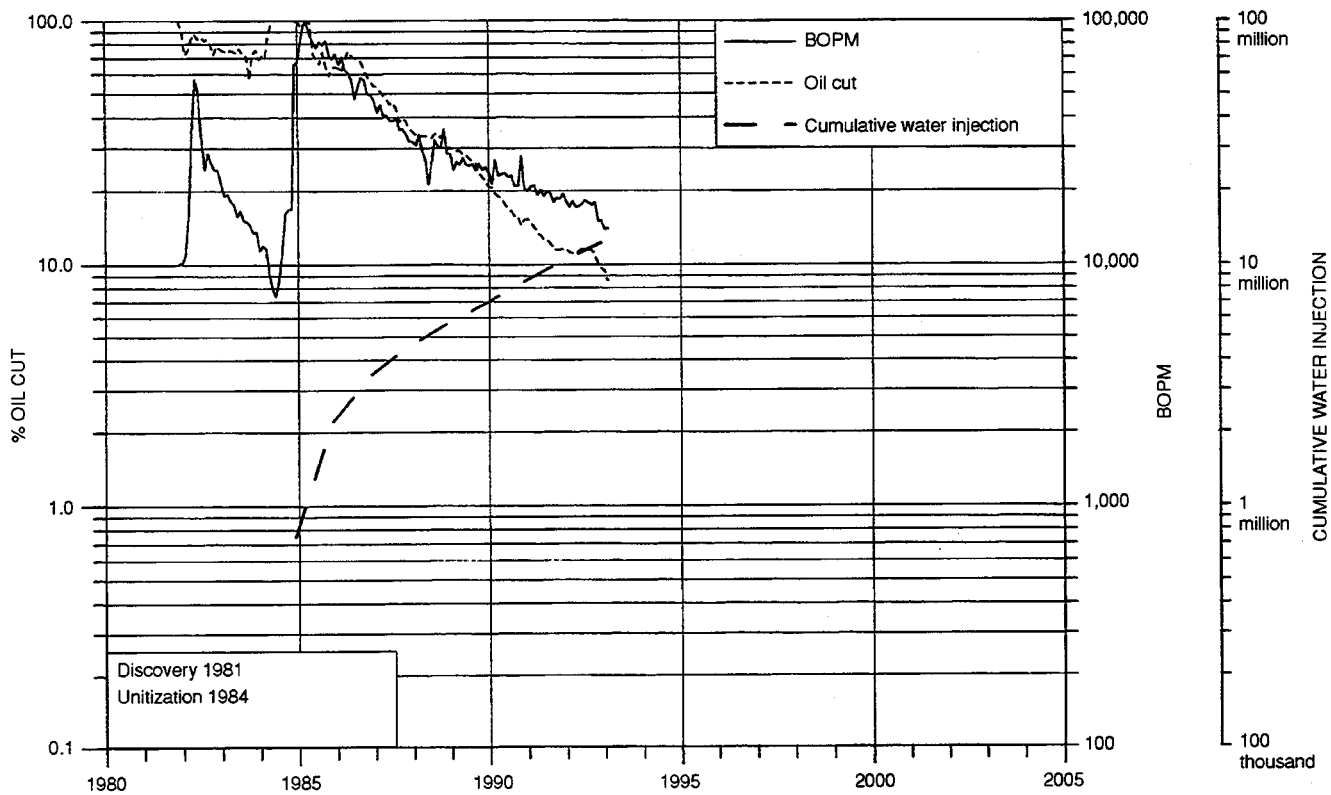


Fig. 2 Production and injection information for Edsel Field, Minnelusa Upper B. BOPM, barrels of oil per month.

TABLE 3

**Chemical Oil Recoveries of the Radial Corefloods
(4-in. Radial Discs)**

Chemical injected	Waterflood recovery, % S_{oi}^*	Chemical flood recovery, % S_{oi}	Combined recovery, % S_{oi}
Waterflood followed by 37% PV ASP†	45.4	12.6	58.0
Waterflood followed by 13% PV ASP	47.7	5.5	53.2
29% PV ASP-10% PV polymer	-	61.2	-
13% PV ASP-26% PV polymer	-	52.7	-
94% ASP-no polymer	-	65.9	-
43% polymer	-	40.0	-
40% polymer	-	50.2	-

* S_{oi} , initial oil saturation.
†ASP, alkaline-surfactant-polymer.

References

1. S. R. Clark, M. J. Pitts, and S. M. Smith, Design and Application of an Alkaline-Surfactant-Polymer Recovery System to the West Kiehl Field, *SPE Advanced Technology Series*, 1(1): 172-179 (April 1993).
2. J. J. Meyers, M. J. Pitts, and K. Wyatt, *Alkaline-Surfactant-Polymer Flood of the West Kiehl, Minnelusa Unit*, Report SPE/DOE 24144.

**MODIFICATION OF RESERVOIR
CHEMICAL AND PHYSICAL FACTORS
IN STEAMFLOODS TO INCREASE
HEAVY OIL RECOVERY**

Contract No. DE-FG22-90BC14899

**University of Southern California
Los Angeles, Calif.**

**Contract Date: Feb. 22, 1993
Anticipated Completion: Feb. 21, 1996
Government Award: \$150,000
(Current year)**

**Principal Investigator:
Yanis C. Yortsos**

**Project Manager:
Thomas Reid
Bartlesville Project Office**

Reporting Period: July 1–Sept. 30, 1993

Objectives

The objectives of this contract are to continue previous work and to carry out new fundamental studies in these areas of interest to thermal recovery: displacement and flow properties of fluids involving phase change (condensation–evaporation) in porous media; flow properties of mobility control fluids (such as foam); and the effect of reservoir heterogeneity on thermal recovery. The specific projects are motivated by and address the need to improve heavy oil recovery from typical reservoirs as well as from less conventional fractured reservoirs producing from vertical or horizontal wells.

Thermal methods, and particularly steam injection, are currently recognized as the most promising for the efficient recovery of heavy oil. Despite significant progress, however, important technical issues remain. Specifically, knowledge of the complex interaction between porous media and the various fluids of thermal recovery (steam, water, heavy oil, gases, and chemicals) is still inadequate, and the interplay of heat transfer and fluid flow with pore- and macro-scale heterogeneity is largely unexplored.

Summary of Technical Progress

Vapor–Liquid Flow

During this quarter investigations continued on phase change in porous media and on steam drive mechanisms. A substantial effort was devoted to summarizing many previous theoretical and experimental results on bubble growth in

porous media.^{1–4} Two topical reports on this subject were also prepared. In these papers patterns and rates of growth, the stability of interfaces, and the competition between various growing clusters are discussed. A pore network simulator has been developed that allowed investigation of mass transfer and heat transfer effects on the growth of the gas clusters. Further work on the effects of solid conduction and liquid convection in the pore space is being currently completed. Whereas the effect of solid conduction is found to be minimal, the effect of liquid convection on the growth rate is quite important. Work continues on effects of gravity and on the pore network simulation of the injection problem.

Further experimental work was conducted to investigate the recovery of trapped oil from dead-end pores in glass micromodels by steam injection. A substantial recovery was observed. Two mechanisms were identified as contributing to this result: a viscous coupling between the injected gas phase and oil films, which was also found to exist in typical gas injection experiments, and film flow of oil between the vapor phase and condensed water. The process to model these mechanisms is under way. A theoretical effort is also in place to model the oscillatory behavior of steam front propagation observed in many of these experiments.

Heterogeneity

In parallel, glass micromodel experiments were conducted to investigate the injection of steam in fractured systems. The displacement of the nonwetting phase from the matrix is possible by two mechanisms, one involving imbibition by the condensed water and another involving penetration of the vapor phase, provided that injection rates are sufficiently high and that condensation effects are limited. The latter process has many similarities with drainage in fractured systems, which was explored in a previous study.⁵ Imbibition of the matrix was modeled with a pore network simulator, the elements of which were presented at the Society of Petroleum Engineers Annual Fall Meeting in October 1993 in Houston, Tex.⁶ Comparison of experiments and simulations for imbibition in a fracture-matrix system, which were shown to be in good agreement, are reported.⁷

Continuing also is an effort to provide alternatives to the conventional description of low-rate imbibition and to assess effects of heterogeneity in such processes. In parallel, a numerical study of capillary invasion in anisotropic systems is nearing completion. In this study the capillary pressure curve in anisotropic systems is direction-dependent; namely, it also depends on the saturation gradient, in addition to the saturation, even in systems where the pore-size distribution is the same in both directions (complete overlap). These results have important implications for displacements in anisotropic systems. Work also continues on the use of Vertical Equilibrium concepts to the description of displacement problems, including steam injection.

Chemical Additives

During the past quarter, displacement experiments of a Bingham plastic by the injection of a Newtonian fluid in Hele-Shaw cells and packed cells were conducted to mimic the displacement behavior of some heavy oils. The experiments were successfully simulated with pore network models previously developed. A technical report on the general properties of Bingham plastics and their displacement was also prepared.⁸ Finally, a summary is given of the past research on single-phase power law fluid flow in porous media in a technical paper.⁹

In parallel, progress continued in the modeling of foam flow in porous media. Two efforts are made in this direction. In one an investigation is conducted of the suitability of macroscopic continuum models. Analysis of the system of hyperbolic equations that have been proposed to describe foam propagation found some useful solution methods, even though this particular system of equations also involves nonhomogeneous (reaction rate) terms. However, such models were found inadequate to describe the experiments of Baghdikhian and Handy.¹⁰ To reconcile these differences, work continued on the development of pore-network models to describe foam generation and propagation.

References

1. X. Li and Y. C. Yortsos, Bubble Growth in Porous Media, *Chem. Eng. Sci.* (submitted in 1993).
2. G. Satic, X. Li, and Y. C. Yortsos, Scaling of Bubble Growth in Porous Media, *Phys. Rev. Lett.* (submitted in 1993).
3. X. Li and Y. C. Yortsos, Visualization and Numerical Simulation of Bubble Growth in Pore Networks, *A.I.Ch.E. J.* (submitted in 1993).
4. X. Li and Y. C. Yortsos, Bubble Growth and Stability in an Effective Porous Medium, *Phys. Fluids A* (submitted in 1993).
5. M. Haghighi, B. Xu, and Y. C. Yortsos, Visualization and Simulation of Immiscible Displacement in Fractured Systems Using Micromodels: I. Drainage, *J. Colloid Interface Sci.* (submitted in 1993).
6. M. Chaouche, N. Rakotomalala, D. Salin, B. Xu, and Y. C. Yortsos, paper SPE 26658 presented at the 1993 SPE Annual Fall Meeting, October 1993, Houston, Tex.
7. M. Haghighi, B. Xu, and Y. C. Yortsos, Visualization and Simulation of Immiscible Displacement in Fractured Systems Using Micromodels: II. Imbibition, *J. Colloid Interface Sci.* (submitted in 1993).
8. C. Shah and Y. C. Yortsos, paper presented at the Heavy Oils and Tar Sands Symposium, Nov. 18-19, 1993, Lexington, Ky.
9. C. Shah and Y. C. Yortsos, Aspects of Flow of Power-Law Fluids in Porous Media, *A.I.Ch.E. J.* (submitted in 1993).
10. S. Baghdikhian and L. L. Handy, *Transient Behavior of Simultaneous Flow of Gas and Surfactant Solution in Consolidated Porous Media*, DOE Topical Report, July 1991.

GEOSCIENCE TECHNOLOGY

**CHARACTERIZATION AND MODIFICATION
OF FLUID CONDUCTIVITY IN
HETEROGENEOUS RESERVOIRS
TO IMPROVE SWEEP EFFICIENCY**

Contract No. DE-AC22-89BC14474

**University of Michigan
Ann Arbor, Mich.**

**Contract Date: Sept. 26, 1989
Anticipated Completion: Sept. 26, 1993**

**Principal Investigator:
H. Scott Fogler**

**Project Manager:
Robert Lemmon
Bartlesville Project Office**

Reporting Period: July 1–Sept. 30, 1993

Objective

The objective of this work is to develop effective flow-diverting techniques through experimentation with the use of neutron imaging for flow characterization before and after treatment. Theoretical modeling will be used to identify the

important parameters that govern the process of diverting fluids.

Summary of Technical Progress

During the final quarter of this year all research was compiled and the final report written. The primary focus of the work conducted was the development and study of new profile modification techniques. The following is a summary of the investigations into the fundamental aspects of each fluid diversion system.

The main objectives of this project were to develop new treatment strategies that would improve the efficiency of oil production and stimulation procedures. Treatment strategies were developed to treat injection well matrix heterogeneities, production well matrix or saturation heterogeneities, and fractured wells. The treatment strategies investigated included a particulate system, a foamed gel for injection well profile modification, a foam-acid injection strategy for improving acidization of carbonates, an acid reactive gel for controlling acid leak-off into fractures, and a water-reactive gel for water shutoff at production wells. The research performed focused on discovering the principles governing the performance of the treatment strategies to provide a fundamental basis for further development of these techniques. Other goals of this project were to demonstrate the use of neutron imaging for real-time imaging of fluid flow through heterogeneous porous media and develop a kinetic model to

simulate the effect of diagenetic processes on reservoir porosity and permeability.

Injection Well Profile Modification

A foamed gel was studied for use as an injection well profile modification treatment. Advantages of foamed gel include a controllable residual resistance factor, inhibited gel migration (slumping) after placement, and fewer chemical requirements than bulk gels. Visual experiments demonstrated that foamed gel efficiently plugs porous media via the formation of gelled lenses in pore-throat constrictions. The foamed-gel-filled region remained impermeable until the pressure-induced rupture of successive gelled lenses led to percolation of conductive channels. Although gel remained in the pore throats after rupture and hindered fluid flow, the foamed-gel plug permeability increased as the conductive channel network increased in size. The percolation rupture pressure was found to depend on the foamed-gel quality, the gel strength, and the permeability of the porous medium. These trends were supported by experiments that revealed a relationship between the rupture pressure of the individual gelled lenses and the ratio of the gelled lens length to the capillary constriction diameter. The foamed gel was proven effective for profile modification treatments on the laboratory scale.

The development of a model that simulates foamed-gel breakdown hinged on proper characterization of the gelled lenses in the pore space. In the interest of estimating the characteristics of a foamed gel (specifically location and number of gelled lenses), the formation of a foamed gel in porous media was studied with glass micromodels of different pore configurations and two different types of gelling solutions. For long gelation times, the foamed gel consisted of one bubble in each pore body and one gelled lens in each pore throat. For short gelation times or high aspect ratio pore bodies, however, more than one bubble remained in each pore body.

The experimental studies provided the basis for development of a phenomenological model that simulates the breakdown of foamed gel. A network-type model was used because of conceptual similarities with the experimental system as well as the ability to account for microscopic heterogeneities of foam and porous medium structure. The model determined foamed-gel breakdown on the basis of the deformation and subsequent rupture of gelled lenses. Experimentally determined relationships between gel properties and measurable parameters are used in the model. The model agreed qualitatively with trends found for foamed-gel plugging of macroscopically homogeneous pore spaces. With further refinement, the foamed-gel breakdown model will be helpful in evaluating treatments on systems with matrix heterogeneities.

Acid Stimulation

Although acidization has been used for many years as a successful method for increasing the productivity of petro-

leum wells in carbonate formations, there are ever-increasing demands on the performance and application of the acidizing process. This study investigated the use of foamed acid for stimulating carbonate formations. Foamed acid has the potential to be used as a diverting agent as well as to increase the depth of acid penetration.

The goal of the experiments described in this report was to better understand the foamed acid diversion process by studying the dissolution patterns in carbonate samples. The experiments were initiated by preflushing the carbonate core with an aqueous surfactant solution. Either nitrogen or a comingled acid was then injected to generate a foam. When stimulation was complete, the wormholes were characterized by Wood's metal castings and neutron radiographs. Such parameters as acid flow rate, gas flow rate, acid concentration, and the presence of foam were studied to determine their effect on the amount of acid required for wormhole breakthrough. Images of wormholes that were stimulated in the presence of foam are longer, thinner, and less branched. The reason for these structures can be understood from the fundamental concepts that describe pore-level dissolution, two-phase flow, and interfacial phenomena.

Water Control

As production wells age and undergo secondary recovery, water production often becomes a problem. Not only is separation and disposal of produced water difficult but also acidizing these wells often results in stimulation of the water-bearing regions. Reactive diverting agents are designed to selectively plug watered-out zones either for water-control purposes or as acid preflush treatments. They are organic-based agents that form a gel or precipitate upon contact with water and are meant to plug zones where this contact occurs while leaving oil-producing zones undamaged.

This study has shown that these diverting agents do not perform as they are ideally designed to work. Specifically, the permeability reduction that occurs in water-bearing zones is often not sufficient, and more importantly, damage is common in producing intervals. The reasons for the lack of selectivity are related first to the organic nature of the diverting fluid, which displaces water away from the wellbore, and second to the reaction of the diverting agent with low water saturations in oil-rich zones.

This project has defined what is required of the diverting agent in terms of permeability reduction. More importantly, a simple method has been developed that provides a high degree of selectivity with slow-gelling reactants. This procedure, called the injection-backflow procedure, is a promising new technology to help control water production in the future.

Fluid Loss Control

Acid fracturing is a common production operation to increase the drainage area of low-permeability carbonate formations. In this process acid etches surfaces of natural or

artificial fractures to create conductive channels for flow. One of the factors that limits the success of this technique is excessive fluid leak-off that results from channeling the acid into the formation. Acid leak-off cannot be controlled with methods designed to control fluid loss. Polymers that form gels in acid can theoretically control acid loss effectively. Such gels should be reversible to ensure that the formation is not damaged after the treatment. Sodium alginate is a commercial polysaccharide that exhibits acid gelling properties. The objective of this study is to evaluate the feasibility of using acid gelling polymers in permeability reduction and fluid loss control.

- Batch studies have demonstrated the reversible nature of the gel and the influence of mixing on the gel structure.
- Permeability modification has been realized in both high- and low-permeability cores along with cores having significant permeability variations such as wormholes. In highly permeable cores, the mechanism of permeability reduction seems to be pore area reduction rather than pore blockage. The mechanism of permeability reduction in low-permeability cores seems to be governed by size exclusion.
- The effectiveness of the polymer in controlling nonreactive leak-off has been demonstrated with the use of a hollow core reactor. The mechanism of leak-off control in this case seems to be either an external or an internal filter-cake formation.

- Constant pressure acidization runs have demonstrated the effectiveness of the acid gelling polymer in delaying wormhole formation. This result demonstrates the feasibility of using such a model system in controlling reactive leak-off.

Modeling Particulate Injection for Injection Well Profile Modification

The efficiency of any flooding process depends on the number and type of different layers through which sweeping must be accomplished. Matrix treatments are often performed to improve sweeping efficiencies in multilayered formations which exhibit large differences in permeability. The various methods used to remedy this bypassing of the low-permeability layers in heterogeneous strata include injection of particulate diverting agents, in situ cross-linking polyacrylamide-chromium gel systems, lignosulfate gels, and alumina precipitates.

The success of these diverting methods depends to a large extent on the understanding of the fundamental mechanisms occurring in these systems. Phenomena occurring in porous media have been modeled by various approaches, including continuum, stochastic, and network models. Network models can provide an understanding of the phenomena occurring at the pore scale and can predict macroscopic changes with sufficient accuracy. The previous work involving network models has included only pore-scale heterogeneities. In this work network modeling has been extended to simulate particulate flow in media with macroscopic heterogeneities.

ELECTRICAL AND ELECTROMAGNETIC METHODS FOR RESERVOIR DESCRIPTION AND PROCESS MONITORING

**Lawrence Berkeley Laboratory
University of California
Berkeley, Calif.**

**Contract Date: Oct. 1, 1990
Anticipated Completion: Sept. 30, 1993
Government Award: \$195,000**

**Principal Investigators:
H. Frank Morrison
Ki Ha Lee
Alex Becker**

**Project Manager:
Robert Lemmon
Bartlesville Project Office**

Reporting Period: July 1–Sept. 30, 1993

Objectives

This project is part of an integrated effort by Lawrence Berkeley Laboratory (LBL)–University of California at Berkeley (UCB), Lawrence Livermore National Laboratory (LLNL), and Sandia National Laboratories (SNL) in the electrical and electromagnetic (EM) geophysical method development research and development (R&D) program for petroleum reservoir characterization and process monitoring. The overall objectives of the program are to (1) integrate research funded by the Department of Energy (DOE) for hydrocarbon recovery into a focused effort to demonstrate the technology in the shortest time with the least cost; (2) assure industry acceptance of the technology developed by having industry involvement in the planning, implementation, and funding of the research; and (3) focus the research on real-world problems that have the potential for solution in the near term with significant energy payoff.

Research conducted through this integrated effort focuses on five general activities:

1. EM forward modeling development.
2. Data interpretation methods development.

3. Hardware and instrumentation development.
4. Enhanced Oil Recovery (EOR) and reservoir characterization.
5. Controlled field experiments.

Lawrence Berkeley Laboratory–University of California at Berkeley research is focused on activities 1, 2, and 5. The primary focus is in the development of reliable inversion and imaging schemes that can yield conductivity distribution from measured electrical and electromagnetic field data. The development of accurate forward modeling algorithms and the acquisition of high-quality scale-model data are necessarily the early part of the inversion scheme develop-

ment for ultimately monitoring the front tracking in existing reservoirs.

Summary of Technical Progress

During the last quarter of FY93, field experiments and the preliminary data analysis were summarized in report number LBL-34734. The field experiment was done initially at British Petroleum's test site in Devine, Tex., and later at the University of California's Richmond field station under a controlled environment. Born inversion technique was developed and used to interpret data obtained from these experiments. The report has been submitted for publication to *Geophysics*.

LAWRENCE BERKELEY LABORATORY/ INDUSTRY HETEROGENEOUS RESERVOIR PERFORMANCE DEFINITION PROJECT

Lawrence Berkeley Laboratory
University of California
Berkeley, Calif.

Contract Date: April 1, 1992
Anticipated Completion Date: September, 1995
Funding for FY 1993: \$274,000

Principal Investigators:

J. C. S. Long
E. L. Majer
L. R. Myer

Project Manager:

Robert Lemmon
Bartlesville Project Office

Reporting Period: July 1–Sept. 30, 1993

Objectives

The purpose of this work is to validate geophysical and hydrological techniques for characterizing heterogeneous reservoirs in the most optimal/economic manner. The overall goal of the project is to develop a methodology that can be used by the petroleum industry in a variety of heterogeneous regimes for characterizing and predicting the performance of petroleum reservoirs.

This will be accomplished through a cooperative research program between Lawrence Berkeley Laboratory (LBL),

British Petroleum, Inc. (BP), and the University of Oklahoma (OU), which is focused on the characterization of heterogeneous reservoirs in a meander-belt porous-medium formation. BP has done characterization and data integration at several test facilities. The present program will continue BP's multiyear efforts at the Gypsy site in northeastern Oklahoma. The resulting research will integrate various geophysical and hydrological methods and apply them at a well-calibrated and characterized site, where their utility can be assessed. This cooperation will allow techniques developed for waste storage and geothermal energy to be adapted for use in heterogeneous and fractured reservoirs. The work will be coordinated with the cross-well electromagnetic (EM) research and development (R&D) project and the LBL/Morgantown Energy Technology Center (METC) reservoir performance definition project.

Summary of Technical Progress

Hydrologic-Related Work

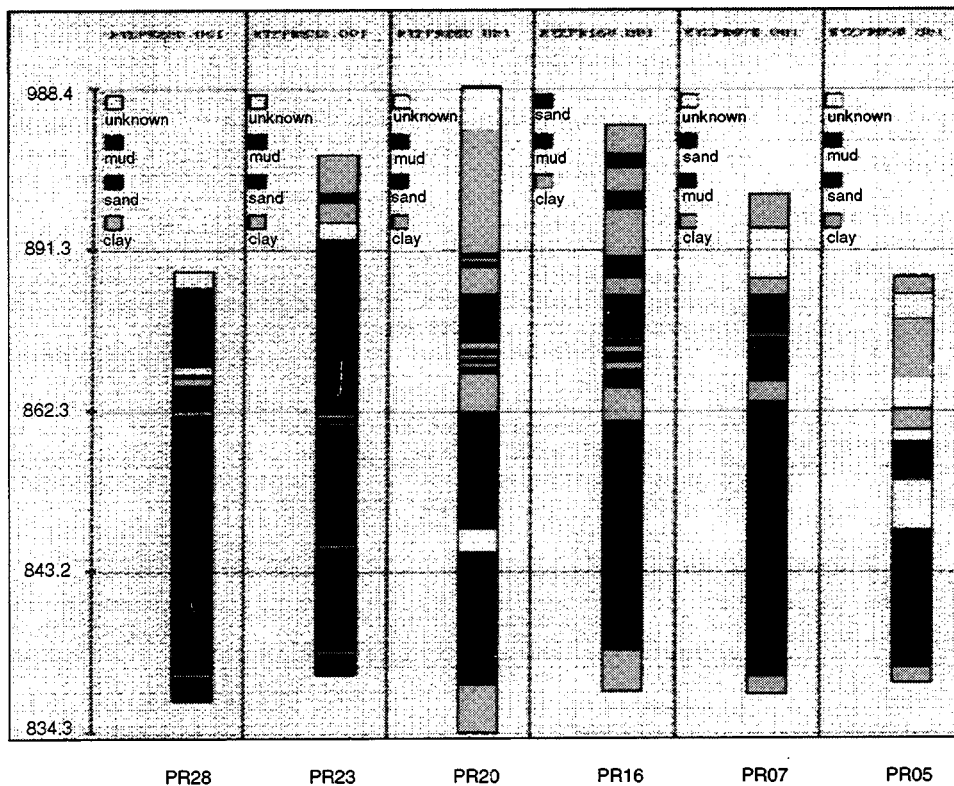
Two tasks related to the hydrological inversion of the pilot-site well tests were carried out this quarter. First, 3D-Rock, an integrated database and visualization package tailored to geologic media, was used to develop ways of looking at lithological data from the outcrop-site boreholes and pilot-site wells. Second, several co-inversions of tests 90/S3/T1 and 90/S4/T1 were done. Each of these tasks is briefly summarized below, and plans for future activities are outlined.

3D-Rock: A Three-Dimensional Visualization Technique for Geophysical Data

Figure 1 shows a plan view of the outcrop-site boreholes, generated by 3D-Rock, with two cross sections marked. The

North

South



West

East

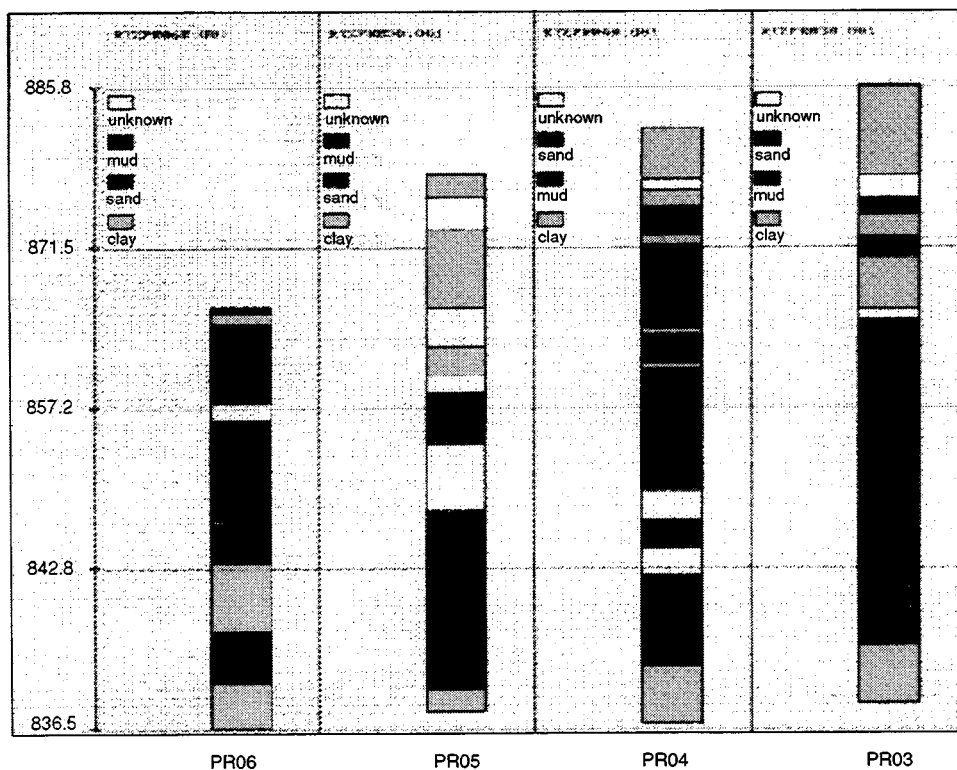


Fig. 2 Borehole lithologies for two cross sections at the Gypsy outcrop site. (Art reproduced from best available copy.)

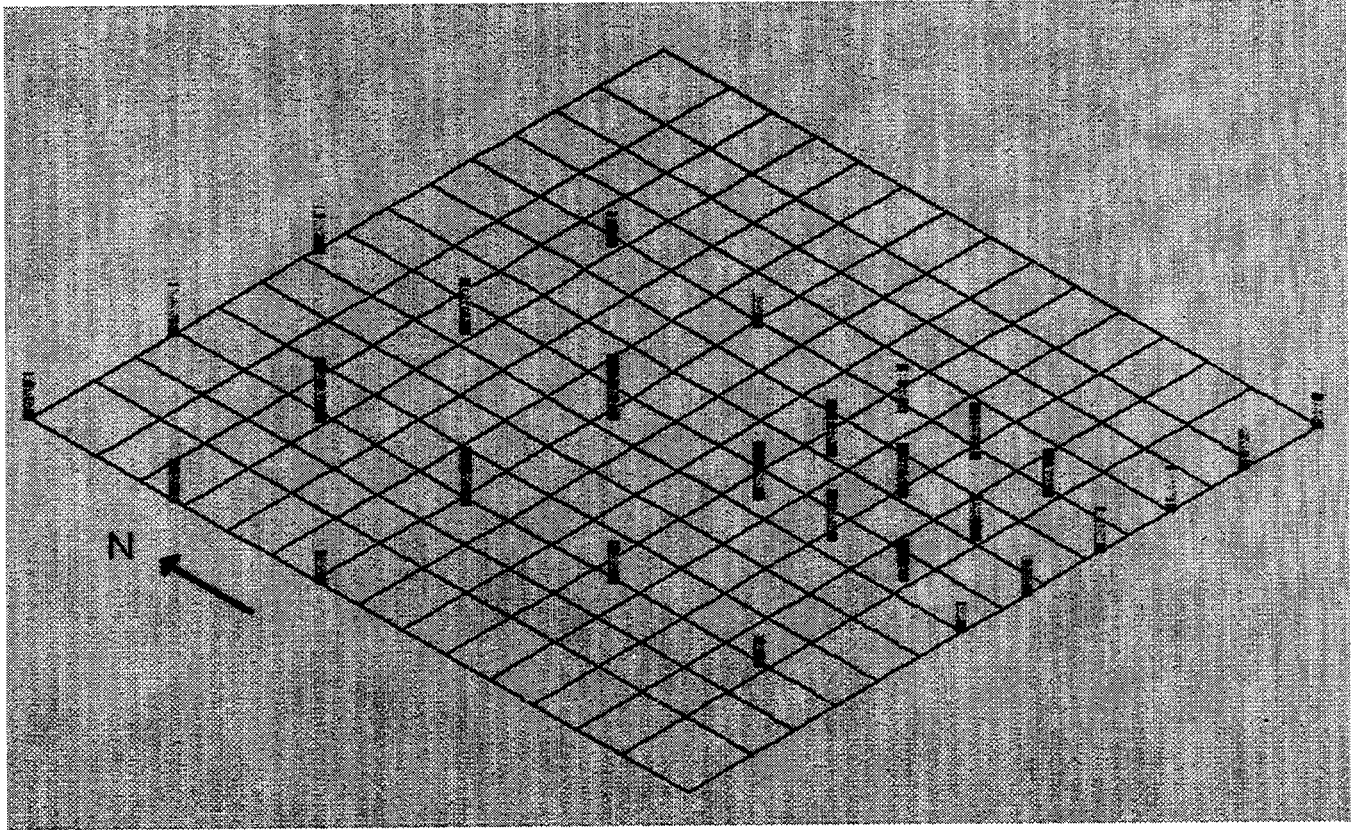


Fig. 3 Three-dimensional view of the outcrop-site boreholes. (Art reproduced from best available copy.)

instead, the pressure changes are reset to zero at the end of the first test. The inversion procedure tries a variety of permeability distributions as it attempts to match both sets of pressure transients. In fact, it really considers the two tests as one long test, with one set of long pressure transients. This is the first time a co-inversion of multiple well tests has been done using the iterated function system (IFS) inversion program, and several surprising results are emerging.

Typical results are shown in Figs. 6 and 7, which display observed and calculated pressure transients and a gray-scale representation of the permeability distribution used to generate them. It is notable that the pressure-transient matches do not look appreciably better for the final result than do those for a uniform medium, despite the decrease in energy (the value of the objective function) from $E=11.3$ to $E=3.6$. This is because the observed data points are equally spaced in log time for each of the individual tests, but since they are plotted against linear time, casual examination of the mismatch between observed and modeled pressures does not properly reflect the energy. Two consecutive tests cannot be plotted on one log-time scale because the second test would be too compressed to show anything. The log-time weighting was chosen to emphasize early time behavior, which should reflect near well-field heterogeneities. The use of log-time weighting in co-inversion of sequences of tests,

however, may not be appropriate. This issue is currently being reconsidered.

Another problem with the co-inversion of multiple tests is that the inversion seems to get stuck addressing either one part of the co-inversion or the other. In Fig. 6, the permeability distribution has primarily been modified between well 8-7 and the observation wells, in effect addressing the S3/T1 part of the pressure transients. Individual inversions of tests S3/T1 and S4/T1 yielded comparably low energies around $E=2.5$, but the starting point for these inversions, a uniform medium, gave substantially higher energy for S3/T1 ($E=28$) than for S4/T1 ($E=3.5$). Hence a co-inversion of the two tests shows a much larger decrease in energy by making permeability changes that the S3/T1 portion of the test is sensitive to (i.e., the region between well 8-7 and the observation wells). Use of IFSs composed of greater numbers of affine transforms (the inversions done so far use $k=4$) will provide permeability distributions with more distinct regions of variability, which may be appropriate for co-inverting multiple well tests. This option is currently being examined.

A few more studies will be done with the lower sand channel data in an attempt to fine tune the co-inversion procedure to make it more practically usable and to get good enough results to do cross-validation. However, the

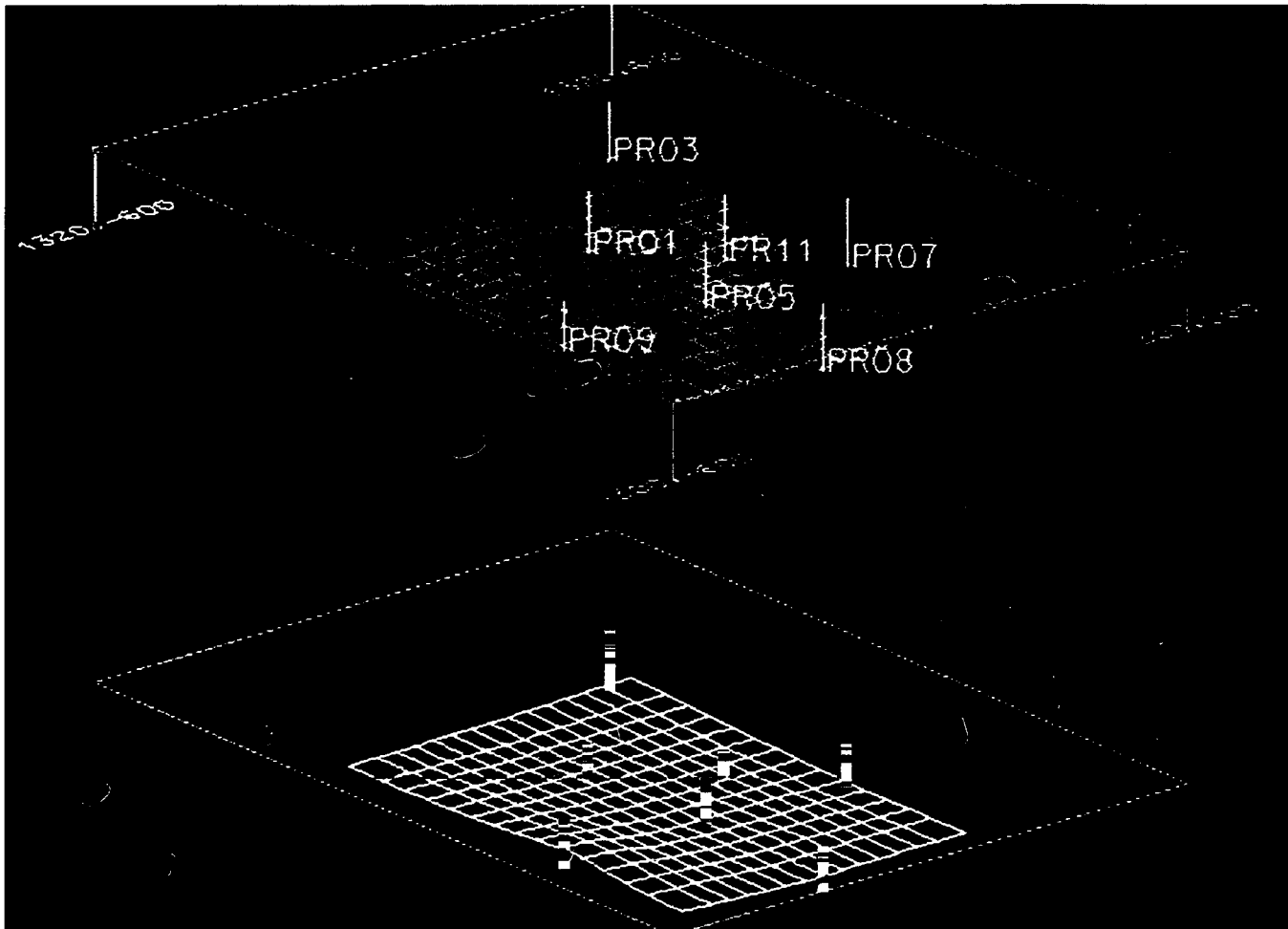


Fig. 4 Three-dimensional view of the pilot-site wells, identifying sand (light) and clay (dark) layers. (PR01 is well 1-7, PR05 is well 5-7, etc.) (Art reproduced from best available copy.)

subtle nature of intra-sand channel heterogeneities may be making this exercise unduly difficult. A more productive approach may be to invert the well tests conducted in the upper and middle sand channels, where the heterogeneities involve sand and clay, in which permeability contrasts are several orders of magnitude. These inversions will begin soon and will require a 3-D numerical model.

Seismic-Related Work

The last week of September a series of mini cross-well seismic surveys were conducted at the Gypsy outcrop site. Although the data have not yet been analyzed, some preliminary findings from the field work are reported. An updated diagram of the four wells used for the surveys, boring 4 and new wells A, B, and C, is shown in Fig. 8. Previously the borehole which the new wells surround was misidentified as boring 5. Each of the new wells A, B, and C was sealed and cased and filled with water for the surveys; each is about 75 ft deep. Boring 4 is believed to be uncased; it holds water with a level about 10 ft below the ground surface and is at least

70 ft deep. Four surveys were done, using the following source-receiver pairs:

Source	Receiver
A	4
B	4
C	4
A	C

In addition, a single-well reflection survey was obtained in Well A. The source signal consisted of a linear sweep from 300 Hz to 4000 Hz at a sample rate of 25,000 samples per second and a sweep length of 1/10th second. During the surveys the source location was moved in 0.25-m increments and the receiver spacing was also 0.25 m. For each of the surveys, the seismic signal was strongly attenuated when either the source or receiver was above the water table, which is located near the bottom of the outcrop, at a depth of about 50 ft, near the Gypsy-Tallant contact. It is possible that the way the wells were completed is causing the strong signal attenuation, but it may be that the air-filled formation itself is not cohesive enough to transmit the seismic signal well. These

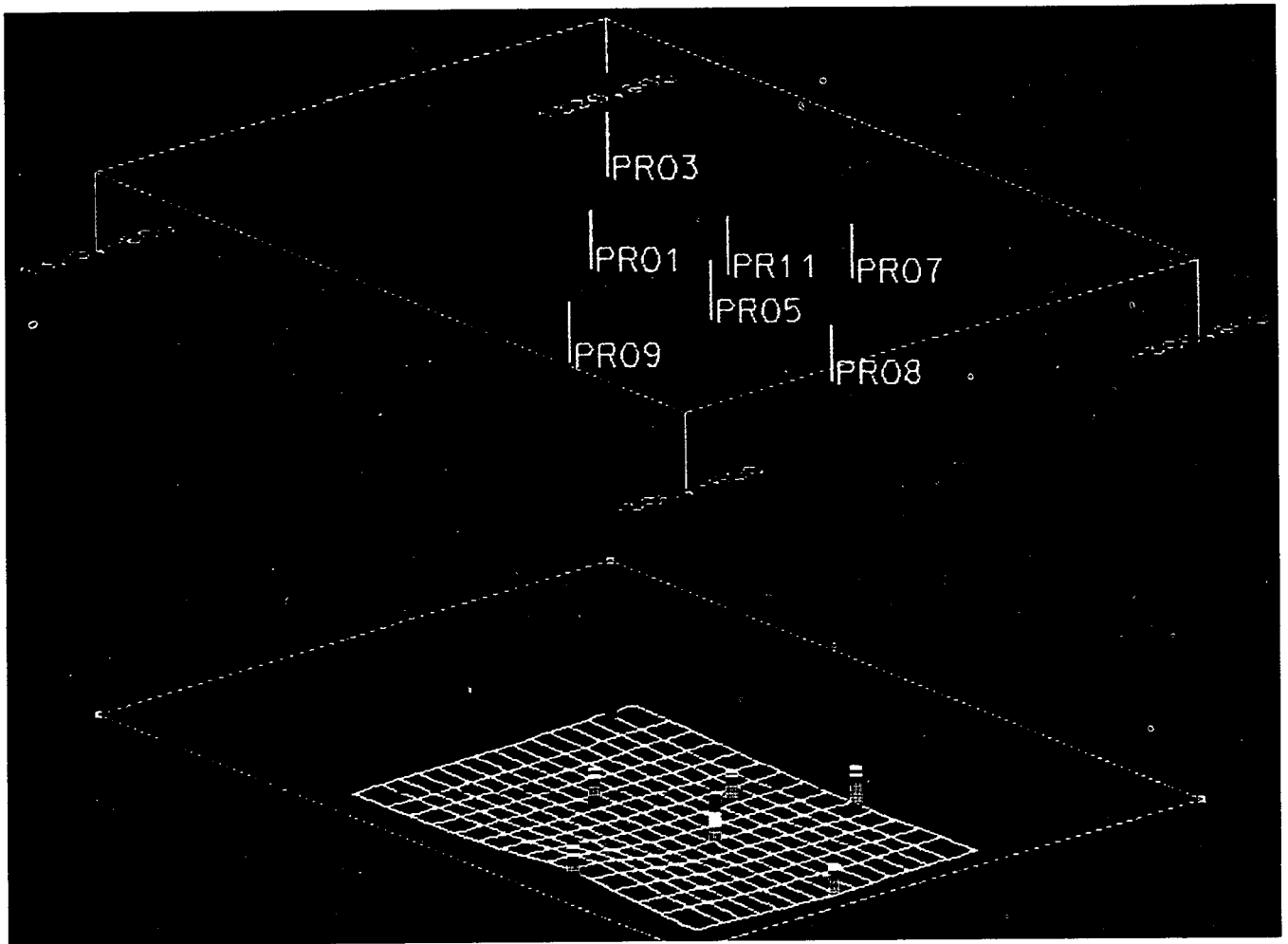


Fig. 5 Three-dimensional view of the pilot-site wells, distinguishing between lower sand channel (gray) and upper/middle sand channels (white), as identified by the hydrologic tests. (Art reproduced from best available copy.)

possibilities will be examined more fully as the data are analyzed. Good signals were transmitted through the water-saturated portion of the formation (the Tallant), which will provide information on the resolution achievable and anisotropy (by comparing results for surveys in perpendicular planes, e.g., A-4 and C-4). However, calibration anticipated between seismic signal and Gypsy formation geology will probably not be possible.

The unlikelihood of success in obtaining usable cross-well seismic data for the Gypsy interval at the outcrop site makes it imperative that the existing pilot-site cross-well seismic data be examined. The need for this data is twofold. First, it is

necessary to see what has already been done in order to plan pilot-site field work for FY94. Second, real seismic data need to be incorporated into the hydrologic inversion process.

Data Transfer

A compact disc (CD) with an assortment of Gypsy data has been received from OU. The data have been transferred from the CD to the Unix computer system, including some of the scanned images. Preliminary examination of the seismic data shows that the data format and organization will be convenient for analysis, but detailed studies have not yet been done.

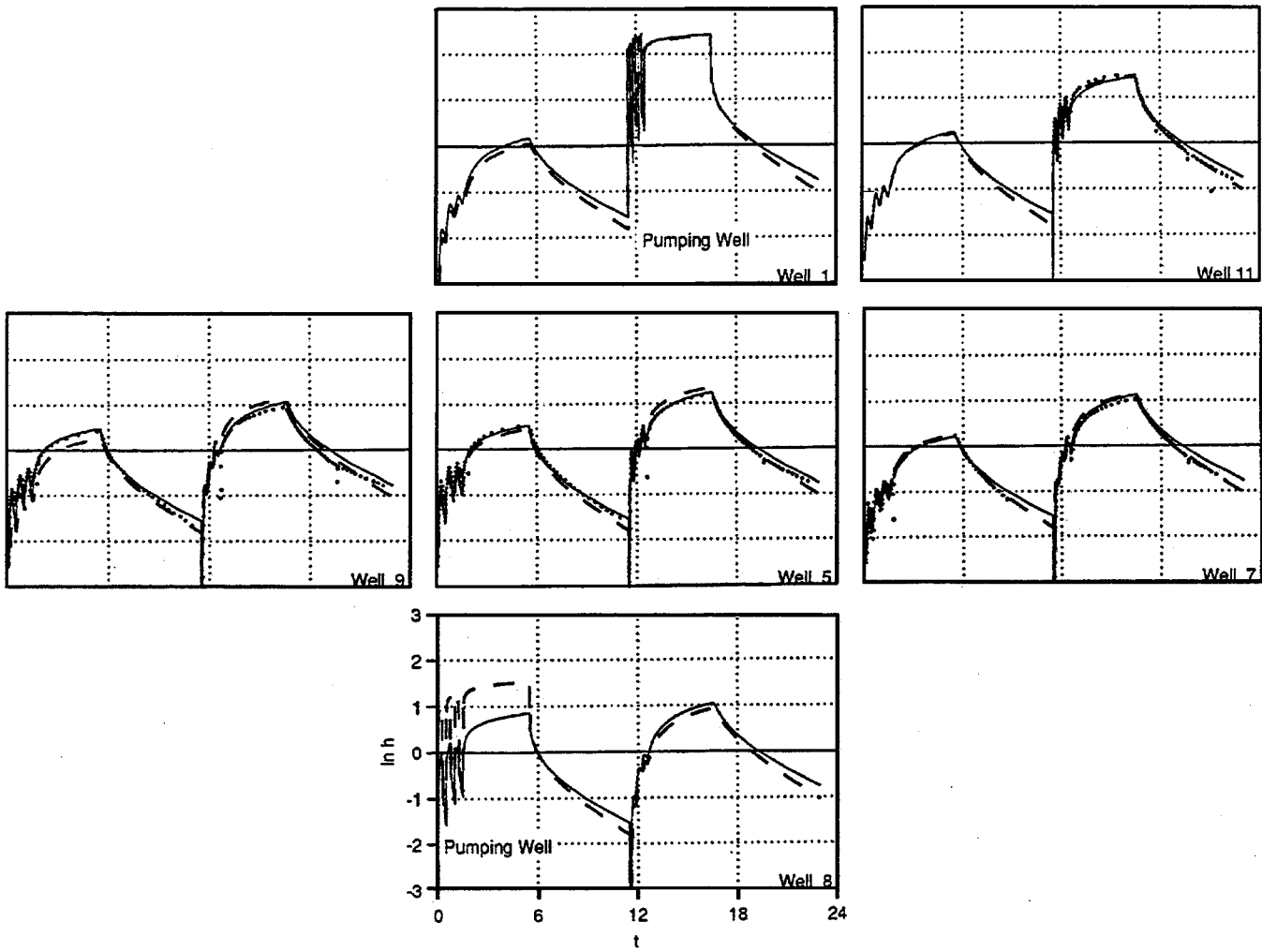


Fig. 6 Pressure transients for a co-inversion of 90/S3/T1 and 90/S4/T1. •, observed data. —, modeled ($E=3.63$). ---, uniform medium ($E=11.3$).

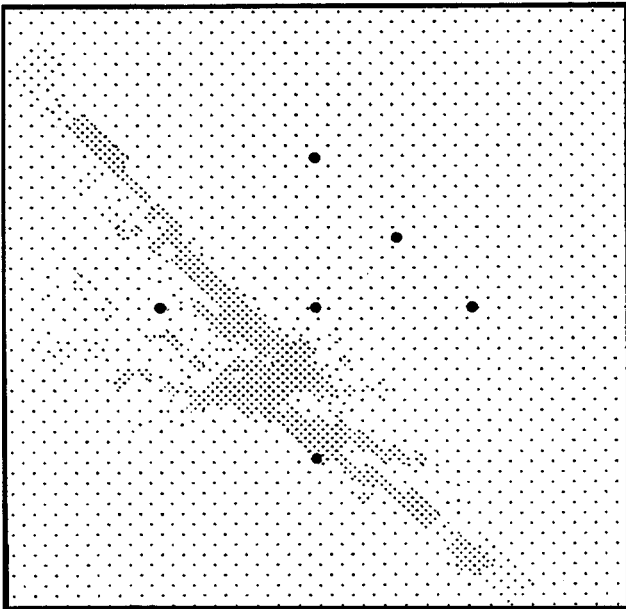


Fig. 7 Permeability distribution for the lower sand channel returned by a co-inversion of 90/S3/T1 and 90/S4/T1. BP29a, $E=3.63$.

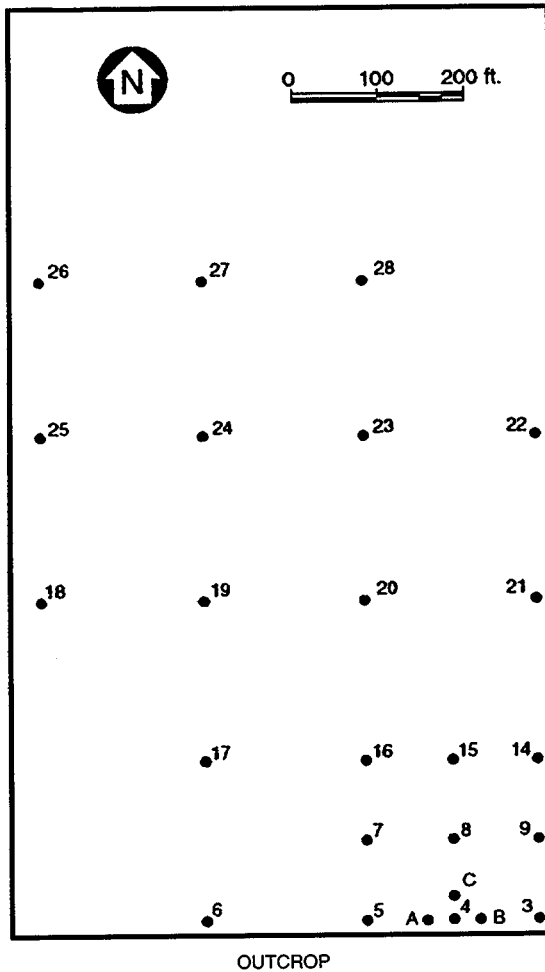


Fig. 8 Gypsy outcrop-site borings showing the new wells A, B, and C, which were drilled for the mini cross-well seismic survey.

Objective

The overall objective of this project is to develop electromagnetic (EM) geophysical methods for imaging and monitoring oil recovery processes and for characterizing oil reservoirs. Information obtained from the application of these methods will aid in the production of existing oil resources. Transfer of this technology to industry is a key element of the objective of this project. Because this is the final quarterly report for this project, project summary and highlights are given at the end of this report.

The status of this project was summarized at the DOE program review in July.

Summary of Technical Progress

For the borehole-to-surface and cross-borehole EM method under development for this project, the primary EM field is produced by a grounded, borehole, vertical electric source (VES). For a borehole VES in the earth operating in the audio frequency range (neglecting displacement currents) with an electrical structure that is axially symmetric about the VES, only a magnetic field (H) concentric with the VES is created, and this field is completely confined to within the earth. In other words, within the audio frequency range there is no vertical H field created in the earth or in the air, nor is there a horizontal H field at the earth's surface and in the air. The presence of a geoelectric section that is not axially symmetric about the VES produces secondary H fields. The measured vertical H fields in a borehole or on the earth's surface and the measured horizontal H fields on the earth's surface are a result of the secondary H fields. The advantage of using the borehole VES is that the non-axially symmetric geoelectric section produces the desired response and the host response is minimized.

As part of the analysis of the VES EM data, the multi-frequency, multisource holographic method, discussed briefly below, is being applied to the data taken at the Marathon site in April/May and that taken in November 1992. For calculated model results in the audio frequency range, targets have been detected and imaged. However, the resolution is limited by the frequencies used but is improved over that expected because of the focusing action of the holographic method. Proper amplitude data are necessary to determine the conductivity structure from the hologram. In this report a brief outline of the theory to determine the conductivity structure from the hologram will be given.

EM Holographic Method

The multisource holography applied to seismic imaging has been adapted for EM waves in earth materials. Multisource holography is a generalization of the traditional single-source holography. It is a numerical reconstruction procedure based on the double focusing principle for both the source

GEODIAGNOSTICS FOR FOSSIL ENERGY RECOVERY

Sandia National Laboratories
Albuquerque, N. Mex.

Contract Date: Oct. 1, 1986
Anticipated Completion: Sept. 30, 1993
Funding for FY 1993: \$340,000

Principal Investigators:
L. C. Bartel
G. A. Newman

Project Manager:
Robert Lemmon
Bartlesville Project Office

Reporting Period: July 1–Sept. 30, 1993

array and the receiver array. The measured scattered (secondary) magnetic wave fields are back propagated (migrated) to the image point and are then in turn back propagated (migrated) to the source point. Summations over all receivers and source points focus both the receiver array and the source array. To enhance the holographic method, multiple frequencies are used. Multifrequency, multisource holography is equivalent to prestack wave migration used in the analysis of seismic data. The holograms have been formed with the use of plane-wave propagators. For the multifrequency holograms, the phase coherency is determined by a Fourier transformation from the frequency domain to the time domain and setting time $t=0$. At time $t=0$ the image is formed when the in-phase part (real part) is not zero and the out-of-phase (imaginary part) is a minimum; that is, the EM wave is phase coherent at its origination.

The resistivity of the scattering anomaly and its relationship to the transmitting antenna will determine the phase structure of the hologram. However, when plane-wave propagators are used, it is difficult to recover the proper magnitudes of the secondary magnetic fields at their origin to determine the resistivity of the scatterer. In order to determine the resistivity structure from the holographic image, a more sophisticated method of back projection is use of the Helmholtz–Kirchhoff integral theorem as in classical diffraction theory. However, in the present context, the full term must be used because one is generally in the near-field and/or transition region and not in the radiation limit. The method extrapolates data taken on an aperture (on the earth's surface or in a borehole) to a "pixel." The extrapolated field at the pixel is deconvolved with a source function. The image is formed when there is phase coherency, that is, constructive interference. This image of the conductivity structure is related to the actual conductivity structure through a Fredholm integral equation of the first kind.

When the sources of the secondary magnetic fields are ignored, the zero order migrated or extrapolated field, H^e , for each transmitter located at x_i is given by

$$H^e(x, x_t, \omega) = - \int_S dS' H^s(x', x_t, \omega) \partial'_n G^*(x, x', \omega) \quad (1)$$

where S = the surface of the aperture

H^s = the secondary magnetic fields measured on the aperture S

G^* = a Green's function

∂'_n = the normal derivative to S

In Eq. 1, x denotes the location of the pixel and the components of H^e and H^s are the components tangential to the aperture S . The migrated image, $\gamma(x, x_t)_M$, is obtained by an imaging condition that consists of deconvolving the back propagated field by the incident field at each image point and evaluating the resulting function at time zero. Specifically

$$\gamma(x, x_t)_M = (1/2\pi) \int_{-\infty}^{\infty} d\omega [H^e(x, x_t, \omega)/P(x, x_t, \omega)] \quad (2)$$

where $P(x, x_t, \omega)$ is the incident "source" field.

If the conductivity structure γ is known, then the secondary magnetic fields on the aperture can be calculated and the migrated or extrapolated field in the Born approximation becomes

$$H^e(x, x_t, \omega) \equiv \sigma_0 \int_{V_s} dv'' \gamma(x'') \Gamma(x, x'', x_t, \omega) \quad (3)$$

where in the zero order

$$\Gamma(x, x'', x_t, \omega) = E^P(x'', x_t, \omega) \times \int_S ds' \nabla' G_1(x', x'', \omega) \partial'_n G^*(x, x', \omega) \quad (4)$$

In Eq. 4, E^P is the primary electric field from the VES. For the Born approximation it is assumed that the primary electric field is significantly larger than the secondary electric fields arising from the electrical anomaly. The conductivity structure γ is defined as

$$\gamma(x'') = [\sigma(x'') - \sigma_0] / \sigma_0 \quad (5)$$

where $\sigma(x'')$ is the anomalous conductivity and σ_0 is the background conductivity. Deconvolving Eq. 3 with the source function, the Fredholm integral equation of the first kind for the unknown conductivity structure becomes

$$\gamma(x, x_t)_M = \sigma_0 \int_V dV'' \gamma(x'') \Lambda(x, x'', x_t) \quad (6)$$

where

$$\Lambda(x, x'', x_t) = (1/2\pi) \int_{-\infty}^{\infty} d\omega \Gamma(x, x'', \omega) / P(x, x_t, \omega) \quad (7)$$

In Eq. 6, V is the volume of the pixels, $\gamma(x, x_t)_M$ is determined from the experimental data using Eqs. 1 and 2, and $\Lambda(x, x'', x_t)$ is known since it only involves the known geometry and the known source function. The final step is to sum over all transmitters. Equation 6 is a Fredholm integral equation of the first kind for the unknown $\gamma(x'')$. $\gamma(x, x_t)_M$ is the image of the conductivity variation from the background value, $\gamma(x)$, when imaged using $\Lambda(x, x'', x_t)$ measured on the aperture S deconvolved with a source function. $\Lambda(x, x'', x_t)$ is the point-spread function for the migrated image at the point x . The migrated image is therefore the true conductivity

variation $\gamma(x)$ "smoothed" by the function $\Lambda(x, x'', x_t)$. The final step is to sum over all transmitters.

The integral equation represented by Eq. 6 is ill-conditioned. Methods to solve this integral equation are being investigated.

Project Summary and Highlights

This project was initiated October 1, 1986. Since that time there have been several significant accomplishments.

Computer Model Verification

Physical simulation facilities were constructed and experiments performed. Electrical and EM computer models have been verified through the physical simulation.

DOE EM Coordinated Program

During the last three years of this project, Sandia led a coordinated program to keep participants informed, reduce unnecessary duplication of effort, and advance the state of the art more rapidly. The coordination was between Sandia National Laboratories (SNL), Lawrence Livermore National Laboratory (LLNL), and Lawrence Berkeley Laboratory with the University of California at Berkeley (LBL/UCB).

EM Technique Development

The grounded VES technique was developed for reservoir characterization and imaging advance petroleum extraction methods. The advantage of the VES method is that the effects of a uniform host response are minimized while desired target responses are enhanced.

Forward Modeling Efforts

Revised EM computer codes were developed by SNL personnel to include borehole sources and receivers. These codes were used for numerous model efforts.

Data Inversion Efforts

Direct inversion techniques were developed to interpret EM data. Inversion methods were applied to field data from

SNL experiments and experiments performed by LLNL. An EM holographic method was developed to image the sub-surface. The holographic imaging method was applied to data taken by SNL at an industry site (Marathon Oil Company). Work to determine the conductivity structure from the holographic images was in progress at the conclusion of this project.

EM Data and Reservoir Simulation Synergism

SNL took the lead in use of EM data to aid in reservoir simulation and, in turn, use of reservoir simulation data to aid in the interpretation of EM data.

Industry Interest

During the past few years, SNL has been interacting with Mobil R&D in the development of the controlled source audio-frequency magnetotellurics (CSAMT) method for imaging a steamflood process. SNL's involvement has been to show that meaningful CSAMT data could be taken in an active oil field environment and aid in the interpretation of data acquired by Mobil through a contractor. Because of SNL's recognized expertise, Marathon Oil Company expressed interest in SNL's participation in their effort to better understand a polymer flood enhanced oil recovery process. This interest resulted in two SNL/Marathon field efforts where the VES method was utilized. Data from these field studies are still being analyzed. Presentation of the study results are to be given to Marathon management and their field office in Bridgeport, Ill., the site of the field studies. Marathon expressed interest in forming a Cooperative Research and Development Agreement (CRADA) with SNL. AMOCO has also expressed interest in utilizing EM methods to characterize oil reservoirs.

Technical Articles and Presentations

Numerous journal articles and professional meeting presentations resulted from this project, giving visibility to the DOE program.

FABRICATION AND DOWNHOLE TESTING OF MOVING THRU CASING RESISTIVITY APPARATUS

Contract No. DE-FG22-93BC14966

**ParaMagnetic Logging, Inc.
Woodinville, Wash.**

**Contract Date: Mar. 23, 1993
Anticipated Completion: June 30, 1994
Government Award: \$109,000**

**Principal Investigator:
W. Banning Vail**

**Project Manager:
Robert Lemmon
Bartlesville Project Office**

Reporting Period: July 1–Sept. 30, 1993

Objective

The objective of this project is to validate recently discovered technology dealing with oil well measurement instrumentation that will allow the industry to find "missed oil" and "bypassed gas." This breakthrough technology, already endorsed in principle by the oil and gas industries, will allow identification of missed oil and bypassed gas locations in currently abandoned fields as well as in existing offshore wells, and will also allow increased productivity from low-production wells. There is no other proven technology today that will detect such oil behind steel casing, lower the discovery risk, and improve the success rate of recovery of otherwise accessible but undetected oil and gas reserves.

Summary of Technical Progress

It is believed that there may be more potential bypassed oil horizons around existing wells than will be found in the future by wildcat drilling in the continental United States. This new technology could substantially increase the petroleum reserves in the continental United States and obviate greatly the need to drill new wells, particularly in environmentally sensitive areas. This technology may be of particular interest initially to the independent oil companies and will ultimately be of great economic value to the major oil companies as well.

The technology will also be used to monitor enhanced oil recovery projects in the future.

This is a continuing research effort into the new field of measuring resistivity of geological formations from within cased wells. Additional data confirming the feasibility of the technology are to be taken in a test well with the existing stop-and-lock apparatus that is called the Thru Casing Resistivity Apparatus (TCRA). After those data are obtained, the already existing mechanical apparatus developed in an earlier phase of the project will then be modified and new electronic components will be fabricated to test the concept of a moving apparatus called the Moving Thru Casing Resistivity Apparatus (Moving TCRA). These steps are considered sufficient for subsequent commercial development by industry. The study by ParaMagnetic Logging, Inc., of measuring resistivity through casing with the TCRA is of great importance to the oil and gas industries. It is important to measure resistivity through casing for at least the following reasons: locating bypassed oil and gas; measuring water breakthrough during waterflooding operations; evaluating reservoirs measuring through a drill string when the drilling bit is stopped; and environmental monitoring of disposal wells, water wells, etc.

Continued Data from Test Well

Data were taken during the months of July, August, and September. These data showed the following:

- The apparent resistivity data are reproducible below about 200 Ω -m.
- The apparent resistivity data agree quantitatively with the open-hole LateroLog Survey (LLS) to resistivities in excess of 70 Ω -m.
- Casing collars can be located easily as a by-product of the measurements.

Hydraulic Section of the Apparatus

The hydraulic sections were taken to Houston and tested in the test chamber of Atlas Wireline Services. These tests proved that the hydraulics would be able to withstand use in the deep well.

Choice of Deep Test Well

The well has been chosen for the first deep tests of the 4¼ in. O.D. apparatus. It is the "MWX" site near Grand Junction, Colo. The first logs at the test well are to provide an initial blind test of the apparatus.

**RESEARCH CONSORTIUM ON FRACTURED
PETROLEUM RESERVOIRS**

Contract No. DE-AC22-91BC14835

**Reservoir Engineering Research Institute
Palo Alto, Calif.**

**Contract Date: Oct. 1, 1992
Anticipated Completion: Nov. 30, 1993
Government Award: \$50,000**

**Principal Investigator:
Abbas Firoozabadi**

**Project Manager:
Rhonda Lindsey
Bartlesville Project Office**

Reporting Period: July 1–Sept. 30, 1993

Objective

The objective of this project is to quantify the physics of multiphase flow in fractured porous media. Because the roles of capillary, diffusive, gravity, and viscous forces will be addressed, the topics of natural depletion, gas injection (both miscible and immiscible), and water injection in light and heavy oil reservoirs will all be studied in a unified approach.

Summary of Technical Progress

Immiscible Gas–Oil Gravity Drainage in Layered Porous Media

Layered reservoirs with distinct permeability for each layer may have certain characteristics similar to those of

fractured reservoirs. The contrast in capillary pressure of different media may have significant influence on oil recovery of the less permeable medium. In the experimental work to be presented in this report, it has been demonstrated that the less permeable layer may not reach gravity–capillary equilibrium in field-scale time frame. Therefore, appropriate use of capillary pressure data in the study of layered reservoirs by a simulation model may be very important.

Another feature of gas–oil gravity in layered porous media is the downward gas fingering in the less permeable layer, which is related to the permeability ratio, capillary threshold height of the less permeable layer, and thickness of the more permeable layer.¹ The theory of downward gas fingering was introduced in Ref. 1. The experiments of this report verify the validity of the theory.

The capillary pressure of the two types of media used for the two layers are currently being measured. With capillary pressure and relative permeability data, analysis of the laboratory experiments can proceed. The next quarterly report will cover analysis of the experiments presented in this report.

Experimental Study of Viscous Gas–Oil Displacement in Fractured Porous Media

Six experiments have been carried out to study the influence of viscous forces on gas–oil displacement in fractured porous media. In these experiments, two different matrix/fracture configurations have been used. Two types of experiments were conducted: (1) constant injection rate and (2) constant pressure drop. Comparison of the gravity drainage performance and the viscous displacement in the same matrix/fracture configuration reveals a strong effect of viscous forces.

Reference

1. A. C. Correa and A. Firoozabadi, *Concept of Gas–Oil Gravity Drainage in Layered Porous Media*, SPE 26299 (paper in review).

RESOURCE ASSESSMENT TECHNOLOGY

**CONTINUED SUPPORT OF THE
NATURAL RESOURCES INFORMATION
SYSTEM FOR THE STATE
OF OKLAHOMA**

Contract No. DE-FG22-92BC14853

**Oklahoma Geological Survey
University of Oklahoma
Norman, Okla.**

**Contract Date: May 18, 1992
Anticipated Completion: May 17, 1994
Government Award: \$350,000**

**Principal Investigators:
Charles J. Mankin
Terry P. Rizzuti**

**Project Manager:
R. Michael Ray
Bartlesville Project Office**

Reporting Period: July 1–Sept. 30, 1993

Objective

The objective of this research program is to continue developing, editing, maintaining, using, and making publicly

available the Oil and Gas Well History File portion of the Natural Resources Information System (NRIS) for the state of Oklahoma. This contract funds the ongoing development work as a continuation of earlier contract numbers DE-FG19-88BC14233 and DE-FG22-89BC14483. The Oklahoma Geological Survey (OGS), working with Geological Information Systems at the University of Oklahoma Sarkeys Energy Center, has constructed this information system in response to the need for a computerized, centrally located library containing accurate, detailed information on the state's natural resources. Particular emphasis during this phase of NRIS development is being placed on computerizing information related to the energy needs of the nation, specifically oil and gas.

Summary of Technical Progress

The NRIS Well History File contains historical and recent completion records for oil and gas wells reported to the Oklahoma Corporation Commission (OCC) on Form 1002-A. At the start of this quarter, the Well History File contained 321,771 records, which provides geographical coverage for most of Oklahoma (all but the northeast part of the state). Data elements on this file include American Petroleum Institute (API) well number, lease name and well number, location information, elevations, dates of significant activities for the well, and formation items (e.g., formation names, completion and test data, depths, and perforations). In addition to the standard Well History File processing, special projects have

been undertaken to add supplemental data to the file from well logs, scout tickets, and core and sample documentation.

A large portion of the Well History File work involves photocopying the completion reports for use in coding before data entry. The historical completion reports are checked out of the OGS Archive Library and copied at an average rate of about 1500 forms per week. All new completion reports are copied as soon as they are received from the OCC. Completion reports for areas of the state that have already been (or are being) "worked" are entered into the processing stream immediately. All others are filed for processing at the appropriate times. More than 379,000 completion reports had been copied by the end of the quarter, which represents all the 1002-A completion reports available in-house.

Processing of the OCC's oil and gas well completion reports (Form 1002-A) is proceeding smoothly. Well records are being prescanned, keyed, and edited for the following counties in northeastern Oklahoma: Craig, Kay, Nowata, Osage, Ottawa, and Washington. Approximately 27,000 well records were keyed and added to the file this quarter. As of September 1993, 348,996 records were on the database. The Well History File progress by NRIS Regional Division is shown in Table 1. The current status of county coverage and the total record counts by county are shown in Figs. 1 and 2.

Both general and specialized edit procedures continued on the well data. Search strategies are used to research well records with incorrect township-range-section (TRS) or county location data and well records that should be cross-referenced. Oklahoma Tax Commission lease numbers are being assigned to well records through a combined machine and manual matching process between the lease and well files. The state-wide Lease File/Well File match used to identify sections with significant discrepancies in the lease and well counts has been facilitated by cooperation from NRIS users and from Sooner Well Log Service located in Oklahoma City. Since the start of the contract, efforts to locate missing 1002-A forms for areas identified through these methods have been highly successful.

By early next quarter all the completion reports available in-house will have been processed, which will result in approximately 353,000 forms on the file. Future work will emphasize three areas of research to obtain the remaining records, an estimated additional 47,000 forms. One, efforts

TABLE 1
Well History File Progress by
Regional Division

Area of coverage	Start of Contract	Start of quarter	Current
Southeast Region	65,712	66,815	66,954
Southwest Region	69,453	71,266	71,669
Northeast Region	23,467	93,943	117,181
Northwest Region	32,507	33,185	33,355
North Central Region	40,883	56,562	59,837
Total	232,022	321,771	348,996

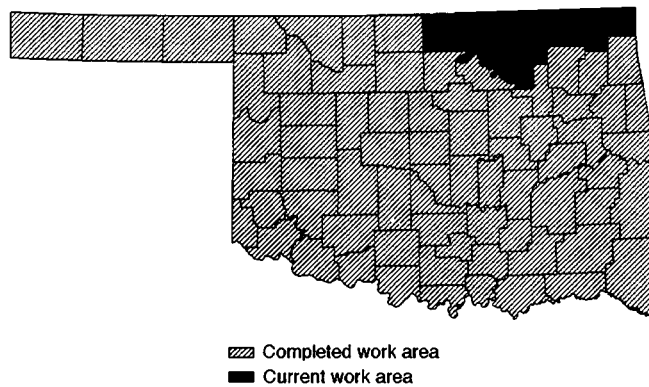


Fig. 1 Status of Well History Database project by county coverage as of September 1993.

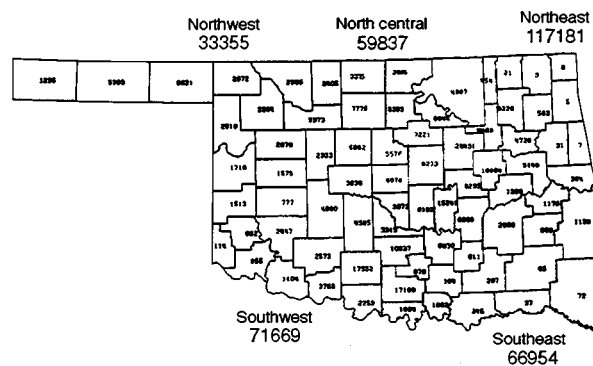


Fig. 2 Status of Well History Database project. Total well records, 348,996.

are under way to obtain access to Osage County records available through the Osage Tribal Agency. Indications are that these records will be made available to the project sometime next quarter. Two, the Lease File/Well File matching efforts described in the preceding paragraph will continue as a means of identifying areas with missing 1002-A forms. Three, research efforts will match well records currently on file against hard-copy scout tickets available through the Lawrence Youngblood Energy Library here at the University of Oklahoma. Initial efforts will be concentrated in the northeastern part of the state. Scout tickets identified for wells not on the Well History File will be sent to Sooner Well Log Service, and any missing 1002-A's available through their collection will be obtained and added to the file; those scout tickets for which no corresponding 1002-A records can be identified will be added to the Well History File to ensure a more complete file.

Efforts are ongoing for standardizing the formation names on the Well History File. A PC-based program uses a conversion table to standardize spellings and allows the user to interactively build new entries for the conversion table as new spelling variations are encountered. In the southeast, southwest, and northwest regions, over 99% of the reported names have been standardized in this effort. Efforts on the northeast

region have been completed with 97% standardized. Efforts on the north-central region were resumed with 95% of the region standardized. This formations-editing process is further enhanced by the addition of a table to determine the standard "Franklinized" abbreviation for each reported name following the convention with which industry users are familiar.

One goal of the NRIS system involves efforts to "assign" leases and wells to fields on the basis of official field outlines as designated by the Midcontinent Oil and Gas Association's Oklahoma Nomenclature Committee (ONC). Some areas exist in which significant field extension drilling has taken place, but the ONC has had insufficient resources to update the field boundaries accordingly. To assist the ONC in updating their field outlines, information packages are produced from the NRIS system for selected areas; these packages include well data listings and well spot maps. On the basis of this input, the Committee began by first updating several gas-field boundaries; emphasis has now shifted to oil-field boundaries as work proceeds on a separate Department of Energy (DOE) project involving the identification and evaluation of Oklahoma's fluvial-dominated deltaic reservoirs. Overall, unassigned gas production is 13% of the annual average production, whereas unassigned oil production is 20%.

The July 1993 data release was finalized this quarter. The Well History subsystem operations guide, which documents the weekly processing jobs, was completed. The Oil and Gas Production (OGP) subsystem operations guide was also completed. The Well History subsystem and the OGP subsystem system specifications should be completed next quarter.

Public Data Release

Efforts have been made since early 1991 to disseminate NRIS information through meetings, workshops, OGS annual reports, and mass mailings to numerous individuals, companies, and organizations. As a result, a dramatic response to the release of NRIS data began during the summer of 1991 and has continued. Feedback from the public continues to reflect a great deal of excitement about this new resource for the oil and gas industry in Oklahoma. Data and analyses have been

provided that would not have been feasible before construction of the NRIS system.

One commercial firm subscribes to the Well History File, and several inquiries are received each quarter from small companies and independents who typically acquire NRIS subsets to evaluate within their specific computer systems before committing to larger data acquisitions.

Also, as previously reported, NRIS well data have been made available through the Oklahoma City Geological Society Library with very positive results. The high level of interest by library members has led to the acquisition of several thousand records by several members as well as constructive feedback on user-detected data anomalies. Also, the Library, which is cataloging its extensive well log collection and tying each log to the corresponding NRIS well record, will be providing a listing of logs for which no NRIS records are on file. This should greatly enhance efforts to locate missing well records.

The OGS is establishing a computing facility to promote user access to the NRIS data, initially by Survey staff and eventually by the public. A PC-level relational database management system called Advanced Revelations is being used to develop a menu-driven retrieval system customized to NRIS data. A large digitizer, large plotter, and desk-top scanning equipment enhance the capabilities available through GeoGraphix and Radian CPS/PC contour mapping software as well as through ARC/INFO, a Geographical Information Systems (GIS) spatial analysis tool.

The NRIS data factor significantly in several projects. One such project, under way in conjunction with the Geography department, involves the creation of a GIS database of oil and gas pipelines for the Oklahoma Ad Valorem Task Force. Four Oklahoma counties were used as a pilot study. (NRIS well data related to data layers are being included.) Another, a DOE project, involves the study of Oklahoma's fluvial-dominated deltaic reservoirs. A third, involving cooperative research with the School of Civil Engineering and Environmental Science, is the creation of a GIS database (with a wellhead protection component) containing current and potential waste sites located on Oklahoma's Cheyenne/Arapaho tribal lands.

FIELD DEMONSTRATIONS IN HIGH-PRIORITY RESERVOIR CLASSES

**GREEN RIVER FORMATION
WATERFLOOD DEMONSTRATION
PROJECT, UINTA BASIN, UTAH**

Contract No. DE-FC22-93BC14958

**Lomax Exploration Company
Salt Lake City, Utah**

**Contract Date: Oct. 21, 1992
Anticipated Completion: Oct. 20, 1995
Government Award: \$1,304,000**

Principal Investigators:

**John D. Lomax
Dennis L. Nielson
Milind D. Deo**

Project Manager:

**Edith Allison
Bartlesville Project Office**

Reporting Period: July 1–Sept. 30, 1993

Objective

The project is designed to increase recoverable petroleum reserves in the United States. The Green River Formation in

Utah's Uinta Basin contains abundant hydrocarbons that are hard to recover by primary means. The successful Lomax Monument Butte Unit waterflood will be evaluated under this contract, and, on the basis of this information, waterfloods will be initiated in nearby Travis and Boundary units. In 1987, Lomax Exploration Company started a waterflood in the Monument Butte Unit of a Douglas Creek member of the Green River Formation. This was a low-energy, geologically heterogeneous reservoir producing a waxy crude oil. Primary production yielded about 5% of the original oil in place (OOIP). As a result of the waterflood project, total production will yield an estimated recovery of 20% OOIP.

Summary of Technical Progress

Field Drilling and Production Results

The Monument Butte Unit No. 10-34 and the Travis Unit No. 14A-28 were put on production the last quarter of 1992. Formation microimaging (FMI) and magnetic resonance imaging logs were used to evaluate these wells as commercially productive. Through Sept. 30, 1993, the Monument Butte No. 10-34 (Nov. 27, 1992, first production) has produced 7,526 bbl of oil and 7,824 Mcf of gas and the Travis No. 14A-28 (Jan. 1, 1993, first production) has produced 7,953 bbl of oil and 23,045 Mcf of gas.

As a result of fracture information provided by the FMI log and subsequent completion in the D sand in the Travis No. 14A-28 well, the behind pipe D sand zones in the Travis

Federal No. 14-28 were recompleted in March of 1993 and the Travis No. 10-28 in May of 1993. Through Sept. 30, 1993, the Travis No. 14-28 and 10-28 wells have produced 5,529 bbl of oil (31,993 Mcf of gas) and 2,907 bbl of oil (4,929 Mcf of gas), respectively. As a result of the success of the D sand interval of the Green River Formation, water injection will begin in October 1993 in the Travis No. 14A-28.

Water injection continued in the Travis Unit No. 15-28 throughout the third quarter of 1993. The average daily water injection rate for the report period was 275 bbl. Lomax and the Department of Chemical and Fuels Engineering agreed to a slower injection rate in the No. 15-28 because of the fractures found in the logging and coring of the No. 14A-28 well. The Travis No. 3-33 was converted into a water injector to inject into the Lower Douglas Creek member of the Green River Formation in October 1993.

Monument Butte Wireline Log Analysis

The wireline logs for the Monument Butte Unit were reduced to a scale of 40 ft per inch to facilitate a reevaluation of the distribution of reservoir rocks. Well Monument Federal 13-35 was designated the type log for the unit (Fig. 1). One of the principal difficulties in the Uinta Basin is that the stratigraphic nomenclature is not standardized. Each operator has developed its own designations, and thus correlation of reservoir units on a regional scale is extremely imprecise. By illustrating a type log, the stratigraphic details will aid other operators in the area.

The B limestone marker is the lowest marker bed shown in Fig. 1. On the basis of correlation with wells in the Duchesne field to the west, the B limestone is equivalent to the "Top of the Carbonate Marker Unit."¹ Because the B limestone is a clearly recognizable unit across the southern portion of the basin, it represents open lacustrine deposition.

The prominent marker above the B limestone is termed the Bicarbonate marker. In the section between these two markers, the B sandstones constitute important petroleum reservoirs.

The Douglas Creek marker is the uppermost marker shown in Fig. 1. Imaging logs through this unit suggest that it is a sandy limestone. Between the Bicarbonate and Douglas Creek markers are the D and C sandstones. The principal reservoir units discussed in this report are the D and B sandstones, which are the principal reservoirs involved in the waterflood.

B Sandstone

This unit occurs within the stratigraphic interval between the B limestone and the Bicarbonate markers. There appears to be at least three, and perhaps five, stratigraphically distinct sands. The important sandstones in terms of thickness and porosity are located near the base of the section above the B limestone. At times the sandstones are deposited directly

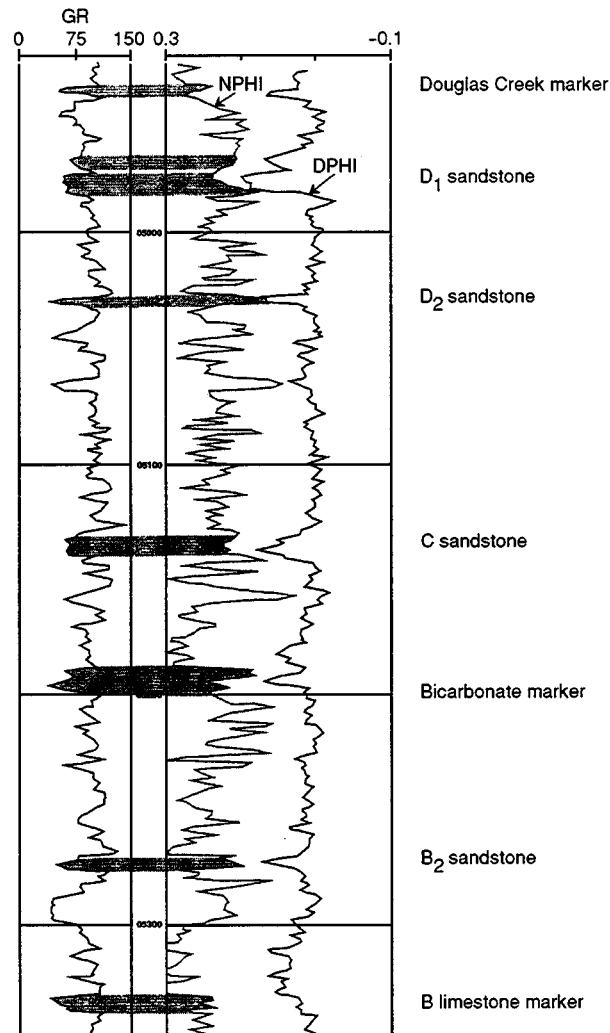


Fig. 1 Type log for reservoir sandstone in Monument Butte field, Utah. Log is from well Monument Federal No. 13-35. GR, gamma ray (in API units); NPHI, neutron porosity; DPHI, density porosity.

on the B limestone, and it is clear that there is an erosional unconformity above the B limestone.

Figure 2 is an isopach map of the B₂ and B₃ sandstones. It is interpreted as representing a meandering fluvial system, although more information is needed to eliminate the possibility that it does not represent the effects of a fluvial system superimposed upon a delta, where, as seen in the D₁ sandstone, accumulations greater than 30 ft are possible. Nevertheless, it is the interpretation that the B sandstone represents a delta plain environment with fluvial systems separated by mud flats.

The northwest trend of the thickest portions of the sandstone is notable. This trend is parallel to the trends of gilsonite dikes, which are certainly younger than the channel system, but the two may have resulted from similar structural controls. From the standpoint of the waterflood, the sandstones are probably well confined by shale horizons, which provides a good geometry for the waterflood sweep.

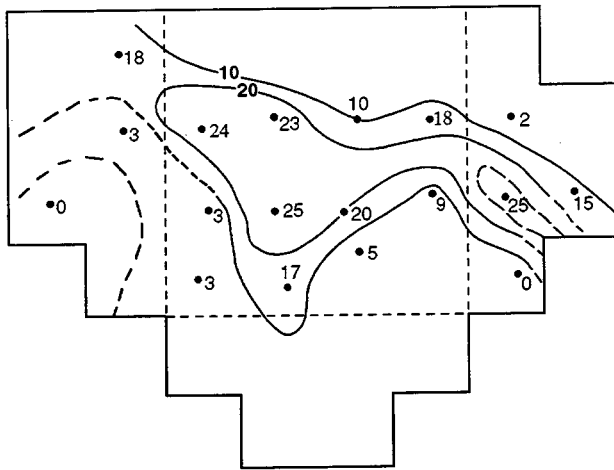


Fig. 2 B₂ and B₃ net sandstone isopach, Monument Butte Unit. Central portion of unit is located in sec. 35, T. 8 S., R. 16 E., shown by light dashed lines. Bold numbers indicate value of contour interval.

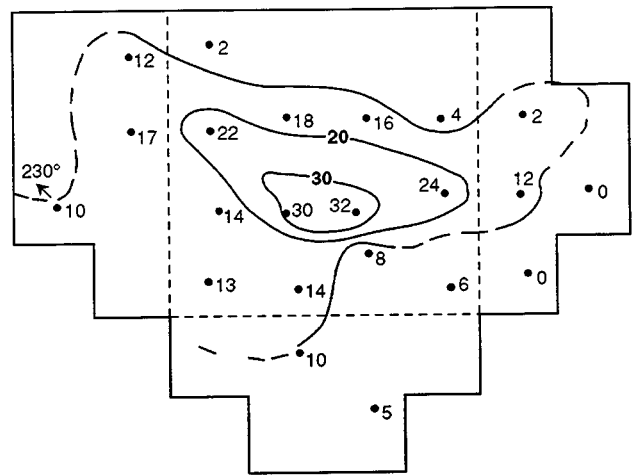


Fig. 3 D₁ net sandstone isopach, Monument Butte Unit. Central portion of unit is located in sec. 35, T. 8 S., R. 16 E., shown by light dashed lines. Bold numbers indicate value of contour interval.

C Sandstone

Beneath the D₂ sandstone is the C sandstone reservoir unit. The C sandstone is present in most wells. It is normally thin but is over 30 ft thick in some wells. This reservoir is not involved in the waterflood at this time.

D Sandstone

The D sandstone interval has been well characterized from full-diameter core taken in the 6-35 and 12-35 wells. These sandstones are characterized as deposits of a playa environment formed along the margins of a larger permanent lake. Terrigenous clastics were carried onto the playa by unchanneled sheetfloods and braided fluvial channels.

An isopach map of the D₁ sandstone is shown in Fig. 3. This shows a maximum thickness of 32 ft with a lensoid shape having a WNW-ESE orientation. Although the thicker portions of the body occur as a single unit, sections through the margins show that, as the body gets thinner, it also breaks up into two or three separate sands separated by shale horizons that are generally 2 to 4 ft thick.

An FMI image through the D₁ in well 10-34 shows that the bedding is oriented 230° (Fig. 3), showing sediment transport away from the thicker portions of the body. This section of side-wall cores suggests that the D₁ was deposited as a sublacustrine bar. The presence of abundant rounded micrite clasts and micrite-coated quartz and feldspar grains suggests formation of the grains in a shallow bay or lagoon and then transportation to an offshore environment. The overall fine grain size and lack of strong grading preclude deposition as channelized sands.

An isopach of the D₂ sandstone is shown in Fig. 4. In contrast to the D₁, the D₂ is much less continuous, probably the result of its deposition in channels. The nature of the sandstone distribution suggests that the depositing streams were meandering. Because of its irregular distribution, the D₂ is not a good drilling target.

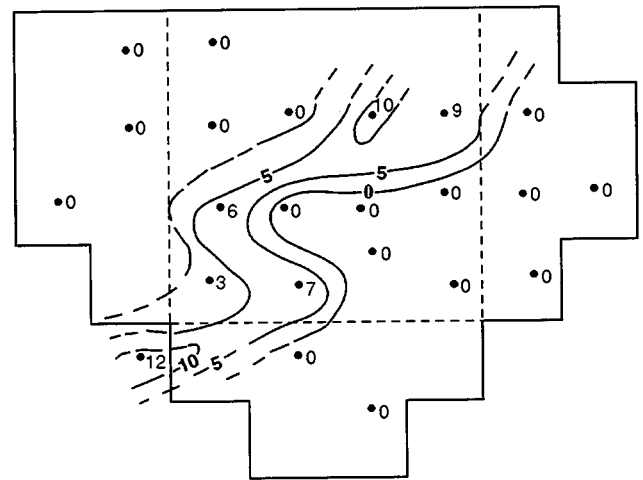


Fig. 4 D₂ net sandstone isopach, Monument Butte Unit. Central portion of unit is located in sec. 35, T. 8 S., R. 16 E., shown by light dashed lines. Bold numbers indicate value of contour interval.

Travis Unit—Preliminary History Match of Primary Production

A preliminary model of the Travis field was developed at the University of Utah. Simulations carried out with the model match overall field gas and oil production within 5%, and simulated production from individual wells was matched within 15 to 20% of actual production.

The model makes use of isopach data (Lomax Exploration) for reservoir zone thickness estimation. The model representation is preliminary and will be tuned to incorporate a more accurate geologic description later. The model also does not account for permeability improvements that result from occasional hot oil treatments that have been applied.

All the Travis reservoir simulations were performed with a black oil simulator (IMEX) developed by the Computer

Modeling Group. These studies made use of the dual-porosity, dual-permeability option of the IMEX simulator to describe the fractured reservoir. The use of this option requires separate sets of descriptive reservoir data for the reservoir matrix and for the fracture system.

The Travis Unit consists of moderately fractured sands vertically separated by shale strata and by layers of unproductive sand. Seven wells (five producers and two injectors) now operate in the unit. The wells have been perforated in numerous sands, but the three main sands account for the great majority of production from the unit.

The model description of the reservoir consists of a $5 \times 7 \times 8$ cartesian coordinate grid with total areal dimensions of 3300 by 4620 ft. The variable thickness of the productive sands of the reservoir was modeled by variable grid-block thickness. The top two layers of the model correspond to the D sands, the next to an impermeable separation zone, the following two to the Lower Douglas Creek Sands, the next to another separation zone, and the bottom two layers to the Castle Peak Sands. Zone thicknesses were assigned on the basis of isopach information and perforated interval data from individual wells.

A constant matrix permeability of 1.0 mD and a fracture permeability of 18.75 mD in the horizontal direction and 36.50 mD in the vertical direction were assumed. The matrix permeability, as determined from core data, is typically 1 to 5 mD. Fracture permeability was not evaluated from core data.

A base porosity of 0.132 was used over the entire reservoir, this being the average of the measured values from cores. A uniform oil saturation of 0.78 was assumed for the entire field. No free gas was present in the reservoir initially; therefore initial water saturation was set to a value of 0.22, which represents the difference between unity and the oil saturation.

Oil and gas samples were collected from several producing wells in the Travis Unit. The characterization of reservoir fluid properties consisted of the following measurements and calculations:

- Measurement of the bulk properties of the oils (API gravities and viscosities).
- Prediction of bubble points and oil formation volume factors at different gas/oil ratios from oil and gas gravities.
- Assumption that oil and gas compositions were the same as those from the Monument Butte Unit.²

For reproducible measurements of API gravities and viscosities, the oils were filtered through a cloth to remove small amounts of water and particulates. The three oils from the Travis Unit that were tested had API gravities of about 26 °API (specific gravity, 0.90).

Oil viscosities were measured at the reservoir temperature of 140 °F with a Brookfield cone and plate viscometer, model LVT, equipped with a spindle CP-41 (3° cone). The viscosity of oil from well 10-28 was 31.7 cP. Established correlations were used to adjust the oil viscosities at reservoir conditions for the presence of solution gas.³ Relative permeabilities and capillary pressures typical of water-wet sands were used in all the simulations.

The cumulative oil production from the field data and the production predicted by simulations are compared in Fig. 5. Both the oil production trend and the overall oil production are represented fairly well by the simulations. The simulated and actual cumulative gas productions are compared in Fig. 6. The initial field gas production is higher than the simulated; however, the simulated production catches up to the field production, and the final cumulative production predicted by the simulations is in reasonably close agreement with the field data.

Technology Transfer

The success of the Monument Butte Unit has influenced the start and the development of the Jonah Unit by Equitable Resources Energy Company. Equitable received approval from the state of Utah on June 23, 1993, to unitize 4222 acres approximately 1 mile southeast of the Monument Butte Unit. In Equitable's testimony before the state of Utah, it was stated that the waterflood unit would spend in excess of \$10 million to increase oil reserves from 1.6 million bbl to over 4 million bbl over the next 10 yr.

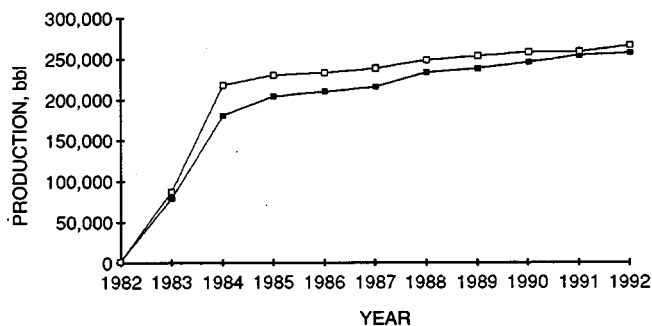


Fig. 5 Cumulative Travis oil production. —■—, field data. —□—, simulation.

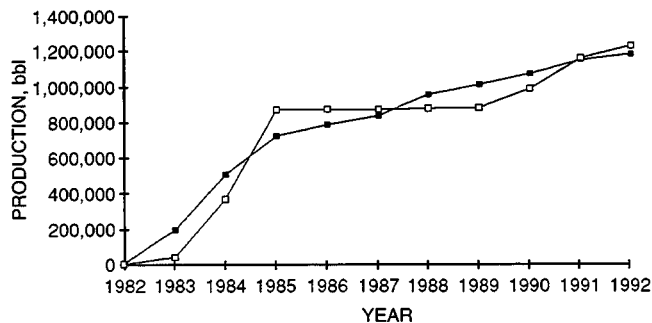


Fig. 6 Cumulative Travis gas production. —■—, field data. —□—, simulation.

References

1. T. D. Fouch, Distribution of Rock Types, Lithologic Groups, and Interpreted Depositional Environments for Some Lower Tertiary and Upper Cretaceous Rocks from Outcrops at Willow Creek-Indian Canyon Through

the Subsurface of Duchesne and Altamont Oil Fields, Southwest to North Central Parts of the Uinta Basin, Utah, U.S. Geological Survey, Chart OC-81, 1981.

2. L. A. Neer and M. D. Deo, Simulated Distillation of Oils with Wide Carbon Number Distributions, submitted to *J. Chromatogr. Sci.* (in review).
3. W. D. McCain, Jr., *The Properties of Petroleum Fluids*, second edition, Pennwell Books, PennWell Publishing Company, Tulsa, Okla., 1989.

DYNAMIC ENHANCED RECOVERY TECHNOLOGIES

Contract No. DE-FC22-93BC14961

**Columbia University
New York, N.Y.**

**Contract Date: July 5, 1993
Anticipated Completion: Oct. 30, 1995
Government Award: \$7,742,000**

**Principal Investigator:
Roger N. Anderson**

**Project Manager:
Edith Allison
Bartlesville Project Office**

Reporting Period: July 1–Sept. 30, 1993

Objectives

Dynamic enhanced recovery technologies are intended to identify the locations of moving streams of hydrocarbons in the process of migration. A field demonstration experiment

will be conducted in Eugene Island Block 330 (EI 330) field to determine if enhanced oil recovery can be maximized by drilling into such a conduit that directly connects the geopressured source accumulation to the presently producing reservoir rocks. The integration of a variety of geophysical, geochemical, geological, and reservoir engineering technologies can image ongoing fluid-flow processes. Techniques will be developed for the exploitation of these new enhanced oil recovery technologies. Time-dependent three-dimensional (3-D) seismic surveys; structural and stratigraphic, pressure, and temperature mapping; and production histories will be used to image the dynamic fluid-flow processes ongoing within a large growth fault of the EI 330 Block. Finite-element fluid-flow modeling will be used to simulate the observed pressure and temperature conditions and to design optimal stimulation strategies. A well will be drilled in the fault zone test site to test predictions of enhanced subsurface fluid flow from within the fault zone. This project will focus on which rates of the fluid-flow processes result in transient rupture and expulsion of hydrocarbon-charged fluids from the geopressed strata. The locations and magnitudes of present day hydrocarbon expulsion events will be identified, as well as the locations of focused fluid-flow that have the potential to deliver large quantities of additional hydrocarbons to reserves estimates for the Gulf Coast.

This dynamic enhanced recovery project is broken into seven major tasks:

- Management Start-Up
- Database Management
- Field Demonstration Experiment
- Reservoir Characterization
- Modeling
- Geochemistry
- Integration

Summary of Technical Progress

Management Start-Up

The purpose of this task is to equip the project with staff and resources (computer and otherwise) to accomplish the other tasks associated with this project, to negotiate contracts with several industry and university subcontractors to achieve the task objectives, and to initiate technology transfer to industry and the public as a result of this project.

Technology transfer includes the following publications, exhibitions, and workshops to date.

1. Global Basins Research Network (GBRN)/Department of Energy (DOE) project workshop at the Society of Exploration Geophysicists (SEG) convention held in New Orleans, La., October 25–29, 1992.
2. Semiannual GBRN meeting held in Houston, Tex., in January 1993.

3. GBRN/DOE project exhibition at the Annual American Association of Petroleum Geologists (AAPG) convention in New Orleans, La., April 26–28, 1993.
4. Semiannual GBRN meeting held in Baton Rouge, La., June 1993.
5. Recovering Dynamic Gulf of Mexico Reserves and the U.S. Energy Future, *Oil and Gas Journal*, 85-88, 90-92 (April 26, 1993).
6. Several videotapes:
 - a. June 1993—"Migration of Hydrocarbons in the Offshore Gulf of Mexico"
 - b. March 1993—"Dynamic Enhanced Recovery Technologies"
 - c. October 1992—IHRDC Video Journal: "Dynamic Fluid Flow Modeling"
 - d. November 1992—"Seismic Images Model Structure of Proposed Well"
 - e. November 1992—"AVS Compilation"
 - f. September 1992—"Dynamic Exploration & Production Technologies"
7. *Seismic Amplitude Analysis Technique for Predicting Top-of-Geopressure and Its Application to the Pleistocene Offshore Louisiana Gulf of Mexico*, Master's Thesis, Columbia University, Lamont-Doherty Earth Observatory, September 1993 (Ref.1).

Database Management

The objectives of this task are to accumulate, archive, and disseminate the geological information available within the area of research of this project: networked database creation, generation of new seismic interpretation with high-tech software, and real-time visualization of the online database.

4-D Seismic Interpretation

A GBRN file directory hierarchy including data, networks, and source code for new modules has been implemented at Lamont-Doherty Earth Observatory (LDEO) and other sites. To date, visualization work at LDEO has centered on data from two (Pennzoil and Texaco) 3-D seismic surveys over the EI 330 area.

Two specific visualization networks depict (1) isosurfaces of the two data sets shown together and (2) isosurfaces showing the similarities and differences between the data sets. Images of these isosurfaces were incorporated into an April 26, 1993, *Oil and Gas Journal* article titled "Recovering Dynamic Gulf of Mexico Reserves and the U.S. Energy Future."

In June 1993, a patent application was filed for "Seismic Interpretation and Imaging Utilizing Amorphous Diffuse Inter-Period (ADIP) Projectors." This invention investigates the association of high-amplitude events between multiple data sets of a region over time. This invention is of considerable utility in the identification of the locations and migration pathways of oil, gas, and other fluids in the subsurface of the Earth and potentially in other applications.

Recently, efforts have been directed at being able to accurately show isosurfaces of 3-D seismic amplitude data with well locations and block boundary lines. This brought up several issues, including

- Getting precise coordinate information in order to line up data sets
- Transforming coordinate systems between data sets
- Data ordering differences between AVS and Landmark software
- Redefining the boundaries of the data files to make smaller data sets
- Reengineering previously created software to reflect the current steps

Most of these issues have been resolved and some modifications to data files and source code have been made.

Field Demonstration Experiment

The Pathfinder well is scheduled to spud on October 15, 1993. Pennzoil will drill the first portion of the hole and set 9⁵/₈-in. casing. At this point, the GBRN/DOE well extension will begin. The field demonstration experiment should take 25 d to complete. The experiments are divided into three stages:

- Whole coring and completion of drilling
- Wireline logging, sidewall coring, and formation pressure tester
- Stress test, completion, flow test, and pressure transient test

Reservoir Characterization

Stratigraphic Interpretation

The 16-Block 2-D analysis is now at the stage of final write-up. The final report on this subtask will be a paper submitted to the *American Association of Petroleum Geologists, Bulletin*. This task will be completed with a final report available by Jan. 1, 1994.

Salt Analysis and Paleogeographic Reconstruction

This task involves integrating the regional sequence stratigraphic interpretations with a palynospastic restoration to understand regional structural and stratigraphic evolution. A final write-up is planned to be completed by Feb. 1, 1994.

From the regional stratigraphic interpretations an initial structural restoration of the regional seismic profiles was done. This report of the study is critical to placing important constraints on the timing of fluid migration into the EI 330 field. Preliminary results indicate that initial migration of petroleum into the EI 330 minibasin started somewhere between 3.4 and 2.7 Ma.

Fluid Potential Analysis

Two levels of structure maps are being produced. Regional structure maps have been completed based on 16-block

stratigraphic mapping. Detailed field-scale structure maps, where not previously accomplished by Pennzoil, are being constructed.

The acquisition of all deviation data for the 330 area has allowed much more detailed location of pressure horizons. At this stage only 2-D "cross sections" of pressure can be constructed (see Fig. 1). This technique will be extended to 3-D pressure mapping.

The objective of this task is to build the complete 3-D temperature distribution inside the data-cube from a data set of temperatures from the different wells. The temperatures used are mostly bottom-hole temperatures; therefore, the information must be either corrected from the time of circulation, when available, or calibrated by more accurate data, like DST temperatures. A first mapping has been produced, but some areas with scattered temperatures must be reevaluated with new data in order to produce the final results.

Modeling

Two-dimensional Access.Basin models that describe fluid flow, salt and sediment diapirism, sedimentation and erosion, faulting, temperature evolution, salt transport, and fluid flow (by all possible fluid drive mechanisms) have been developed and nearly all aspects have been successfully tested. The realistic 2-D algorithms have been about 75% converted to 3-D. Methods for the 3-D visualization of input data and model results are nearly complete.

Geologic Input

Two geologic cross sections that run through the South Eugene Island (SEI) area and eight two-way time seismic

structural maps showing the location of all faults and the thickness (in time) of the major stratigraphic subdivisions have been prepared.

From this data four flat files (N-S cross sections) defining the faults and strata across the SEI minibasin have been prepared. Each flat file consists of 37 horizons and 11 pseudo-wells.

The four 2-D sections (flat files) described previously compose a realistic 3-D flat file on the South Eugene Minibasin scale.

Very detailed sequence stratigraphic interpretation of 2-D seismic data and well logs in the SEI Minibasin has been completed and a paper prepared. Fault plane mapping of the principal structures has been largely completed and shows where sand-on-sand contacts allow water flow and hydrocarbon spillage across the major faults in Block 330 area. Three-dimensional seismic data have been used in this interpretation.

Model Simulations

Five 2-D flat files describing the geologic evolution of four N-S cross sections of the SEI area have been generated. Access.Basin 2-D simulations have been carried out on two of these sections. On one, calculations have been carried through the development of overpressure, seal rupture, and venting. Variations in porosity over the 2-D section have been made, assuming both exponential and linear compaction laws and fixed and migrating seals. Migrating seals have been found capable of producing an arrested profile of porosity reduction similar to that observed in some of the SEI wells. The thermal anomalies produced by venting are similar to those defined by subsurface well data. Modeling shows the flow required to

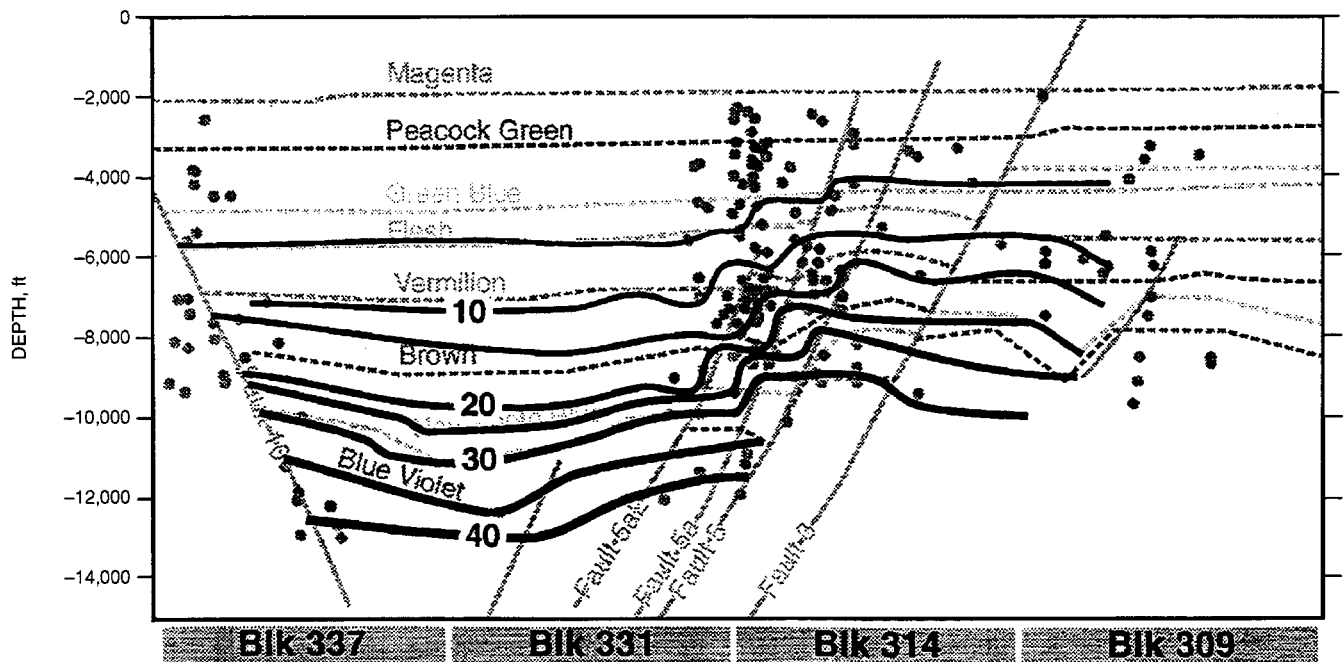


Fig. 1 Sample 2-D pressure interpretation. Pore pressure-hydrostatic pressure. Overpressure, MPa.

produce the anomalies is compatible with that required to refill the Pennzoil Block 330 reservoirs at the rate required to account for their apparent refilling.

Regional salt movement and pressure build-up and dissipation across salt welds has been simulated in two regional scale 2-D cross sections. The calculations have been carried out with both migrating and static seals and show the evolution and exchange of overpressures between adjacent compartments. The model runs show second-order temperature anomalies around individual salt domes because of the high thermal conductivity of salt. Hot domains lie above domes; cold domains below the domes reach all the way to the bottom of the basin (basement depth at > 12 km).

Investigation of the thermal and mechanical evolution of sediments in the Gulf of Mexico basin, including the effects of overpressuring and halokinesis, is progressing. To achieve this goal, a set of differential equations that describe the flux of heat and fluid in an evolving sedimentary basin was derived. The finite element method is used to solve these differential equations because of its suitability in discretizing complex geometry with intricate distribution of physical properties. As sedimentation proceeds, the fluids tend to escape from the sediments and the rate of fluid flow depends on sediment and fluid properties, such as permeability, viscosity and hydraulic diffusivity, and sediment rheology. If the fluids cannot escape from the sediments, they may become undercompacted and overpressured, decreasing the thermal conductivity of the sediments. The salt rock movement plays an important role on the temperature and pressure distribution history in a sedimentary basin because of the thermal conduc-

tivity in salt rock that may be five times the average sediment thermal conductivities and is practically impervious. With the predicted temperature and pressure history for the basin, the maturity level of the organic matter is estimated by using the kinetic reactions that describe the transformation of the kerosene to hydrocarbons. Finally, this technique is aimed at the partial assessment of the hydrocarbon generation, migration, and accumulation associated with salt and overpressure.

Geochemistry

Illite/Smectite Transformation in Sidewall Cores from the Red Fault Zone

The early results for the illite/smectite (I/S) transition on the Red Fault are shown in Table 1. These data indicate that the I/S transition occurs early, or high, in the section in the vicinity of the Red Fault and has been interpreted as evidence for rapid (?) migration of hot fluids, both brines and hydrocarbons.

Because the I/S data in the Red Fault zone are possibly anomalous, it is necessary to conduct studies away from the zone to see if the I/S transition occurs at the same or lower depths. To date, material (cuttings) has been obtained from Texaco Block 336.

Texaco Samples from Block 331

The X-ray data have not been interpreted as yet, but preliminary indications are that the I/S transition is lower in this well. If so, the new data support to some degree the interpretation that the Red Fault zone is thermally anomalous.

TABLE 1
Illite/Smectite Ratios for Pennzoil Sidewall Cores
Eugene Island Block 330

Number	Sample	Depth, ft	Smectite, %	Number	Sample	Depth, ft	Smectite, %
1	P1	7445	55	22	P53	7319	55
2	P3	7443	60	23	P55	7317	60
3	P4	7441	55	24	P56	7316	60
4	P6	7439	55	25	P57	7315	60
5	P8	7437	55	26	P59	7313	60
6	P10	7435	50	27	1	7349	60
7	P12	7433	55	28	11	7329	60
8	P15	7357	50	29	12	7327	60
9	P17	7355	55	30	14	7323	60
10	P19	7353	55	31	16	7321	60
11	P21	7351	60	32	22	7313	60
12	P23	7349	55	33	23	7289	60
13	P25	7347	55	34	24	7283	60
14	P27	7345	55	35	25	7279	25
15	P29	7343	50	36	26	7269	50
16	P31	7341	55	37	49	7107	50
17	P43	7329	60	38	52	6843	80
18	P45	7327	55	39	54	6833	80
19	P47	7325	55	40	55	6827	80
20	P49	7323	50	41	57	5803	90
21	P51	7321	55	42	58	5801	90

Organic Geochemistry

Initial hydrous pyrolysis experiments showed that a single activation energy, as used previously by Lewan² does not adequately describe gas evolution from the oxidized gas-prone Gulf Coast Cretaceous Eutaw Shale. Therefore, isothermal hydrous pyrolysis gas results from this rock were fitted to a distributed activation energy model^{3,4} in which carbon dioxide evolves at both low and high energies (maxima at 42 and 62 kcal/mol); ethane at about 54 kcal/mol, and methane at high energy (75 to 78 kcal/mol) (Fig. 2). Frequency factors, which are not assumed in these calculations, were also calculated and were found to depend somewhat on the spacing picked for calculating the distribution.

The oil generated in this initial experiment is much heavier than found for the EI-330 oils. The EI-330 oils all appear to belong to a single genetic family which, based on molecular composition, is sourced from a more marine, anoxic, and possibly evaporitic facies than a Eutaw Shale type rock.

These initial results suggest that even a relatively poor petroleum source rock such as this is capable of generating part of the methane which could solubilize and aid in migration of oil formed or trapped at depth below EI-330. However, methane generation from this rock would only occur at substantial depths and very high temperatures. A second finding from this work not previously reported is that substantial quantities of carbon dioxide are generated from this kerogen at high temperatures so that carbon dioxide must also be considered as a potential agent to aid in reactions or migration processes in deep Gulf Coast formations.

A paper entitled "Organic Geochemical Indicators of Dynamic Fluid Flow Processes in Petroleum Basins" was presented at the European Association of Organic Geochemists meeting, Stavanger, Norway, Sept. 19-24, 1993. This paper summarizes what is currently known about the oils, gases, and

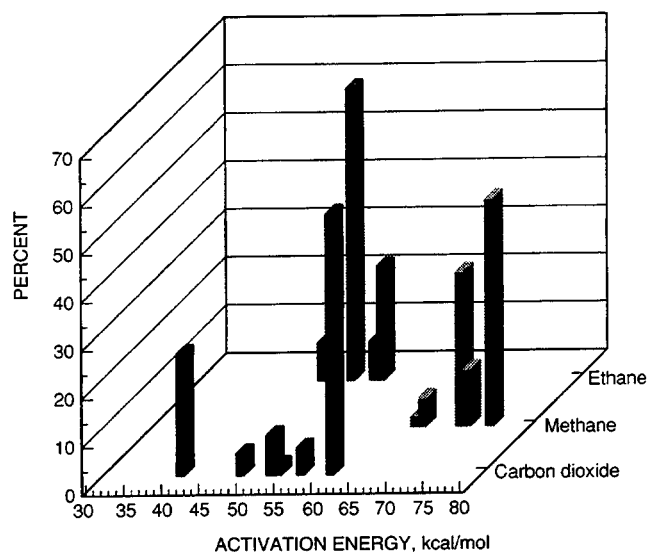


Fig. 2 Eutaw shale gas generation.

kerogens in EI-330 reservoirs and provides a framework for future organic geochemical analyses to be performed on the DOE Pathfinder Well samples.

References

1. Wei He, *Seismic Amplitude Analysis Technique for Predicting Top-of-Geopressure and Its Application to the Pleistocene Offshore Louisiana Gulf of Mexico*, M.S. Thesis, Columbia University, September 1993.
2. M. D. Lewan, Evaluation of Petroleum Generation by Hydrous Pyrolysis Experimentation, *Phil. Trans. R. Soc. Lond.*, A315: 123-134 (1985).
3. R. L. Braun and A. K. Burnham, Analysis of Chemical Reaction Kinetics Using a Distribution of Activation Energies and Simpler Models, *Energy & Fuels*, 1: 153-161 (1987).
4. R. L. Braun and A. K. Burnham, Mathematical Model of Oil Generation, Degradation, and Expulsion, *Energy & Fuels*, 4: 132-146 (1990).

**ENHANCED OIL RECOVERY UTILIZING
HIGH-ANGLE WELLS IN THE FRONTIER
FORMATION, BADGER BASIN FIELD,
PARK COUNTY, WYOMING**

Contract No. DE-FC22-93BC14950

**Sierra Energy Company
Reno, Nev.**

**Contract Date: July 10, 1993
Anticipated Completion: Dec. 31, 1994
Government Award: \$1,124,127
(Current year)**

**Principal Investigators:
Richard G. Formann
Jerome P. Walker**

**Project Manager:
Edith Allison
Bartlesville Project Office**

Reporting Period: July 1—Sept. 30, 1993

Objective

The objective of this study of the Frontier Formation in Badger Basin Field, Park County, Wyo., is to use three-dimensional (3-D) seismic and core data to analyze the diagenetic history, rock properties, and natural fracture system. This will provide the basis for increasing recovery with slant and horizontal wells to intersect oil-bearing fractures.

Summary of Technical Progress

Acquire 3-D Seismic Data

Process data. Vector Seismic Data Processing, Inc., began processing the 3-D seismic data in May 1993 and completed the work Sept. 8, 1993, with the delivery of migrated tapes. Processing consisted of demultiplex/reformat, 3-D geometry assignment, preliminary data analyses, gain recovery, brute stacks, deconvolution, spectral

balancing, 3-D velocity analysis, surface-consistent 3-D autostatics via Ronen–Claerbout method, preliminary stacks, final data analyses, normal moveout (NMO) and trace mute applications, common depth point (CDP) correlation autostatics, final stacks, bandpass filter, trace balancing, 3-D refraction statics, and 2-pass finite difference migration. Final decisions concerning tape copies and archival methods will be addressed in the near future.

Interpret data. Interpretation of the 3-D seismic survey has begun on a Sun Sparcstation 10 workstation (UNIX based), using Landmark Graphics' latest version of Seisworks 3D software. The first step in the interpretation process was to identify the seismic reflectors. This was accomplished by constructing synthetic seismograms from sonic and density logs for the No. 8 and No. 16 Badger Basin Field Unit (BBFU) wells (formerly the Apache No. 2-8 Federal and the Arapaho Petroleum No. 18-1 Federal). These seismograms (see Figs. 1, 2a, and 2b) were used to tie the formation picks to the seismic reflectors. The next step was to pick the normal and reverse faults seen on the survey in order to constrain the productive structure. Then, the following reflectors were picked on a 10 × 10 (inline by crossline) grid: (1) Eagle Sandstone Member of the Mesaverde Formation, (2) Cody marker, (3) Frontier Formation, (4) 2nd Frontier sandstone, (5) 3rd Frontier sandstone, (6) Lakota Formation (the Pryor Conglomerate equivalent). An autopicking routine (ZapIII) will be used to fill in the picks throughout the remainder of the survey for the three Frontier reflectors. Each crossline (NW–SE orientation) within the productive area of the field will then be checked for quality of the auto picking and edited if necessary. The crossline orientation is chosen because it is optimally placed for identification of the normal faulting, which is believed to be key to well productivity. Subsequently, time-structure maps and amplitude maps will be constructed for the three Frontier reflectors. A conversion from time-structure to depth will be made once a satisfactory velocity-gradient map is achieved. The location for the slant and horizontal wellbores will be chosen with the use of the appropriate structure maps.

Drill Slant Hole

Solicit bids and award. Various service companies, including drilling contractors, well-site geologists, mudloggers, core-analysis companies, etc., will be contacted and requested to supply bids for their anticipated services.

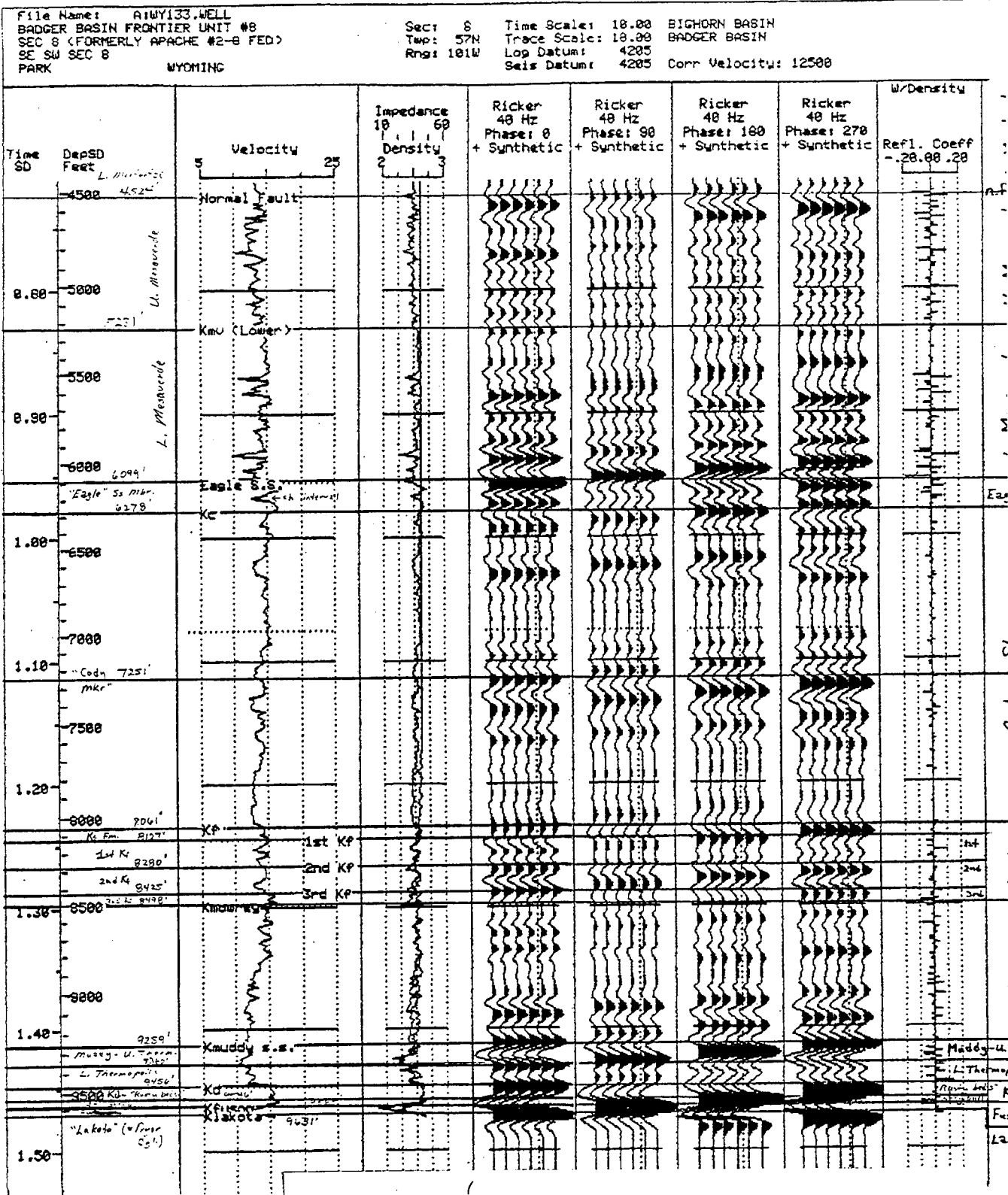


Fig. 1 Synthetic seismogram for the No. 8 Badger Basin Field Unit well. (Art reproduced from best available copy.)

File Name: AsWY134.WELL
 BADGER BASIN FRONTIER UNIT #16
 (FORMERLY ARAPAHO PETROLEUM #18-1 FED)
 528 FNL 1120 FEL SEC 18
 PARK WYOMING

Sec: 18 Time Scale: 10.00 BIGHORN BASIN
 Top: 57N Trace Scale: 10.00 BADGER BASIN
 Rng: 101W Log Datum: 4198
 Seis Datum: 4198 Corr Velocity: 8000

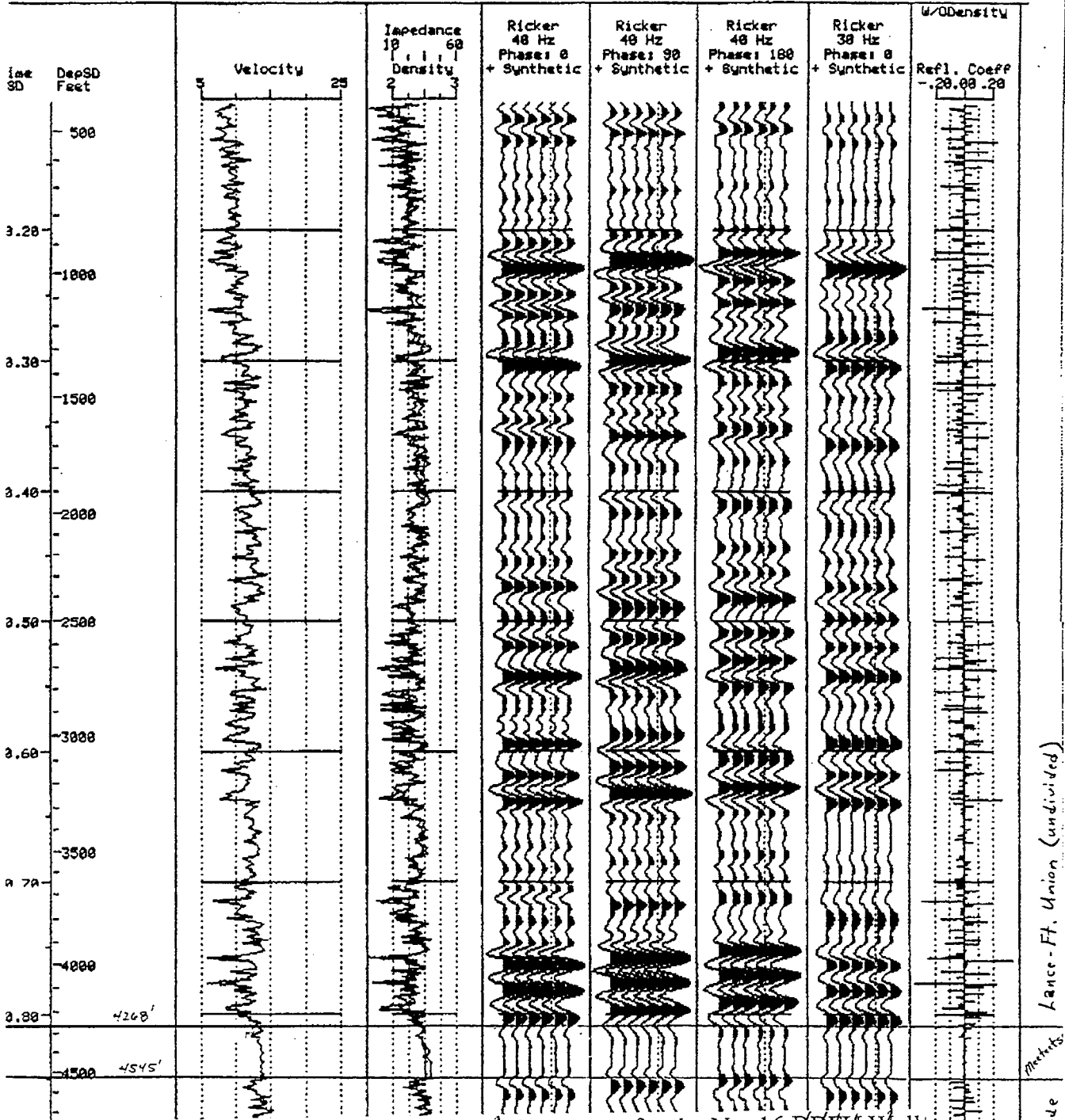


Fig. 2a Synthetic seismogram for the No. 16 Badger Basin Field Unit well. (Art reproduced from best available copy.)

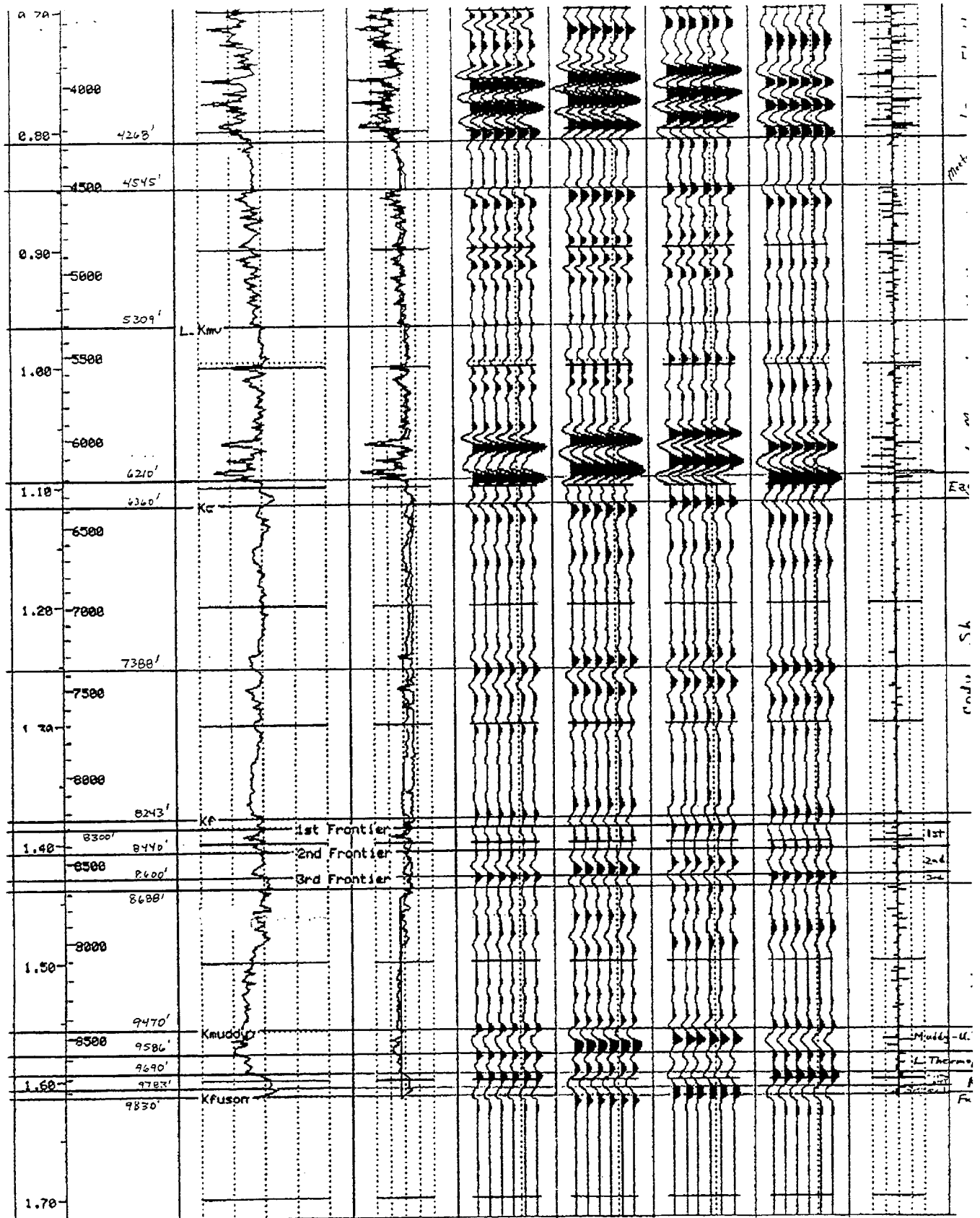


Fig. 2b Synthetic seismogram for the No. 16 Badger Basin Field Unit well. (Art reproduced from best available copy.)

IMPROVED OIL RECOVERY IN FLUVIAL DOMINATED DELTAIC RESERVOIRS OF KANSAS—NEAR-TERM

Contract No. DE-FC22-93BC14957

**University of Kansas
Lawrence, Kans.**

Contract Date: June 18, 1993

Anticipated Completion: Dec. 31, 1998

Government Award: \$2,007,450

Principal Investigators:

Don W. Green

G. Paul Willhite

Project Manager:

Rhonda Lindsey

Bartlesville Project Office

Reporting Period: July–Sept. 30, 1993

Objective

The objective of this project is to address waterflood problems of the type found in Cherokee Group reservoirs in southeastern Kansas and in Marrow sandstone reservoirs in southwestern Kansas. Two demonstration sites operated by different independent oil operators are involved in the project. The Nelson Lease (an existing waterflood) is located in Allen County, Kans., in the northeastern Savonburg Field and is operated by James E. Russell Petroleum, Inc. The Stewart Field (on latter stage of primary production) is located in Finney County, Kans., and is operated by Sharon Resources, Inc.

Topics to be addressed include (1) reservoir management and performance evaluation; (2) waterflood optimization; and (3) the demonstration of recovery processes involving off-the-shelf technologies that can be used to enhance waterflood recovery, increase reserves, and reduce the abandonment rate of these reservoir types.

The reservoir management portion of the project will involve performance evaluation and will include such work as (1) reservoir characterization and the development of a reservoir database, (2) identification of operational problems, (3) identification of near wellbore problems, (4) identification of unrecovered mobile oil and estimation of recovery factors, and (5) identification of the most efficient and economical recovery process.

The waterflood optimization portion of the project involves only the Nelson Lease. It will be based on the performance evaluation and will involve (1) design and implementation of a water cleanup system for the waterflood, (2) application of well remedial work such as polymer gel

treatments to improve vertical sweep efficiency, and (3) changes in waterflood patterns to increase sweep efficiency.

Finally, an improved recovery process will be implemented, possibly polymer augmented water flooding on both field demonstration sites.

Summary of Technical Progress

Savonburg Project

Engineering and Geological Analysis

A computer database that includes (1) well locations, (2) elevations, (3) perforations, (4) elevations of geological horizons, and (5) formation properties has been developed on a personal computer. Geological and engineering studies have been started to determine flow paths, reservoir continuity, and the existence of uncontacted compartments within the reservoir. A geological study is in the final stages of being completed. Preliminary cross sections have been constructed on the field.

A poster session entitled "Reservoir Characterization of Pennsylvanian Sandstones, Nelson Lease, Savonburg Field, Allen County, Kansas" was presented at the Oklahoma Class 1 Reservoir Characterization Meeting in March 1993. This is part of the technology transfer work.

A polymer flood streamtube five-spot simulation has been conducted on the Nelson Field to determine the applicability of polymer flooding.

A build-up test was conducted on Well H-17 to determine skin and reservoir properties.

During the next quarter, the field will be characterized by refining the computer database and cross sections as additional information becomes available. Patterns with high potential for improvement of production will be identified by calculating remaining mobile oil in place using the computer database. These potential patterns will be candidates for pattern changes and wellbore cleanups.

Water Plant Development

The supply and produced waters have been analyzed and mixtures tested to determine possible water quality problems with regard to the waterflood.

One air flotation vendor has been notified of needs for high water quality.

A water cleanup process will be designed on the basis of volume requirements and economics. Once a process that will economically clean the brine has been identified, the equipment will be placed on location and tested.

Pattern Changes and Wellbore Cleanup

Five-spot pattern investigations have been conducted to determine the effect of past acid treatments on oil production. Possible workover/wellbore cleanup techniques have been investigated.

In July, the following injection wells were washed and acidized: RW-1, RW-3, RW-14, HW-23, HW-29, and HW-31. In September, the following injection wells were washed and acidized: RW-8, RW-9, RW-13, RW-3, and KW-6.

Possible pattern changes will be considered on the basis of identified mobile oil saturation. New injection lines to converted injection wells will be placed. Pumping units will be placed on converted production wells. Wells exhibiting skin problems will be cleaned using appropriate methods. Treatments will be designed on the basis of the problem(s) identified.

Field Operations

Normal field operations have included (1) monitoring wells on a daily basis; (2) repairing water plant, piping, and wells as required; (3) collecting daily rate and pressure data; and (4) solving any other daily field operational problem that might occur.

Month	Average oil production
June	16.4 bbl/d
July	16.5 bbl/d
August	18.2 bbl/d
September	22.0 bbl/d

The field operations will be continued.

Stewart Field

Geological and Engineering Analysis

All the electric log data for the field have been digitized into a computer database. Existing core analyses and log data have been analyzed to find a relationship between core porosity vs. log porosity and porosity vs. permeability. A cumulative porosity plot was used to determine a porosity cutoff as related to net pay. Net pay thicknesses for individual wells have been completed using porosity cutoff values based on this study. A net pay map has been constructed for the purpose of the waterflood feasibility study. This map was planimetered to determine the reservoir volume of the Morrow and oil recovery factors.

Water saturation calculation work has begun and the current understanding is that water saturations cannot be calculated with sufficient accuracy to tabulate values for individual wells. Key problems are identified to be thin bed effects, thin conductive beds from pyrite cementation material, and conductive chloride clays. Capillary tests on cores may need to be employed.

Production data for all wells in the Stewart Field have also been entered into the computer database. Production data have been tabulated by month since the discovery of the field.

The wells have been grouped by tank battery so that allocations for each well can be monitored. The production is allocated to each well by monthly barrel tests. Water production is estimated by applying the percentage of water as determined by a grind-out test and relating that to the oil volume produced. The sales numbers for each tank battery are also listed for comparison with the production numbers supplied by the operators. Production has been divided between Morrow and non-Morrow for the wells that have produced from other zones. Gas production from the field is minimal and is used to power the pumping units or vented. Preliminary decline curve analysis to identify remaining primary reserves has begun.

The Stewart Field pressure history, including drill stem tests (DST) conducted on 31 wells, 2 field-wide shut-in surface pressure tests, and individual well fluid level tests, has also been tabulated into the database. Pressure tests indicate the continuity of the reservoir over the 4.5 mile length of the field. Isobar maps have been constructed for the field. Pressure histories of all DSTs, shut-in pressures, bottomhole pressure (BHP) from fluid levels, and BHP vs. cumulative production plots have been made for each well and the entire field.

Material balance calculations were performed from the initial field pressure to the two field-wide shut-in pressure tests. At this time a large difference exists between the volumetric mapping of the net sand and the material balance calculations.

A log stratification study has been completed which indicates the Morrow formation can be divided into as many as eight different flow units. Three main flow units were identified as separate depositional sequences that appear to possess similar porosity and permeability characteristics. These three flow units correlate along the deepest parts of the channel, with some minor discrepancies within the thinner boundary wells.

Initial steps have been taken to connect Sharon Resources via Internet to the workstation at the University of Kansas so simulation work on the field can be started.

Future Work

Computerized reservoir simulation of the field will begin in the next quarter. Preliminary screening models will be conducted to evaluate polymer flooding potential vs. waterflooding. Net pay maps will be refined to better define reservoir volume. The initial discrepancies that have arisen in the comparison of material balance calculations versus volumetric analysis will be further investigated. Decline curve analysis from existing production data will be continued to identify remaining oil reserves. Techniques to accurately conduct water saturation calculations will continue to be investigated.

APPLICATIONS OF ADVANCED PETROLEUM PRODUCTION TECHNOLOGY AND WATER-ALTERNATING-GAS INJECTION FOR ENHANCED OIL RECOVERY—MATTOON OIL FIELD, ILLINOIS

Contract No. DE-FC22-93BC14955

**American Oil Recovery, Inc.
Decatur, Ill.**

Contract Date: Dec. 29, 1992

Anticipated Completion: Dec. 31, 1994

**Government Award: \$702,091
(Current year)**

**Principal Investigator:
Michael R. Baroni**

**Project Manager:
Gene Pauling
Metairie Site Office**

Reporting Period: July 1–Sept. 30, 1993

Objectives

The objectives of this project are to continue reservoir characterization of the Cypress Sandstone; identify and map facies-defined waterflood units (FDWS); and design and implement water-alternating-gas (WAG) oil recovery utilizing carbon dioxide (CO₂). The producibility problems are permeability variation and poor sweep efficiency. Part 1 of the project focuses on the development of computer-generated geological and reservoir simulation models that will be used to select sites for the demonstration and implementation of CO₂ displacement programs in Part 2. Included in Part 1 is the site selection and drilling of an infill well, coring of the Cypress interval, and injectivity testing to gather information used to update the reservoir simulation model. Part 2 involves field implementation of WAG. Technology transfer includes outreach activity, such as seminars, workshops, and field trips.

Summary of Technical Progress

Drilling, Geophysical, and Petrophysical Analyses of Seaman No. 15

A joint team of American Oil Recovery, Inc. (AOR) project personnel, and Illinois State Geological Survey (ISGS) geoscientists selected sec. 35, T. 12 N., R. 7 E. for location of the infill well, AOR/Seaman No. 15, based on the isopach of the target facies-defined subunit (E-interval) in the Sawyer Unit and information from surrounding wells (Fig. 1).

AOR–Seaman No. 15 was drilled from Sept. 12 to 22, 1993. The whole cores recovered from 1738 to 1822.5 ft contained live oil in the B, C, and E intervals of Cypress Formation (Fig. 2). Core analyses showed that the E interval has a higher average porosity and permeability than the B and C intervals respectively (Table 1). A suite of geophysical logs composed of dual induction focus log, natural gamma ray log, compensated densilog/caliper, compensated neutron log, minilog, dielectric log and analysis, and epilog–complex reservoir analysis were run. The in situ water saturation of the E interval predicted from the logs was very high. For example, the C interval was calculated to have a water saturation of 100% by the dielectric log despite the fact that the whole core portion of the C interval was observed to be oil saturated and bleeding oil and gas. Because of the uncertainty of the water saturations determined by use of rule-of-thumb values of exponent “n” and the formation cementation factor “m” employed in the log interpretation, Cypress core samples from the B, C, and E intervals were submitted for an extended analysis of these critical factors.

Cypress Rock/Injected Brine Compatibility Tests

Two core plugs taken from the E interval at depths of 1750.5 and 1751 ft, respectively, were tested for compatibility with (1) Cypress formation brine from Strohl No. 8; (2) produced brine from the Pennsylvanian formations; (3) pit brine consisting of Rosiclare and Cypress effluents, effluents from Pennsylvanian formations, and rain water; and (4) laboratory brine consisting of 1% NH₄Cl and 1% NaCl. The resistivity and pH of the various test brines were measured at room temperatures ranging from 74.9 to 77.3 °F (Table 2). The fluids were injected into the plugs in the order shown in Table 3.

All field brines were first passed through the Whatman filter paper (No. 4) prior to injection into the core plug. The brines retained a yellowish taint after filtration. Liquid permeability was observed to decrease as the field brines were consecutively injected into the core plugs (Table 3). Also, the color of the core effluents was clear, which suggests that the plugs filtered out the yellowish taint. A dark-brown solid buildup was also observed on the inlet face of the core plugs. The liquid permeability increased from 14 to 19.3 mD after the flow direction was reversed in plug No. 2 (Table 3), a sure indication that particle plugging occurred in the core sample. These observations suggest that these field brines may impair formation permeability if injected into the reservoir without adequate filtration.

Slim-Tube CO₂–Oil Miscibility Tests To Determine Minimum Miscibility Pressure of Cypress Oil

CO₂–crude oil miscibility tests were conducted in a slim-tube apparatus using Cypress crude oil sampled from the No. 8 Strong well (Fig. 1). The test conditions were 85 °F and

Core # 1 1738-1760
Core 22', recover 20.35'

Core # 2 1761-1791
Core 30', recover 30'

Core # 3 1792-1822.5
Core 30.5', recover 28.9'

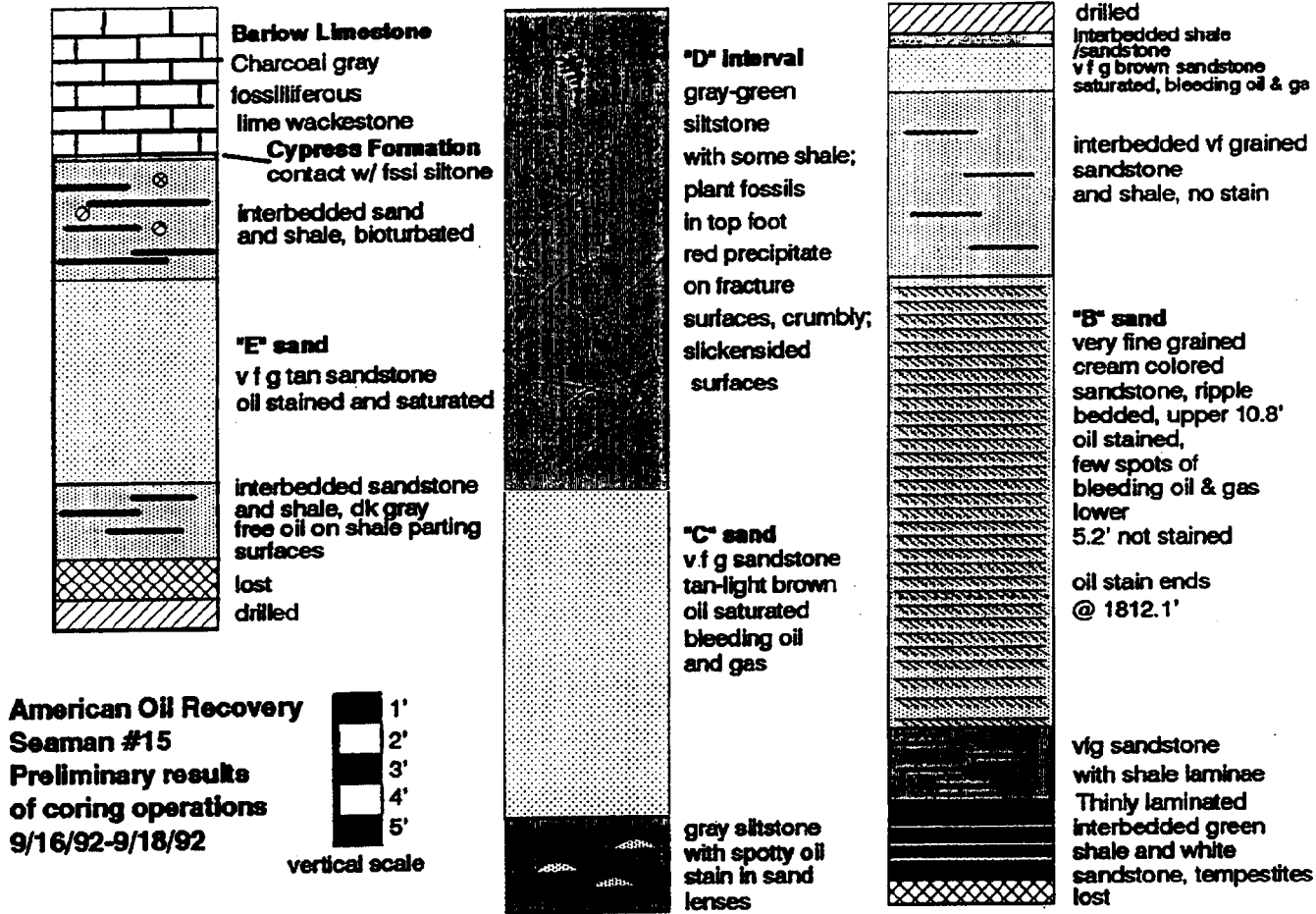


Fig. 2 First-pass whole core description of Cypress interval from American Oil Recovery, Inc.-Seaman No. 15 well.

TABLE 1
Core Analysis Summary

Formation	Depth, ft	Average permeability, mD		Average Porosity, %	Average Liquid Saturation, %	
		Horizontal	Vertical		Oil	Water
Cypress	1748.9-1758.0	61.0	57.0	19.6	15.3	25.2
	1777.8-1788.3	24.0	7.1	19.5	21.7	43.4
	1799.7-1810.8	11.0	0.93	16.7	10.6	37.9

pressure ranges of 1250 to 2500 psig. The slim-tube properties are summarized in Table 4, and the test results are summarized in Table 5. The plot of oil recovery of 1.2 pore volume (PV) of injected CO₂ vs. pressure is illustrated in Fig. 3. The minimum miscibility pressure (MMP) of the Mattoon crude oil with CO₂ was determined to be 1780 psig using the method of Yellig and Metcalf.¹

This result implies that only immiscible CO₂ displacement of oil is possible from the Cypress reservoirs at Mattoon field because the formation parting pressure is about 1800 psia.

Reservoir Simulation

Reservoir simulation models of the Mattoon CO₂ Project have been developed to enhance and verify reservoir characterization and predict optimum CO₂-assisted oil recovery processes. The models, which are being continuously updated, will aid in the design and management of Part 2 of this project. The three major models are the Sawyer CO₂ injection, the Pinnell CO₂-WAG, and the huff 'n' puff (cyclic CO₂ injection with data from the AOR/Seaman No. 15 well) models.

TABLE 2
Chemistry of Brine Used in the Rock/Brine Compatibility Tests

Type of fluid	pH	Resistivity of water, Ω/m^2	Total dissolved solids, ppm	Test temperature, °F
Cypress brine	6.97	0.074	37,768	74.9
Pennsylvanian* pit brine	7.54	0.113	20,804	77.3
Laboratory brine	6.85	0.110	21,652	77.0
Core effluent from Cypress brine	7.26	0.065	42,365	77.1
Cypress brine	7.36	0.076	35,400	76.3

*Pennsylvanian brines consist of commingled produced brines from Pennsylvanian formations.

TABLE 3
Coreflow Data in the Rock/Brine Compatibility Tests

	Plug 1	Plug 2
Depth, ft	1750.5	1751.0
Air permeability, mD	45.2	42.7
Laboratory brine permeability, mD	13.5	-
Cypress brine permeability, mD	-	14.04
Pennsylvanian* brine permeability, mD	10.1	13.33
Pit brine permeability, mD	7.0	8.50
Reverse flow—Cypress brine permeability, mD	-	19.32

*Pennsylvanian brines consist of commingled produced brines from Pennsylvanian formations.

TABLE 4
Slim-Tube Properties

Column material	316 stainless steel
Length	57 ft
Internal diameter	0.457 cm
Packing material	glass bead (100 to 120 mesh)
Porosity	42.1%
Pore volume	120 cm ³
Pressure rating	5000 psi
Permeability	4 D

TABLE 5
Oil Recoveries at Various Slim-Tube Pressures

Pressure, psig	% oil recovery	% PV CO ₂ injected when gas-oil interface/transition zone was observed
1350	74.86	72
1500	81.67	79
2000	90.01	91
2500	91.40	95

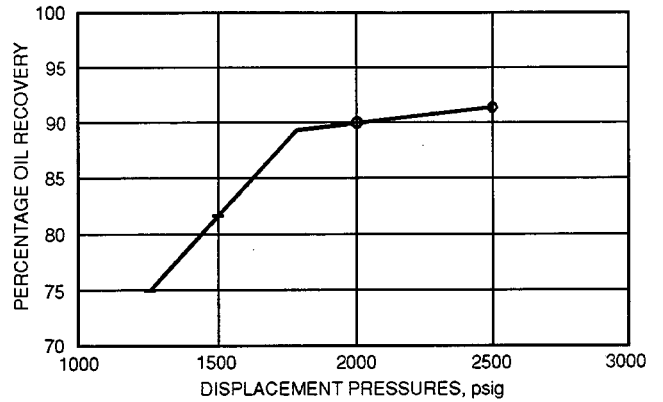


Fig. 3 Percentage oil recovery vs. displacement pressure from slim-tube tests. The minimum miscibility pressure is 1780 psi. Miscible displacement of Mattoon crude oil with CO₂ may only occur above this pressure.

Sawyer Unit CO₂ Project

During the last quarter, approximately 2000 tons of CO₂ were injected into No. 1 Sawyer Community and oil was produced from No. 2 Ed. Morris and No. 1 D. M. Sawyer Community 2 (Fig. 1). ICCR No. 18 and ICCR No. 19 wells were monitored and found to contain CO₂. After the cessation of CO₂ injection on June 30, 1993, ICCR No. 18 and ICCR No. 19 wells and No. 1 Sawyer Community injection well were used to monitor reservoir pressure. There was a general pressure decrease in all these wells as oil production continued from No. 2 Ed. Morris and No. 1 D. M. Sawyer Community wells (Fig. 4). Uniformity of pressure responses confirm communication among these wells in the E interval.

A continuing and extensive search for well information in this unit revealed that twelve wells were completed for oil production from the E interval at various times between June 1946 and February 1962. Furthermore, four wells, including

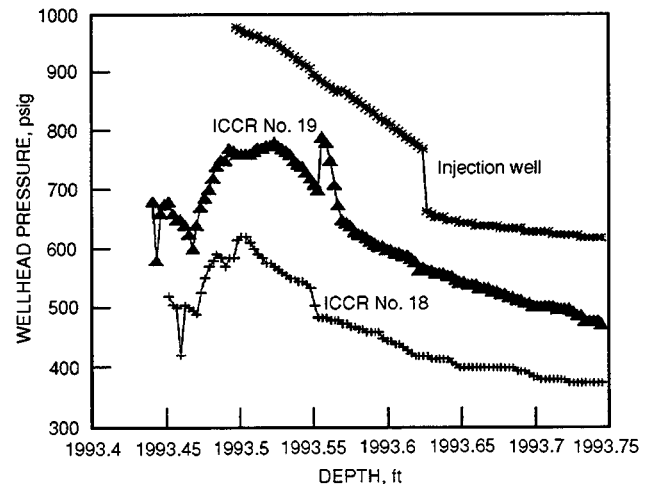


Fig. 4 Wellhead pressures of injection well (Sawyer 1 Community 3), ICCR No. 18, and ICCR No. 19. Identical pressure profiles indicate communication among the wells.

the Railroad No. 18 well, previously used as water injectors, were open in the E interval. Only three wells—No. 1 Sawyer Community No. 3, No. 1 Sawyer Community No. 2, and Railroad No. 19—were opened in the E interval during the current project. The implication of this finding is that the E interval has been produced.

A compositional reservoir simulation model consisting of six pseudo-components (Table 6) was developed to assist in the management of the project in the Sawyer Unit. Reservoir description was initially accomplished by correlations of reservoir quality (clean sand distribution) to porosities and the permeability–porosity correlation of the Cypress sandstone. These data have been greatly improved by the core analysis of the AOR–Seaman No. 15 well in the Sawyer Unit. Pseudo-relative permeability data were replaced with laboratory-measured values using Cypress rock from the newly drilled well, Cypress brine, and CO₂-saturated crude oil. History match was greatly improved. One drawback is that there are no gas data to date and simulated gas production could not be matched by observed data.

Planned predictions with the use of the simulation model include the comparison of the performances of multiple well oil production and gas injection to those of the cyclic CO₂ injection and oil production otherwise called huff 'n' puff. The uncertainty of the integrity of wells that are open in the E interval and the high cost of verifying them favor the use of huff 'n' puff operations in the Sawyer Unit.

Single-Well Cyclic CO₂ Injection in Sawyer and Strong Units

Parameters affecting oil recoveries from huff 'n' puff wells have been investigated by simulation of a single-well model. The core analysis and well data of the AOR–Seaman No. 15 well were used in the simulation (Table 7). The parameters included in the sensitivity analysis are the CO₂ slug size, the number of CO₂ injection cycles, the CO₂–oil mixing ratios, and permeability–thickness of the reservoir interval.

Simulated results show that the oil production rate increases after injecting CO₂ into the single well (Fig. 5). Other results are (1) oil recovery increases with CO₂ slug size reaching a peak after 2% hydrocarbon pore volume (HCPV) [7.64 million standard cubic feet (MMscf)] is injected but

declines between 2% and 3% HCPV; (2) increasing permeability values increases oil recovery and also cumulative gas production at the same slug size (Fig. 6); (3) a second cycle of CO₂ injection may increase the flow rate at the same well conditions; and (4) oil recovery increases with CO₂–crude oil mixing ratio (Fig. 7). Other factors that increase the CO₂–crude oil mixing ratio include absence of thief zones in the reservoir and initial reservoir pressure (Fig. 3).

These results suggest that (1) there is a CO₂ slug size for optimum oil production from a given huff 'n' puff well; (2) oil production from a huff 'n' puff well may be optimized by well stimulation that can increase the well productivity without creating fractures and channels; and (3) a second cycle of CO₂ injection may enhance oil recovery from the huff 'n' puff well.

The next stage of the simulation of the huff 'n' puff process involves matching the simulation model to observed results from actual huff 'n' puff wells in order to develop a suitable model that can be used to advise future applications of huff 'n' puff projects.

Pinnell CO₂–WAG Project

The reservoir simulation study of the Pinnell CO₂–WAG project was performed with a black-oil model. The model was calibrated by matching oil production and pressure history between April 20 and Sept. 30, 1993. Performance of various CO₂ injection scenarios were investigated with Pinnell–Uphoff No. 1 and Pinnell No. 3–W wells as the oil producer and gas–water injector, respectively. The options considered are

- Base case: Continuous production from Pinnell–Uphoff No. 1 without pressure maintenance after May 15.
- Straight CO₂ injection: Continuous CO₂ injection at a rate of 500 Mcf per day.
- Straight water injection: Continuous water injection at a rate of 125 barrels per day.
- Water-alternating-CO₂ injection at various brine-to-CO₂ slug ratios.

The following conclusions can be drawn from the results of this model (Table 8):

- Oil production from WAG injection is higher than that obtained from straight CO₂ flood or straight waterflood.

TABLE 6

Properties and Compositions of Pseudo-Components in Reservoir Crude Oil

Pseudo-component	Composition mole fraction	Components in mixture	Molecular weight, grams/gram mole	Critical temp., °F	Critical pressure, psia
CO ₂	0.0004	CO ₂	44.01	87.9	1070
P2	0.0036	N ₂	28.01	-232.4	493
P3	0.06253	C1,C2,C3	36.11	119.8	639.16
P4	0.08171	C4,C5	65.32	342.84	518.51
P5	0.3522	C6,C7,C8,C9	103.11	553.61	435.76
P6	0.49955	C10,C33	388.53	1104.7	212.15

Note: Reservoir temperature, 80 °F.

TABLE 7

Reservoir Properties Used in Single-Well Simulation (AOR-Seaman No. 15)

Average water saturation, 59% (assumed)
 Oil saturation, 38% (assumed)
 Gas saturation, 3% (assumed)

Depth, ft	Permeability, mD		Porosity, %
	Horizontal	Vertical	
1750	71.0	54.0	20.9
1750-1751	73.0		19.6
1751-1752	119.0		20.2
1752-1753	73.0	67.0	20.7
1753-1754	60.0		21.3
1754-1755	28.0		19.5
1755-1756	54.0	49.0	21.0
1756-1757	11.0		13.5
1757-1758	2.1		13.8

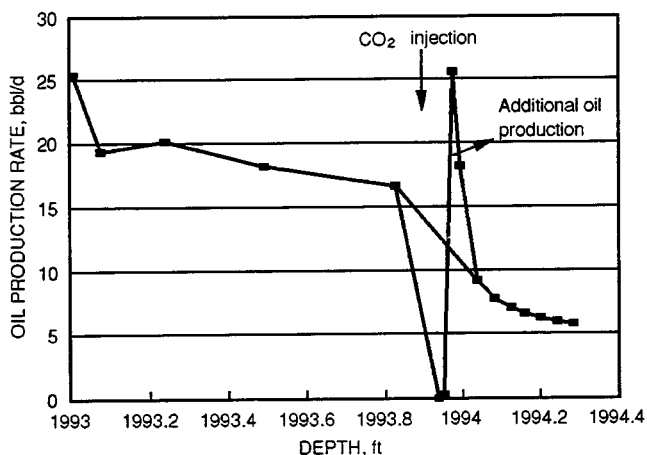


Fig. 5 Oil production rate is increased by the CO₂ cyclic injection processes. 3.82 MMscf of CO₂ was injected into 10 ft of pay.

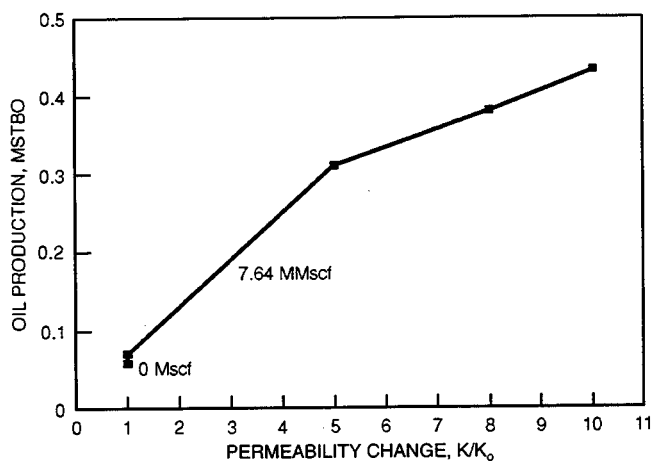


Fig. 6 Oil production after 130 d; oil recovery is enhanced with improved reservoir permeability.

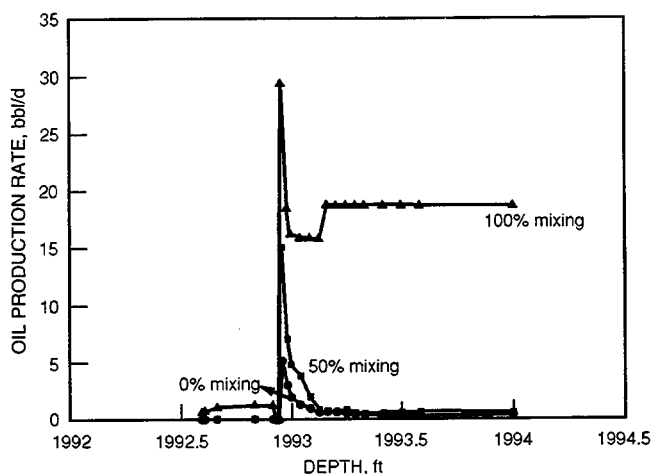


Fig. 7 Oil recovery rate increases with CO₂-crude oil mixing ratio.

TABLE 8

Cumulative Oil Production Ratio (Relative to Base Case) from April 20, 1993, to Dec. 30, 1995

	Mixing Ratio (% of Hydrocarbon Pore Volume contacted by CO ₂)		
	5%	20%	50%
CO ₂ flood	0.75	1.4	3.2
Brine flood	2.4	2.5	3.1
WAG (1:2)*	2.6	3.8	5.7
WAG (1:1)	2.6	3.7	5.0
WAG (2:1)	2.6	3.5	4.2
WAG (3:1)	2.6	3.2	3.8

*WAG (1:2) means water-alternating-gas ratio of 15,000 barrels of water to 30,000 Mcf of CO₂.

- Higher oil recovery was obtained with a WAG ratio higher than 1 Mcf of CO₂ per barrel of brine.
- Oil recovery by immiscible CO₂ displacement of oil is sensitive to the mixing ratio of CO₂ with crude oil. Oil recovery from straight CO₂ flood is poor when the mixing ratio is low (<20%).

Reference

1. W. F. Yellig and R. S. Metcalfe, *Determination and Prediction of CO₂ Minimum Miscibility Pressure*, Paper SPE 7477 presented at the 53rd Annual SPE Technical Conference and Exhibition, Houston, Tex., Oct. 1-3, 1978.

**SECONDARY OIL RECOVERY FROM
SELECTED CARTER SANDSTONE OIL
FIELDS—BLACK WARRIOR BASIN,
ALABAMA**

Contract No. DE-FC22-93BC14952

**Anderman/Smith Operating Company
Denver, Colo.**

**Contract Date: Oct. 21, 1992
Anticipated Completion: Jan. 5, 1996
Government Award: \$369,600**

**Principal Investigator:
James C. Anderson**

**Project Manager:
Gene Pauling
Metairie Site Office**

Reporting Period: July 1–Sept. 30, 1993

Objectives

The objectives of this project are to (1) increase the ultimate economic recovery of oil from the Carter reservoirs and thereby increase domestic reserves and lessen U.S. dependence on foreign oil; (2) extensively model, test, and monitor the reservoirs so that their management is optimized; and (3) assimilate and transfer the information and results gathered to other U.S. oil companies to encourage them to attempt similar projects.

Summary of Technical Progress

Central Bluff

Gas production fell during the quarter. The Fowler–Brashear 7-9 is producing only enough gas to run the pumping unit. With average water injection rates of 200 to 250 BPD, no pressure build-up was observed. The rate was increased in late September to 300 BPD and the injection well began to pressure up. The current injection rate is 300 BPD with 460 psi.

The oil production rate for the Fowler–Dodson 8-12 has increased to about 4 BPD. The gears and gear box on the Fowler–Dodson 8-12 were repaired.

A reservoir modeling study of the Central Bluff Unit is planned in the next quarter.

North Fairview

Annual maintenance for the field was performed. Locations were cleaned, equipment was painted, and firewalls were rebuilt. Water injection rate has been and is 200 BPD with 1240 psi. Pressure was realized almost immediately after injection commenced. Five hundred gallons of xylene were injected into the Bowman 33-8 in an attempt to lower the injection pressure. The pressure remained the same.

Oil production in the field has increased very little this quarter. The Smith 33-8 is up to 4 BPD and the Perkins 33-11 up to 2.5 BPD.

A reservoir modeling study of North Fairview Unit was initiated. The objectives of the study are to (1) improve understanding of primary and secondary recovery, (2) check/confirm no-flow boundaries, (3) develop an improved reservoir management scheme (e.g., optimal water injection strategy), and (4) forecast oil recovery for various operating strategies.

Structure, net pay isopach, and net oil pore volume maps were prepared on the basis of Anderman/Smith Operating Company's previous geologic evaluation of the area. A reservoir simulation grid (24 × 16 × 1) was constructed to cover an area of about 7000 × 5000 ft, or about five times as great as the 150 acres estimated for North Fairview. A transparency of the grid was overlaid on the structure and isopach maps, and values of elevation and thickness were digitized at gridblock centers for input to the simulator.

The reservoir simulator used in the study is ROAST II, a modified version of the Department of Energy's (DOE's) BOAST II simulator. Production and pressure data for the three producing wells (33-6, 33-10, and 33-11) and the injection well (33-5 No. 1) will be history matched using the simulator.

Two post-fracture pressure buildup tests were performed for well 33-11. Analyses of the well tests yielded an estimated permeability of 85 mD with a skin factor of -3.4 as a result of fracture stimulation. Other reservoir properties are being evaluated for input to the simulator. Some parameters for which no data are available, such as relative permeability, will be estimated from matching actual field performance.

South Bluff

There was no activity during the period.

**INTEGRATED APPROACH TOWARD THE
APPLICATION OF HORIZONTAL WELLS TO
IMPROVE WATERFLOODING PERFORMANCE**

Contract No. DE-FC22-93BC14951

**University of Tulsa
Tulsa, Okla.**

**Contract Date: Jan. 1, 1993
Anticipated Completion: Dec. 31, 1996
Government Award: \$250,973**

**Principal Investigator:
Balmohan G. Kelkar**

**Project Manager:
Rhonda Lindsey
Bartlesville Project Office**

Reporting Period: July 1–Sept. 30, 1993

Objective

The overall objective of the proposed project is to improve secondary recovery performance of a marginal oil field through the use of a horizontal injection well. The location and direction of the well will be selected on the basis of detailed reservoir description using the integrated approach. With the use of this method, a recovery of 5% of original oil in place is expected. This should extend the life of the reservoir by at least 10 years.

This project is divided into two stages. In Stage I, part of the Glenn Pool field (William B. Self Unit) will be selected, and additional reservoir data will be collected by conducting cross-borehole tomography surveys and formation micro scanner (FMS) logs through a newly drilled well. In addition, analogous outcrop data will be used. The state-of-the-art data will be combined with conventional core and log data to develop a detailed reservoir description based on the integrated approach. Extensive reservoir simulation studies will be conducted, and a location and direction of a horizontal injection well will be selected. The well will be drilled based on optimized design, and the field performance will be monitored for at least 6 months. If the performance is encouraging, a second stage will be scheduled for the project. If the project is continued, Stage II will involve selection of part of the same reservoir (Berryhill Unit, Tract 7), development of reservoir description with the use of only conventional data, simulation of flow performance with the use of the developed reservoir description, selection of a location and direction of a horizontal injection well, and implementation of the well followed by monitoring of reservoir performance.

A comparison of the results of the two stages will allow an evaluation of the collection of additional data using state-of-the-art technology. In addition, the application of horizontal wells to

improve secondary recovery performance of marginal oil fields will be evaluated. A successful completion of this project will provide a new means of extending the life of marginal oil fields with the use of easily available technology. It will also present a methodology to integrate various qualities and quantities of measured data to develop a detailed reservoir description.

Summary of Technical Progress

This report is divided into three sections. In the first section preliminary results based on the cross-borehole seismic surveys are discussed. In the second section, the geological description of the Self Unit is discussed. In the third section, a petrophysical properties description of the reservoir is presented followed by the flow simulation results. On the basis of a thorough evaluation of the geological and flow simulation results, the initial test well location will be finalized within the next month followed by drilling of the well in early November.

Geophysical Data Collection

A cross-well seismic test was performed in the Self Unit under Upland Resources management (Kiefer, Southeast Creek County) on Aug. 24, 1993. This report focuses on the data acquisition parameters of the test survey. The purpose of the test was to establish the signal quality for various raypath lengths. The information will be used to locate the position of the Vertical Test Well (VTW) relative to the four existing receiver wells. The VTW will be used as the source well. The optimum wavelet quality will be a determining factor in locating the VTW.

Test Data Acquisition

The cross-well test survey was performed in two cased wells 660 ft apart. The receivers were placed in Well 62 and the source in Well 72. The survey was conducted from a recording truck approximately halfway between the source–receiver well pair. Source and incoming signals (raw data) were transmitted through wireline cables. The data were loaded on the computer hard disk, which was then transferred to 88-MB tapes. The size of the test data is approximately 20 to 25 MB.

The basic receiver for this test was a hydrophone group of three receivers inserted in the fluid-filled well. The hydrophone separation was 8 ft. A piezoelectric transducer source was used to generate a sweep signal at a frequency range of 200 to 2000 Hz with a 0.125 ms time sample interval. A “listen time” of 0.5 s yielded 4000 samples per trace ($0.5 \text{ s} / 0.125 \text{ ms} = 4000 \text{ samples}$).

Figure 1 explains the cross-well test survey acquisition geometry in detail. Acquisition is defined by four coverage zones, “fans.” For fans I through III, the maximum and minimum depth of source were 1520 and 704 ft, respectively. The source is pulled up at a constant speed activating eight times in a 2-ft interval. The midpoint of each of the eight sources defines an eight-fold vertical stack location. The consecutive vertical stacks are 16 ft apart, yielding 52 stacked source locations for each fan, I through III. Fan IV has lower areal coverage compared with the first three. However, the 4-ft spacing yielded

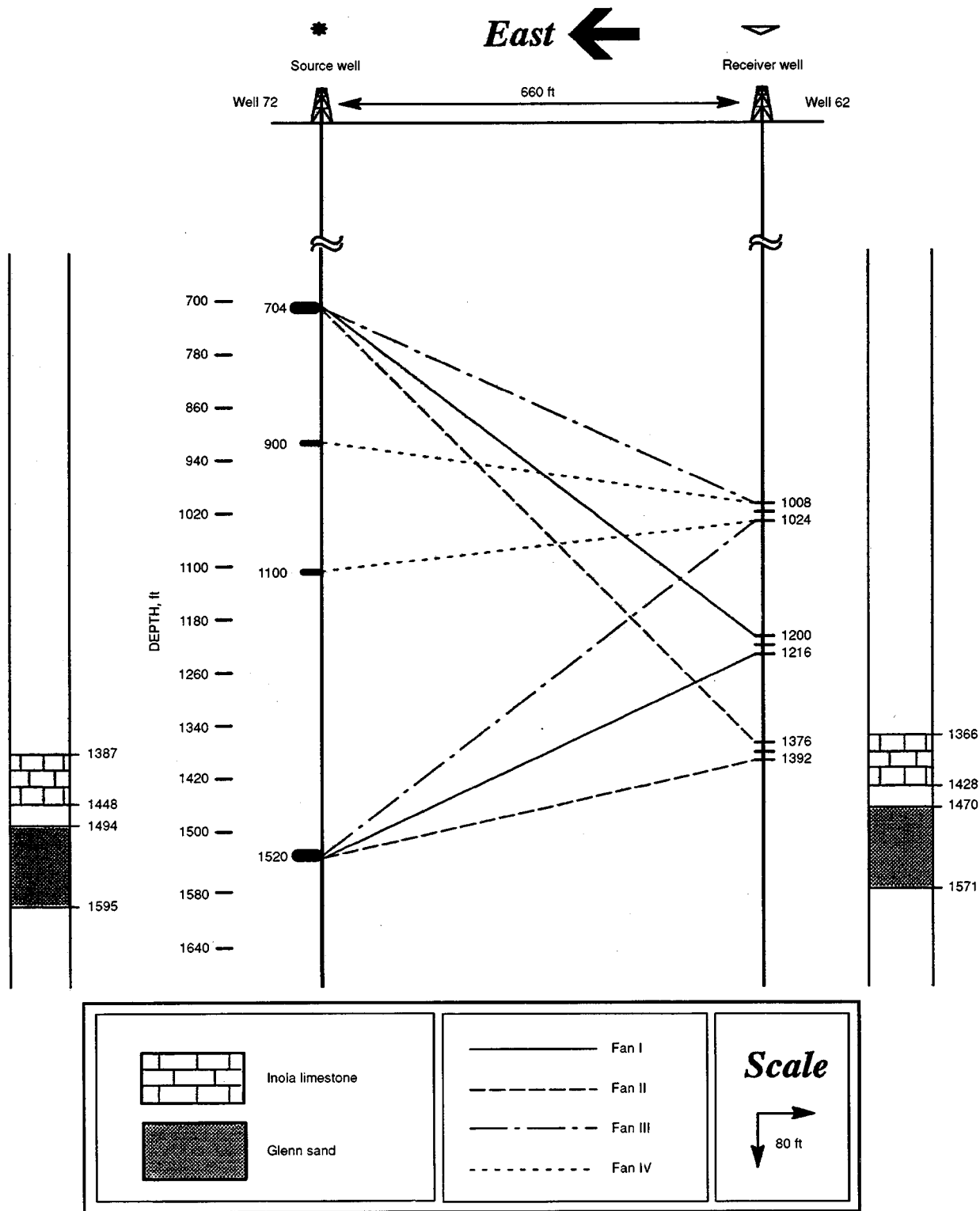
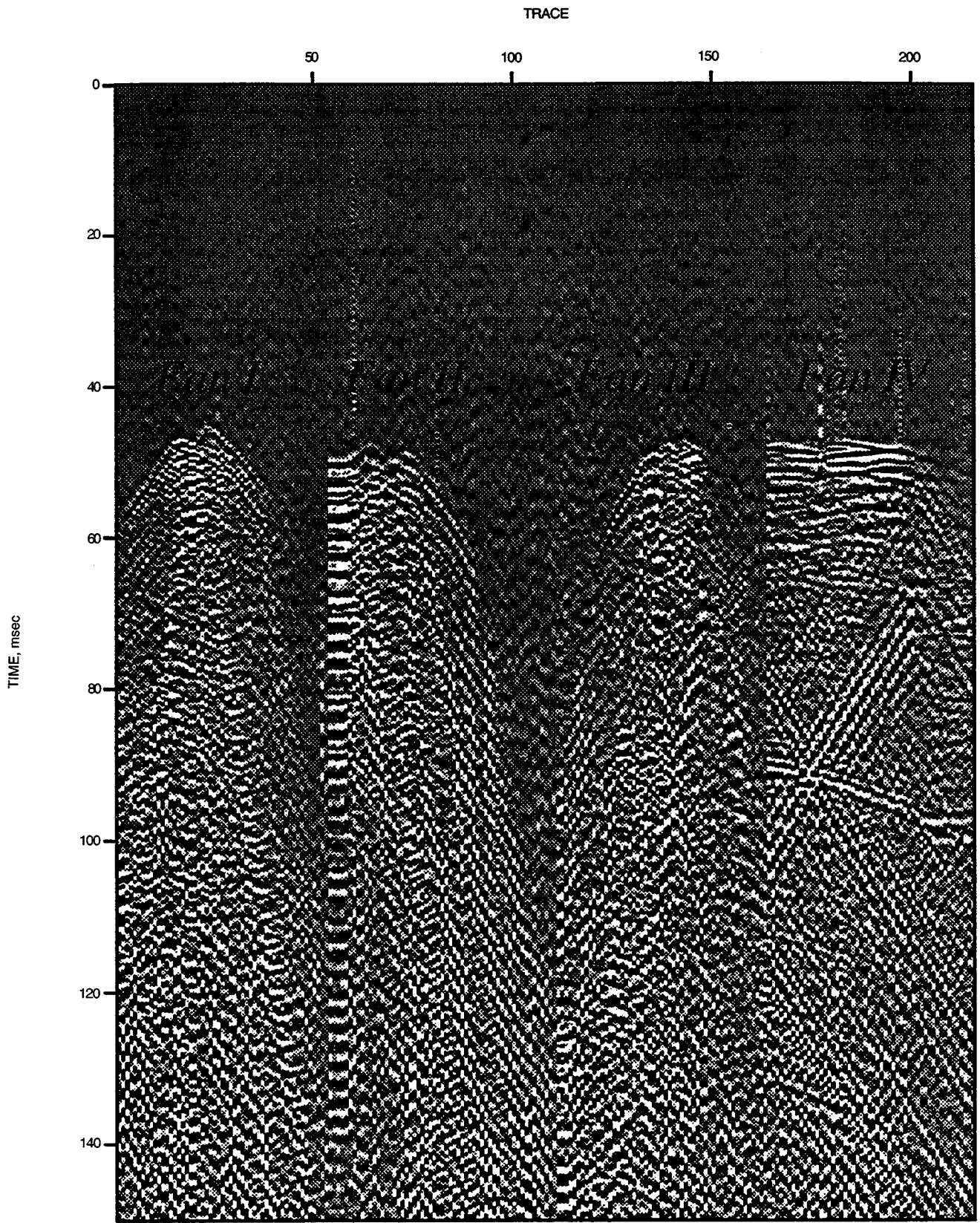


Fig. 1 Glenn Pool cross-well test survey acquisition geometry (day 1).

51 stacked source locations. The test survey includes a total of 207 stacked source locations, each shooting into 3 receivers. This results in 621 rays. More than 4000 rays from unstacked sources were acquired in approximately 5 h.

Figure 2 shows the raw data from the four fans as common receiver (receiver 1) gathers. A first processing attempt on the data is in progress.



CROSS-WELL TEST SURVEY DAY 1, receiver 1

Fig. 2 Common receiver gathers for fans I, II, III, and IV.

Geological Description

Stratigraphic framework of the Glenn Sand reservoir in the Self Unit (160 acres) has been established through a series of northeast to southwest stratigraphic cross sections. Some cross sections extend southwestward into the adjacent Burrows Unit. A thin interval (1 to 2 ft), expressed as high gamma ray and conductivity log response, is used as a marker bed about 12 ft above the Glenn Sand (Fig. 3); two thin intervals, expressed as high conductivity log response, are also used as markers in those wells that penetrate up to 50 ft below the Glenn Sand. In these stratigraphic cross sections, the Glenn Sand has been subdivided into 7 units (A descending through G), each of which is a discrete genetic interval (contiguous facies deposited during a brief, discrete increment of time). The superpositional relationship among discrete genetic intervals is established by the elevation of the top of channel-fill deposits relative to the marker beds.

A combination facies and facies-biased, net-sand isopach maps have been constructed for each of the seven discrete genetic intervals. Units A through E are characterized by channel-fill and splay facies as reservoir rock and floodplain and levee facies as barrier or baffle rock. Within the channel-fill facies, localized isopach closures of the 10-ft isogram typically encompass 15 acres, and the centers of these closures are separated by 1000 ft along a channel-fill facies trend. The channel-fill facies sandstone obtains a maximum thickness of about 30 ft. In the A Unit, the splay facies reaches a maximum thickness of 15 ft in locations proximal to the channel-fill facies and diminishes to zero feet thick up to 2200 ft away; in the other units, the splay facies is more restricted in thickness and lateral extent. Units F and G include a channel-mouth-bar facies as reservoir rock. The channel-mouth-bar facies acquires a maximum thickness of 40 ft at a channel terminus and extends laterally beyond the limits of the Shelf Unit.

Work in progress includes mapping the thickness and lateral extent of nonreservoir rock facies. This will determine the potential for vertical isolation or baffling between each discrete genetic interval.

Shallow stratigraphic correlations were completed in the vicinity of the cross-well tomography test to evaluate possible acoustic reflections observed in the test results. Wells included in the cross section are Self Nos. 72, 62, 55, 66, and 57. Stratigraphic zones identified between top of Glenn Sand (about 1470 ft drill depth) up to the top of the logged interval (about 500 ft) include, in ascending order: upper Boggy Formation to top of the Inola Lime (at 1370 ft); Red Fork to top of Pink Lime (at 1210 ft); Senora Formation, including Skinner Sands to top of Verdigris Lime (at 930 ft); lower Marmaton Formation including Pure Sands to top of the Big Lime (at 750 ft); and Mowata Shale up to the top of the logged interval. All stratigraphic units are continuous between the test source well (No. 72) and receiver well (No. 62), except the Skinner Sands, which clearly terminate between these two wells.

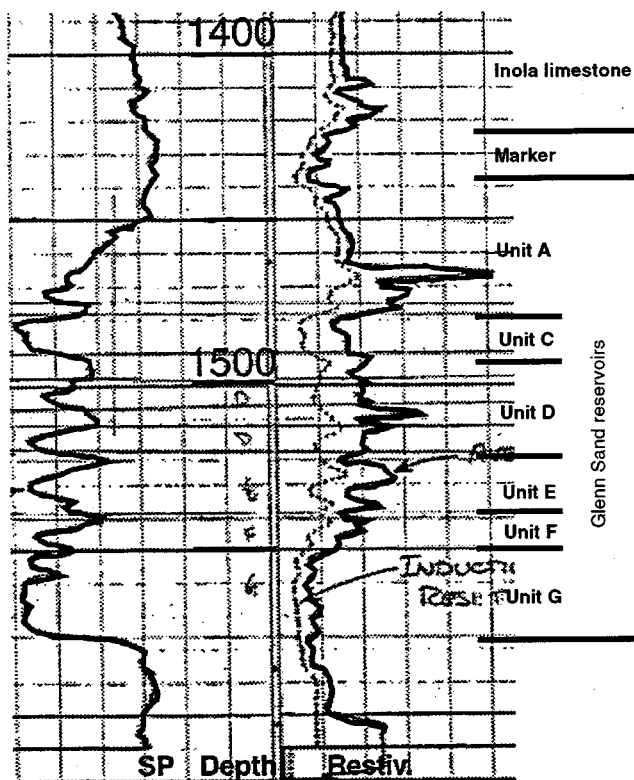
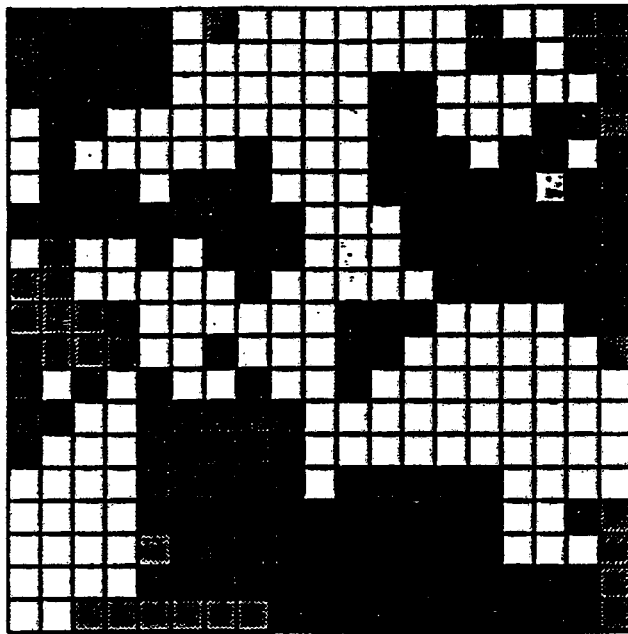


Fig. 3 Discrete genetic intervals in Glenn Sand (William B. Self No. 59).

Engineering Description and Simulation

A two-step procedure is used to construct the spatial description of the reservoir properties. In the first step, a geological description was created using a geostatistical program SISIMPDF.¹ This program allows the different geological units to be described by numerical quantities. For example, sand A was described by the number 1, sand B was described by the number 2, and so on. After assigning numbers to individual sands, vertical and horizontal variograms were constructed, and the sands were simulated at interwell locations. To validate the results, the sands description was compared with the geological maps. Although not identical the simulated descriptions show resemblance to the geological units. For example, in Fig. 4 an areal map at a particular depth is compared with the geological map for sand A, and an areal map of simulated values for sand C is compared with the geological map of sand C.

Once the simulated sands distribution was constructed, the next step was to assign the petrophysical properties to individual grid blocks. To ensure that assignment of permeability and porosity values was consistent with individual sands, all the core information was used and the core data for individual sands were divided on the basis of the sand description at that particular location. As a result, permeability and porosity data were limited for individual sands. The lower sands had much higher permeability compared with the upper sands. With the use of this limited data, porosity variograms for individual

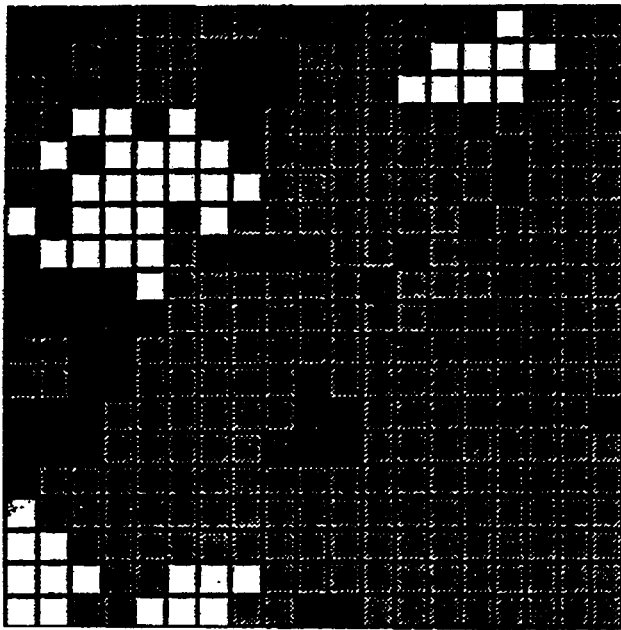


Simulated

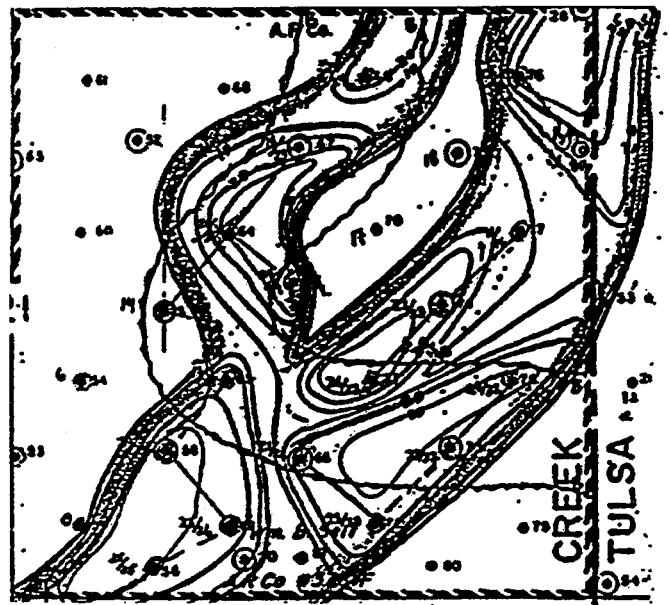


Geological

SAND A



Simulated



Geological

SAND C

Fig. 4 Simulated sands and geological model.

sands in both vertical and horizontal directions were constructed. For horizontal direction, as a result of pure nugget effect, it was necessary to make assumptions with respect to ranges of the variograms. With the help of these variograms, using the method of simulated annealing,² spatial distribution for porosities for all the sands was constructed at every grid point. That is, for eight sands there were eight porosity values

at each grid block. The simulated porosity values were filtered through the simulated sand maps so that a porosity value could be assigned at an individual grid block. For example, if sand A is present at a particular grid block, the porosity value assigned corresponded to sand A porosity simulation. This way, the porosity distribution was consistent with the observed core values. Permeability values at individual grid

block were assigned with the use of a cross plot between log of permeability and porosity for each sand.

For conducting flow simulation, pressure-volume-temperature (PVT) properties are needed. In the absence of any reliable data, an assumption was made that the bubble point pressure of the oil was the same as initial reservoir pressure. A single curve published by ARCO was used for the relative permeability data for the entire Glenn Pool field. It does create significant uncertainty in the reservoir description. The goal is not necessarily to match the historical performance but to observe how close simple forward modeling comes to the historical performance. Figure 5 shows a comparison between the historical performance and the simulated performance. For early years the match simulated performance underpredicts the actual performance.

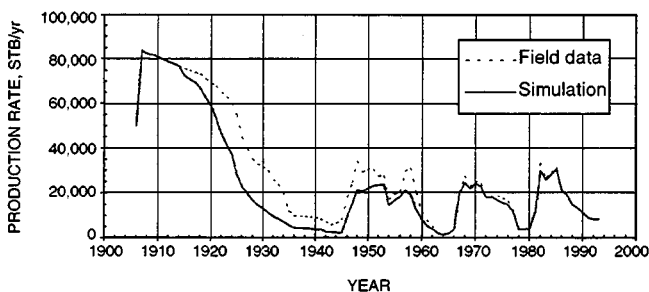


Fig. 5 Field performance and simulated performance.

Several reasons may explain the discrepancy. First, yearly production data are not available until 1935. One single number in 1945 indicates cumulative production until that time. How reliable that number is uncertain. Second, during the early years, all the wells were drilled at the boundary of the Self Unit to protect the drainage of the reserves. As a result, some of the wells may have drained oil from nearby leases. An assumption has been made that the Self Unit is bounded. Overall, considering the uncertainties involved in many of the reservoir parameters, the match is deemed satisfactory.

The simulation results will be investigated more carefully. One goal is to use more grid blocks to investigate the sensitivity of flow performance on smaller scale heterogeneities. Another goal is to vary vertical permeability in the simulation. Vertical permeability is one of the unknowns in the simulation results. The sensitivity of flow performance will be investigated on this parameter as well. Once these studies are complete, the applicability of the horizontal injection well in improving the reservoir performance will be investigated. Such study is still in progress.

References

1. C. V. Deutsch and A. G. Journel, *GSLIB: Geostatistical Software Library User's Guide*, Oxford University Press, New York (1992).
2. G. Perez, *Stochastic Conditional Simulation for Description of Reservoir Properties*, Ph.D. Dissertation, University of Tulsa, Tulsa, Okla., 1991.